

**Climate and Glacier Variability during Past Centuries in the North and
South Patagonian Andes of Argentina**

(Spine Title: Recent Climate and Glacier Changes in the Patagonian Andes)

(Thesis Format: Integrated-Article)

by

Mariano H. Masiokas

Graduate Program
in
Geography (Environmental Science)

Submitted in partial fulfillment
of the requirements for the degree of
Doctor of Philosophy

Faculty of Graduate Studies
The University of Western Ontario
London, Ontario, Canada
January, 2008

© Mariano H. Masiokas 2008



Library and
Archives Canada

Bibliothèque et
Archives Canada

Published Heritage
Branch

Direction du
Patrimoine de l'édition

395 Wellington Street
Ottawa ON K1A 0N4
Canada

395, rue Wellington
Ottawa ON K1A 0N4
Canada

Your file Votre référence
ISBN: 978-0-494-39303-1
Our file Notre référence
ISBN: 978-0-494-39303-1

NOTICE:

The author has granted a non-exclusive license allowing Library and Archives Canada to reproduce, publish, archive, preserve, conserve, communicate to the public by telecommunication or on the Internet, loan, distribute and sell theses worldwide, for commercial or non-commercial purposes, in microform, paper, electronic and/or any other formats.

The author retains copyright ownership and moral rights in this thesis. Neither the thesis nor substantial extracts from it may be printed or otherwise reproduced without the author's permission.

AVIS:

L'auteur a accordé une licence non exclusive permettant à la Bibliothèque et Archives Canada de reproduire, publier, archiver, sauvegarder, conserver, transmettre au public par télécommunication ou par l'Internet, prêter, distribuer et vendre des thèses partout dans le monde, à des fins commerciales ou autres, sur support microforme, papier, électronique et/ou autres formats.

L'auteur conserve la propriété du droit d'auteur et des droits moraux qui protègent cette thèse. Ni la thèse ni des extraits substantiels de celle-ci ne doivent être imprimés ou autrement reproduits sans son autorisation.

In compliance with the Canadian Privacy Act some supporting forms may have been removed from this thesis.

Conformément à la loi canadienne sur la protection de la vie privée, quelques formulaires secondaires ont été enlevés de cette thèse.

While these forms may be included in the document page count, their removal does not represent any loss of content from the thesis.

Bien que ces formulaires aient inclus dans la pagination, il n'y aura aucun contenu manquant.


Canada

The University of Western Ontario
Faculty of Graduate Studies

Certificate of Examination

Chief Advisor

Examining Board

Dr. Brian H. Luckman

Dr. Chris Smart

Advisory Committee

Dr. Katrina Moser

Dr. James Voogt

Dr. Stephen Hicock

Dr. Stephen Hicock

Dr. Greg Wiles

The thesis by
Mariano H. Masiokas

entitled:

**Climate and glacier variability during past centuries in the north and south
Patagonian Andes of Argentina**

is accepted in partial fulfillment of the
requirements for the degree of
Doctor of Philosophy

Date

Chairman of Examining Board

Abstract and Keywords

Updated instrumental hydro-climatic data, tree rings and glacier records from southern South America were used to document the main spatial and temporal patterns of climate and glacier variability across the Patagonian Andes over the past few centuries. Analyses of instrumental records identified four well defined regional patterns with distinct modes of variability. The south Patagonian region has warmed significantly during the 20th century and experienced a concurrent, widespread glacier mass loss. Recent glacier recession is also documented throughout the north Patagonian Andes using repeat photography. Although the gridded temperature data in this region show significant warming, improved homogenized temperature records indicate an overall negative trend. Strong negative trends also occur in regional precipitation and streamflow records. A simple climate-based “glacier mass balance” proxy series was developed to overcome the lack of local, direct mass balance measurements. This series shows a long term negative trend between 1912 and 2002 which is concordant with the widespread glacier recession. Dendrogeomorphic techniques were used to develop detailed Little Ice Age (LIA) glacier chronologies for the past few centuries at the Tronador and Fitz Roy-Lago del Desierto areas in the north and south Patagonian Andes. Trees directly affected by glacier activity at Tronador indicate two main LIA advances culminating in the early-mid 1600s and 1800s followed by several readvances. A hitherto unknown glacier advance was identified and calendar dated to ca. 450 AD. In the southern area the main LIA event probably culminated during the early 17th century, but additional, relatively synchronous advances occurred in the early 1700s and late 1800s-early 1900s. Well-replicated tree-ring records from NW Patagonia were used to develop an annually-resolved “glacier mass balance” proxy series over the past 520 years that partially validates the glacier chronology from the Tronador area. This reconstructed proxy record, viewed cumulatively, shows a noticeable negative trend after the late 1500s and extended intervals of overall “positive” mass balance conditions that roughly precede the two main LIA advances in this region. These results highlight the great potential for future research in this region but several limitations associated with the basic data and/or the methodologies used still need to be addressed.

Keywords: Southern South America, Patagonian Andes, instrumental hydro-climatic data, tree-ring records, glacier fluctuations, Little Ice Age, dendroglaciology, glacier mass balance estimates.

Statement on Co-Authorship

Chapters 2-6 and Appendix 1 were written as stand-alone manuscripts intended for publication. Chapter 3 and Appendix 1 have been published and Chapter 4 accepted for publication. I am the first author in all cases but several co-authors assisted to a variable extent in the preparation of these manuscripts. The specific contribution of each co-author is detailed below. A list of co-authors and the publication information is also provided at the beginning of the appropriate chapters.

I wrote all the papers and except for the analysis of satellite images in Chapter 4 (see below) I also conducted all the data analysis and preparation of figures and tables. With some assistance from co-authors I gathered all hydro-climatic data for Chapters 2, 3 and 6, analyzed and collected or participated in the collection of most tree-ring samples used in Chapters 4 and 5, and collaborated in the collection of some of the tree-ring samples used in Chapter 6.

My supervisor Dr. Brian H. Luckman is co-author of all the manuscripts. Dr. Luckman assisted with the organization and structure of the research and papers, providing useful suggestions regarding the analysis of data, the interpretation of results and the overall presentation of figures and tables. He was also crucial editing the text to improve readability.

Dr. Ricardo Villalba of IANIGLA-CONICET¹ is also a co-author of all the manuscripts. He was critical during the planning stages of the research and manuscripts and subsequently provided useful suggestions regarding data analysis and interpretation of results. He collected or assisted in the collection of most of the tree-ring data used throughout this thesis and provided access to a large proportion of the climatic data analyzed in Chapters 2, 3 and 6.

¹ Instituto Argentino de Nivología, Glaciología y Ciencias Ambientales, Consejo Nacional de Investigaciones Científicas y Técnicas, Mendoza, Argentina.

Dr. Petr Stepanek of the Czech Hydrometeorological Institute is co-author of Chapters 2 and 3. He allowed unrestricted access to his computer programs that permitted a thorough analysis of the relative homogeneity of the climatic data. He also provided useful suggestions during the preparation of these manuscripts.

Drs. Steven A. Mauget of the U.S. Department of Agriculture-Agricultural Research Service and Richard L. Branham of IANIGLA-CONICET are co-authors in Chapter 2. Dr. Mauget provided the source code for the testing algorithm that identifies intra- to multi-decadal modes of variability in time series whereas Dr. Branham facilitated its implementation in a PC Windows environment. Both co-authors provided useful discussions regarding the interpretation of this methodology.

Silvia Delgado of IANIGLA-CONICET is a co-author in Chapters 3 and 4. In Chapter 3 she provided useful suggestions in the interpretation of results, whereas in Chapter 4 she performed with my assistance the analyses of Landsat TM satellite data to determine glacier area changes at the study sites in the south Patagonian Andes.

Marcelo E. Lascano of IANIGLA-CONICET is co-author of Chapter 3. Mr. Lascano facilitated access to updated hydro-climatic data from NW Patagonia and participated in the discussion of preliminary versions of this manuscript.

Alberto Ripalta of IANIGLA-CONICET is co-author of Chapters 4 and 5. He assisted in the collection of the tree-ring samples used in these manuscripts and provided important suggestions in the field that improved the subsequent interpretation of results.

Pedro Skvarca of Instituto Antártico Argentino is co-author in Chapter 4. He provided aerial photographs and useful suggestions to improve readability and interpretation of results.

Dr. Jorge Rabassa of CADIC-CONICET² is co-author of Chapter 5. He collected and supported the analysis of an earlier tree-ring sampling at selected sites in the forefield of Glaciar Río Manso in the early 1980s.

Dr. Antonio Lara and Rocío Urrutia of Universidad Austral de Chile are co-authors in Chapter 6. They provided climate data and most of the Chilean tree-ring series used in this manuscript, including some recently updated tree-ring chronologies that allowed the comparison with climate data to be extended forward for over a decade.

Drs. Carlos Le Quesne of Universidad Austral de Chile and Juan Carlos Aravena of Centro de Estudios Cuaternarios, Chile are co-authors of Appendix 1. They provided useful suggestions during the preparation of this paper. Dr. Le Quesne facilitated access to streamflow and snowpack data from central Chile.

² Centro Austral de Investigaciones Científicas, Consejo Nacional de Investigaciones Científicas y Técnicas, Tierra del Fuego, Argentina.

Acknowledgements

First of all I would like to thank my supervisor Dr. Brian H. Luckman for his invaluable support and patience during all the stages of preparation of this thesis. He was always available and willing to discuss my “quick” questions and responded (with almost no delay in virtually all cases) with an amazing collection of extremely detailed comments and suggestions on how to improve numerous preliminary versions of the different chapters of this thesis. His critical thinking and experience in the fields of dendroclimatology, dendroglaciology and glacial geomorphology have been crucial in my formation as a young researcher and have significantly improved the quality of this thesis. He also provided an important proportion of the financial support needed for the completion of this thesis.

My special gratitude also goes to Dr. Ricardo Villalba of IANIGLA, Mendoza. He introduced me to the world of dendroglaciology and the beautiful Patagonian glaciers several years ago and strongly supported my decision to come to Canada in 2002. He has supported and taken part in the field research throughout the project and unselfishly provided data and additional funds that have contributed to this research. Since coming to Canada he has been my “unofficial” supervisor from afar, constantly providing excellent ideas, comments and energy to continue with this research project. Both he and Dr. Luckman have encouraged me to attend or be aware of important meetings related to my research, and have facilitated my participation at several of these meetings. I feel privileged to have had such extraordinary supervisors.

I would also like to thank Dr. Chris Smart and the members of my advisory committee, Drs. James Voogt and Stephen Hicoek for their friendly help and suggestions during the initial stages of this research. Dr. Voogt’s assistance as a second reader of this thesis is also greatly appreciated.

This research has been partially supported by scholarships and travel funding from the Inter-American Institute for Global Change Research (via funds awarded to them by the

United States National Science Foundation) through their Collaborative Research Network 03 “The Assessment of Present, Past and Future Climate Variability in the Americas from Treeline Environments” and CRN 2047 “Documenting, Understanding and Projecting Changes in the Hydrological Cycle in the American Cordillera” (B.H. Luckman PI). I am also extremely grateful to the several individuals and institutions that provided additional financial support for this research: The University of Western Ontario, the Department of Geography, the Environmental Science Graduate Program (my special gratitude to Dr. Bob Bailey), the Natural Sciences and Engineering Research Council of Canada (NSERC), the Ontario Graduate Scholarships (OGS) Program, and Past Global Changes (PAGES), Switzerland. The Agencia de Promoción Científica y Tecnológica (through grants PICT07-03093 and PICTR02-186 to Dr. Ricardo Villalba) and Consejo Nacional de Investigaciones Científicas y Técnicas (CONICET) provided crucial funding for the activities carried out in Argentina.

The field component of this thesis would have not been possible without the assistance and expertise of many people that are or have been associated with IANIGLA, Mendoza over the past decade. In particular, Dr. Ricardo Villalba, Alberto Ripalta, Silvia Delgado, Salvador Calí, Pepe Hernández and Lidio López were crucial in making the field trips extremely productive and fun. I also thank personnel from Parques Nacionales, Argentina for facilitating our work and providing assistance in the field. The photographic database used in Chapter 3 was developed with the assistance of many individuals and institutions, including the group mentioned above plus Darío Trombotto and Claudia Bottero of IANIGLA, Club Andino Bariloche and Museo de la Patagonia (Bariloche, Argentina), Biblioteca Perito Moreno (Parques Nacionales, Buenos Aires, Argentina), and the Libraries and Department of Geology of the University of Helsinki, Finland. Dr. Högne Jungner, Director of the Dating Laboratory of the University of Helsinki, kindly provided some of the radiocarbon determinations used in this thesis. I greatly appreciate the help and patience of Silvia Delgado (IANIGLA) during our extended email communications regarding the analyses of satellite images for Chapter 4. I would also like to thank Rocío Urrutia (Universidad Austral de Chile, Valdivia) for sending via email many of the Chilean climate and tree-ring records used in this thesis, and Guillermo García Zamora

and Marcelo Lascano (IANIGLA), and Carlos Le Quesne (Universidad Austral de Chile) for providing snow course and streamflow records. J.C. Aravena (CEQUA, Chile) and D. Fernández (El Calafate, Argentina) facilitated access to aerial photographs from Lago del Desierto.

This Canadian experience would have not been so rich and the adaptation so smooth without the unselfish help from Helen and Brian Luckman. Over these years they have taught me a great deal on how to make newcomers feel welcomed and I will always remember your hospitality and delicious suppers. The staff, professors and graduate students of the Department of Geography also facilitated enormously my adaptation and daily life by providing an excellent and friendly environment to conduct research. In particular, I would like to thank the “dendro mafia” (Sean, David, Mike, Richard, Juan Carlos) for discussions and moments at the dendro lab and in the field, Karen from the Cartography Section for her help with my questions regarding maps, figures, scanning, etc, the staff from the Main Office for their help with applications, contracts, faxes, etc, and Joe for patiently answering my many questions regarding the computers/software available at the computer lab and for making these computers run always smooth and reliable.

I would also like to thank our friends in Canada, especially Jorge and Lety Arroyo-Boy, Luis and Marcela Silva, Andrés and Adriana Ramírez, Luis and Iliana Orta, Andrés and Julieta González, Estela Quintero, Gabor and Monica Saas, Roey Egozi, and the historic members of the Mercator soccer team for many great moments. We have also shared many great moments with Juan Carlos Aravena and his family (Waleska, Beatriz and Alejandro) and also with the De León family (Allyson, Gustavo, Ariel and Mateo) and I will always remember those days at Platt’s Lane Estates. Over the years Juan Carlos has become a great friend. I am happy we had the opportunity to share many of our experiences here in Canada together. The Calle family (Indio, Leti, Chula and Ignacio) made us feel right in Mendoza every time we visited them in Toronto and I sincerely thank them for their support and friendship.

Our families in Mendoza were also a constant and unconditional source of energy and emotional support: Mamá, Papá, Melisa, Marcos, Matías, Juan and the kids, Carlos, Ana María, Mar, Puchi and Belén. In one way or another they have all contributed with the successful outcome of this thesis and I wish we can go home soon to share our memories of these years enjoying a great asado together. I also thank my friend Martín Balasch for his constant good humor and support from the other end of the world.

I dedicate this thesis to my angels Carla, Sol and Blas for making these the best (and busiest!) years of my life and for the love and happiness they give me every single day.

Table of contents

Title page	i
Certificate of Examination	ii
Abstract and Keywords	iii
Statement on Co-Authorship	v
Acknowledgments	viii
Table of Contents	xii
List of Tables	xvi
List of Figures	xviii
List of Appendices	xxi
Chapter 1: Introduction	1
1.1 Introduction	1
1.2 Objectives	4
1.3 Context of this research	4
1.4 Thesis outline	5
1.5 References	7
Chapter 2: Instrumental surface temperature variations in southern South America and the Antarctic Peninsula: Data homogenization and identification of main modes of spatio-temporal variability	13
2.1 Introduction	13
2.2 Data and Methods	16
2.2.1 Data Screening	18
2.2.1.1 Southern South American records	18
2.2.1.2 Antarctic Peninsula Records	20
2.2.2 Data homogenization	21
2.2.2.1 Creation of reference series	22
2.2.2.2 Homogeneity testing	25
2.2.3 Identification of main spatial patterns	27
2.2.4 Creation of regionally averaged series	28
2.2.5 Identification of long term modes of variability	29
2.3 Results	30
2.3.1 Homogeneity of records	30
2.3.2 Main spatial patterns	32
2.3.3 Temporal variability of regionally averaged records	38

2.4	Discussion and Conclusions	44
2.5	References	50
Chapter 3:	20th-century glacier recession and regional hydro-climatic changes in northwestern Patagonia	58
3.1	Introduction	58
3.2	Study Area	59
3.3	Data and Methods	61
3.3.1	Repeat ground photography	61
3.3.2	Climate records	66
3.3.3	Regional climatic index, 1912-2002	68
3.3.4	Relationships with regional streamflow records	69
3.4	Results	71
3.4.1	Photographic comparisons	71
3.4.2	Climate changes in northwestern Patagonia, 1912-2002	71
3.4.3	Regional climatic index. Comparison with localized glacier advances	75
3.4.4	Regional streamflow variations and relationships with climate records	77
3.5	Discussion and Conclusions	79
3.6	References	81
Chapter 4:	Little Ice Age fluctuations of small glaciers in the Monte Fitz Roy and Lago del Desierto areas, south Patagonian Andes, Argentina	88
4.1	Introduction	88
4.2	Study Area	90
4.3	Previous studies	91
4.4	Methods	94
4.4.1	Dating the glacier deposits	94
4.4.2	Estimating glacier area changes since the LIA	97
4.5	Results	98
4.5.1	Glaciar Torre	98
4.5.2	Glaciar Piedras Blancas	103
4.5.3	Glaciar Lago del Desierto I	107
4.5.4	Glaciar Lago del Desierto II	110
4.5.5	Glaciar Lago del Desierto III	112
4.5.6	Changes in glacier area	113

4.6	Summary and Conclusions	114
4.7	References	119
Chapter 5:	Late Neoglacial fluctuations of Glaciar Río Manso and Glaciar Frías in the north Patagonian Andes of Argentina	125
5.1	Introduction	125
5.2	Study Area	127
5.3	Previous work	129
5.4	Methodology	133
5.5	Results	136
5.5.1	Glaciar Río Manso	136
5.5.1.1	The north lateral moraine	136
5.5.1.2	The terminal zone	144
5.5.1.3	The south lateral moraine	146
5.5.2	Glaciar Frías	148
5.6	Discussion and Conclusions	151
5.7	References	158
Chapter 6:	Tree-ring based reconstruction of a glacier mass balance proxy record for the past five centuries in the north Patagonian Andes	163
6.1	Introduction	163
6.2	Study area	164
6.3	Data and Methods	168
6.3.1	Developing glacier mass balance proxy series from climate records	168
6.3.2	Tree-ring data	171
6.3.3	Reconstruction Method	173
6.4	Results	176
6.4.1	Instrumental climate records and mass balance proxy series, 1912-2002	176
6.4.2	Tree-ring records	180
6.4.3	Mass balance proxy reconstruction, 1481-2000	181
6.5	Discussion and Conclusions	186
6.6	References	191
Chapter 7:	Summary and conclusions	198
7.1	Introduction	198

7.2	20 th -century climate variations in southern South America	200
7.3	Glacier fluctuations in the Patagonian Andes during the past five centuries	203
7.3.1	Southern study area: Monte Fitz Roy and Lago del Desierto	203
7.3.2	Northern study area: Monte Tronador	204
7.4	North Patagonian glacier mass balance proxy estimates	207
7.5	Recommendations for future related research and final conclusions	208
7.6	References	211
Appendix 1	214
Appendix 2	251
Appendix 3	256
Appendix 4	257
Appendix 5	258
Appendix 6	259
Appendix 7	261
Appendix 8	263
Appendix 9	265
Curriculum Vitae	266

List of Tables

Chapter 2

2.1	Surface air temperature station records used in this study	17
2.2	Selected features identified on the regionally averaged, mean annual temperature records from SSA and the AP	41

Chapter 3

3.1	Stations used to develop regionally-averaged series of annual and seasonal precipitation variations for northwestern Patagonia between 38° and 44°S ...	67
3.2	Streamflow records used in this study	70
3.3	Linear trend analysis for regional temperature, precipitation, climatic index, and streamflow variations in northwestern Patagonia between 1912 and 2002	72
3.4	Glacier advances identified in the Tronador Area (41°10'S) during the 20 th century	77
3.5	Paired correlations between the annual (April-March) streamflow record and annual and seasonal (April-September, October-March) precipitation and temperature series for the northwestern Patagonian region between 1912 and 2002	78

Chapter 4

4.1	Data sources used in this study.....	94
4.2	Evidence for and limitations of dendroglaciological dating	95
4.3	Dendrochronological dating of moraines at Glaciar Torre	100
4.4	As Table 4.3, but for Glaciar Piedras Blancas	105
4.5	As Table 4.3, but for the three glaciers at Lago del Desierto	109
4.6	Approximate changes in glacier area between the LIA, 1984 and 2005 based on the analysis of Landsat TM satellite imagery	114
4.7	Summary of tree-ring based minimum and maximum age estimates for the main moraine systems identified at the five glaciers analyzed in this study	115

Chapter 5

5.1	Summary of the available sources of information for the Argentinean glaciers on Monte Tronador	129
5.2	Evidence for and limitations of dendroglaciological dating	134
5.3	Radiocarbon ages of <i>in situ</i> stumps from Glaciar Río Manso	140
5.4	Comparison between ¹⁴ C determinations from selected <i>in situ</i> stumps at Glaciar Río Manso and their absolute, tree-ring based age range	143
5.5	Chronology of fluctuations for Glaciar Frías over the past ~1600 years	148
5.6	As Table 5.3 but for the <i>in situ</i> and reworked stumps at Glaciar Frías	150

5.7	Tree-ring dating of <i>Fitzroya cupressoides in situ</i> stumps associated with Moraine L at Glaciar Frías	151
------------	--	-----

Chapter 6

6.1	Stations used to develop regionally-averaged climate series for northwestern Patagonia between 38° and 44°S	167
6.2	The eight tree-ring chronologies used to develop the mass balance proxy reconstructions	173
6.3	Calibration/verification statistics and details of the five trial models developed for the reconstruction of the MBPann proxy series	175

Appendix 1

A1.1	Snow courses used to develop a regional averaged series of annual maximum snow water equivalent (MSWE) record for the central Andes, 1951-2005	220
A1.2	Climatic indices used in this study	223
A1.3	Argentinean and Chilean streamflow records used in this study	225
A1.4	The 10 highest and lowest snow accumulation years in the central Andes (1951-2005)	231
A1.5	Multivariate regression trials between 1953-2002 prewhitened versions of the regional snowpack record and seasonally-averaged estimates for the six climatic indices described in Table 2	236
A1.6	Linear trends over the 1951-2004 and 1906-2004 periods for several hydroclimatic parameters	239

List of Figures

Chapter 2

2.1	Location of temperature stations in southern South America, the Antarctic Peninsula and adjacent islands	16
2.2	Correlation fields of four stations with all possible stations in the dataset with at least 20 yrs of overlap	31
2.3	Main modes of spatial variability in SSA and AP mean annual temperature records over the 1969-88 common interval (42 stations)	33
2.4	(A) Map of the loading of each climate station on PC1 (southern Patagonia) over the 1969-88 interval. (B) Variance adjusted, weighted average of mean annual temperature records for stations within the 0.7 contour line in (A). (C) Mann-Whitney Z statistics for running 10-yr samples of the mean annual, regionally averaged record	35
2.5	As Fig. 2.4, but for PC2 (NE SSA)	36
2.6	As Fig. 2.4, but for PC3 (NW Patagonia)	36
2.7	As Fig. 2.4, but for PC4 (central-northern Patagonia)	37
2.8	Main modes of spatial variability in 1970-95 AP mean annual temperature records	37
2.9	As Fig. 2.4B and 2.4C, but for stations located within the 0.8 contour line in AP PC1 for the 1970-95 period	42
2.10	As Fig. 2.9, but for AP PC2	43
2.11	Time series of AP mean annual temperature PC1 and PC2, 1946-2005	43

Chapter 3

3.1	Map of northwestern Patagonia showing the location of the glacier sites, precipitation and streamflow gauge stations used in this study	60
3.2	Selected photographic comparisons showing changes in the glaciers of the north Patagonian Andes. (A) Lanín Norte Glacier, 1896 and 2001. (B) Frías Glacier, Tronador area, 1893 and 2005	63
3.2	(C) Castaño Overo Glacier, Tronador area, 1936 and 2005. (D) Ventisquero Negro Glacier, Tronador area, 1937 and 2005	64
3.2	(E) Esperanza Norte Glacier, ca. 42°S, 1948 and 2001. (F) Torrecillas Glacier, Parque Nacional Los Alerces, 1899, 1937 and 2001	65
3.3	(A) October-March temperature variations in the northwestern Patagonian region between 1912 and 2002. (B) April-September precipitation variations for the study area. (C) Regional climatic index calculated as the difference between Z scores of cold season precipitation totals and warm season mean temperatures. (D) Number of stations contributing to the regionally-averaged temperature and precipitation series in any given year	74
3.4	Comparison of the regional climatic index and glacier advances in the Tronador Area (41°10'S) during the 20 th -century	76

3.5	Comparison between the regional climatic index and the average of seven annual discharge records from east of the Andes	78
-----	---	----

Chapter 4

4.1	(Left) Location of the study area and the North and South Patagonian Icefields. (Center and right) 2005 Landsat TM image showing the Lago del Desierto and Monte Fitz Roy areas	90
4.2	Glacial features and minimum dates of moraines at Glaciar Torre	99
4.3	(A) Glaciar Torre in 1931 and 2005. (B) Frontal positions of Glaciar Torre in 1946, 1952 and 2002	102
4.4	Glacial features and dating of moraines at Glaciar Piedras Blancas	104
4.5	(A) Glaciar Piedras Blancas in 1931 and 2002. (B) Glacier front variations of Glaciar Piedras Blancas between 1952 and 2002	106
4.6	Glacial features of the glaciers studied in the Lago del Desierto area	108
4.7	Age estimates for the main glacier advances in the Fitz Roy and Lago del Desierto areas	117

Chapter 5

5.1	(Left) Location of the Tronador area in the north Patagonian Andes. (Right) April 2003 ASTER image showing the glaciers at Monte Tronador	127
5.2	(Left) Map showing the moraine systems and recent ice margin positions at Glaciar Río Manso. (Upper right) Oblique view of Monte Tronador and Glaciar Río Manso in the late 1990s	137
5.3	Calendar age range for <i>in situ</i> stumps found at the north lateral moraine of Glaciar Río Manso	138
5.4	(A) Location of <i>in situ</i> stumps and living trees at the Río Blanco Site. (B) Stream section of the former lake floor sediments at the Río Blanco Site with a rotten <i>in situ</i> stump embedded in the deposits. (C) 2001 view of Río Blanco channel showing <i>in situ</i> stumps	141
5.5	Calendar age range of 18 <i>in situ</i> stumps at the Río Blanco Site	142
5.6	Panoramic view of Glaciar Frías showing the approximate frontal location of the main advances identified during the past ~1600 yrs	149
5.7	Late Neoglacial age estimates for the main glacier advances at Glaciar Río Manso and Glaciar Frías	152
5.8	An example of the “Bamboo Line” in Area H	155

Chapter 6

6.1	Map of northwestern Patagonia showing (A) the location of the meteorological stations and (B) tree-ring sites used in this study	166
6.2	Temperature, precipitation, proxy mass balance and moraine records for NW Patagonia, 1912-2002. (A) Five-year averages of Z scores of April-	

	September precipitation and October-March temperatures. (B) Regional “glacier mass balance” proxy series calculated as (i) the difference between the Z scores of seasonal precipitation temperature variables (MBP _{sea}), and (ii) using annual precipitation and temperature data (MBP _{ann}). (C) 20 th -century moraine record for four glaciers in the Tronador area	178
6.3	Comparison between the regional “glacier mass balance” proxy series and selected independent data sets	180
6.4	(A) Comparison of the MBP _{ann} series with values predicted from Models 3 and 4. (B) As above using an MBP _{ann} series developed from climate data for 1853-79 from Valdivia, Chile	184
6.5	(A) Reconstruction of the MBP _{ann} series for the NW Patagonian region based on tree-ring data. (B) Cumulative record of the reconstructed MBP _{ann} series. (C) Tree-ring dated moraine records for Glaciar Frías and Glaciar Río Manso in the Tronador area	185

Appendix 1

A1.1	Map of central Chile and central western Argentina, showing the location of snow courses and gauge stations used in this study	217
A1.2	(A-F) Plot of the annual Maximum Snow Water Equivalent (MSWE) records for the six snow courses used in this study. (G) Regional snowpack series (1951-2005) developed from these series expressed as percentages of their 1966-2004 mean	227
A1.3	(A) Correlations over the 1961-1990 period between the prewhitened MSWE regional series and seasonal and annual precipitation totals. (B) Correlations between the prewhitened MSWE regional series and gridded mean seasonal and annual temperature data for central Chile and central western Argentina	228
A1.4	Five-month moving averages of monthly SST anomalies for the Niño 3.4 region (above) and the regional snowpack series from the central Andes (below)	230
A1.5	(A) June-September mean 500-hPa geopotential height anomalies for the 10 snowiest years in the central Andes. (B) As (A), but for the 10 driest years	232
A1.6	The changing seasonal strength in the relationships between the regional MSWE series and seasonally averaged NCEP-NCAR reanalysis 2.5° x 2.5° SST (A-C) and SLP (D-F) gridded data over the 1952-2003 interval	234
A1.7	Correlations between the prewhitened regional snowfall MSWE record and streamflow over the 1955-2002 period	238
A1.8	Relationship between the 1951-2005 MSWE series and the 1906-2004 regionally-averaged November-February discharge from central Chile and central western Argentina	238

List of Appendices

Appendix 1	Snowpack variations in the central Andes of Argentina and Chile, 1951-2005: Large-scale atmospheric influences and implications for water resources in the region	214
A1.1	Introduction	214
A1.2	Study area	215
A1.3	Data and Methods	219
A1.4	Results	225
A1.4.1	Regional snowpack record, 1951-2005	225
A1.4.2	Relationship with local climate conditions	226
A1.4.3	Influence of ENSO events and relationship with 500-hPa geopotential height anomalies	229
A1.4.4	Relationships with gridded SST, SLP and climate indices	233
A1.4.5	Relationships between regional streamflow records and winter snowpack	236
A1.5	Discussion and Conclusions	240
A1.6	References	245
 Appendix 2	 Techniques used to identify the main modes of temporal variability in regionally averaged temperature records	 251
A4.1	Statistical significance of linear trends	251
A4.2	Identification of regime shifts	252
A4.3	Identification of intra- to multi-decadal (IMD) patterns	253
Appendix 3	As Fig. 2.3, but based on the 32 stations for the 1931-60 interval	256
Appendix 4	As Fig. 2.3, but for the 26 stations over the 1961-2001 interval	257
Appendix 5	Dendrochronological data for selected trees sampled at Glaciar Río Manso	258
Appendix 6	Selected tree-ring chronologies used in Chapter 6	259
Appendix 7	Permission to reprint Chapter 3	261
Appendix 8	Permission to reprint Chapter 4	263
Appendix 9	Permission to reprint Appendix 1	265

Chapter 1: Introduction

1.1. Introduction

In contrast to the Northern Hemisphere, South America is the only Southern Hemisphere land mass that extends through mid to high latitudes and offers opportunities for high resolution paleoclimate records to evaluate past climate variability. This makes the proper characterization of past and present climatic variations in Patagonia¹ of crucial importance for the better understanding of the climate system at local, regional and larger spatial scales. Understanding the relative influence and spatial extent of the main large-scale atmospheric forcing mechanisms affecting climate variability in this region is also a critical component in the examination of the differences in climate history and climate forcing between the Northern and Southern Hemispheres. The diverse forest regions, numerous glaciers and lakes along the Patagonian Andes provide an excellent opportunity to incorporate records from several complementary environmental indicators (e.g. tree rings, laminated lake sediments and glacier records) to reconstruct past climate fluctuations. These data, in combination with studies of instrumental records, allow the evaluation of the relative magnitude of recent fluctuations in a longer-term perspective (Bradley 1999, 2000). However, despite recent efforts (e.g. Villalba et al. 2003) and the promising combination of geographic location and abundance of environmental indicators, past and present climate variability in this region remains poorly documented and understood. This thesis seeks to improve our understanding of climate and glacier variability in Patagonia through the detailed analysis of available instrumental climate data, dendrochronological (tree-ring) series and selected glacier histories.

The first critical step in examining present climate variability in a given region is to develop an instrumental climate database from records that are as up to date, reliable and homogeneous as possible². Such data are also an essential prerequisite for the development of reconstructions of past climates. A major limitation to the accurate

¹ In this thesis, Patagonia is broadly defined as South America south of 37°S. At these latitudes this region is the only continental land mass outside Antarctica.

² A homogeneous climate series is defined as one where variations are free of non-climatic discontinuities and caused only by variations in weather and climate (Conrad and Pollack 1962; Peterson et al. 1998).

depiction of 20th-century climate variability in Patagonia is the poor quality of instrumental climate data and the inadequate spatial distribution of meteorological stations, which make this region “among the least known (land) areas of the world” (Rosenblüth et al. 1997:67). Despite the fact that several agencies have and are collecting hydro-meteorological data, many of these data are not readily available or are of unknown quality. Except for a few global climatological databases (such as the Global Historical Climatology Network, Peterson and Vose 1997), the absence of a comprehensive, regional database of updated, reliable and homogeneous hydro-climatic records has probably contributed to the limited number of detailed studies dealing with climatic variations in Patagonia during the 20th century. Only a few studies have applied homogeneity tests and data correction to Patagonian climate records (e.g. Rosenblüth et al. 1997). In most cases, given the scarcity of long and complete records for comparison, the homogeneity tests were performed using a very small number of stations and it is possible that important non-climatic inhomogeneities may remain undetected. Therefore, this thesis begins with an evaluation of the temperature records for the region.

Most paleoclimatic inferences in southern South America have been based on palynological, lacustrine, dendrochronological or glaciological evidence. Pollen and lake sediment studies have been mainly focused on the late Quaternary and the Holocene periods (e.g. Stine and Stine 1990; Heusser et al. 2000; Markgraf et al. 2003; Whitlock et al. 2006), but the coarse resolution and climatic sensitivity of the records available are usually inadequate for the detailed study of decade- to century-scale climate variations in this region³. In contrast, tree-ring records from the Patagonian Andes are particularly suitable for high resolution studies because they provide continuous, annually resolved and precisely dated series that usually extend for several centuries (and in some cases, for millennia). Unlike other proxies where the response to climate is difficult to evaluate using climate station data (Jones et al. 1998), tree-ring series can be statistically calibrated and verified against instrumental climate records prior to the development of reconstruction models. These factors make dendrochronological records the best source

³ Recent paleolimnological studies (e.g. Mayr et al. 2005; Haberzettl 2006) indicate however that lacustrine records from isolated basins in the southeastern Patagonian steppe have the potential to provide decade- to century scale information of paleoenvironmental change in this region.

of paleoclimatic information for the last millennium in this region, and several studies have used tree-ring series to reconstruct annual and seasonal variations in temperature, precipitation and other atmospheric variables at local and larger spatial scales (Boninsegna 1992; Villalba 2000). However, the majority of these paleoclimatic studies are only based on tree-ring data and few studies have exploited the potential combination of independent proxy climate reconstructions to provide a more comprehensive picture of climate changes (e.g. Luckman and Villalba 2001).

Glaciers and their deposits have been widely used as indirect indicators of past and present climatic variability (Porter 1981; Grove 2004; Haeberli 2005). The precise dating of glacial deposits provides records that, although not continuous, can reach a reasonable (i.e. decadal) resolution, particularly during the past centuries and for small valley glaciers (Luckman 1993, 2000). Thus, detailed glacier histories from selected sites could be used to validate the low frequency climatic variability inferred from tree rings or other high resolution proxy climate data (e.g. Luckman 1996; Watson and Luckman 2004). In southern South America glacier studies have generally examined variations from a long-term, late Glacial-Holocene perspective (e.g. Mercer 1976, 1982; Röthlisberger 1986; Glasser et al. 2004), or they have focused on 20th-century glacier changes (Aniya et al. 1996, 1997; Rivera et al. 2000, 2007; Rignot et al. 2003). Few studies have focused on glacial fluctuations during the past few centuries (e.g. Villalba et al. 1990; Harrison and Winchester 1998) for which the glacial evidence is relatively more abundant, well preserved and easily dated. This interval also encompasses the period for which high resolution proxy climate information derived from tree rings are generally available for comparison with the glacier records. Furthermore, since most of these glaciological studies were focused on a few large calving glaciers with complex responses to climate fluctuations (Warren 1994; Warren et al. 1995), the glacier history and detailed glacier/climate relationships in the region are not well established (Clapperton and Sugden 1988, Warren and Sugden 1993). According to Luckman and Villalba (2001:136), “there remains a significant need for detailed, well-dated records of glacier fluctuations, coupled with a better understanding of the factors that control glacier mass balance” during this time frame. In this thesis I address these issues through a

combination of dendrochronological, geomorphic and paleoclimatic approaches in a mix of regional and detailed local studies.

1.2. Objectives

The main purposes of this study are:

1. To utilize updated and homogenized surface temperature records to characterize the major patterns of spatio-temporal variability during the 20th century in the Patagonian region.
2. To develop detailed glacial histories for the past ~1000 years at study areas in the north and south Patagonian Andes of Argentina that each contain several small glaciers.
3. To develop a proxy measure of glacier mass balance from instrumental and tree-ring data and compare the regional glacial history from the northern study area with this mass balance proxy.
4. To evaluate the relative magnitude of late 20th century climate and glacier changes in a longer term (i.e. multi-century) perspective.

1.3. Context of this research

This thesis originated from a dendroglaciological research project initiated in 1998 by Dr. Ricardo Villalba from IANIGLA⁴ that was intended to document the past 1000 years of glacier, climate and tree-ring fluctuations across a latitudinal transect in the Patagonian Andes of Argentina. Eight glaciated areas were originally selected for study based on several criteria such as the presence of a dense forest cover in or adjacent to the glacier forefields, the existence of historical documents and aerial photographs showing past glacier positions, and accessibility. This thesis examines two of these glaciated areas at contrasting sites in the north and south Patagonian Andes in an attempt to evaluate the relative magnitude and synchronicity of climate fluctuations and the major glacial events within and between the two areas. This work has involved the assembly of a network of tree-ring records across the region and the compilation of a regional hydro-climate database and historical records by many individuals in addition to the author which are

⁴ Instituto Argentino de Nivología, Glaciología y Ciencias Ambientales, Mendoza, Argentina.

acknowledged in the papers that arise from this work and in the introductory preface to each chapter. There remain strong linkages with national and international ongoing projects at IANIGLA (Villalba et al. 2006, Grosjean and Villalba 2006) and with the IAI collaborative networks CRN03 and CRN2047 (Luckman 2005, 2007). There are also strong linkages (though with somewhat different emphases) with the parallel study of climate history in this timeframe from Chilean Patagonia (Aravena 2007).

1.4. Thesis outline

The thesis is written in manuscript format. Each chapter was written as a stand-alone manuscript and is intended for publication. As a result, the introductory sections and methodological descriptions have been kept purposely short but there is some repetition of concepts, especially between Chapters 4 and 5 that deal with the development of glacier histories for sites in the south and north Patagonian Andes.

The sequence of chapters follows a logical structure based on the main objectives of this thesis. However, some of the aims and methodologies have been modified and/or improved as the research progressed over the past few years. Brief introductory comments are therefore provided in each chapter to address these issues and discuss its context within the thesis.

Chapter 2 presents the analysis of an updated, greatly expanded surface temperature station dataset from southern South America and the northern Antarctic Peninsula and adjacent islands. Homogenized mean annual temperature records from these regions are developed and comprehensively analyzed to determine the existence of common spatial patterns of variability. Regionally-averaged time series are subsequently analyzed to assess the relative magnitude of the main low frequency patterns in each subregion and place the last few decades of the records into a longer, 20th-century context. In a related study, an original record of snowpack variations was developed from the central Andes of Argentina and Chile and is presented in Appendix 1. This study illustrates the methods that could be used to develop the data and evaluate the influences of large-scale phenomena on the regionally-averaged surface temperature series developed in Chapter

2⁵. The results from Appendix 1 also provide a regional context and important information on recent hydro-climatic variability in a region close to the site studies in the north Patagonian Andes.

Chapter 3 documents the occurrence of significant glacier and hydro-climatic changes in northwestern Patagonia during the past century. Repeat photography of some of the earliest images of glaciers in southern South America is complemented by the analysis of regionally-averaged winter precipitation and summer temperature records from which a “glacier mass balance proxy” is developed. This series is subsequently compared to reported 20th-century intervals of glacier advance and mean annual streamflow records east of the Andes.

Chapter 4 describes and analyzes the dendro-geomorphological evidence for Little Ice Age (LIA) and post-LIA activity⁶ for several small neighboring glaciers in the Monte Fitz Roy and Lago del Desierto areas of the south Patagonian Andes. Numerous glacier advances are identified from field surveys and the examination of aerial photographs. These events are dated mainly using living trees, but *in situ*, subfossil material is also used to provide key dating controls at some specific sites. Estimates based on Landsat TM imagery provide an indication of glacier area loss since the LIA maximum at these glaciers.

Chapter 5 presents revised chronologies of LIA and post-LIA fluctuations for the Río Manso and Frías Glaciers in the Monte Tronador area of the north Patagonian Andes. These chronologies are based on the integration of results from previous studies and an extensive collection and analysis of living and subfossil tree-ring material. The variety of evidence available at these sites highlights the great potential for dendroglaciological investigations of this area and provides the most detailed chronology of LIA glacier

⁵ The analysis of instrumental climate data in relation to large-scale atmospheric indices and variables was one of the original objectives of this thesis but was subsequently excluded because of time constraints. Seasonal analyses have also been performed on these data but were excluded for similar reasons.

⁶ The term “Little Ice Age” generally refers to the latest glacier expansion episode of the late Holocene (Grove 2004; Matthews and Briffa 2005). In Patagonia, the limited evidence available indicates that the main LIA glacier advances occurred between the 17th and 19th centuries (Luckman and Villalba 2001; Glasser et al. 2004).

fluctuations for the north Patagonian Andes. However, this evidence also highlights some of the main limitations associated with the dating of glacier deposits from dendro-geomorphological determinations, and both chapters 4 and 5 discuss this issue critically. Some evidence for pre-LIA glacier activity in the study areas is also discussed as it provides important additional information for placing the most recent glacier events into a longer, late Holocene perspective.

Chapter 6 discusses the development of the first tree-ring based reconstruction of a glacier mass balance proxy record for the Patagonian region. The instrumental record used is different from that used in Chapter 3 (individual temperature station data instead of gridded series) to compute mean annual estimates of glacier mass balance conditions. A multi-species network of tree-ring width chronologies from sites on both sides of the north Patagonian Andes is used to develop a ~500-yr long proxy mass balance record. The low frequency (i.e. multi-decadal) patterns in this series are compared to the dates of moraine formation identified in Chapter 5, and the potential usefulness and inherent limitations of this approach are discussed.

Chapter 7 summarizes the findings from this research and discusses their significance in relation to the main objectives of this thesis. Main conclusions are provided together with recommendations for future related research in this region.

1.5. References

- Aniya, M., Sato, H., Naruse, R., Skvarca, P and Casassa, G. 1996. The use of satellite and airborne imagery to inventory outlet glaciers of the Southern Patagonian Icefield, South America. *Photogrammetric Engineering and Remote Sensing* 62, 1361–69.
- Aniya, M., Sato, H., Naruse, R., Skvarca, P., and Casassa, G., 1997. Recent glacier variations in the Southern Patagonia Icefield, South America. *Arctic and Alpine Research* 29, 1-12.
- Aravena, J.C. 2007. Reconstructing climate variability using tree rings and glacier fluctuations in the southern Chilean Andes. Ph.D. Thesis, Department of Geography, University of Western Ontario, 236 pp.

- Boninsegna, J.A. 1992. South American dendroclimatological records. In: Bradley, R.S., and Jones, P.D. (eds.) *Climate since A.D. 1500*. Routledge, London, pp. 446-462.
- Bradley, R.S. 1999. *Paleoclimatology. Reconstructing Climates of the Quaternary*. Academic Press, 2nd ed. 610 pp.
- Bradley, R.S. 2000. Past global changes and their significance for the future. *Quaternary Science Reviews* 19, 391-402.
- Clapperton, C.M. and Sugden, D.E. 1988. Holocene glacier fluctuations in South America and Antarctica. *Quaternary Science Reviews* 7, 185-198.
- Conrad, V. and Pollack, C. 1962. *Methods in Climatology*. Harvard University Press, Cambridge, MA, 459 pp.
- Glasser, N.F., Harrison, S., Winchester, V. and Aniya, M. 2004. Late Pleistocene and Holocene palaeoclimate and glacier fluctuations in Patagonia. *Global and Planetary Change* 43: 79-101.
- Grosjean, M. and Villalba, R. 2006. Regional climate variations in South America over the late Holocene. *PAGES News, Workshop reports* 14, 26.
- Grove, J.M. 2004. *Little Ice Ages: Ancient and Modern* (2 vols), Routledge, London, 718 pp.
- Haberzettl, T. 2006. Late Quaternary hydrological variability in southeastern Patagonia – 45,000 years of terrestrial evidence from Laguna Potrok Aike. Ph.D. Dissertation, Universität Bremen. 142 pp.
- Haeberli, W. 2005. Mountain glaciers in global climate-related observing systems. In: Huber, U.M., Bugmann, H.K.M. and Reasoner, M.A. (eds.) *Global change and mountain regions – An overview of current knowledge*. Springer, pp. 169-175.
- Harrison, S. and Winchester, V. 1998. Historical fluctuations of the Gualas and Reicher Glaciers, North Patagonian Icefield, Chile. *The Holocene* 8, 481-485.
- Heusser, C.J., Heusser, L.E., Lowell, T.V., Moreira, M.A. and Moreira, M.S. 2000. Deglacial palaeoclimate at Puerto del Hambre, subantarctic Patagonia, Chile. *Journal of Quaternary Science* 15, 101-114.
- Jones, P.D., Briffa, K.R., Barnett, T.P. and Tett, S.F.B. 1998. High-resolution palaeoclimatic records for the last millennium: interpretation, integration and comparison with General Circulation Model control-run temperatures. *The Holocene* 8, 455-471.

- Luckman, B.H. 1993. Glacier fluctuation and tree-ring records for the last millennium in the Canadian Rockies. *Quaternary Science Review* 16, 441–450.
- Luckman, B.H. 1996. Reconciling the glacial and dendrochronological records of the last millennium in the Canadian Rockies. In: Jones, P.D., Bradley, R.S. and Jouzel, J. (eds.), *Climatic Variations and Forcing Mechanisms of the Last 2000 Years*. NATO ASI Series I-41, Springer-Verlag, Berlin, pp. 85–108.
- Luckman, B.H. 2000. The Little Ice Age in the Canadian Rockies. *Geomorphology* 32, 357-384.
- Luckman B.H. (ed) 2005. Assessment of Present, Past and Future Climate Variability in the Americas from Treeline Environments: Final report of IAI CRN03. Submitted to the Inter American Institute for Global Change Research, São José dos Campos, Brazil, August 2005, iii + 177 pp.
- Luckman B.H. (ed) 2007. Documenting, understanding and projecting changes in the hydrological cycle in the American Cordillera: IAI Collaborative Research Network 2047. Report of activities carried out between April 2006 and July 2007. Submitted to the Inter American Institute for Global Change Research, São José dos Campos, Brazil, 12 July 2007, iii + 97 pp.
- Luckman, B.H., and Villalba, R. 2001. Assessing the synchronicity of glacier fluctuations in the western cordillera of the Americas during the last millennium. In: Markgraf, V. (ed.), *Interhemispheric Climate Linkages*, Academic Press, London, pp. 119–140.
- Markgraf, V., Bradbury, J.P., Schwalb, A., Burns, S.J., Stern, C., Ariztegui, D., Gilli, A., Anselmetti, F.S., Stine, S. and Maidana, N. 2003. Holocene palaeoclimates of southern Patagonia: limnological and environmental history of Lago Cardiel, Argentina: *The Holocene* 13, 581-591.
- Matthews, J.A. and Briffa, K.R. 2005: The ‘Little Ice Age’: reevaluation of an evolving concept. *Geografiska Annaler* 87A, 17–36.
- Mayr, C., Fey, M. Habertzettl, T., Janssen, S., Lücke, A., Maidana, N.I., Ohlendorf, C., Schäbitz, F., Schleser, G.H., Struck, U., Wille, M. and Zolitschka, B. 2005. Palaeoenvironmental changes in southern Patagonia during the last millennium recorded in lake sediments from Laguna Azul (Argentina). *Palaeogeography, Palaeoclimatology, Palaeoecology* 228, 203-227.
- Mercer, J.H. 1976. Glacial history of the southernmost South America. *Quaternary Research* 6, 125-166.
- Mercer, J.H. 1982. Holocene glacier variations in southern South America. *Striae* 18, 35-40.

- Oerlemans, J. 1994. Quantifying global warming from the retreat of glaciers. *Science* 264, 243-245.
- Oerlemans, J. and Fortuin, J.P.F. 1992. Sensitivity of glaciers and small ice caps to greenhouse warming. *Science* 258, 115-117.
- Peterson, T.C. and Vose, R.S. 1997. An overview of the Global Historical Climatology Network temperature data base. *Bulletin of the American Meteorological Society* 78, 2837-2849.
- Peterson, T.C. and 20 others. 1998. Homogeneity adjustment of in situ atmospheric climate data: a review. *International Journal of Climatology* 18, 1493-1517.
- Porter, S.C. 1981. Glaciological evidence of Holocene climatic change. In: Wigley, T.M.L., Ingram, M.J. and Farmer, G. (eds.), *Climate and History*. Cambridge University Press, pp. 83-110.
- Rignot, E., Rivera A. and Casassa, G. 2003. Contribution of the Patagonia icefields of South America to global sea level rise. *Science* 302, 434-437.
- Rivera, A., Benham, T. Casassa, G., Bamber, J. and Dowdeswell, J. 2007. Ice elevation and areal changes of glaciers from the Northern Patagonia icefield, Chile. *Global and Planetary Change*, doi:10.1016/j.gloplacha.2006.11.037.
- Rivera, A., Casassa, G., Acuña, C. and Lange, H. 2000. Variaciones recientes de glaciares en Chile. *Revista de Investigaciones Geográficas* 34, 25-52.
- Rosenblüth, B., Fuenzalida, H. and Aceituno, P. 1997. Recent temperature variations in southern South America. *International Journal of Climatology* 17, 67-85.
- Röthlisberger, F. 1986. 1000 Jahre Gletschergerichte der Erde. Salzburg, Verlag Sauerlander.
- Stine, S. and Stine, M. 1990. A record from Lake Cardiel of climate in southern South America. *Nature* 345, 705-708.
- Villalba, R. 2000: Dendroclimatology: a Southern Hemisphere Perspective. In: Smolka P. and Volkheimer, W. (eds.), *Paleo- and Neoclimates of the Southern Hemisphere: the state of the arts*. Springer, pp. 105-143.
- Villalba, R. Masiokas, M.H., Lascano, M., Boninsegna, J.A., Garibotti, I., Flamenco, E., Delgado, S., Morales, M., Gil Montero, R., Ferrero, M.E., Srur, A.M., Casteller, A., Paolini, L. Present and past climatic variability across the Argentinean Andes: Current studies in the context of CRNII-47 (Changes in the Hydrological Cycle in the American Cordillera). First Meeting IAI-CRNII 047: Documenting,

Understanding and Projecting changes in the hydrological cycle in the American Cordillera. Mendoza, April 2-3, 2006.

- Villalba, R., Lara, A., Boninsegna, J.A., Masiokas, M., Delgado, S., Aravena, J.C., Roig, F.A., Schmelter, A., Wolodarsky, A., and Ripalta, A. 2003. Large-scale temperature changes across the southern Andes: 20th-century variations in the context of the past 400 years. *Climatic Change* 59, 177-232.
- Villalba, R., Leiva, J.C., Rubulis, S., Suarez, J.A., 1990. Climate, tree rings and glacier fluctuations in the Rio Frias Valley, Rio Negro, Argentina. *Arctic and Alpine Research* 22, 215-232.
- Warren, C.R. 1994. Freshwater calving and anomalous glacier oscillations: recent behaviour of Moreno and Ameghino glaciers, Patagonia. *The Holocene* 4, 422-429.
- Warren, C.R. and Sugden, D.E. 1993: The Patagonian Icefields: a glaciological review. *Arctic and Alpine Research* 25, 316-331.
- Warren, C.R., Sugden, D.E. and Clapperton, C.M. 1995. Asynchronous response of Patagonian glaciers to historic climate change. *Quaternary of South America and the Antarctic Peninsula* 9, 89-108.
- Watson, E. and Luckman, B.H. 2004. Tree-ring estimates of mass balance at Peyto Glacier for the last three centuries. *Quaternary Research* 62, 9-18.
- Whitlock, C., Bianchi, M.M., Bartlein, P.J., Markgraf, V., Walsh, M., Marlon, J.M. and McCoy, N. 2006. Postglacial vegetation, climate, and fire history along the east side of the Andes (lat 41-42.5 S), Argentina. *Quaternary Research* 66, 187-201.

The following chapter discusses the development and analysis of an updated collection of surface temperature records from southern South America and the Antarctic Peninsula and surrounding islands. The main modes of spatio-temporal variability in these regions are identified using homogenized records. This analysis provides an important large-scale perspective to better understanding of the climate and glacier changes observed at the two study areas discussed in subsequent chapters.

This chapter will be submitted for publication in the near future with the following list of co-authors: Masiokas, M.H.^{1,2}; Luckman, B.H.¹; Villalba, R.²; Stepanek, P.³; Mauget, S.⁴ and Branham, R.²

¹ Department of Geography, University of Western Ontario, London, Ontario, Canada.

² Instituto Argentino de Nivología, Glaciología y Ciencias Ambientales (IANIGLA-CONICET), Mendoza, Argentina.

³ Czech Hydrometeorological Institute (CHMI), Regional Office Brno, Czech Republic.

⁴ U.S. Department of Agriculture-Agricultural Research Service, Lubbock, Texas.

Chapter 2: Instrumental surface temperature variations in southern South America and the Antarctic Peninsula: Data homogenization and identification of main modes of spatio-temporal variability

2.1. Introduction

Southern South America (SSA) is the only land mass that extends through mid to high latitudes in the Southern Hemisphere and represents one of the few opportunities for studying instrumental climate variations since the beginning of the 20th century in this part of the world¹. This makes the proper characterization of climatic variability in SSA and adjacent areas of crucial importance for the better understanding of the climate system at local, regional and larger spatial scales. This knowledge is also critical in the assessment of the relative influence and spatial extent of the main large-scale atmospheric forcing mechanisms affecting climate variations in this region and may provide useful information in the examination of the differences in climate history and climate forcing between the Northern and Southern Hemispheres. Given the abundance and variety of proxy climate indicators in SSA (e.g. tree rings, laminated lake sediments), the correct identification of the main modes of variability in instrumental climate data is also a prerequisite for the development of reliable high-resolution paleoclimatic reconstructions that allow the evaluation of 20th-century conditions over a long term perspective.

Climate stations are sparsely distributed in SSA and many meteorological records are of poor quality and have an uneven temporal coverage. Probably because of these limitations, very few studies have focused on the spatio-temporal behavior of instrumental surface air temperatures from SSA. The scarcity of long, reliable climate series and complete station history reports (metadata) has also hampered the evaluation of the relative homogeneity² of these records, and few studies have addressed this issue prior to assessing long-term temperature changes in this region (e.g. Rosenblüth et al. 1995, 1997). In most cases, such changes have been assessed statistically through linear

¹ South of 38°S, SSA is the only continental land mass outside Antarctica. In this study SSA is defined as South America south of 36°S.

² A relatively homogeneous climate record is usually referred to as a time series in which variations are only caused by variations in weather and climate (Conrad and Pollack 1962; Peterson et al. 1998).

trend analyses of individual station data (e.g. Rosenblüth et al. 1997) or regionally representative time series (e.g. Villalba et al. 2003). South of 38°S Villalba et al. (2003) identified three main temperature patterns with distinct long term trends over the 1931-90 period: cooling over NW Patagonia west of the Andes, no significant trend over NE Patagonia, and a significant warming trend over the southernmost tip of the continent. Although based on different time periods and sets of stations, roughly similar results are reported by other studies for stations located in Villalba's subregions. Hoffmann (1990) and Hoffmann et al. (1997) analyzed only Argentinean stations, Aceituno et al. (1993) focused only on Chile, and Rosenblüth et al. (1995, 1997) used selected data from both countries. The few existing spatial classifications of Argentinean-Chilean temperature variations that included SSA (Pittock 1980; Coronato and Bisigato 1998) have found somewhat different patterns to those in Villalba et al. (2003) but used different areas of study, time periods and sets of stations.

Comparatively more information is available for the limited records of the Antarctic Peninsula and adjacent islands (hereafter AP), and several studies (mostly based on the analysis of individual station records) report a strong, highly significant surface warming trend (Limbert 1974; King 1994; Skvarca et al. 1998; King and Harangozo 1998; King et al. 2003; Vaughan et al. 2003). For example, mean annual surface temperatures at Faraday (65°24'S, 64°24'W; now Vernadsky) in the western portion of the peninsula have increased by about 2.5°C since the 1950s, making this area one of the fastest warming regions on Earth (Vaughan et al. 2001; Turner et al. 2005). To our knowledge, the relative homogeneity of available surface temperature records in the AP has not been specifically examined. Recent studies have, however, partially acknowledged this issue by carefully selecting only high-quality station records that are assumed to be largely free of non-climatic inhomogeneities (i.e. the SCAR READER dataset, Turner et al. 2004, 2005). The reduction in sea ice extent on the western side of the AP in recent decades (Jacobs and Comiso 1997), the collapse of large sections of the Larsen and other AP ice shelves (Doake and Vaughan 1991; Vaughan and Doake 1996; Rott et al. 1996; Skvarca and De Angelis 2003; Scambos et al. 2003), and the generalized retreat of glaciers and icefields in both SSA and the AP (Aniya et al. 1997; Rignot et al. 2003; Rau et al. 2004;

Cook et al. 2005), have all been linked to the observed warmer conditions in recent decades on both sides of the Drake Passage. However, despite their proximity (Fig. 2.1), updated, homogenized surface temperature records from SSA and the AP have not yet been comprehensively analyzed to determine the existence of common patterns of spatio-temporal variability. Only a few studies focused on surface temperature variations in Antarctica or the AP have incorporated any station data from SSA (e.g. Rogers 1983; King 1994; Jacka et al. 2004). Likewise, only Hoffmann (1990) and Hoffmann et al. (1997) have analyzed and compared the temperature variations between stations in SSA and the sub-Antarctic islands adjacent to the peninsula. Moreover, as linear trend analysis has usually been the main tool for the statistical assessment of the long-term behavior of instrumental temperature records in SSA and the AP, very little is known regarding the relative magnitude and statistical significance of the main intra- to multi-decadal (IMD) modes of temperature variability in these regions.

In this paper we utilize a recently updated compilation of climate data that includes the high-quality SCAR READER records from the AP and a greatly expanded dataset of mean monthly surface temperature records from SSA to a) test the relative homogeneity of the available station records; b) develop relatively homogeneous mean seasonal and annual station records for SSA and the AP; c) identify the dominant modes of spatial variability in these surface temperature data; and d) evaluate the magnitude and statistical significance of linear and intra- to multi-decadal (IMD) variations in each of the main regional patterns of common variability. The techniques applied in this study are considered the most appropriate to handle the heterogeneous spatio-temporal coverage of data available and enhance the regional common climatic signal while minimizing the impact of undetected non-climatic inhomogeneities in the original series. In this context, instead of analyzing individual mean monthly station records, we specifically targeted and analyzed regionally averaged temperature series derived from carefully selected, updated and homogenized mean seasonal and annual station records. This analysis will focus only on mean annual records. Although by no means definitive, these results will hopefully provide useful information for the study of surface climate variability at a

regional scale and facilitate the evaluation of atmosphere-ocean-cryosphere interrelationships in this part of the world.

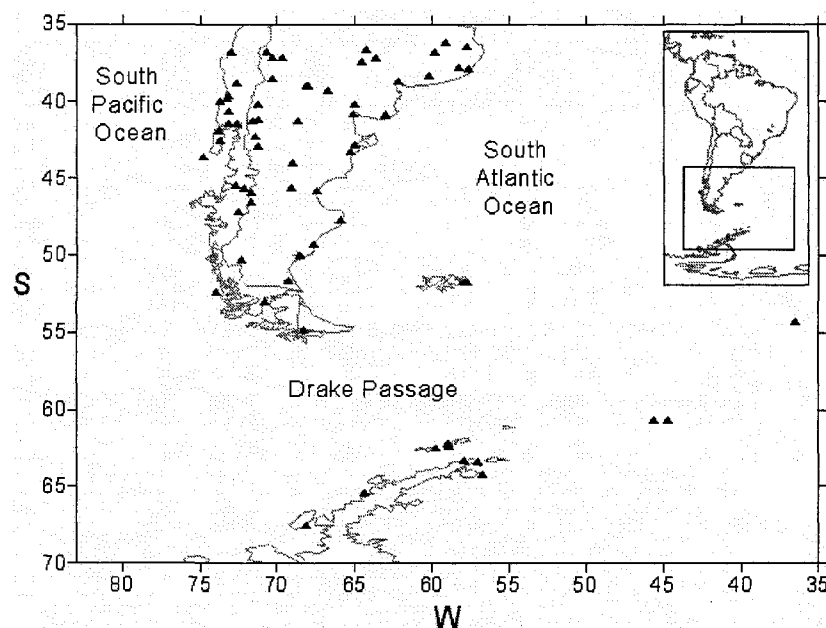


Fig. 2.1. Location of temperature stations with ≥ 20 yrs of data and $\leq 15\%$ missing values in southern South America, the Antarctic Peninsula and adjacent islands (see Table 2.1 for details). The width of the Drake Passage between the tip of South America and the Antarctic Peninsula is ca. 1000 km.

2.2. Data and Methods

This study uses mean monthly surface air temperature records from stations south of 36°S in South America and north of 70°S in the Antarctic Peninsula and surrounding areas (Fig. 2.1). Most of these records were assembled from global, national and regional databases, but a few local sources provided additional material (Table 2.1). This extensive, updated compilation complements the existing dataset of hydro-climatological variables available at Instituto Argentino de Nivología, Glaciología y Ciencias Ambientales (IANIGLA-CONICET, Mendoza) for the study of recent climate and environmental changes in southern South America and neighboring regions.

Table 2.1. Surface air temperature station records used in this study. Data sources: 1: Global Historical Climatology Network; 2: World Weather Records; 3: Servicio Meteorológico Nacional, Argentina; 4: Dirección Meteorológica de Chile; 5: British Antarctic Survey; 6: Subsecretaría de Recursos Hídricos, Argentina; 7: Jones and Reid (2001); 8: Estancia Collunco (pers. Comm.), 9: CORFO, Chile; 10: S. Rubulis (pers. comm.); 11: Universidad Austral de Chile.

Station (source)	Lat (S), Long (W), Elev (m)	Period (% miss.)	Station (source)	Lat (S), Long (W), Elev (m)	Period (% miss.)
Las Flores (1)	36.1, 59.1, 38	1931-1960 (3.3)	Castro (4)	42.5, 73.7, 5	1958-1988 (3.3)
Dolores (1,2)	36.4, 57.7, 9	1931-2005 (8.8)	Puerto Madryn (1)	42.8, 65.0, 7	1901-1933 (0.5)
Santa Rosa (1,2)	36.6, 64.3, 191	1941-2005 (3.7)	Esquel (1,2,3)	42.9, 71.2, 785	1901-2005 (0.4)
Azul (1,2)	36.8, 59.8, 132	1931-1994 (4.0)	Trelew (1,2)	43.2, 65.3, 43	1901-2005 (2.9)
Varvarco (6)	36.8, 70.7, 1246	1977-2004 (1.2)	Isla Huafo (1,2)	43.6, 74.8, 140	1909-1968 (8.4)
Concepción (1,2,4)	36.8, 73.0, 12	1942-1992 (0.0)	Paso de Indios (1,3)	44.0, 69.0, 460	1969-2005 (13.1)
Macachín (1)	37.1, 63.7, 142	1931-1960 (0.0)	Puerto Aysen (1,2,4)	45.4, 72.7, 11	1931-1992 (5.1)
Buta Ranquil (6)	37.1, 69.7, 850	1966-2004 (1.1)	Sarmiento A (1)	45.6, 69.1, 268	1903-1963 (1.4)
Chos Malal A (1,3)	37.1, 70.3, 864	1916-1961 (1.8)	Sarmiento B (6)		1985-2004 (6.0)
Chos Malal B (3)		1975-2005 (6.1)	Coyhaique (2,4)	45.6, 72.1, 310	1961-2001 (0.8)
Gral. Acha (1)	37.4, 64.6, 230	1931-1960 (3.3)	C. Rivadavia (1,2,3)	45.8, 67.5, 46	1931-2005 (0.3)
Balcarce (1)	37.8, 58.3, 100	1931-1960 (0.8)	Balmaceda (1,2,4)	45.9, 71.7, 520	1961-2005 (0.6)
Mar del Plata (1,2)	37.9, 57.6, 21	1931-2005 (4.0)	Chile Chico (4)	46.5, 71.7, 327	1965-2001 (5.4)
Tres Arroyos A (1,2)	38.3, 60.2, 115	1931-1960 (0.0)	Cochrane (4)	47.2, 72.5, 182	1969-2001 (2.6)
Tres Arroyos B (1)		1971-2005 (8.6)	Puerto Deseado (1,2)	47.7, 65.9, 80	1961-2005 (6.9)
Las Lajas (3)	38.5, 70.3, 770	1916-1973 (13.2)	San Julian (1,2,3)	49.3, 67.7, 62	1970-2005 (0.5)
Bahía Blanca (1,2)	38.7, 62.2, 72	1896-2005 (4.4)	Santa Cruz (1)	50.0, 68.6, 111	1901-1962 (4.2)
Temuco (1,2,4)	38.8, 72.6, 114	1930-2005 (2.6)	Lg. Argentino (1,2,3)	50.3, 72.3, 220	1961-2005 (1.5)
Cipolletti (1,2)	39.0, 68.0, 265	1931-1990 (4.3)	Rio Gallegos (1,2,3)	51.6, 69.3, 19	1931-2005 (6.7)

Table 2.1. Cont'd.

Neuquén (1,2,3)	39.0, 68.1, 271	1957-2005 (0.0)	Cape Pembroke (1)	51.7, 57.7, 16	1895-1947 (3.6)
Choele Choel (1)	39.2, 66.8, 100	1931-1960 (4.2)	Stanley (1)	51.7, 57.9, 51	1922-1982 (1.0)
Valdivia (1,2,4)	39.6, 73.1, 13	1912-2003 (7.3)	Evangelistas (4)	52.4, 75.0, 52	1901-1934 (0.2)
Isla Teja (11)	39.8, 73.2, 9	1960-2001 (0.2)	Punta Arenas (1,2,4)	53.0, 70.8, 37	1888-2005 (1.0)
Punta Galera	40.0, 73.7, 40	1899-1957 (0.6)	Grytviken (5)	54.3, 36.5, 3	1905-1988 (3.2)
Gral. Conesa (1)	40.1, 65.0, 100	1931-1960 (4.7)	Ushuaia (1,2,3)	54.8, 68.3, 14	1901-2005 (4.8)
Collunco (8)	40.1, 71.2, 875	1912-1989 (0.6)	Orcadas (5)	60.7, 44.7, 6	1903-2005 (0.0)
Osorno (1,2,4)	40.6, 73.1, 65	1961-2003 (5.3)	Signy Island (5)	60.7, 45.6, 6	1947-1995 (0.0)
Patagones (1)	40.8, 63.0, 10	1931-1960 (0.6)	Bellingshausen (5,7)	62.2, 58.9, 16	1944-2005 (1.6)
S. Antonio O. (1,2)	40.8, 65.1, 20	1931-2005 (8.1)	Great Wall (5)	62.2, 59.0, 10	1985-2005 (0.0)
Viedma (1,3)	40.9, 63.0, 7	1969-2005 (3.8)	Marsh (5)	62.4, 58.9, 10	1969-2005 (6.3)
Bariloche (1,2,3)	41.1, 71.2, 840	1914-2005 (0.0)	Arturo Prat (5)	62.5, 59.7, 5	1966-2003 (3.7)
Maquinchao (1,2,3)	41.2, 68.7, 888	1961-2005 (3.5)	O'Higgins (5)	63.3, 57.9, 10	1963-2005 (0.4)
Mascardi (10)	41.2, 71.6, 842	1969-1995 (0.3)	Esperanza (5,7)	63.4, 57.0, 13	1945-2005 (6.2)
Desague Chapo (9)	41.4, 72.6, 330	1964-1989 (1.4)	Marambio (5)	64.2, 56.7, 198	1970-2005 (0.2)
Puerto Montt (1,2,4)	41.4, 73.1, 85	1911-2005 (4.5)	Faraday (5,7)	65.4, 64.4, 11	1944-2005 (0.0)
Ancud (1,2)	41.9, 73.8, 114	1961-1980 (3.8)	Rothera (5,7)	67.5, 68.1, 16	1946-2005 (11.2)
Epuyen (3)	42.2, 71.4, 450	1964-1983 (0.0)			

2.2.1. Data Screening

2.2.1.1. Southern South American records

The examination of available SSA records revealed repeated, “duplicate” series for the majority of stations. Except for the cases where the same records were obtained from different data sources, these duplicate series consist of identical values for an overlapping period of variable length, and are probably the result of meteorological agencies reporting

different portions of the same data on different occasions. As a first step to develop the longest, most complete record for each location, all duplicate mean monthly station records were merged into a single series. In addition to these duplicate series, we also found “parallel” series (i.e. highly correlated yet not exactly the same records) for many SSA stations. Unfortunately, the limited information available did not allow us to determine whether these differences relate to differences in data processing or result from simultaneous measurements made at nearby stations. In view of the scarcity of climate data from this area, rather than discarding these parallel series or using them as separate, shorter, incomplete records, we combined all data for a given station-month-year to create a mean “composite” series following the averaging technique described in Hansen et al. (1999). Only parallel series with a period of overlap were used, and records with three or more years of consecutive missing data were treated as separate series. We calculated the average difference between two series over their overlapping interval and, using the most recent series as a base record, adjusted the second series by the mean difference prior to averaging the two series (see Hansen et al. 1999). If more than two parallel series with some overlapping interval were available for a given location, they were averaged with the mean of the other two records in the same way until all series were combined into a single record. Careful examination of parallel records from SSA stations revealed strong similarities with positive correlations above 0.9 for most cases. Yet, to minimize the influence of spurious/erroneous values at this stage, only records with correlations ≥ 0.8 in their overlapping interval were averaged into composite series. Although not ideal, this averaging approach has the advantage of maximizing the information available for each site and allows a further extension of the records by combining highly correlated series covering different time intervals. In addition, using adjusted data from parallel series can considerably reduce the percentage of missing values. After averaging all suitable parallel series from each location we obtained a single record of mean monthly values (in some cases over 90 years long and updated to 2005) for most sites in SSA. The few station records that contained two periods of valid data separated by more than three years of missing values were treated independently (Table 2.1). Mean monthly values outside ± 3 standard deviations from the long term mean were flagged as potential outliers, but were considered valid if the same month/year of the

nearest station was outside ± 2 standard deviations in the same direction. Otherwise, data from the three nearest stations were used as a basis for the decision to accept or reject the suspect value. Only records with less than 15% missing values and more than 20 years of data were selected for further analysis (Fig. 2.1 and Table 2.1).

2.2.1.2. Antarctic Peninsula Records

The main source for mean monthly surface temperature records for the AP was the SCAR READER dataset recently published by the British Antarctic Survey (Turner et al. 2004, data available online at <http://www.antarctica.ac.uk/met/READER/>). This database is a compilation of high-quality Antarctic station records that are largely free of discontinuities related to changes in observation times, etc. In developing this dataset, Turner et al. (2004) used a minimum threshold of 90% of available daily data to compute the monthly means for each station. However, monthly means calculated from less than 90% of available days are included in the database for completeness. Examination of the AP stations used in this study revealed that the number of available days is very rarely below 19-20 days (i.e. 65%) and most monthly means have been calculated using 75-90% of daily data. Thus, rather than extrapolating values from other stations, we relaxed the 90% threshold and used all data available to compute the monthly means for each station, regardless of the percentage of days available. Although not ideal, we consider that using monthly averages based only on e.g. 20 days (65%) of data is preferable to estimating missing months from neighboring stations often located several hundred kilometers away from the candidate site.

The records from four stations in the AP (Bellingshaussen, Esperanza, Rothera Point, and Faraday/Vernadsky, Table 2.1) were extended back in time using adjusted data from nearby discontinued stations as described in Jones and Limbert (1987)³. This approach has the advantage of extending the period under study back to the 1940s in all cases and allows a better assessment and intercomparison of the low frequency temperature patterns in this region. It is especially valuable for the western side of the AP where very limited

³ Updated data were published online by Jones and Reid (2001), <http://cdiac.ornl.gov/epubs/ndp/ndp032/>, and also at <http://www.antarctica.ac.uk/met/gjma/>.

data are available (Fig. 2.1). Potential discontinuities arising from this procedure (or present in the original records) are expected to be identified and adjusted during the homogenization process. Any undetected, (likely minor) inhomogeneity in monthly data will be further minimized by seasonally and regionally averaging the individual station records (see below). As with the SSA series, the decision whether to accept or reject extreme values was made based on the information available from the nearest stations, and only AP station records with ≥ 20 years of data and $\leq 15\%$ missing values were included in further analysis (Table 2.1).

2.2.2. Data homogenization

Surface air temperature station records can be influenced by several non-climatic factors such as station moves, changes in instrumentation and times of observation, modifications to the station surroundings, etc. If unaccounted for, these factors may ultimately impact the station records and result in biased interpretations regarding the true climatic changes occurring at any particular site. Homogeneous climate time series can be developed either by only using stations that are considered relatively homogeneous, or by applying homogeneity adjustment techniques to obtain an adjusted homogeneous record [see Peterson et al. (1998) and Aguilar et al. (2003)]. In SSA the first strategy would result in very few stations being considered relatively homogeneous, considerably reducing the spatial representativeness of any study. The lack of accurate metadata for many SSA and AP records would make this an almost impossible task for our study area. In the second case the validity of the adjustments may be questioned in regions that lack metadata or where there are no reliable stations nearby to test the homogeneity of the candidate station. Nevertheless, two differently adjusted versions of the same station's data are usually much more similar to each other than they are to the unadjusted records (Peterson et al. 1998), suggesting that using adjusted data can significantly reduce the uncertainty of the resulting regional climate series. To our knowledge only a few studies have applied homogeneity tests and data corrections to SSA records (e.g. Rosenblüth et al. 1997). In most cases, given the scarcity of long and complete records for comparison, previous homogeneity tests were performed using a very small number of stations and therefore it is possible that important inhomogeneities may remain undetected. The

greatly expanded spatial and temporal coverage of station records presented here has allowed us to reevaluate this issue critically by developing reference series from several neighboring stations to perform consistent homogeneity tests on the records from SSA and the AP.

Most temperature records in SSA come from cities or towns, where the lack of long, reliable proximal and purely rural records for comparison can seriously hamper the identification of any potential urbanization signal present in the individual urban records (e.g. Karl et al. 1988; Jones et al. 1990). However, given the strong, almost constant influence of westerly winds in Patagonia (Miller 1976; Prohaska 1976) and the fact that in most cases the meteorological observations have been collected at the local airports (usually located several kilometers away from the urban centers), we believe that the urbanization effect is probably not a major factor affecting these records⁴.

2.2.2.1. Creation of reference series

Several methods for the formation of “reference” climate time series, and for the evaluation of the relative homogeneity of “candidate” series, have been discussed in the literature (e.g. Peterson and Easterling 1994). Basically, the idea is that, by comparing/testing a candidate record against a representative reference series (supposedly largely free of non-climatic inhomogeneities and usually derived from several well-correlated neighboring records), it is possible to detect (and adjust if necessary) major discontinuities in the candidate record and obtain a new, homogenized candidate series. Since the techniques that utilize several neighboring stations in the construction of an area-averaged reference time series must necessarily introduce a regional climate signal into the individual station data, the most appropriate use of homogeneity-adjusted series is in creating and analyzing such regional area-averaged climate records (Peterson et al. 1998).

⁴ One approach to this issue would be to apply the population-based correction algorithms from Karl et al. (1988), who estimated adjustment factors for urban records in the U.S. based on their differences with neighboring, purely rural stations and their population growth over time. We did not apply these correction algorithms because they could result in an additional, unknown source of error that is not justified until more detailed analyses of SSA stations and conditions are developed.

Unfortunately, there is no period in common to all stations in our study area (Table 2.1). Thus, it was not possible to develop reference series using weighted averages of anomalies calculated from a common reference period (e.g. Alexandersson and Moberg 1997) without seriously compromising the spatial and temporal coverage of the records. Instead we used (with some modifications, see below) the technique proposed by Peterson and Easterling (1994) that does not necessarily require a common period for the development of reference series. This method first identifies the most suitable reference stations for a candidate site by correlating the first-differenced time series (FD) that are created by subtracting the previous year's data (T_{t-1}) from the current year values (T_t). That is,

$$FD_t = T_t - T_{t-1}$$

Since any jump or discontinuity that may be present in the raw, original records will only affect one year in the FD series, the use of FD series in correlation analyses will provide a more reliable estimate of the strength of the relationship between series (Peterson and Easterling 1994). This simple data transformation also brings the records closer to a normal distribution and minimizes the influence of serial persistence in the estimation of the statistical significance of the correlations between stations (e.g. Dawdy and Matalas 1964). Because FD series are not tied to a common reference interval but reflect the year-to-year changes in the records, well-correlated neighboring series covering different time intervals can be readily combined into FD reference series.

The average of FD monthly correlations between all possible pairs of stations was first tested for significance (t-test), and only those records positively correlated with each candidate site at the 99% level and with ≥ 20 years of overlap were considered for the development of the reference series. The significance level of the correlations was used rather than the raw correlation coefficients because of the variable periods of overlap between stations. Briefly, the creation of reference series involved:

- 1- Selection of a minimum (maximum) of three (10) of the most significantly correlated stations within 750 km of the candidate site (for a few isolated stations in the south Atlantic, the distance threshold was extended to 1500 km). As small correlation coefficients can become statistically significant if the number of years in common between two series is sufficiently large, stations correlating at <0.5 with the candidate were excluded at this stage, regardless of their statistical significance. The only exception was the use of Port Stanley (correlation 0.483) in the creation of the reference series for Orcadas (the longest record in Antarctica and surrounding regions south of 60°S) as this allowed sufficient neighboring stations to extend the reference record for Orcadas back to 1922.
- 2- The FD monthly series from the stations selected above were averaged using a 40% trimmed mean to exclude anomalously high or low values caused by possible jumps or discontinuities in the original data. For example, for a candidate monthly record for which five reference stations are available, only the three central values are used to calculate a monthly average, minimizing the impacts of possible discontinuities in the creation of the FD reference series.
- 3- The full reference series were created from the averaged FD monthly reference series obtained in the previous step. Essentially, this is the reverse of the process for creating the FD series. In order to facilitate the visualization of the data, the most recent value of the FD reference series is set equal to the final value of the candidate series, and the reference series is created working backwards in time from that final value (Peterson and Easterling 1994).

Recently, Menne and Williams (2005) evaluated the impacts of different methodologies for the creation of reference series and homogeneity testing in the proper identification of abrupt discontinuities imposed on simulated climate time series. They showed that reference series created from FD series containing missing values may be affected by non-climatic random walks that, originating in those missing points, will propagate back in time due to the way these reference records are created. This can impact the number, magnitude and location of discontinuities attributed to the candidate series during subsequent homogeneity tests, reducing the overall reliability of this approach. In order to

minimize this problem we obtained serially complete station records prior to the creation of the reference series by estimating missing values in each series. This was accomplished by setting the departure of each missing month as the average departure (calculated from the mean of a 30-yr window around that value) of the eight best correlated (99% significance level or better) neighboring stations.

2.2.2.2. Homogeneity testing

A number of measures were taken to ensure that the surface temperature records developed were as homogeneous as possible with respect to the surrounding stations. First, using the reference series described above, we objectively tested the relative homogeneity of individual records using three different, well-known homogeneity tests. The combination of multiple tests to detect abrupt inhomogeneities in simulated climate records has been shown to reduce the number of “false alarms” that may appear when only a single homogeneity test is applied to the data (Menne and Williams 2005). The three homogeneity tests used were the standard normal homogeneity test for single shifts (Alexandersson 1986), Potter’s bivariate test (Potter 1981), and the two-phase regression approach of Easterling and Peterson (1995). Rigorous comparison of these techniques with other homogeneity tests (Easterling and Peterson 1992, 1995) showed that they were the best option for identifying sudden shifts in artificial data. Thus, they were considered the most appropriate choice to minimize the manipulation of the original data and to obtain robust, reliable information about the location, magnitude and statistical significance of any discontinuities identified in the records.

These purely empirical analyses were complemented, whenever possible, with metadata obtained from the extensive compilation of Southern Hemisphere surface station histories by Jones et al. (1986), the British Antarctic Survey website, and local meteorological agencies. Dates for station moves in southern Chile were also obtained from Rosenblüth et al. (1997). Unfortunately the metadata available is quite limited: it does not include all stations, and in most cases the information is only available for part of the period covered by the station records. Nevertheless, dates (years) indicating station moves and/or changes in instrumentation, formulae to calculate mean temperatures, and times of

observation were flagged as possible locations for inhomogeneities in each candidate series. These dates were combined with the information obtained from the homogeneity tests to identify (and adjust if appropriate) the most important temporal discontinuities in the candidate records.

For each test and candidate record, the analyses were run using the difference series between the candidate and the reference record (this difference series should, in theory, be stationary and randomly distributed around zero if the candidate is relatively homogeneous). Although we applied the necessary adjustments to monthly data, we used the less variable mean seasonal and annual records to improve detection of discontinuities in the candidate series. This process is briefly described below:

- 1- Test statistics were calculated for each year of the candidate series starting in year 5 and ending in year $n - 5$ to avoid the less reliable test estimates associated with the start and end of the series. Extreme values in test statistics outside the 95% level were recorded as potential discontinuities, and the difference series was subdivided into two parts (before and after the discontinuity). Each subsection was then tested in the same manner, significant discontinuities were recorded, and the series was subdivided again if necessary. This process continued until no significant discontinuities were found or the series was too short for testing.
- 2- The combined record of potential inhomogeneities derived from each individual test and mean seasonal candidate record was assessed and adjustments were applied only if a) at least two of the three tests identified a significant (95% confidence level) jump in the same year, or b) if a significant discontinuity identified by at least one of the tests occurred within one year of a change at the station documented by the available metadata.
- 3- Keeping the portion with most recent records as the base period, adjustment values were calculated from the difference series using (when possible) a 20-yr window before and after the year with the discontinuity. Although the identification of the most important discontinuities was based on seasonal series, adjustments were applied to the monthly values for each season (DJF for summer, etc).

- 4- The adjusted monthly values were re-averaged into seasonal series and steps 1-3 were performed again to identify (and adjust, if still present) any further discontinuities in the records.
- 5- If no further discontinuities were found in the seasonal series, the entire test was performed again using annually averaged records, and adjustments were applied if necessary. This process continued until no significant discontinuities were found in both seasonal and annual series. In most cases, this process resulted in only minor adjustments and allowed us to obtain serially complete records that are considered as homogeneous as possible (at the mean seasonal and annual levels) with respect to their surrounding area and present measuring conditions at each site.

2.2.3. Identification of main spatial patterns

The main patterns of spatial variability in surface temperature series from the study area were identified using obliquely rotated principal component analyses (Richman 1981). Initially the annual and seasonal homogenized records from SSA and the AP were analyzed together to define the dominant spatial patterns across the whole study area. Subsequently, records from SSA and the AP were examined separately to characterize the main modes of variability in each region and identify the most suitable stations for the development of regionally averaged time series. The uneven temporal coverage of the records (Table 2.1) makes it impossible to utilize a common period for all 68 stations to analyze their regional patterns of variability (e.g. Pittock 1980). Therefore we performed several trials using different time intervals (1931-60, 1969-88, 1970-95, and 1961-2001) that maximized either the number of sites or the temporal coverage under analysis and objectively identified the main spatial patterns associated with our data. The 1969-88 period is shared by the highest number of stations (42) in the dataset and is the basis for most of the results for the combined SSA and AP analyses. Tests of the 1931-60 and 1961-2001 periods (32 and 26 stations, respectively) allowed the evaluation of the temporal stability of the main spatial patterns identified, providing additional information that facilitated their spatio-temporal interpretation. The highest possible subset of stations for SSA and the AP were 1969-88 (33 sites) and 1970-95 (10 sites), respectively (Table 2.1).

Extensive revision and testing of several principal component rotation methods has revealed that obliquely rotated solutions perform significantly better than unrotated and orthogonally rotated methods in objectively decomposing spatial arrays of real and simulated climate data into regional clusters or patterns (Richman 1986; White et al. 1991). As obliquely rotated solutions do not constrain orthogonality of the vectors, they tend to reflect the natural regional patterns of common variability present in the original records in a more physically realistic manner (Richman 1981; White et al. 1991). Following Richman (1986) we used an oblique Promax rotation (Hendrickson and White 1964) with a power $k = 2$, but we also examined the Varimax orthogonal rotation (Kaiser 1958) as an alternative validation. The analyses were performed using a correlation input matrix in which all series are equally weighted: the resulting map types are not biased by areas of high and low variance and therefore will not concentrate the synoptic centers in areas of maximum variance (Richman 1981). This may be of relevance given the size of the study area and the inherent variability observed in the records. For example, some AP stations show three to four times larger interannual variability than records located further north along the Atlantic and Pacific coasts of SSA. Significant components were identified as those with eigenvalues ≥ 1 (Kaiser 1960).

2.2.4. Creation of regionally averaged series

To reflect accurately the major modes of intra- to multi-decadal variability in the study area, regionally averaged mean annual time series were derived from separate principal component analyses of SSA and AP records using the 1969-88 and 1970-95 common intervals, respectively. However, as these common time intervals are significantly shorter than the full period covered by the station records, it was deemed inappropriate to use the principal component (factor) scores to evaluate the long-term temperature variability of each subregion (e.g. Villalba et al. 2003). Instead, regionally representative time series were created using a weighted average (weighted by the square of the component loading of each station selected) of homogenized data from stations with component loadings \geq

0.70 (0.80) with each principal component identified in SSA (AP) data⁵. These mean regional series were adjusted to account for the temporal changes in variance due to changes in sampling size (Jones et al. 1997, 2001), and variance adjustment factors were derived from the average correlation between all possible pairs of station records within each subregion and the number of records available for any given year (Osborn et al. 1997). Although the choice of a different time interval and loading threshold would have slightly modified the shape of the resulting subregions, several trials performed using different rotation solutions, number of stations and time intervals suggest that the main spatial domains characterized over these regions are relatively robust and have remained relatively time stable over the instrumental period (see below).

2.2.5. Identification of long term modes of variability

Linear trend analysis has been commonly used in previous studies as a simple, easy-to-interpret measure of long term temperature changes in SSA and the AP (e.g. Villalba et al. 2003; King et al. 2003). However, this type of analysis assumes a relatively monotonic rate of change that is rarely the case in climate time series, and the magnitude and significance of linear trends can be highly influenced by many factors such as the degree of serial correlation in each time series, the length of the series under analysis and the existence of extreme values at the beginning or the end of the series (Santer et al. 2000). Thus, despite being a useful, informative measure, linear trends give a rather limited picture of the full range of climatic variability that may be present in a given regional climate time series. Here we characterized the temporal variability observed in the regionally averaged records using three different approaches (see Appendix 2 for additional details):

- 1- The statistical significance of least-squares linear trends was assessed following a conservative approach which accounts for the serial correlation in the regression residuals of each time series (Santer et al. 2000).

⁵ Since these principal component loadings can be interpreted as simple correlation coefficients between each factor and the original variables, these threshold values ensured a strong common signal for each subregional record while almost completely avoiding the overlap between subregions.

- 2- The most important step-like changes in mean conditions that have occurred during the observational period were identified using a simple, robust regime shift detection technique (Rodionov 2004, 2006). This procedure is based on the calculation of a Regime Shift Index combined with the sequential application of Student's *t*-tests to determine the timing and significance of the regime shifts. Unlike most shift detection techniques, significant jumps near the end of the series can be readily identified and subsequently validated with the inclusion of new data once they become available. This offers the opportunity of detecting potential climate shifts relatively early and allows the assessment of their magnitude changes over time (Rodionov 2004). This methodology was recently improved by Rodionov (2006), who implemented a set of procedures to account for the impacts of serial correlation in the identification of significant regime shifts in time series.
- 3- The magnitude and statistical significance of time-varying moving windows of different lengths (e.g. 6-30 years) and location in each regional time series were tested using an innovative nonparametric technique that uses Mann-Whitney U statistics and Monte Carlo simulations (Mauget 2003, 2004). This procedure allowed us to characterize the most important low frequency patterns in each subregion and evaluate objectively the nature of the last 10-15 years in a longer term temporal context.

2.3. Results

2.3.1. Homogeneity of records

The correlation analyses between first-differenced mean monthly series for all possible pairs of stations with at least 20 years of overlap revealed strong, coherent patterns of common interannual variability in the study area. For almost every candidate series regardless of their location and period of coverage, we found highly significant positive correlations with neighbors located up to several hundred kilometers distant (Fig. 2.2). These highly consistent results were unexpected given the variety of sources and the different, often unknown, methods originally used to derive the mean monthly records in our dataset. However, the results highlight (at least at the inter-annual level) the overall good quality of the records from which the reference series were derived. They also underline the potential contribution that the usually neglected, early climate records from

discontinued stations can make to improve our understanding of climate variability and change in this region.

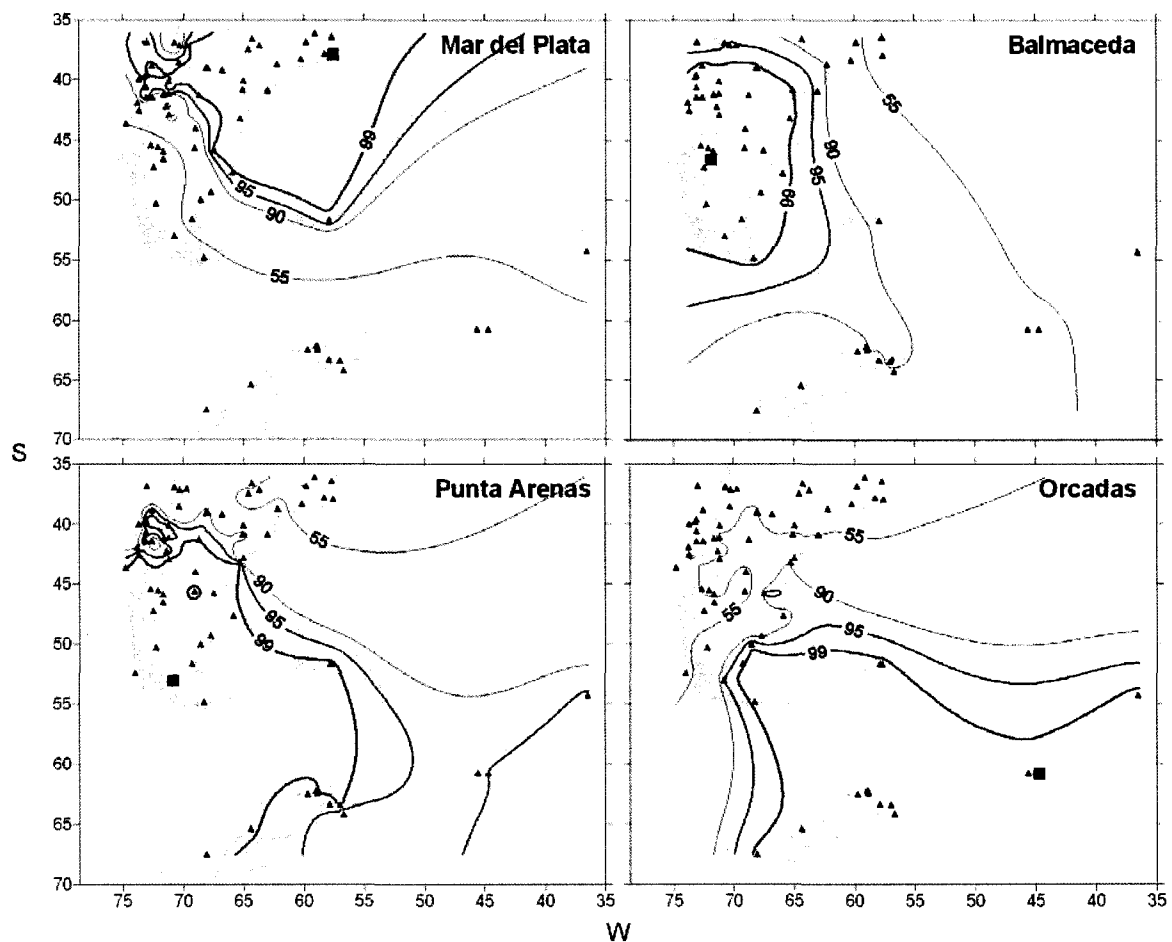


Fig. 2.2. Correlation fields of four selected candidate stations (red boxes) with all possible stations in the dataset (triangles) with at least 20 years of overlap. The average of monthly correlations of first difference series and the number of years in common between the two series being tested were used to determine probability (p) which is mapped here as $[(1-p)*100]$. Interpolated lines of equal probability are shown in color. In each map, stations located within the blue lines are correlated at the 99% confidence level with the candidate series, showing strong similarities in year-to-year variations across large regions.

The choice of techniques that utilize first-differenced data allowed the use of many series that otherwise would have been excluded from the analysis because of the lack of an overlapping common reference interval with those longer records employed in previous studies (e.g. Villalba et al. 2003). It also allowed the creation of reference series from at least 3 neighboring stations for most of the period covered by almost all candidate series, thereby increasing the reference sites used to identify discontinuities in the original records. In SSA only the Evangelistas station (Table 2.1) was excluded from the analysis because it lacked a sufficient number of significantly correlated neighboring stations to develop an adequate reference series. The combination of multiple tests for evaluating the relative homogeneity of records effectively restricted the number of adjustments to only those major discontinuities that could be cross-validated empirically. Whenever possible, discontinuities were also identified using the available metadata. For the majority of records this combined approach resulted in usually only minor adjustments to conform to the regional climate conditions inferred from well-correlated records from 3-10 neighboring stations. The analyses and discussions reported here are based on mean annual series: seasonal analyses will be reported elsewhere.

2.3.2. Main spatial patterns

Obliquely rotated principal component analyses of 1969-88 homogenized mean annual station records from SSA and the AP identified five major spatial patterns (Fig. 2.3). The strongest component was centered in southern Patagonia between 45°-50°S and explained over 42% of the total variance⁶ (PC1, Fig. 2.3). Principal components PC2, 3 and 5 were concentrated on the NE, NW and central-northern sectors of SSA and explained about 31%, 20% and 10% of the total variance. PC4 grouped the stations in the AP and explained about 18% of the variance. Except for the pattern centered in central-northern Patagonia (which was identified using 1931-60 data but is not evident during the 1961-2001 period), the first four modes of variability are readily identifiable over different time intervals and sets of stations (see Appendices 3 and 4). Puerto Montt and Desague del Chapo (Table 2.1) showed spatial inconsistencies in their PC loadings with

⁶ Note however that obliquely rotated principal components are not constrained to be orthogonal. As a result, some of this variance may be explained by more than one component and therefore the sums of their squared loadings cannot be added to obtain total variance.

respect to their neighboring stations in NW Patagonia and were excluded from further analysis for this region. Analyses using an orthogonally rotated Varimax eigensolution of SSA and AP data for this same intervals gave similar results (not shown) with the same number of significant components explaining between 81-89% of the total variance in the original records. These results indicate that the patterns in Fig. 2.3 can be regarded as reliable indicators of the main spatial modes of 20th-century temperature variability across this region.

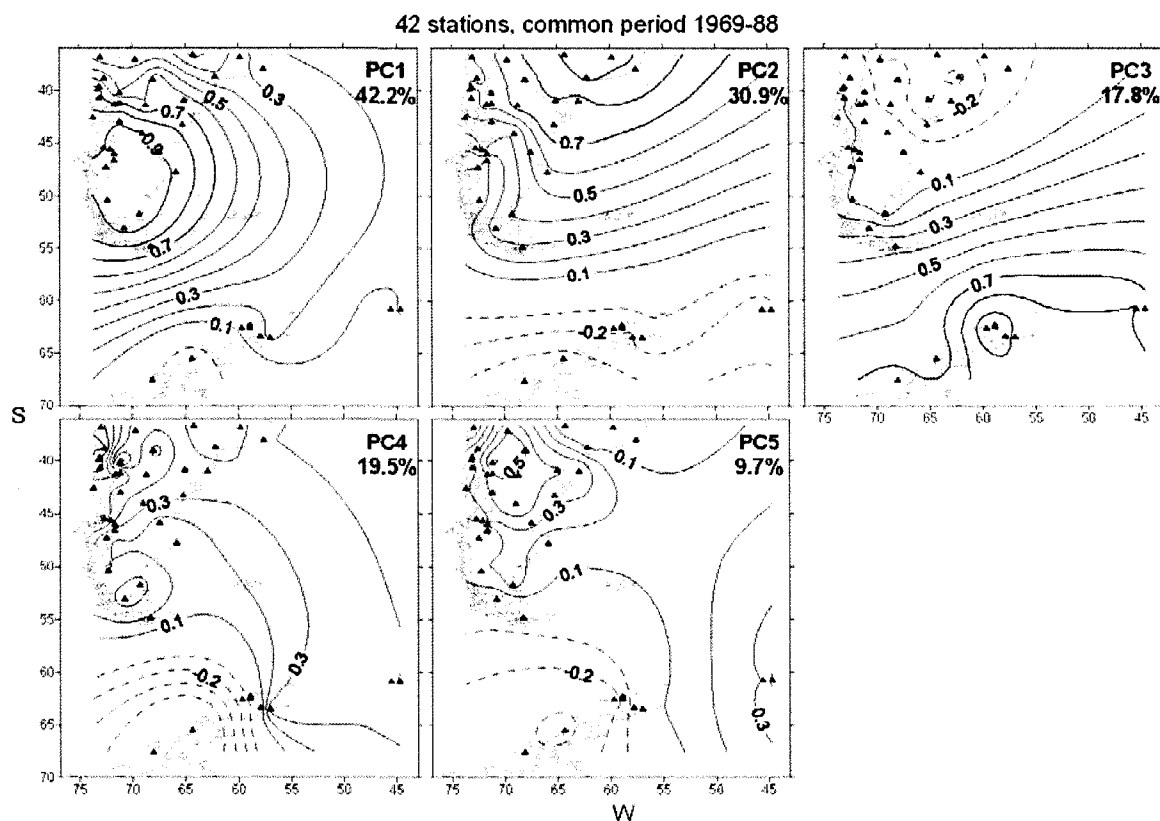


Fig. 2.3. Main modes of spatial variability in SSA and AP mean annual temperature records derived from obliquely rotated eigensolutions using the 1969-88 common interval with the highest possible subset of stations for analysis (42 stations). PCs with eigenvalues ≥ 1 are shown, and the 0.7, 0.8, and 0.9 loading contour lines are colored in red to highlight areas with a strong common signal. Triangles indicate station locations, negative loadings are shown as dashed lines, and the zero line is omitted. Percentage of total variance explained by each component is noted but should be interpreted with caution because the components are not truly independent. Equivalent maps for the 1931-60 and 1961-2001 intervals are shown in Appendices 3 and 4.

The separate analysis of 1969-88 mean annual temperature records from SSA revealed similar spatial patterns to those identified in Fig. 2.3. The strongest PC in SSA records (PC1, Fig. 2.4A) was again centered in southern Patagonia and explained almost 48.5% of the total variance of this dataset. The three remaining patterns concentrated the highest loadings in the NE, NW and central-northern SSA sectors and explained about 31%, 33%, and 36% of the variance, respectively⁶ (Fig. 2.5A-2.7A). The spatial domains of PCs 1-3 (see Fig. 2.4A-2.6A) closely resemble those identified by Villalba et al. (2003) in a subset of SSA records analyzed over the 1931-90 interval. A fourth pattern, centered on central-northern Patagonia (Fig. 2.7A), has not been documented before and emerged clearly in this analysis of SSA data. Apart from having a mixed signal probably influenced by the surrounding modes of variability, the identification of this pattern (located at the southernmost tip of the “Arid Diagonal” biogeographical unit; Cabrera and Willink 1973) may be dependent on the number of sites available for this data-poor area at the different time intervals.

When tested alone using the 1970-95 maximum overlapping interval, AP records segregated into two regions concentrated over the NE and SW sectors of the peninsula (Fig. 2.8). These subregional patterns explain about 67% and 46% of the total variance⁶ and corroborate previous studies that observed contrasting patterns of variability between the NW and the SE sectors of the AP (e.g. Schwerdtfeger 1970; Martin and Peel 1978; King and Comiso 2003). Unfortunately the scarcity of climate station data in the southern portion of the AP (Fig. 2.8) hampers a more detailed examination of the spatial variability of surface temperatures across this region.

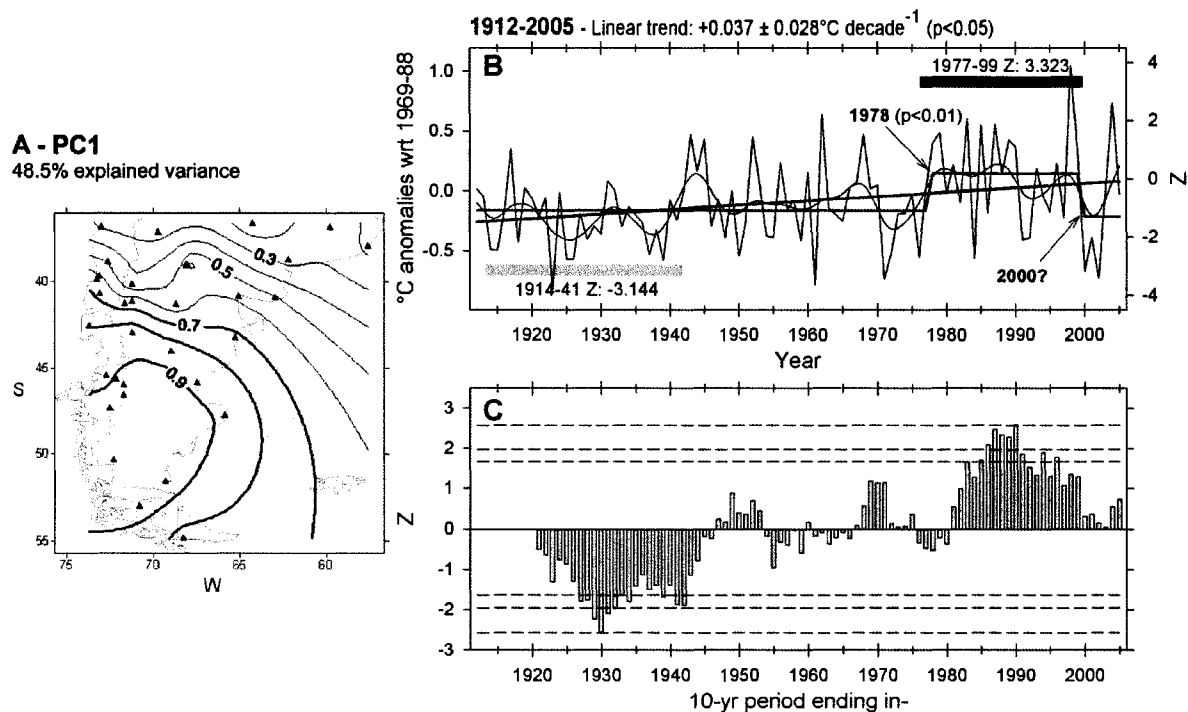


Fig. 2.4 (A). Map of the loading of each climate station on PC1 (southern Patagonia) derived from 33 SSA mean annual series over the 1969-88 interval. **(B)** Variance adjusted, weighted average mean annual temperature records for stations within the 0.7 contour line in (A). The linear trend (thick black line), a 10-yr spline (blue line) and mean regime levels before and after significant shifts (red line) are also shown to emphasize the low-frequency variability in this record. Significant shift years ($p < 0.05$) are indicated together with their significance levels [potential shifts ($p > 0.05$) identified by the algorithm at the end of the series are also included for completeness (see text)]. Periods with the highest (lowest) MWZ values of all possible moving windows of 6-30 years in length are indicated by the light (dark) gray horizontal bars. **(C)** Mann-Whitney Z statistics for running 10-yr samples of the mean annual, regionally averaged record. Horizontal dashed lines indicate positive and negative significance at the 90%, 95%, and 99% confidence levels.

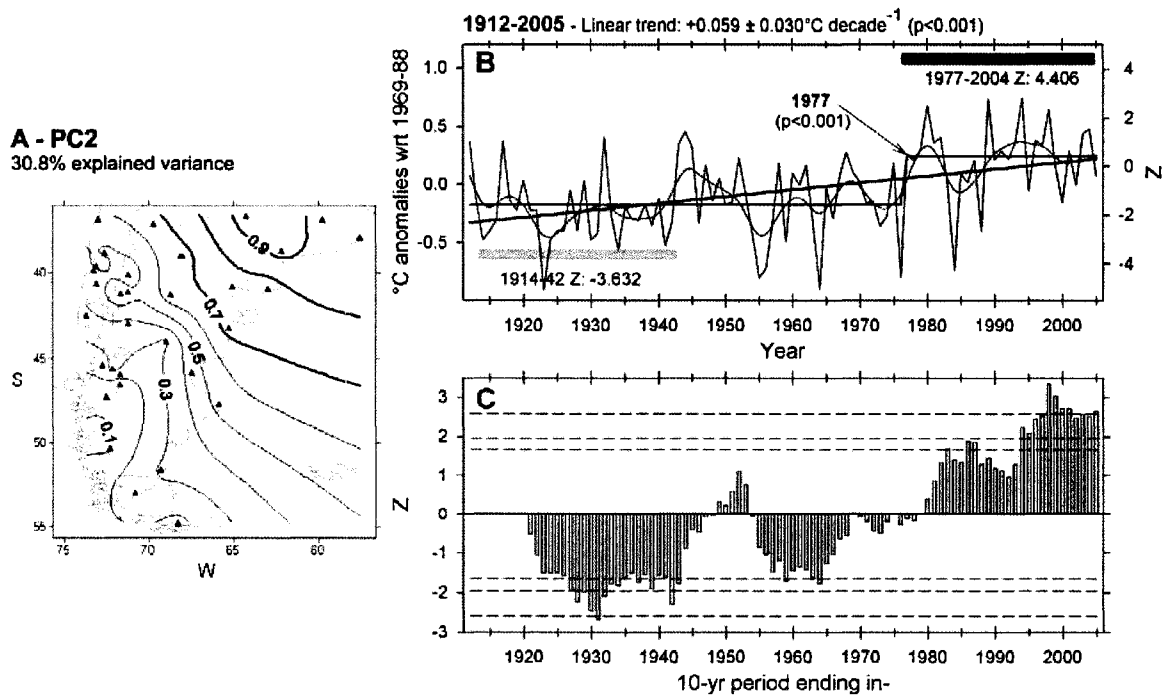


Fig. 2.5. Same as Fig. 2.4, but for PC2 (NE SSA).

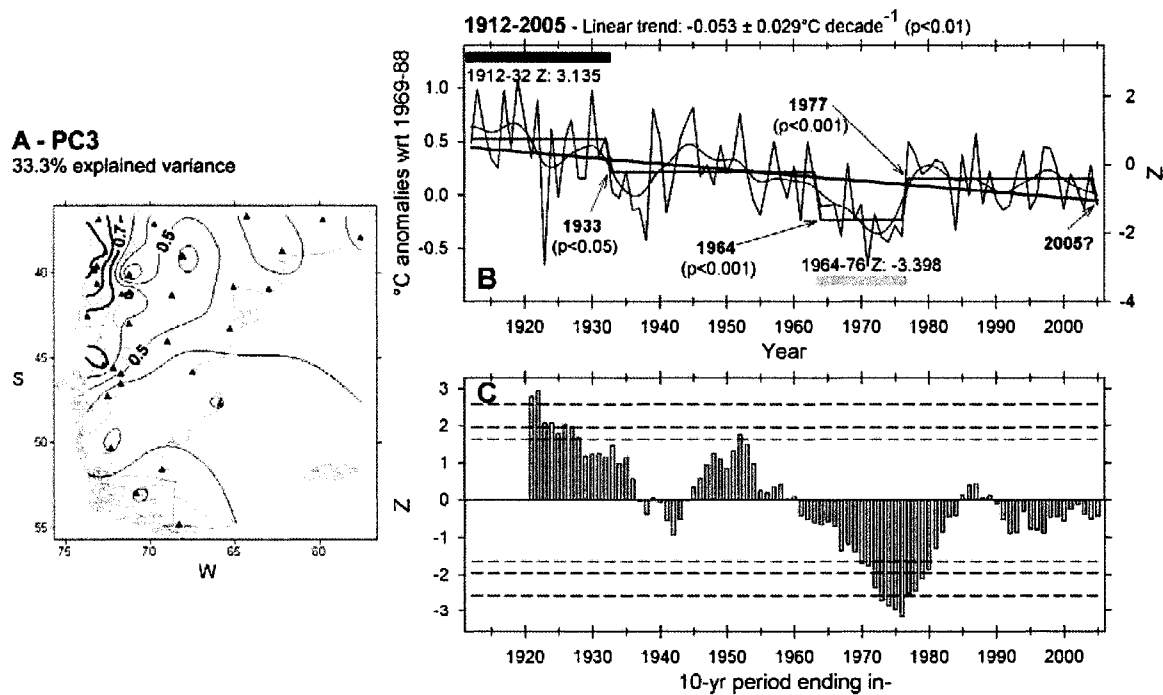


Fig. 2.6. As Fig. 2.4, but for PC3 (NW Patagonia).

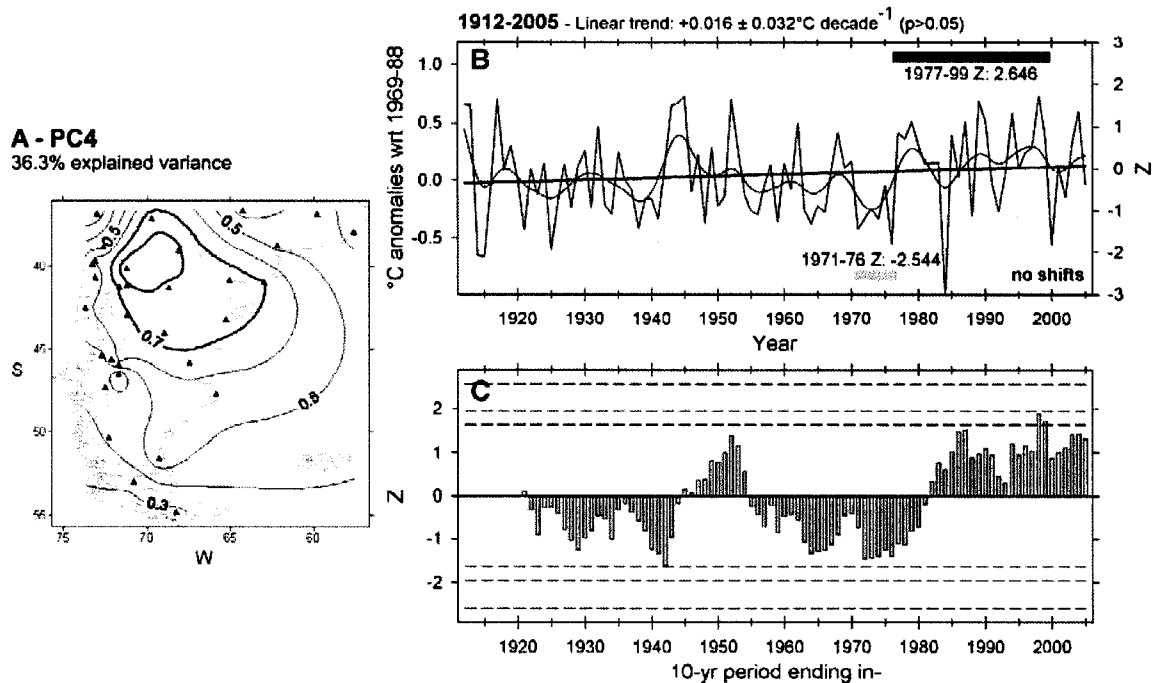


Fig. 2.7. As Fig. 2.4, but for PC4 (central-northern Patagonia). No significant regime shifts were identified in this case.

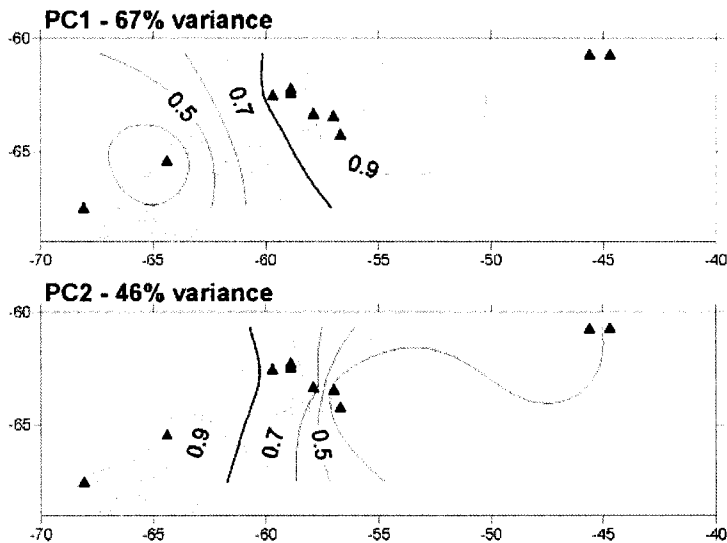


Fig. 2.8. Main modes of spatial variability in 1970-95 AP mean annual temperature records derived from an obliquely rotated Promax eigensolution. The 0.8 loading threshold (thick red line) was used to identify stations included in the regionally averaged records from each subregion (see text).

2.3.3. Temporal variability of regionally averaged records

Regionally averaged mean annual records derived from the four main SSA spatial patterns showed intriguing differences at inter-annual and intra- to multi-decadal timescales (Fig. 2.4BC-2.7BC). Positive, statistically significant linear trends over the 1912-2005 interval were found in the southern and NE SSA sectors (i.e. PC1 and PC2, Fig. 2.4B-2.5B) even after accounting for serial correlation in these series. The warming rates reached almost 0.04°C per decade (PC1) and 0.06°C per decade (PC2) and are statistically significant at the 95% and 99.9% confidence levels, respectively. In contrast, the pattern in NW Patagonia (PC3, Fig. 2.6B) showed a marked, statistically significant negative trend of $-0.053^{\circ}\text{C decade}^{-1}$ over the same period. Located between these major modes of variability, central-northern Patagonia (PC4, Fig. 2.7B) has experienced a weak, non significant warming trend of 0.016°C per decade between 1912 and 2005. Several significant regime shifts were also identified superimposed to the long-term trends in three of these regional series, with the shift towards warmer conditions in 1977-78 emerging as a clear discontinuity in temperature records across SSA (Fig. 2.4B-2.6B). Two sharp, statistically-significant decreases in temperature occurred in NW Patagonia in 1933 and 1964 (Fig. 2.6B). The regime shift testing algorithm also detected potentially significant temperature decreases in 2005 in NW Patagonia (Fig. 2.6B) and in 2000 for the southern sector of SSA (Fig. 2.4B). Although additional, more recent data are required to corroborate the true significance of these later events, this exercise may prove useful as an early detection tool of the latest temperature shifts in these specific areas.

Complementary, much more detailed insights on the low-frequency variability in regionally averaged mean annual temperatures over SSA were obtained from the non-parametric Mann-Whitney / Monte Carlo analysis of moving windows of 6-30 yr duration (Fig. 2.4BC-2.7BC). This simple and objective procedure allowed the assessment of the relative magnitude and statistical significance of a wide range of intra- to multi-decadal (IMD) regimes against an essentially stationary time series and corroborated the regional nature of the shift towards warmer conditions after 1977-78. In

fact, the analysis of IMD intervals with the highest and lowest ranked MWZ values⁷ in these four series for all possible moving windows revealed that the 23-yr interval between 1977-99 has been the warmest period on record for southern (central-northern) Patagonia with at least a 99.9% (99%) level of confidence (Fig 4A and 7A). The warmest interval in NE SSA occurred between 1977 and 2004 and is also highly statistically significant (Fig. 2.5A). Both regional records derived from PCs 1 and 2 (Fig. 2.4B and 2.5B) showed the coldest periods between 1914 and 1941-42. In contrast, the peak warm and cold intervals in NW Patagonia (Fig. 2.6B) occurred in 1912-32 and 1964-76, respectively, and are responsible for the marked cooling trend observed in this subregion over the observational period. The cold interval between 1964 and 1976 has been identified in previous studies as a clear feature of north Patagonian climate west of the Andes (e.g. Villalba et al. 2003) and coincides with the well-dated glacier advances that culminated in 1977 in the north Patagonian Andes (see Chapter 3). The coldest period in central-northern Patagonia occurred between 1971 and 1976 (Fig. 2.7B). The similarities between this record and those in NE and NW Patagonia (i.e. Fig. 2.7B vs. 2.5B and 2.6B) reflect the flexibility of obliquely rotated eigensolutions in allowing mixed influences of nearby patterns in this transitional region.

Based on an arbitrarily selected 10-year reference window, we evaluated the statistical significance of “moving decades” throughout the instrumental period and found additional evidence that clearly differentiates the low-frequency modes of variability in each subregion (Fig. 2.4C-2.7C). Moving decade analysis for southern Patagonia showed 1977-86 as the beginning of a significantly warmer interval that peaked in 1981-90 (Fig. 2.4C). No other decade in this regional record reached the warmth of the 1977-1990 intervals. Except for minor variations in the middle of the record, the MWZ values for this series have slowly increased from the lowest point in 1921-30 to the observed warm peak in the 1981-90. In contrast, the MWZ values for moving decades in NE SSA show a much more drastic increasing trend and all 10-yr windows after 1985 are outside the 95% confidence level (Fig. 2.5C). The 1989-98 period contains the highest number of extreme

⁷ The 95%, 99% and 99.9% confidence intervals are defined by the ± 1.960 , ± 2.576 , and ± 3.290 MWZ values, respectively.

warm years on record and is statistically significantly warmer at the 99.9% level. The coldest decade in this series occurred in 1922-31 (Fig. 2.5C), and several extreme cold intervals in the 1920s and early 1930s plus the warmth of recent decades account for the strong warming trend observed in this region (Fig. 2.5B). As expected, the coldest decades in NW Patagonia occurred between the mid 1960s and late 1970s, particularly over the 1964-76 period (Fig. 2.6C). Following this period decadal temperatures have warmed but not extremely so: the only statistically significant warm decades in this region are concentrated in the early record and peaked in 1913-22 (Fig. 2.6C). Low-frequency patterns have been less marked in central-northern SSA with no decades being statistically significantly warmer or colder (Fig. 2.7C). However, extended periods of warm conditions are clearly evident during the 1940s until the mid 1950s and especially after the mid 1980s. Cold conditions prevail until the early 1940s and also between the mid 1950s and late 1970s (Fig. 2.7B, C).

The inherent flexibility of the nonparametric time series analysis technique and the existence of updated temperature records allowed an objective assessment of the relative magnitude of temperature changes during recent years in a long term context. For each subregion in SSA we examined the 1991-2005 period which is known to include some of the warmest years on record (e.g. Villalba et al. 2003) but has not been fully evaluated in previous studies. This analysis showed that, when compared to a hypothetical time series with similar levels of persistence but essentially stationary over the long term, only the last 15 years of record in NE SSA are collectively significantly warmer than expected by chance alone (Table 2.2). In both southern and central-northern SSA this period showed positive but non-significant MWZ values, whereas the same interval in NW Patagonia showed colder-than-average conditions that were not statistically significant (Table 2.2).

Table 2.2. Selected features identified on the regionally averaged, mean annual temperature records from SSA and the AP (Fig. 2.4BC-2.7BC, 2.9 and 2.10). The significance of least squares linear trends is calculated after accounting for the serial correlation in each series. The first year after a regime shift is indicated and positive (negative) signs denote a change towards warmer (cooler) conditions. Extreme warm and cold IMD intervals are identified from the analysis of all possible moving windows of 6-30 yr duration. The MWZ value of the last 15 years (i.e. 1991-2005) is also included to evaluate this most recent period in a long term context. Notes: One, two and three asterisks denote statistical significance at the 95%, 99%, and 99.9% confidence levels, respectively; (ns) $p > 0.05$; (#) Potential regime shift ($p > 0.05$) identified by the testing algorithm near the end of the series (see text for details).

	PC (period)	Linear trend ($^{\circ}\text{C decade}^{-1}$)	Regime shifts (sign)	Warmest IMD	Coldest IMD	Warmest decade	MWZ last 15 yrs
SSA	PC1 (1912-2005)	$0.037 \pm 0.028^*$	1978(+)** 2000(-)#	1977-99***	1914-41**	1981-90**	0.316ns
	PC2 (1912-2005)	$0.059 \pm 0.030^{***}$	1977(+)**	1977-2004***	1914-42***	1989-98***	3.429***
	PC3 (1912-2005)	$-0.053 \pm 0.029^{**}$	1933(-)* 1964(-)** 1977(+)** 2005(-)#	1912-32**	1964-76***	1913-22**	-0.873ns
	PC4 (1912-2005)	$0.016 \pm 0.032^{\text{ns}}$	None	1977-99**	1971-76*	1989-98ns	1.165ns
AP	PC1 (1922-2005)	$0.214 \pm 0.086^{***}$	1981(+)**	1976-2005***	1922-50***	1996-2005***	3.528***
	PC2 (1946-2005)	$0.317 \pm 0.267^*$	None	1983-2005***	1948-69***	1996-2005**	2.167*

Both regionally averaged records from the NE and SW sectors of the AP (Fig. 2.9 and 2.10) showed marked positive linear trends over their observational periods (1922-2005 and 1946-2005, respectively). As expected, these strong warming trends determine that the coldest and warmest regimes are invariably found towards the beginning and the end of each series (Fig. 2.9 and 2.10). The most extreme warm (cold) interval in the NE AP record occurred between 1976 and 2005 (1922-50) and reached extremely high levels of significance (Fig. 2.9). In addition, a significant warming of about 1.0°C was identified in 1981 for this record, providing strong empirical evidence for the highly unusual late 20th-century temperature changes in this part of the world. Although no regime shift was

identified in the SW AP series, the coldest and warmest intervals occurred between 1983-2005 and 1948-69 and reached the 99.9% level of significance (Fig. 2.10). In both regional AP series the last decade (i.e. 1996-2005) has been the warmest on record (Fig. 2.9 and 2.10). The last 15 years have been particularly warm over the NE sector of the peninsula (Table 2.2).

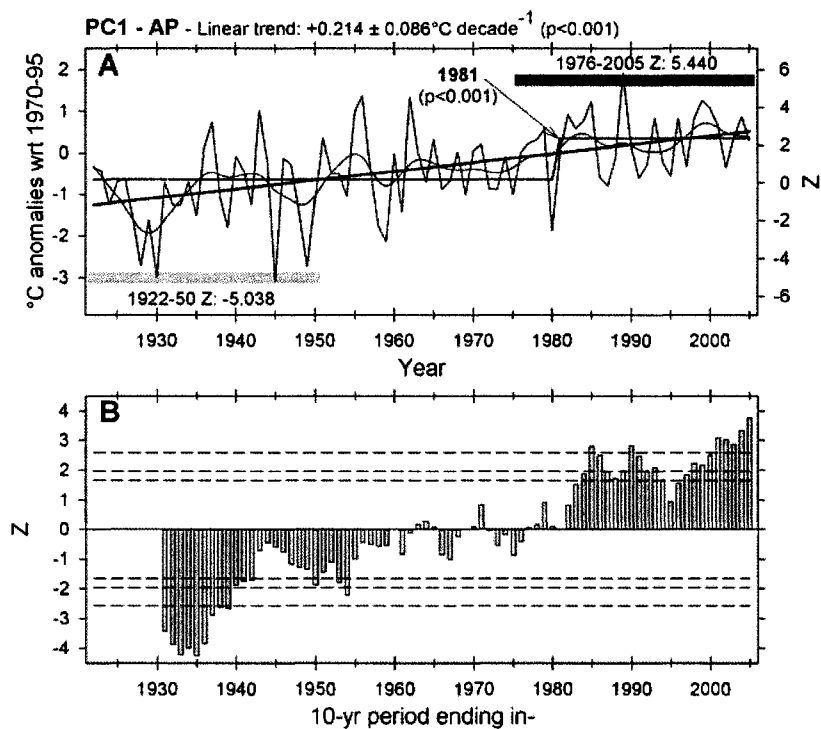


Fig. 2.9. As Fig. 2.4B and 2.4C, but for stations located within the 0.8 contour line in AP PC1 (see Fig. 2.8) for the 1970-95 reference period.

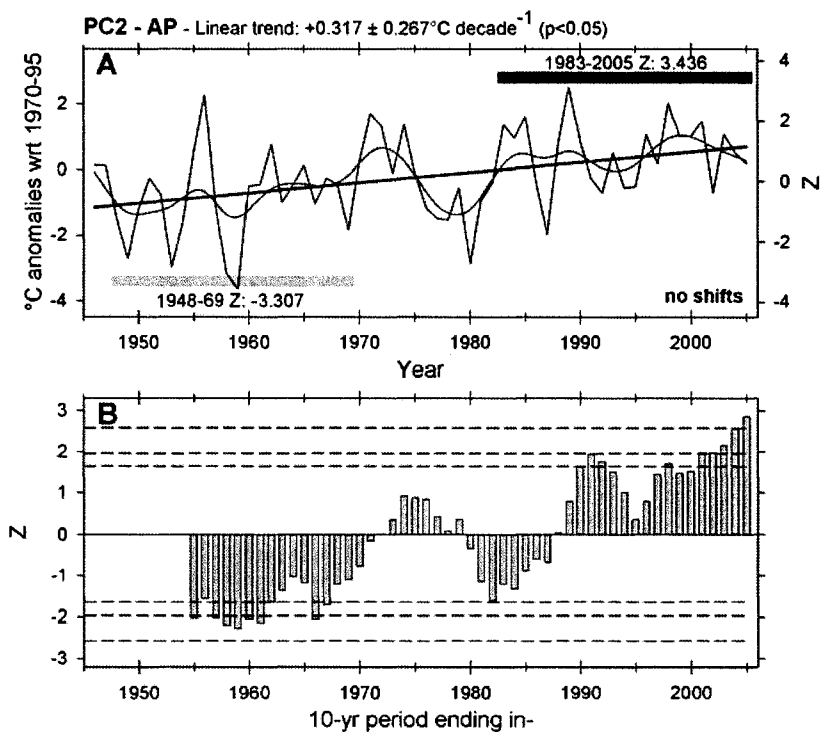


Fig. 2.10. As Fig. 2.9, but for AP PC2 (see Fig. 2.8).

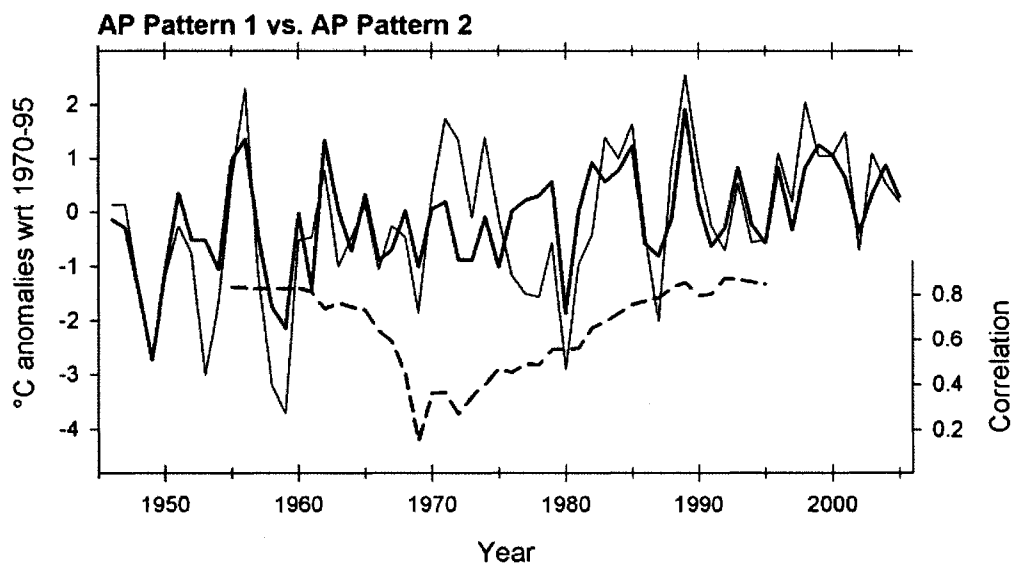


Fig. 2.11. Time series of AP mean annual temperature PC1 (thick line) and PC2 (thin line) over their 1946-2005 overlapping period (see Fig. 2.8). Correlations calculated over 20-yr moving windows (dashed line) are shown to emphasize the disagreement between these two records between about 1970 and 1980.

2.4. Discussion and Conclusions

Previous studies of instrumental surface temperature records from southern South America (SSA) and the northern Antarctic Peninsula and adjacent islands (AP) have found marked, statistically significant warming trends on both sides of the Drake Passage. However, despite their proximity, homogenized temperature records from these regions have not yet been comprehensively analyzed to determine whether there is a common pattern of temporal variability. The proper characterization of climate variations in these areas and across Patagonia is of crucial importance for the better understanding of the regional climate system at local and larger spatial scales and could provide important information regarding the relative influence and spatial extent of the main large-scale atmospheric forcing mechanisms affecting climate variability in this region. The great variety of high resolution proxy climate indicators in this areas (e.g. ice cores in the AP: Peel et al. 1996; tree rings in SSA: Villalba et al. 2003) offers numerous opportunities for the development of paleoclimatic reconstructions that require a good quality instrumental dataset for calibration purposes.

Given the heterogeneous temporal and spatial coverage of available instrumental surface temperature records, previous work in this region has usually selected and analyzed only the longest, most complete records while discarding many shorter series from discontinued stations. In this study we attempted to include as much of this information as possible using two complementary approaches. First, we compiled as much mean monthly temperature data as possible from several local, regional and global sources including updated records and discontinued stations. We then used techniques that maximized the information available from each site and permitted the largest number of stations to be included in the homogeneity analyses, allowing a consistent and objective assessment of the relative homogeneity of these station records. This approach uses first differenced series from highly correlated neighboring stations (that need not have a fixed overlapping period) to develop reference records to assess the relative homogeneity of each candidate station. The homogeneity testing relied on three statistical tests, namely the standard normal homogeneity test for single shifts (Alexandersson 1986), Potter's

bivariate test (Potter 1981), and a modified version of the two-phase regression approach of Easterling and Peterson (1995). The combined results from these tests together with available metadata for each station are the basis for the correction of identified discontinuities.

This methodology was applied to the updated, greatly expanded, surface temperature station dataset (Fig. 2.1 and Table 2.1) to develop a series of relatively homogeneous mean annual station records that cover most of the 20th century. Principal component analyses reduced these records to five distinct regional patterns centered in the AP and the NW, NE, central-northern and southernmost sectors of SSA (Fig. 2.3). The composition of these subregions remained relatively stable when tested over different time intervals (i.e. 1931-60, 1961-2001 and 1969-88, each containing variable combinations of individual station records), indicating that the regional patterns identified over the 1969-88 period are a relatively reliable representation of 20th-century spatial variability across the study area (Fig. 2.3). Based on these results, surface temperature variability in the AP seems to be only weakly related to that observed in the southern tip of SSA and therefore the recent warming reported in previous studies for these two regions is possibly caused by different atmospheric forcing mechanisms. This issue will be explored in a companion study in the near future.

Separate analyses of mean annual data from SSA alone (Figs. 2.4A-2.7A) revealed similar spatial domains to those identified in Fig. 2.3. The dominant strongest pattern was concentrated in the southern tip of the continent and explained almost 50% of the variance in the homogenized station records (Fig. 2.4A). The second and third strongest modes of spatial variability were centered in the NE and NW sectors of SSA and each explained just over one third of the variance (Figs. 2.5A-2.6A)⁶. Similar spatial patterns centered in southern, NE and NW Patagonia were reported by Villalba et al. (2003) using a smaller subset of SSA records (13 vs. 33 stations here) over a longer common interval (1931-90 vs. 1969-88). This suggests that it could be sufficient to utilize only the longest, more complete series if they are relatively evenly distributed spatially and have been carefully checked and corrected for non-climatic discontinuities. However, given the

scarcity of such series and the great size of the study area, the use of the shorter and/or discontinued records *in combination* with the longer and more complete series seems beneficial in at least two aspects. First, the development of relatively well replicated reference series for the homogeneity assessment of the original records was possible only because of the existence of this larger dataset. In most cases, the entire length of almost all original series could be objectively tested, and only a few portions of some station records (e.g. the first decades of the Punta Arenas records, Table 2.1) were considered untestable and excluded from further analysis due to the lack of at least three well correlated neighboring sites for comparison. As we also specifically targeted station data that were as up to date as possible, this approach ultimately resulted in a much larger population of relatively homogeneous series with a longer period of coverage than that analyzed in previous studies (e.g. Rosenblüth et al. 1997; Villalba et al. 2003). Second, the higher density of stations across SSA also offered the opportunity to characterize the spatial variability of recent temperature variations in this region in more detail. This allowed the identification of a fourth spatial pattern concentrated in central-northern Patagonia, that had not been documented previously but emerged clearly in analyses that used the highest station density in both the combined (SSA-AP) and the separate (SSA only) datasets (see Figs. 2.3 and 2.7A).

Based on SSA data we developed four regionally-averaged, variance-adjusted time series over the 1912-2005 interval (Figs. 2.4B-2.7B). In part, our results corroborate those from previous studies that reported warming trends in the southern tip of SSA and a long term cooling tendency in the stations of NW Patagonia west of the Andes (e.g. Rosenblüth et al. 1997; Villalba et al. 2003). However, by combining the analyses of linear trends with the identification of step-like changes and intra- to multi-decadal (IMD) fluctuations over a longer period, our results provide additional, important new information regarding regional temperature variations in SSA. Statistically significant positive trends of 0.037°C and 0.059°C per decade were identified in the 1912-2005 regional series from the southernmost and NE sectors of SSA, with the coldest IMD intervals all occurring in the first three decades of record (Figs. 2.4BC-2.5BC and Table 2.2). Both of these series showed a significant shift towards warmer temperatures around 1977-78 and all the

statistically significant warm intervals occurred after these dates. However, while the southernmost sector experienced the warmest period on record mainly in the 1980s (Fig. 2.4BC), the most extreme warm conditions in the NE sector occurred in the last portion of the series and reached remarkable significance levels when compared against an essentially stationary time series (Fig. 2.5BC and Table 2.2). In contrast, the NW Patagonian sector showed a statistically significant cooling tendency of $-0.053^{\circ}\text{C decade}^{-1}$ and significant decreases in mean annual temperatures following 1933 and 1964 (Fig. 2.6B and Table 2.2). The warmest periods in this record were mainly prior to the mid 1930s and the coldest conditions occurred between 1964 and 1977 (Fig. 2.6BC). Interestingly however, a significant increase towards warmer conditions was observed in the NW SSA sector in 1977, suggesting the late 1970s shift was a widespread, large-scale phenomenon observable across SSA despite differences in the low frequency variability at the subregional level (see Figs. 2.4-2.6). Rosenblüth et al. (1997) and Villalba et al. (2003) also report a noticeable shift towards warmer conditions around 1976 for most stations (and especially those located in the Pacific domain) which was related to changes in the long-term behavior of the Southern Oscillation Index (SOI; Rosenblüth et al. 1997) and the Pacific Decadal Oscillation (PDO; Villalba et al. 2003).

The fourth regional time series, based on records from central-northern Patagonia (Fig. 2.7), showed a positive, non-significant linear trend of $0.016^{\circ}\text{C per decade}$ between 1912 and 2005 and shared some common features with the patterns located immediately to the east and west. We believe this is probably a more realistic representation of climate conditions in this transitional area and confirms the utility of the oblique rotation of the principal components for identifying the main spatial modes of variability across this region. Although no significant positive or negative shifts were detected in this record, significant warm conditions occurred mainly after 1977 in this series (Fig. 2.7BC and Table 2.2). This corroborates the regional extent of the late 1970s climate shift in SSA and possibly contributes to the generalized pattern of glacier recession observed across the Patagonian Andes in recent decades (e.g. Rignot et al. 2003; Masiokas et al. 2007). Identification of these differences also underlines the inappropriateness of using large scale gridded data to characterize regional climates in areas with strong climatic

gradients. Finally, the nonparametric analysis of the relative magnitude of the last 15 years of record in the four SSA series indicates that only the warmth experienced between 1991 and 2005 in the NE sector could be considered statistically significant (Figs. 2.4B-2.7B, Table 2.2). This most recent interval actually exceeded the 99.9% level of significance and is an important contributor to the highly significant positive linear trend observed between 1912 and 2005 in NE SSA (Fig. 2.5BC).

When the limited data from the northern Antarctic Peninsula and adjacent islands (AP) were tested separately, the stations in the NE sector segregated clearly from the two stations in the SW portion of the AP (Fig. 2.8). This contrasting pattern agrees with previous studies which have usually recognized differences between temperature variation in the eastern and western sectors of the AP (e.g. Schwerdtfeger 1970; Martin and Peel 1978; King and Comiso 2003). However, despite this clear spatial differentiation, the two regionally-averaged time series showed significant warming trends with the NE (SW) sector warming at about 0.21°C (0.32°C) decade^{-1} between 1922-2005 (1946-2005) (Figs. 2.9 and 2.10). Although the magnitude of these trends is smaller than previously reported, they are statistically significant even after accounting for the serial correlation observed in the records (Table 2.2). Interestingly, these regional mean annual series showed remarkable similarities during the first and last portions of the records but deviated markedly between ca. 1970-80 (Fig. 2.11). This change in the temperature field is a significant influence on the principal component analysis presented in Fig. 2.8 and was first observed by Schwerdtfeger (1976) between the Orcadas (60.7°S , 44.7°W) and Argentine Island (65.3°S , 64.3°W) stations in the NE and SW sectors of the AP. He ascribed this phenomenon to a relatively local increase of warm air advection and a concurrent decrease in summer sea ice on the west side of the Peninsula between 1970 and 1975. Rogers (1983) suggested that this contrasting pattern could be linked to mid-latitude circulation changes. More detailed investigations, beyond the scope of this study, are needed to resolve this issue.

Despite the 1970-80 discrepancy the two regional AP series show roughly similar results at the IMD level. The coldest and warmest intervals are in the first and last 2-3 decades of

record respectively and reached highly significant levels of significance (Figs. 2.9 and 2.10 and Table 2.2). For example, in the NE sector the warmest regime occurred between 1976 and 2005 and reached a MWZ value of +5.440, well beyond the 99.9% level of significance. This finding, together with a statistically significant jump of ca. 1.0°C identified in 1981 (Fig. 2.9 and Table 2.2) emphasize the exceptional recent warming in this subregion and provide strong, empirical evidence of the highly unusual nature of this phenomenon, at least in a 20th-century perspective.

Although the methodological approach presented here was considered appropriate given the resources available and the spatial and temporal heterogeneity of the records, more work is needed to improve (especially for SSA) the quality and quantity of surface temperature records (and metadata) available. Additional research is also required to evaluate and compare the impacts of different methodologies for testing and correcting for non-climatic inhomogeneities in the available station records. Of special interest for the evaluation of the long-term temperature variations in SSA is the proper identification of the impact of urbanization on the urban and sub-urban stations (e.g. Karl et al. 1988; Parker 2006). We believe this issue has probably had a minor impact in our results because of the windy nature of the Patagonian region and the fact that most stations have or are collecting meteorological information at the local airports located several kilometers from the city centers. The analysis of additional climate variables (such as wind measurements in combination with minimum and maximum daily temperatures, Parker 2006) could help elucidate this issue and provide more accurate surface temperature estimations in SSA.

Our results indicate that most of the instrumental temperature variability observed in SSA and the AP can be explained by few, well defined and relatively time stable dominant modes with distinct low frequency patterns. Linear trend analyses were useful tools in characterizing the long term behavior of the regional time series and, despite minor differences, showed an overall good agreement with the results from previous related studies in SSA and the AP. The differences in trends are to be expected given the way the original records were processed and analyzed (e.g. regionally-averaged series vs.

individual station records) and/or the different time intervals considered in each case. The implementation of two innovative, relatively simple time series analysis techniques provided a much more detailed picture of the complexity of climate changes that occurred at different timescales in each subregion and will hopefully contribute to the understanding of past and present climate variability in this part of the world.

2.5. References

- Aceituno, A., Fuenzalida, H., Rosenblüth, B., 1993. Climate along the extratropical west coast of South America. In: Mooney, H.A., Fuentes, E.R., Kronberg, B.I., (eds.), *Earth system responses to global change – Contrasts between North and South America*. Academic Press, pp. 61-69.
- Aguilar, E., Auer, I., Brunet, M., Peterson, T.C., Wieringa, J. 2003. Guidelines on climate metadata and homogenization. WCDMP-No. 53, WMO-TD No. 1186. World Meteorological Organization, Geneva. 52 pp.
- Akaike, H. 1974. A new look at the statistical model identification. *IEEE Transactions on Automatic Control*, AC-19, 716-723.
- Alexandersson, H. 1986. A homogeneity test applied to precipitation data. *Journal of Climatology* 6, 661-675.
- Alexandersson, H. and Moberg, A. 1997. Homogenization of Swedish temperature data. Part I: homogeneity test for linear trends. *International Journal of Climatology* 17, 25-34.
- Aniya, M., Sato, H., Naruse, R., Skvarca, P. and Casassa, G. 1997. Recent glacier variations in the Southern Patagonia Icefield, South America. *Arctic and Alpine Research* 29, 1-12.
- Cabrera, A.L. and Willink, A. 1973. *Biogeografía de América Latina*. Programa Regional de Desarrollo Científico y Tecnológico, Departamento de Asuntos Científicos, Secretaría General de la Organización de los Estados Americanos, Washington, D.C. 120 pp.
- Conrad, V. and Pollack, C. 1962. *Methods in Climatology*. Harvard University Press, Cambridge, MA, 459 pp.
- Cook, A., Fox, A.J., Vaughan, D.G. and Ferrigno J.G. 2005. Retreating glacier fronts on the Antarctic Peninsula over the last 50 years. *Science* 22, 541-544.
- Coronato, F. and Bisigato, A. 1998. A temperature pattern classification in Patagonia. *International Journal of Climatology* 18, 765-773.

- Dawdy, D.R. and Matalas, N.C. 1964. Statistical and probability analysis of hydrologic data, part III: analysis of variance, covariance and time series. In: Chow, V.T., (ed.), Handbook of Applied Hydrology, A Compendium of Water-Resources Technology, McGraw-Hill Book Company, New York, pp. 8.68-8.90.
- Doake, C.S.M. and Vaughan, D.G. 1991. Rapid Disintegration of Wordie Ice Shelf in Response to Atmospheric Warming. *Nature* 350, 328-330.
- Duchon, C.E. 1979. Lanczos Filtering in one and two dimensions. *Journal of Applied Meteorology* 18, 1016-1022.
- Easterling, D.R. and Peterson, T.C. 1992. Techniques for detecting and adjusting for artificial discontinuities in climatological time series: a review. Proceedings of the 5th International Meeting on Statistical Climatology, Toronto, pp. J28-J32.
- Easterling, D.R. and Peterson, T.C. 1995. A new method for detecting undocumented discontinuities in climatological time series. *International Journal of Climatology* 15, 369-377.
- Hansen, J., Ruedy, R., Glascoe, J. and Sato, M. 1999. GISS analysis of surface temperature change. *Journal of Geophysical Research* 104, 30997-31022.
- Hendrickson, A.E. and White, P.O. 1964. Promax: A quick method for rotation to oblique simple structure. *British Journal of Statistical Psychology* 17, 65-70.
- Hoffman, J.A.J. 1990. De las variaciones de la temperatura del aire en la Argentina y estaciones sub-antárticas adyacentes desde 1903 hasta 1989 inclusive. *Meteorológica* 17(1-2), 11-16.
- Hoffman, J.A.J., Nuñez, S.E. and Vargas, W. 1997. Temperature, humidity and precipitation variations in Argentina and the adjacent sub-Antarctic region during the present century. *Meteorologische Zeitschrift* 6, 3-11.
- Jacka, T.H., Budd, W.F. and Holder, A. 2004. A further assessment of surface temperature changes at stations in the Antarctic and Southern Ocean, 1949-2002. *Annals of Glaciology* 39, 331-338.
- Jacobs, S.S. and Comiso, J.C. 1997. Climate Variability in the Amundsen and Bellingshausen Seas. *Journal of Climate* 10, 697-709.
- Jones, P.D. and Limbert, D.W. 1987. A data bank of Antarctic surface temperature and pressure data. In: Jones, P.D. (ed.). Office of Energy Research, Report no. TR038, US Department of Energy, Washington.

- Jones, P.D. and Reid, P.A. 2001. A databank of Antarctic surface temperature and pressure data. ORNL/CDIAC-27, NDP-032. Oak Ridge, Tennessee, Carbon Dioxide Information Analysis Center, Oak Ridge National Laboratory, US Department of Energy.
- Jones, P.D. and Wigley, T.M.L. 1986. Southern Hemisphere surface air temperature variations: 1851-1984. *Journal of Climate and Applied Meteorology* 25, 1213-1230.
- Jones, P.D., Groisman, P.Ya., Coughlan, M., Plummer, N., Wang, W.C. and Karl, T.R. 1990. Assessment of urbanization effects in time series of surface air temperature over land. *Nature* 347, 169-172.
- Jones, P.D., Osborn, T.J., Briffa, K.R., Folland, C.K., Horton, E.B., Alexander, L.V., Parker, D.E. and Rayner, N.A. 2001. Adjusting for sampling density in grid box land and ocean surface temperature time series. *Journal of Geophysical Research* 106, 3371-3380.
- Jones, P.D., Osborn, T.J. and Briffa, K.R. 1997. Estimating sampling errors in large-scale temperature averages. *Journal of Climate* 10, 2548-2568.
- Kaiser, H.F. 1958. The varimax criterion for analytic rotation in factor analysis. *Psychometrika* 23, 187-200.
- Kaiser, H.F. 1960. The application of electronic computers to factor analysis. *Educational and Psychological Measurement* 20, 141-151.
- Karl, T.R., Diaz, H.F. and Kukla, G. 1988. Urbanization: its detection and effect in the United States climate record. *Journal of Climate* 1, 1099-1123.
- King, J.C. 1994. Recent climate variability in the vicinity of the Antarctic Peninsula. *International Journal of Climatology* 14, 357-369.
- King, J.C. and Harangozo, S.A. 1998. Climate change in the western Antarctic Peninsula since 1945: Observations and possible causes. *Annals of Glaciology* 27, 571-575.
- King, J.C. and Comiso, J.C. 2003. The spatial coherence of interannual temperature variations in the Antarctic Peninsula. *Geophysical Research Letters* 30(2): 1040. doi: 10.1029/2002GL015580.
- King, J.C., Turner, J., Marshall, G.J., Connolley, W.M. and Lachlan-Cope, T.A. 2003. Antarctic Peninsula climate variability and its causes as revealed by instrumental records. In: Domack, E., Burnett, A., Convey, P., Kirby, M., and Bindaschadler, R. (eds.) *Antarctic Peninsula Climate Variability: A Historical and Paleoenvironmental Perspective*. Antarctic Research Series 79, American Geophysical Union, Washington, DC, pp. 17-30.

- Limbert, D.W.S. 1974. Variations in the mean annual temperature for the Antarctic Peninsula, 1904–1972. *Polar Record* 17, 303-306.
- Mann, H.B. and Whitney, D.R. 1947. On a test of whether one of two random variables is stochastically larger than the other. *Annals of Mathematical Statistics* 18, 50-60.
- Martin, P.J. and Peel, D.A. 1978. The spatial distribution of 10m temperatures in the Antarctic Peninsula. *Journal of Glaciology* 20, 311-317.
- Mauget, S.A. 2003. Intra-to multidecadal climate variability over the continental United States: 1932-99. *Journal of Climate* 16, 2215-2231.
- Mauget, S.A. 2004. Low frequency streamflow regimes over the central United States: 1939-1998. *Climatic Change* 63, 121-144.
- Menne, M.J. and Williams, C.N. 2005. Detection of undocumented change points using multiple test statistics and composite reference series. *Journal of Climate* 18, 4271-4286.
- Miller, A. 1976. The Climate of Chile. In: Schwerdtfeger, W. (ed.) *World Survey of Climatology* 12, Climate of Central and South America. Elsevier, Amsterdam, pp. 113-145.
- Osborn, T.J., Briffa, K.R. and Jones, P.D. 1997. Adjusting variance for sample-size in tree-ring chronologies and other regional-mean time-series. *Dendrochronologia* 15, 89-99.
- Parker, D.E. 2006. A demonstration that large-scale warming is not urban. *Journal of Climate* 19, 2882–2895.
- Peel, D.A., Mulvaney, R.M., Pasteur, E.C. and Chenery, C. 1996. Climate changes in the Atlantic sector of Antarctica over the past 500 years from ice-core and other evidence. In: Jones, P. D. Bradley, R. S. and Jouzel, J. (eds.) *Climatic variations and forcing mechanisms of the last 2000 years*. Springer-Verlag, 243-262.
- Peterson T.C., Easterling D.R. 1994. Creation of homogeneous composite climatological reference series. *International Journal of Climatology* 14: 671-679.
- Peterson, T.C. and Vose, R.S. 1997. An overview of the Global Historical Climatology Network temperature data base. *Bulletin of the American Meteorological Society* 78, 2837-2849.
- Peterson, T.C., Easterling, D.R., Karl, T.R., Groisman, P., Nicholls, N., Plummer, N., Torok, S., Auer, I., Boehm, R., Gullett, D., Vincent, L., Heino, R., Tuomenvirta, H., Mestre, O., Szentimrey, T., Salinger, J., Førland, E.J., Hanssen-Bauer, I.,

- Alexandersson, H., Jones P., and Parker, D. 1998. Homogeneity adjustments of in situ atmospheric climate data: a review. *International Journal of Climatology* 18, 1495-1517.
- Pittock, A. 1980. Patterns of climatic variation in Argentina and Chile, II. Temperature, 1931-1960. *Monthly Weather Review* 108, 1362-1369.
- Potter, K.W. 1981. Illustration of a new test for detecting a shift in mean in precipitation series. *Monthly Weather Review* 109, 2040-2045.
- Prohaska, F., 1976. The climate of Argentina, Paraguay and Uruguay. In: Schwerdtfeger, W. (ed.) *World Survey of Climatology* 12, Climate of Central and South America. Elsevier, Amsterdam, pp. 13-112.
- Rau, F., Mauz, F., De Angelis, H., Jaña, R., Arigony Neto, J., Skvarca, P., Vogt, S., Saurer, H., Gossmann, H. 2004. Variations of glacier frontal positions on the Northern Antarctic Peninsula. *Annals of Glaciology* 39, 525-530.
- Richman, M.B. 1981. Obliquely rotated principal components: an improved meteorological map typing technique? *Journal of Applied Meteorology* 20, 1145-1159.
- Richman, M.B. 1986. Rotation of principal components. *Journal of Climatology* 6, 293-335.
- Rignot, E., Rivera A. and Casassa, G. 2003. Contribution of the Patagonia icefields of South America to global sea level rise. *Science* 302, 434-437.
- Rodionov, S.N. 2004. A sequential algorithm for testing climate regime shifts. *Geophysical Research Letters* 31, L09204, doi:10.1029/2004GL019448.
- Rodionov, S.N. 2006. The use of prewhitening in climate regime shift detection. *Geophysical Research Letters* 33, L12707, doi:10.1029/2006GL025904.
- Rogers, J.C. 1983. Spatial variability of Antarctic temperature anomalies and their association with Southern Hemisphere atmospheric circulation. *Annals of the Association of American Geographers* 73, 502-518.
- Rosenblüth, B., Casassa, G. and Fuenzalida, H. 1995. Recent climatic changes in western Patagonia. *Bulletin of Glacier Research* 13, 127-132.
- Rosenblüth, B., Fuenzalida, H. and Aceituno, P. 1997. Recent temperature variations in southern South America. *International Journal of Climatology* 17, 67-85.
- Rott, H., Skvarca, P. and Nagler, T. 1996. Rapid collapse of northern Larsen Ice Shelf, Antarctica. *Science* 271, 788-792.

- Santer, B.D., Wigley, T.M.L., Boyle, J.S., Gaffen, D.J., Hnilo, J.J., Nychka, D., Parker, D.E., Taylor, K.E., 2000. Statistical significance of trends and trend differences in layer average atmospheric temperature time series. *Journal of Geophysical Research* 105, 7337-7356.
- Scambos, T., Hulbe, C. and Fahnestock, M. 2003 Climate-induced ice shelf disintegration in the Antarctic Peninsula. In: Domack, E., Burnett, A., Convey, P., Kirby, M., and Bindshadler, R. (eds.) *Antarctic Peninsula Climate Variability: A Historical and Paleoenvironmental Perspective*. Antarctic Research Series 79, American Geophysical Union, Washington, DC, pp. 79-92.
- Schwerdtfeger, W. 1970. The Climate of the Antarctic. In: Orvig, S. (ed.) *World Survey of Climatology, Climates of the Polar Regions*. Elsevier, New York, pp. 320-322.
- Schwerdtfeger, W. 1976. Changes of temperature field and ice conditions in the area of the Antarctic Peninsula. *Monthly Weather Review* 104, 1441-1443.
- Skvarca, P. and De Angelis, H. 2003. Impact assessment of regional warming on glaciers and ice shelves of the northeastern Antarctic Peninsula. In: Domack, E., Burnett, A., Convey, P., Kirby, M., and Bindshadler, R. (eds.) *Antarctic Peninsula Climate Variability: A Historical and Paleoenvironmental Perspective*. Antarctic Research Series 79, American Geophysical Union, Washington, DC, pp. 69-78.
- Skvarca, P., Rack, W., Rott, H., and Ibarzabal y Donangelo, T. 1998. Evidence of recent climatic warming on the eastern Antarctic Peninsula. *Annals of Glaciology* 27, 628-632.
- Turner, J., Colwell, S.R., Marshall, G.J., Lachlan-Cope, T.A., Carleton, A.M., Jones, P.D., Lagun, V., Reid, P.A. and Iagovkina, S. 2004. The SCAR READER project: towards a high-quality database of mean Antarctic meteorological observations. *Journal of Climate* 17, 2890-2898.
- Turner, J., Colwell, S.R., Marshall, G.J., Lachlan-Cope, T.A., Carleton, A.M., Jones, P.D., Lagun, V. Reid, P.A. and Iagovkina S. 2005. Antarctic climate change during the last 50 years. *International Journal of Climatology* 25, 279-294.
- Vaughan, D.G. and Doake, C.S.M. 1996. Recent atmospheric warming and retreat of ice shelves on the Antarctic Peninsula. *Nature* 379, 328-331.
- Vaughan, D.G., Marshall, G.J., Connolley, W.M., Parkinson, C.L., Mulvaney, R., Hodgson, D.A., King, J.C., Pudsey, C.J. and Turner, J. 2003. Recent rapid regional climate warming on the Antarctic Peninsula. *Climatic Change* 60, 243-274.

- Villalba, R., Lara, A., Boninsegna, J.A., Masiokas, M., Delgado, S., Aravena, J.C., Roig, F.A., Schmelter, A., Wolodarsky, A., and Ripalta, A. 2003. Large-scale temperature changes across the southern Andes: 20th-century variations in the context of the past 400 years. *Climatic Change* 59, 177-232.
- White, D., Richman, M. and Yarnal, B. 1991. Climate regionalization and rotation of principal components. *International Journal of Climatology* 11, 1-25.
- Wilcoxon, F. 1945. Individual comparisons by ranking methods. *Biometrics Bulletin* 1, 80-83.

The preceding chapter identified the main spatio-temporal modes of variability in observed surface temperatures in southern South America and the Antarctic Peninsula using updated, homogenized records. Chapter 3 focuses on a smaller area (the NW Patagonian region) but uses a more diverse set of data (i.e. repeat photographs, climate and streamflow data, and moraine records) to assess the main glacier and hydro-climatic changes observed in this region during the past century. Regional precipitation and temperature records are used to develop a climatic index or “mass balance proxy” series that mimics glacier conditions in this region. The improved temperature records developed in Chapter 2 were not available when Chapter 3 was written and gridded records from a widely used global dataset were used instead. An improved, extended analysis using data from Chapter 2 is presented in Chapter 6.

Chapter 3 was published in *Global and Planetary Change*, Vol. 60, pages 85-100, Copyright Elsevier (2008). The list of co-authors is:

Mariano H. Masiokas^{1,2}, Ricardo Villalba¹, Brian H. Luckman², Marcelo E. Lascano¹, Silvia Delgado¹, and Petr Stepanek³

¹ Instituto Argentino de Nivología, Glaciología y Ciencias Ambientales (IANIGLA-CONICET), Mendoza, Argentina.

² Department of Geography, University of Western Ontario, London, Ontario, Canada.

³ Czech Hydrometeorological Institute (CHMI), Regional Office Brno, Czech Republic.

Chapter 3: 20th-century glacier recession and regional hydroclimatic changes in northwestern Patagonia

3.1. Introduction

In most mountainous areas of the world, glaciers are critical sources of fresh water and a crucial contributor to the sustainability of numerous socio-economic activities such as hydroelectric power generation, agriculture, and tourism (e.g. Coudrain et al. 2005). In such regions long, complete climate records are usually scarce. Glaciers can provide a longer term perspective for the study of climatic variations (e.g. Klok and Oerlemans 2004), and are considered key indicators for the early detection of global climate changes (Dyurgerov and Meier 2000; Hoesle et al. 2003; Oerlemans 1994, 2001, 2005; Haeberli 2005).

The Patagonian Andes (Fig. 3.1) contain over 20,000 km² of glaciers, by far the largest glacierized area in South America. Glaciers are mostly concentrated south of 45°S, with the Northern and Southern Patagonian Icefields covering ca. 4,200 and 13,000 km², respectively (Aniya et al. 1988, 1996). Unfortunately, the absence of long (>10 years) annual mass balance records in this region seriously hampers the study of interannual glacier variations and the assessment of the relative influence of the main climate variables on the mass balance of these glaciers (Warren and Sugden 1993; Rivera et al. 2000). Nevertheless, the noticeable retreat of Patagonian glaciers during the 20th century has been generally linked to the combined effect of increased temperatures and decreasing precipitation (Rosenblüth et al. 1995, 1997; Rivera 2004; Rivera et al. 2000, 2002; Villalba et al. 2003, 2005). Recent studies by Bown (2004) and Rivera et al. (2005) suggest that the drastic ice mass loss observed during the past four decades in the northern Patagonian Andes might also be related to the significant tropospheric warming trend observed in radiosonde records in the region (e.g. Aceituno et al. 1993). However, few studies have analyzed the short-term (i.e. sub-decadal) climate variations during the last century and their influence on local glacier behavior (particularly related to periods of glacier readvance) is still poorly understood. Most previous glacier studies have focused on the large glaciers of the southern Patagonian Andes, and the potential

contribution of the relatively small glaciers located north of 45°S to studies of past and present climate changes in the region has not been fully exploited.

In this paper we present selected paired photographs documenting glacier recession in the north Patagonian Andes¹ over the past 110 years. In most cases, these include the earliest known photographs for these glaciers and are part of a recent compilation of such materials by Instituto Argentino de Nivología, Glaciología y Ciencias Ambientales (IANIGLA) to study climate and glacier fluctuations in this region. We have also analyzed updated, homogenized climate records from 1912-2002 for stations between 39°S and 45°S to develop a simple climatic index or “mass balance proxy” based on April-September (long winter) precipitation and October-March (long summer) temperature series. Given the lack of mass balance records for this region, this index provides a rough measure of the relative magnitude of the accumulation and ablation seasons in any given year. Comparison of available glacier history with decadal scale variations in the climatic index provides insight into the causes of glacier fluctuations of this region during the 20th century. In an additional test the reliability of the regional climatic series developed in this study was assessed by comparing them with independently measured streamflow records east of the Andes. As river discharge is mainly fed by winter precipitation, close agreement between these variables provides mutual verification of the quality of these records.

3.2. Study Area

The north Patagonian Andes (Fig. 3.1) form an effective topographic barrier to the westerly air masses that dominate circulation in this region and therefore produce steep climatic gradients across the mountain range. At ca. 40°-41°S, the main cordillera experiences over 4000 mm precipitation per year (Prohaska 1976) whereas the xeric Patagonian steppe less than 100 km east of the Andes, receives less than 200 mm/year (Veblen and Lorenz 1988; Villalba et al. 2003). Mean annual temperatures vary from around 11°C at the Chilean coast to ca. 8°C in the forest-steppe limit in Argentina (Prohaska 1976; Miller 1976). Although absolute minimum temperatures in this region

¹ Considered here as the portion of the Andes between 38°S and 45°S.

can fall below -15°C , mean temperatures for the coldest month (July) vary between 4°C to 8°C in Chile to 2°C to 4°C in Argentina. Mean temperatures for the warmest month (January) range from 14° to 18°C (Prohaska 1976). These mild environmental conditions and the lower elevations of the north Patagonian Andes result in a limited glacierized area with relatively small glaciers on the highest peaks and volcanoes along the mountain range (Lliboutry 1998).

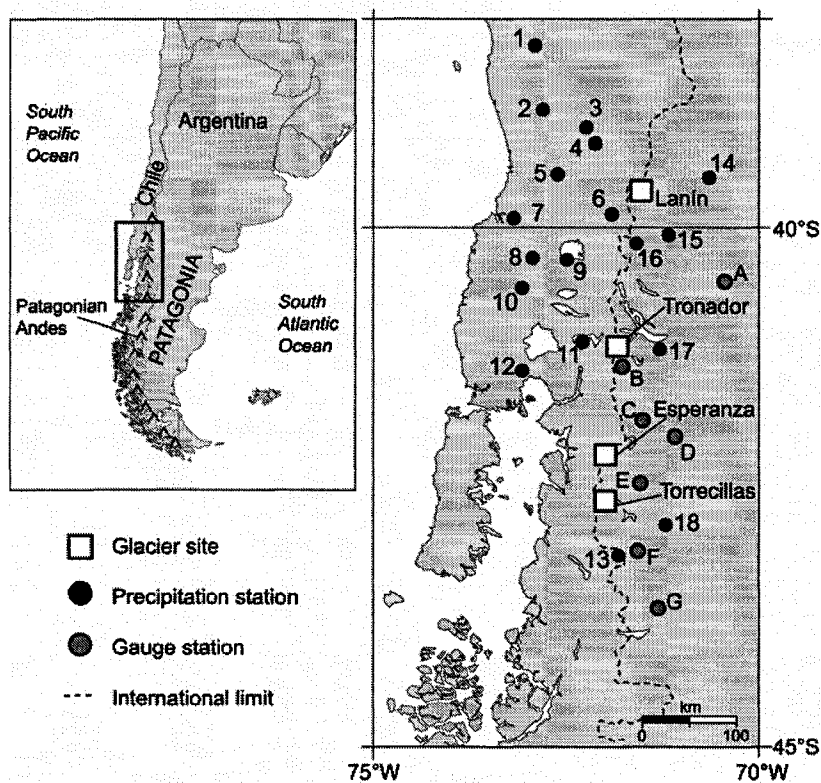


Fig. 3.1. Map of northwestern Patagonia showing the location of the glacier sites (white squares), the precipitation (black dots) and streamflow gauge stations (grey dots) used in this study. Mean monthly temperature anomalies for the grid cell between 40° - 45°S and 70° - 75°W grid cell were obtained from the CRUTem2v gridded dataset (Jones and Moberg 2003). The codes for precipitation and streamflow gauging stations are described in Tables 3.1 and 3.2, respectively.

Twentieth-century glacier changes in the north Patagonian Andes have been studied using aerial photographs, satellite imagery, historical documents, tree-ring records, and field measurements (e.g. Rabassa et al. 1978; Villalba et al. 1990; Bown 2004; Rivera et

al. 2002, 2005). However, and in contrast to the south Patagonian Andes (i.e. south of 45°S), few preliminary glacier inventories are available for this area. Lliboutry (1998) estimates that glaciers cover an approximate area of 300 km² between 35°S and 45°S and occur mainly west of the continental divide. The relatively small size of glaciers in this area makes them particularly sensitive to synoptic changes in climate (Oerlemans and Fortuin 1992), and thereby valuable sources of information for the study of hydroclimatic variations in this region.

Rivers originating in the north Patagonian Andes have a huge socio-economic importance at regional and national scales as sources of fresh water for domestic consumption, irrigation, industries, hydroelectric generation, and recreational activities. For example, 51.8% of Argentina's total hydroelectric generation in 2003 was based on the rivers flowing from the north Patagonian Andes (Secretaría de Energía 2004). On the Chilean side, the multi-million dollar scale salmon industry closely depends on fresh water volumes from the mountains to regulate the salinity and oxygen of the estuarine environments where the farming structures are located (Lara et al. 2005). Fortunately, a remarkably good database of mean monthly discharges exists for most of the rivers east of the Andes. In some cases the available records extend for almost 90 years and contain very few missing months, which makes them one of the longest, most complete runoff records in South America. Of particular relevance for the purposes of this study, these records can be used as an independent variable to further verify the validity of the limited climatic information available for this area.

3.3. Data and Methods

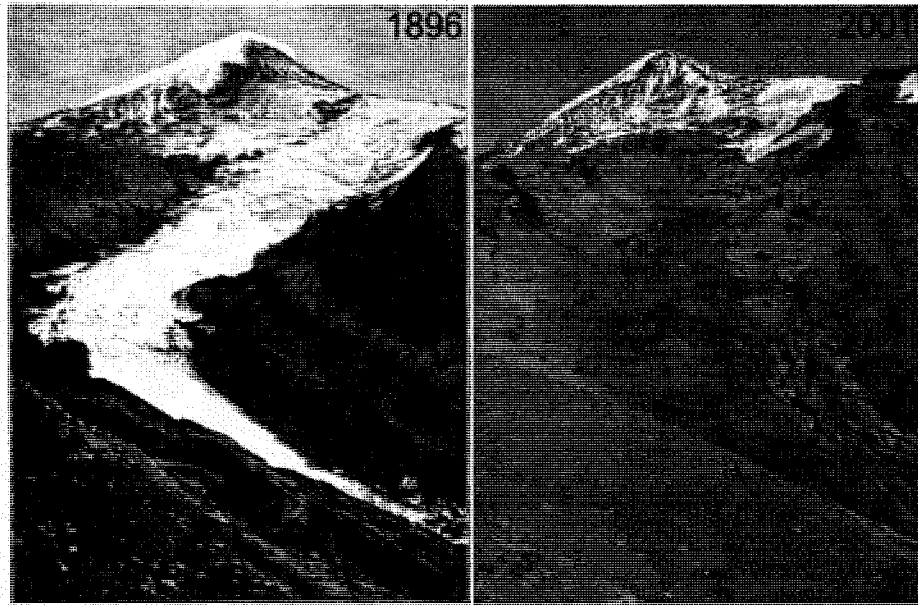
3.3.1. Repeat ground photography

Historical records represent a valuable tool to study glacier fluctuations because they can provide precise information about glacier volumes and frontal positions in past decades and even centuries (e.g. Zumbühl and Holzhauser 1988). Paired with recent photographs, these historical documents can also be used to show, in a simple yet powerful way, the impacts of recent climate changes on these remote, climate-sensitive environments (Hamilton 1965; Rogers et al. 1984). The beauty and remoteness of the Patagonian Andes

have attracted explorers, climbers and researchers since the beginning of the 20th century, and a relatively good collection of historical documents exists for some specific areas (e.g. Kölliker et al. 1917; De Agostini 1945). Many publications contain maps, site descriptions and terrestrial photographs that can be used to establish the former position of the glaciers. For example, the detailed 1857 drawing of the Frías valley and Mount Tronador (Fonck and Hess 1857), and a picture of Frías Glacier taken by De Agostini in the 1930s were used by Villalba et al. (1990) to complement their tree-ring based chronology of ice front positions at Frías Glacier.

Until recently these valuable documents have not been analyzed or compiled into an accessible regional database that could facilitate glaciological and environmental studies in Patagonia. In the late 1990s, IANIGLA began to collect available scientific and non-scientific bibliographic materials concerning Patagonian environments and compile the historical documents (photographs, maps, diagrams, notes, etc) for glaciers in Patagonia. In order to evaluate the changes in glacier areas, volumes, and ice front positions, this initiative was complemented, whenever possible, by repeat photography of the same views. This expanding database now contains several hundred historical documents and sets of paired photographs showing glacier change over the last century. We selected six glaciers between 39°S and 43°S for which good quality comparative photographs are available (Fig. 3.2). These include the earliest known photographs for these glaciers, and are among the earliest in Patagonia.

A - Lanín Norte Glacier (39° 39'S, 71° 30'W)



B - Frías Glacier (41° 09'S, 71° 51'W)

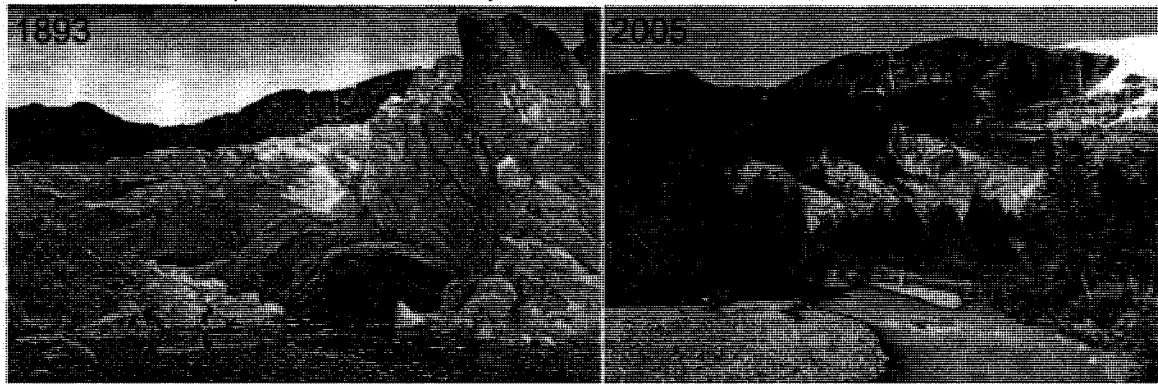
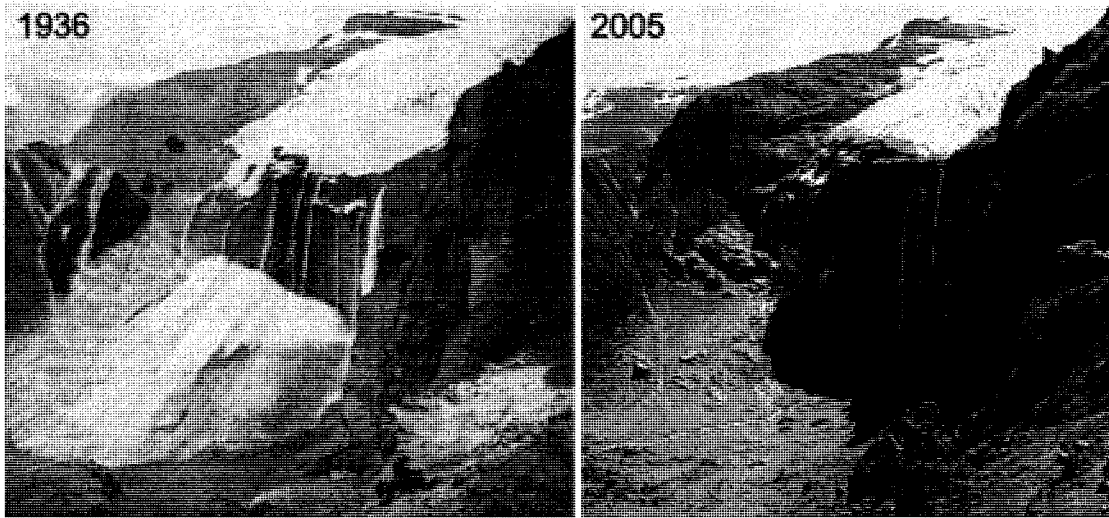


Fig. 3.2. Selected photographic comparisons showing changes in the glaciers of the north Patagonian Andes between 40° and 44°S. (A) The Lanín Norte Glacier in 1896 (Hauthal 1904) and 2001 (photo R. Villalba). (B) The Frías Glacier in the Tronador Area has receded markedly between 1893 (Steffen 1909) and 2005 (photo M. Masiokas).

C - Castaño Overo Glacier



D - Ventisquero Negro Glacier

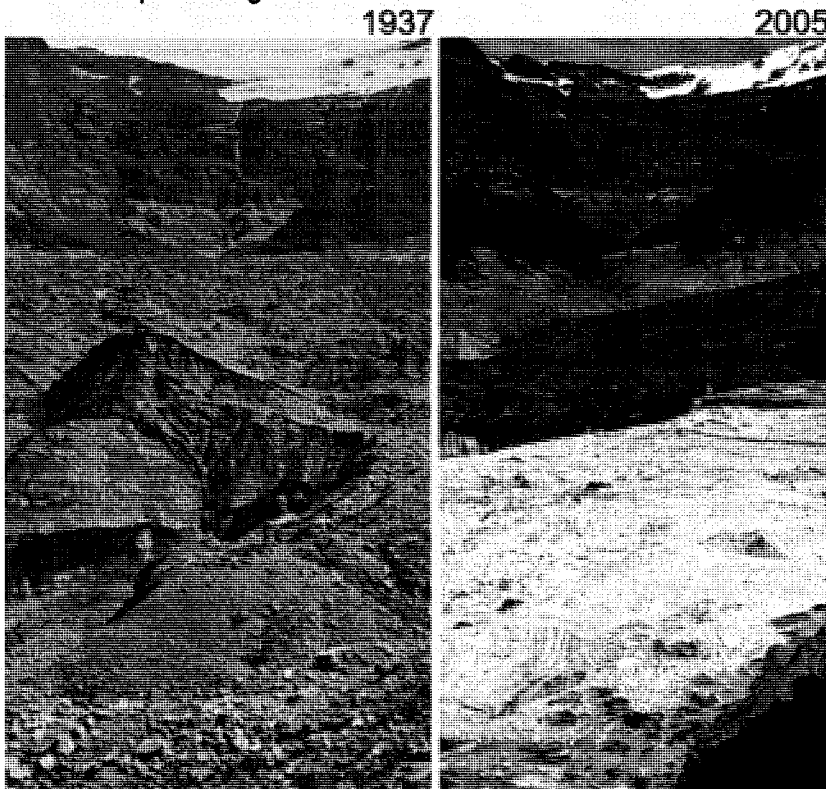
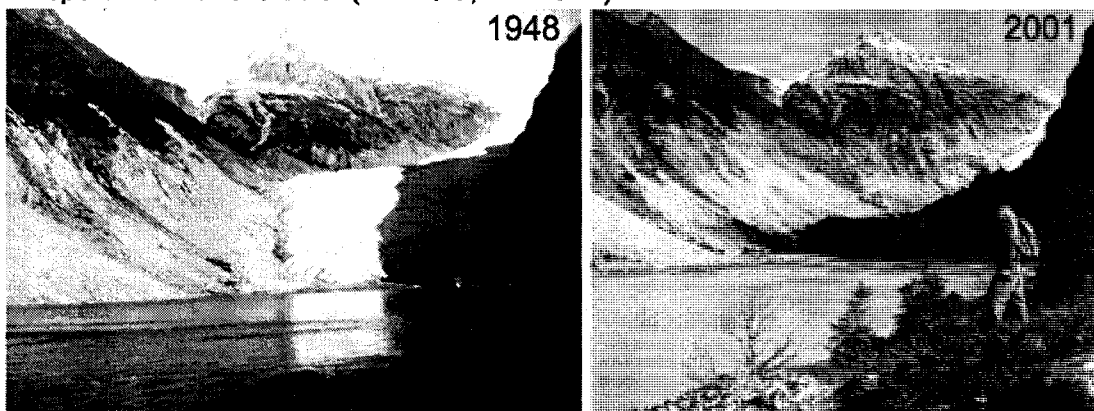


Fig. 3.2 (cont'd). (C) The Castaño Overo Glacier in the Tronador Area shown in 1936 (Jakob 1936) and 2005. (D) The southernmost of the Argentinean glaciers in the Tronador Area, the Ventisquero Negro Glacier (also known as Río Manso Glacier) has thinned markedly between 1937 (Jakob 1937) and 2005. Note the ice-covered proglacial lake in the foreground of the most recent view. Both 2005 photos were taken by R. Villalba.

E - Esperanza Norte Glacier ($42^{\circ} 15'S$, $72^{\circ} 10'W$)



F - Torrecillas Glacier ($42^{\circ} 40'S$, $71^{\circ} 55'W$)

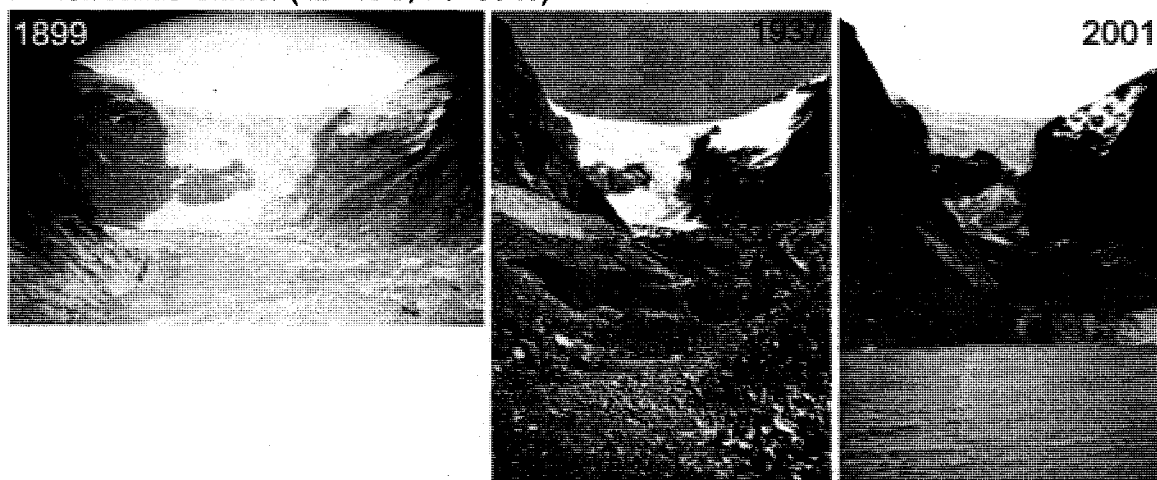


Fig. 3.2 (cont'd). (E) The Esperanza Norte Glacier is located in a largely unexplored portion of the north Patagonian Andes around $42^{\circ}S$ and has receded drastically between 1948 (Neumeyer 1949) and 2001. (F) The Torrecillas Glacier, a conspicuous feature of Parque Nacional Los Alerces, has thinned and retreated markedly during the past century. The photograph on the left was taken by F.P. Moreno in 1899 and is courtesy of Museo de la Patagonia, Bariloche, Argentina. Although it is not exactly matched (it was not at hand when we visited the area), we have included this view to assess the glacier changes over an extended period. The view in the middle was published by Koutche and Ladvoat in 1937. Both 2001 photos were taken by R. Villalba.

3.3.2. Climate records

The poor quality of climatic data and the inadequate spatial distribution of meteorological stations in Patagonia mean that the climatic variability of this region is poorly documented and therefore difficult to characterize (Rosenblüth et al. 1997). Furthermore, it is very difficult and often impossible to obtain the station metadata (data about the stations' histories) to evaluate possible non-climatic variation or inhomogeneities in the records. We have compiled climate data from several sources to obtain a relatively complete, updated climatic dataset for the region. Mean monthly temperature series were obtained for the 40°-45°S and 65°-70°W grid cell from the CRUTem2v dataset (Jones and Moberg 2003, Climatic Research Unit, UK, <http://www.cru.uea.ac.uk/>). These are homogenized data for land stations only expressed as anomalies from the 1961-1990 reference period. These monthly records were averaged into annual (April-March), cold season (April-September), and warm season (October-March) temperature anomaly series for the analysis of two hypothetical "accumulation" and "ablation" seasons over the 1912-2002 period. Each year or season is identified by the year of the earliest month (e.g. the 2002 year runs from April 2002 to March 2003).

Monthly total precipitation records for sites between 38°S and 44°S were obtained from Version 2 of the Global Historical Climatology Network (Vose et al. 1992), and various institutions in Chile and Argentina (Table 3.1). Since many of these records are short or incomplete, we selected 18 stations that provided the most complete (< 7% missing) and longest (>30 years long) records covering the 1961-1990 interval (Fig. 3.1 and Table 3.1). Missing months were estimated by linear regression using reference series created from up to 10 neighboring stations significantly correlated with the candidate series. These reference series were also used to evaluate potential inhomogeneities (see Pittock 1980) in the data for each station. The Alexandersson ratio test (Alexandersson 1986) was used to obtain adjustment coefficients, identify the location and evaluate the statistical significance of potential inhomogeneities. Given the absence of metadata for these precipitation stations, each series was adjusted only when the ratio test reached the 95% critical level. Following Jones and Hulme (1996), annual and seasonal totals for each station were converted to percentages of their 1961-1990 mean and averaged to

create a set of annual, cold season, and warm season precipitation series from 1912 to 2002 for the region.

In the absence of long, complete climatic data from high elevation sites, most of the climatic records used in this analysis come from lowland stations that are distant from the mountain range and therefore their representativeness may be questioned. To address this issue we correlated the annual regional temperature and precipitation series with 1969-1995 annual records from the Mascardi meteorological station ($41^{\circ} 16'S$, $71^{\circ} 39'W$, 842 m). Although this record was too short to be included in the regional climate series, this station is 15 km east of the Tronador glaciers (Fig. 3.2B-D) and is thought to be representative of climate conditions that influence these glaciers (Rabassa et al. 1978; Villalba et al. 1990). Thus, the Mascardi records provide a partial validation of the regional temperature and precipitation series. In addition we performed a Principal Component Analysis (PCA) on the 18 annual precipitation records to evaluate the strength of the climatic signal on both sides of the mountain range.

Table 3.1. Stations used to develop regionally-averaged series of annual and seasonal precipitation variations for northwestern Patagonia between 38° and $44^{\circ}S$. Data sources: (GHCN) Global Historical Climatology Network Version 2 (Vose et al. 1992); (DGA) Dirección General de Aguas, Chile; (DMC) Dirección Meteorológica de Chile; (ENDESA) Empresa Nacional de Electricidad, Chile; (AIC) Autoridad Interjurisdiccional de Cuencas de los Ríos Neuquén, Limay y Negro, Argentina.

Station (code in Fig. 3.1)	Lat., Long.	Elev.	Period	1961-90 annual mean	Apr-Sep contrib. to annual totals	Data source
Lumaco (1)	$38^{\circ} 09'S$ $72^{\circ} 54'W$	60 m	Jan 1948- Dec 2001	1352.2 mm	72.9 %	DGA
Temuco (2)	$38^{\circ} 48'S$ $72^{\circ} 48'W$	114 m	Jan 1912- Apr 2003	1147.2 mm	72.5 %	GHCN
Los Laureles (3)	$38^{\circ} 59'S$ $72^{\circ} 14'W$	190 m	Jan 1947- Dec 2001	2021.8 mm	72.9 %	DGA
Flor del Lago (4)	$39^{\circ} 09'S$ $72^{\circ} 07'W$	300 m	Jan 1961- Dec 2001	2592.1 mm	74.3 %	DMC
Purulón (5)	$39^{\circ} 28'S$ $72^{\circ} 36'W$	95 m	Jan 1936- Dec 2000	2145.9 mm	75.9 %	DMC
Puerto Fuy (6)	$39^{\circ} 52'S$ $71^{\circ} 54'W$	596 m	Jan 1961- Dec 1996	4297.4 mm	70.7 %	ENDESA
Valdivia (7)	$40^{\circ} 00'S$ $73^{\circ} 06'W$	19 m	Jan 1912- Apr 2003	1953.7 mm	77.0 %	GHCN

Table 3.1. (cont'd).

Río Bueno (8)	40° 18'S 72° 56'W	70 m	Jan 1940- Dec 2000	1126.3 mm	72.6 %	DMC
Lago Ranco (9)	40° 18'S 72° 30'W	79 m	Jan 1931- Dec 2000	1938.1 mm	69.8 %	DMC
Osorno (10)	40° 36'S 73° 04'W	65 m	Jan 1961- Dec 2001	1325.2 mm	72.9 %	DMC
Punta Huano (11)	41° 08'S 72° 17'W	200 m	Jan 1961- Dec 2000	3146.2 mm	71.0 %	DMC
Puerto Montt (12)	41° 24'S 73° 06'W	81 m	Jan 1907- Apr 2003	1770.7 mm	65.1 %	GHCN
Futaleufú (13)	43° 12'S 71° 49'W	317 m	Jan 1961- Dec 2001	2073.4 mm	70.0 %	DMC
Ea. Campo Grande (14)	39° 30'S 70° 38'W	960 m	Jan 1947- Dec 1998	471.9 mm	77.2 %	AIC
Ea. Collún Co (15)	40° 04'S 71° 10'W	875 m	Jan 1912- Dec 1998	900.2 mm	80.4 %	AIC
Ea. Quechuquina (16)	40° 09'S 71° 35'W	640 m	Jan 1957- Dec 1998	2145.9 mm	75.9 %	AIC
Bariloche (17)	41° 12'S 71° 12'W	840 m	Jan 1931- Apr 2003	802.5 mm	79.0 %	GHCN
Esquel (18)	42° 54'S 71° 12'W	785 m	Jan 1916- Apr 2003	497.9 mm	73.1 %	GHCN

3.3.3. Regional climatic index, 1912-2002

The lack of long glacier mass balance records seriously hampers the analysis of interannual and interdecadal climatic impacts on glacier behavior in the Patagonian Andes (see e.g. Hodge et al. 1998; McCabe et al. 2000; Rasmussen and Conway 2004; Nesje 2005). We therefore developed a regional climatic index (or “mass balance proxy”) which estimates the relative magnitude of surrogates for winter accumulation (cold season precipitation) and summer ablation (warm season mean temperatures) in the study area. The regional winter anomaly series was developed by averaging anomalies (Z scores) of the April-September precipitation totals from the individual stations, each standardized to the 1961-1990 mean. The October-March gridded temperature records were also converted to Z scores. The climatic index was developed by subtracting the temperature anomalies from the precipitation anomalies such that relatively wet winters and cool summers result in positive indices (overall “positive” mass balance conditions in the region), and vice versa. In years when heavy winter precipitation was followed by warm summers the climatic index is close to zero. In developing these proxies the choice of specific months and length of season is somewhat arbitrary and only intended to

provide a simple yet reasonable surrogate for the relative importance of accumulation vs. ablation in any given year. It is not known for example whether precipitation or temperature variability is the more significant driver of mass balance variations in this region: obviously, as future north Patagonian glacier mass balance data become available (e.g. Rivera et al. 2005), more realistic selection and weighting for these proxies can be developed. We compared the smoothed, low-frequency (i.e. decadal or longer) variations in the regional climatic index with the periods of glacier advances that have been reported for this region during the 20th century (such data are only available for the Tronador Area at around 41°10'S, Fig. 3.1). Although preliminary and largely qualitative, this exercise was attempted to provide the first assessment of the potential influence of decadal climate variations on glacier behavior in northwestern Patagonia. Given the small size of these glaciers (7-19 km²; Rabassa et al. 1978) we expect them to have a relatively short response time to climate fluctuations (Johannesson et al. 1989). However, the possible influence of non-climatic, site-specific factors (such as bed topography, debris cover, etc) at individual glaciers, coupled with the small sample size and inherent limitations in dating glacier deposits (Porter 1981) suggest such comparisons should be interpreted cautiously.

3.3.4. Relationships with regional streamflow records

The northwestern Patagonian climate usually has dry summers and wet winters: 65-80% of annual precipitation falls between April and September (Table 3.1). Therefore the climatic index described above may also be used as a measure of the balance between winter moisture input and summer evapotranspiration in a given basin. In addition, and given the relatively small glacierized area in the north Patagonian Andes, variations in this index should be strongly related to the discharge of local rivers that are mainly fed by winter precipitation. Therefore agreement between the independent estimates of regional river discharges and regional climatic records should provide an additional test of the quality and consistency of these records.

Mean monthly discharges were obtained for seven of the most important rivers between 40° and 44°S that have the longest and most complete flow records in Patagonia (Fig. 3.1

and Table 3.2). Missing monthly values in each gauge station were estimated using a reference series created from those remaining streamflow records significantly correlated with the candidate series. The gauge station records for the Futaleufú and Limay rivers (discontinued in 1976 and 1990 respectively due to dam construction) were updated with data from active gauging stations upstream from the original sites. Subsequently, mean annual (April-March) streamflow records were expressed as percentages of their 1961-1990 mean and averaged to create a regional streamflow series for 1903-2004.

Table 3.2. Streamflow records used in this study. Mean annual discharges refer to an April-March water year and were obtained mostly from Subsecretaría de Recursos Hídricos (SSRH 2004). Notes: (†) April 1990 – September 2005 completed with data from Aluminé (at Huechahue), Chimehuin (at Puesto Confluencia), Caleufú (at Puesto Córdoba) and Limay Superior (at Villa Llanquín); (‡) April 1976 – September 2005 from Futaleufú Embalse (43° 07'S, 71° 39'W, 320m); data from E. Flamenco (pers. comm.), and Compañía Administradora del Mercado Mayorista Eléctrico (CAMMESA), <http://memnet2.cammesa.com/>.

River (basin area)	Gauge station (code)	Lat., Long.	Elev.	Period of record (% missing)	Mean annual discharge
Limay (26400 km ²)	Paso Limay (A)	40 32'S 70 26'W	538 m	Apr 1903 – Sep 2005 (†)	717.3 m ³ s ⁻¹
Manso (750 km ²)	Los Alerces (B)	41 23'S 71 46'W	728 m	Apr 1951 – Mar 2003 (1.7%)	44.7 m ³ s ⁻¹
Quemquemtreu (650 km ²)	Escuela No. 139 (C)	41 54'S 71 30'W	750 m	Apr 1956 – Mar 2003 (1.6%)	9.5 m ³ s ⁻¹
Chubut (1200 km ²)	El Maitén (D)	42 06'S 71 10'W	680 m	Apr 1943 – Mar 2003 (0.8%)	19.5 m ³ s ⁻¹
Carrileufú (580 km ²)	Cholila (E)	42 30'S 71 32'W	535 m	Apr 1957 – Mar 2003 (2.3%)	48.4 m ³ s ⁻¹
Futaleufú (4650 km ²)	Balza Garzón (F)	43 09'S 71 34'W	320 m	Apr 1948 – Sep 2005 (‡)	277.7 m ³ s ⁻¹
Carrenlufú (1500 km ²)	La Elena (G)	43 42'S 71 18'W	802 m	Apr 1954 – Mar 2003 (1.5%)	33.3 m ³ s ⁻¹

Simple correlation analyses were used to evaluate the strength of the relationships between the regionally-averaged streamflow record, the climatic index, and the annual and seasonal temperature and precipitation composites from the study area. The statistical significance of these correlations was estimated using an “effective sample size” (based

on the lag-1 autocorrelation of the raw data, Dawdy and Matalas 1964). The statistical significance of least-squares linear trends in these regional records was assessed following a conservative approach which also accounts for the temporal autocorrelation in these time series (the AdjSE + AdjDF approach of Santer et al. 2000, see Appendix 2).

3.4. Results

3.4.1 Photographic comparisons

Figure 3.2 includes some of the oldest documentation of glacier positions in Patagonia and clearly indicates that glacier recession has been a generalized phenomenon in the north Patagonian Andes during the past century. However, the large temporal gap between observations (>100 years in some cases) indicates that these images can only be used as endpoints of the sequence of glacier variations during this time frame. In addition to the marked glacier front retreats of, for example, the Lanín Norte and Frías glaciers (Fig. 3.2A and 3.2B), some of the less steep glaciers (e.g. Ventisquero Negro Glacier, Fig. 3.2D) have lost ice mass mainly by thinning. Overall, these comparisons reveal that over the past century the climate conditions in the region have clearly favored ablation over accumulation in the mass balance of these glaciers.

3.4.2. Climate changes in northwestern Patagonia, 1912-2002

A series of long, homogeneous annual (April-March), cold season (April-September), and warm season (October-March) regionalized temperature and precipitation records between 1912-2002 were used to complement the photographic comparisons and analyze the possible climatic influence in this noticeable ice mass loss. Despite the broad spatial extent and inherent low-elevation nature of these climatic series, the regionalized climate records revealed a strong coherent signal that provides reliable indicators of climatic conditions across northwestern Patagonia (Fig. 3.1). These records are significantly correlated ($r = 0.87$ for temperature; 0.86 for precipitation,) with the 1969-1995 records from the higher elevation Mascardi station, ca. 15 km east of the Tronador glaciers (Fig. 3.2B-D). In addition, even though annual precipitation totals vary from over 4000 mm to less than 500 mm (Table 3.1), a Principal Component Analysis performed on the 18

precipitation stations indicated that 62.9% of the variance was contained in the first PC over the 1961-1995 common interval.

The linear trend analyses performed on the annual (April-March), cold season (April-September), and warm season (October-March) regional temperature and precipitation series (Table 3.3) showed that these variables have experienced opposite long-term patterns between 1912 and 2002. Annual and seasonal gridded temperature records showed similar, statistically significant positive linear trends of around +0.056 °C per decade even after a marked adjustment to the degrees of freedom due to the serial correlation in their regression residuals (Table 3.3). Highly significant negative linear trends were found for the equivalent precipitation records with cold season totals showing the steepest decrease at -4.89% per decade (Table 3.3).

Table 3.3. Linear trend analysis for regional temperature, precipitation, climatic index, and streamflow variations in northwestern Patagonia between 1912 and 2002. The lag-1 autocorrelation coefficient in the regression residuals of each series (r_1) was used to calculate an “effective sample size” ($neff$) and estimate the statistical significance (t test) of linear trends (Santer et al. 2000). Notes: *(**) Significant at the 95% (99%) confidence level.

Variable	r_1	$neff$	Linear trend (values per decade)
Temp. Apr-Mar	0.386	40	+0.056°C **
Temp. Apr-Sep	0.360	43	+0.056°C *
Temp. Oct-Mar	0.202	60	+0.056°C **
Precip. Apr-Mar	0.040	84	-4.67% **
Precip. Apr-Sep	0.025	89	-4.89% **
Precip. Oct-Mar	0.031	86	-3.71% **
Climatic Index	0.095	75	-0.399 Z scores**
Runoff Apr-Mar	0.145	68	-3.91% **

Temperatures in the northwestern Patagonian region have experienced a marked interannual variability and distinctive low-frequency (decadal-scale) patterns within this long term trend (Fig. 3.3A). The highest warm season temperatures occurred in 1943 (average anomaly of +0.82°C) with extended warm temperatures between 1950 and the

early 1960s, and again between the late 1970s to about 1990. It is interesting to note that, although the post-1990 values have remained warmer than the long-term mean, they have not reached the early 1940s extreme levels in this region. Intervals of extended below-average temperatures occurred during the first three decades in these series and again between the mid 1960s and mid 1970s when the two coldest years on record (1970 and 1975) reached -0.87°C below the mean. The analysis of annual (April-March) values revealed very similar low-frequency patterns throughout the century. The marked cooling trend between the early 1940s and the late 1970s (Fig. 3.3A) has been identified by previous studies as the most noticeable feature in northwestern Patagonia west of the Andes (e.g. Rosenblüth et al. 1997; Villalba et al. 2003) However, our results indicate that when analyzed over the extended 1912-2002 period, this cooling trend is not sufficient to counteract the overall warming tendency observed in the region.

Above-average cold season precipitation totals dominate the first four decades of the regional series and culminate around the mid 1950s. Subsequently there is a strong decrease in winter totals, interrupted by short periods of increased precipitation around 1970, 1980, and the mid 1990s (Fig. 3.3B). The extended below-average interval between 1983 and 1992 is the most conspicuous feature of this later portion of the regional series. The two driest years on record are 1998 (averaging 59.5% of the 1961-1990 precipitation) and 1996 (65.3%, Fig. 3.3B). As the cold season totals average between 65% and 80% of the annual (April-March) total (Table 3.1) these series are almost identical, highlighting the strong influence of winter totals on annual precipitation variations at interannual and interdecadal timescales.

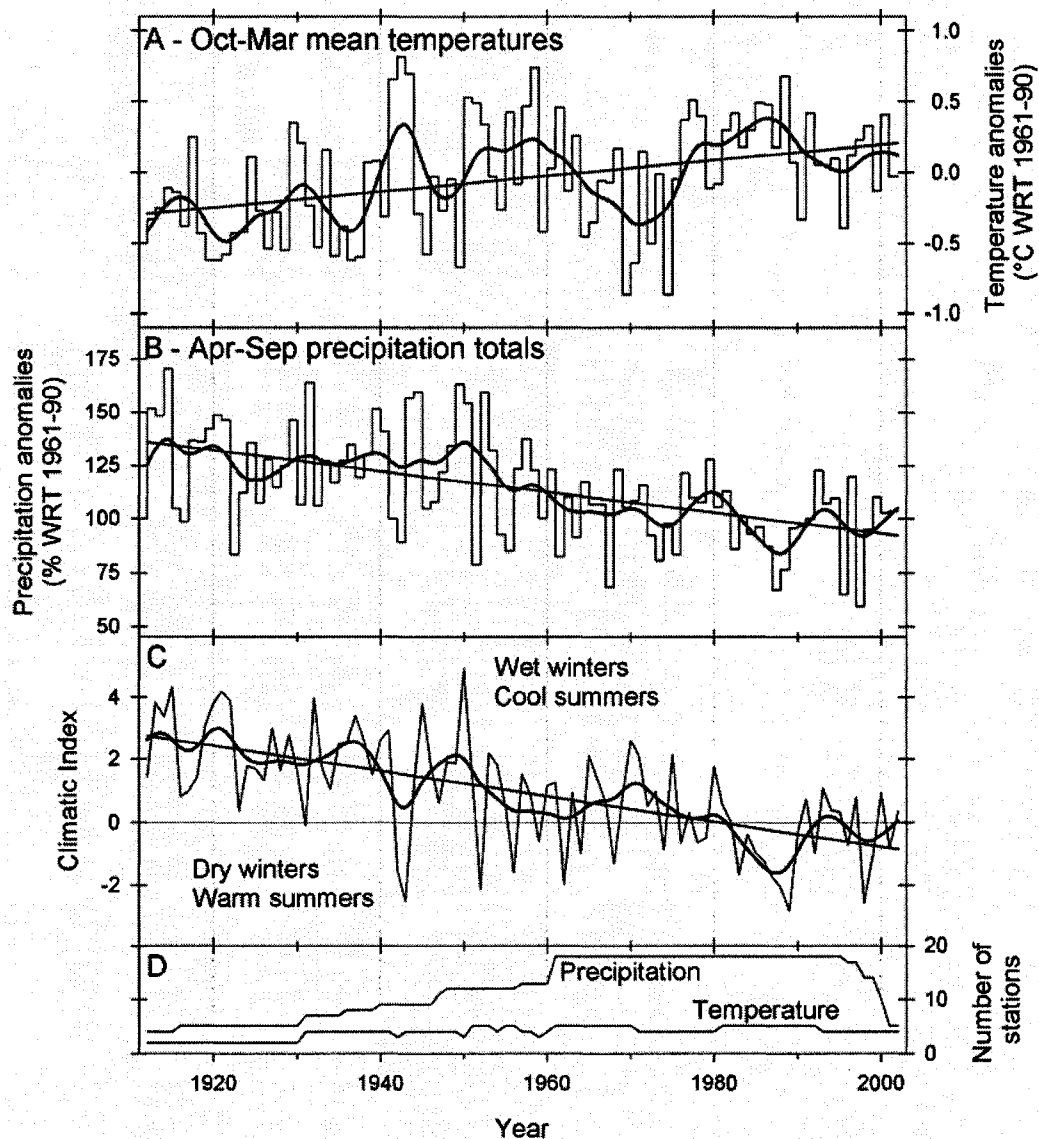


Fig. 3.3. (A) Warm season (October-March) temperature variations in the northwestern Patagonian region between 1912 and 2002 (CRUTem2v grid cell bounded between 40°-45°S and 70°-75°W), expressed as anomalies (°C) with respect to the 1961-1990 reference period. (B) Cold season (April-September) precipitation variations for the study area. Adjusted totals for the 18 selected stations between 38° and 44°S were converted to percentages of their 1961-1990 mean and subsequently averaged to create this regional record. (C) Regional climatic index calculated as the difference between the standardized anomalies (Z scores) of cold season precipitation totals and warm season mean temperatures. In general, positive values are interpreted as the result of wet winters being followed by cool summers, and vice versa. Least squares linear trends and smoothed (10-yr, 50% cutoff spline) versions of each climatic series are shown to highlight the low-frequency patterns in these records. (D) Number of stations contributing to the regionally-averaged temperature and precipitation series in any given year.

3.4.3. Regional climatic index. Comparison with localized glacier advances

The climatic index based on these standardized precipitation and temperature series (Fig. 3.3C) shows a strong negative trend that broadly agrees with the dramatic ice mass losses seen in Fig. 3.2. Between 1912 and 2002, the linear trend is -0.399 standardized anomalies per decade, significant at the 99% level (Table 3.3). Within this long-term pattern, several intervals of extended positive and negative indices are also evident. Positive values (i.e. wet winters followed by cold summer conditions) dominate the series until 1941, when a sharp shift to strongly negative anomalies occurs. Beginning in 1944, a short-lived period of positive values culminates in 1950 with the highest index ($+4.89$) in this time series. From 1950 until the late 1980s, annual values show a sharp declining trend only interrupted by periods of positive values between the mid 1960s and 1970s. One of the most intriguing features of this time series is the interval of successive negative indices between 1983 and 1990, with 1989 being the lowest (-2.80) on record. Afterwards winter precipitation and summer temperature anomalies are roughly balanced and the resulting index values oscillate around zero with an overall mean of -0.12 .

The decadal patterns in the regional climatic index show fair correspondence with the known periods of glacier advances in the region during the 20th-century (Fig. 3.4 and Table 3.4). The smoothed regional climatic index shows peaks in the early 1920s, 1940s and 1950s which roughly precede moraine formation at the Frías and Ventisquero Negro Glaciers dated by tree rings and field observations (Table 3.4). The best documented glacier readvances in the Tronador Area (identified mainly from field studies, Table 3.4) started in the early 1970s and ended in 1977. This short-lived interval of glacier advances closely follows the peak in the climatic series around 1970 (Fig. 3.4). To our knowledge, no evidence has been reported for glacier advances during the 1990s in response to the slight increase in the climatic index evident at that time. On the contrary, most sources indicate accelerating retreating rates after the 1970-1977 event, with the strongest glacier mass loss occurring during recent years (e.g. Rivera et al. 2005).

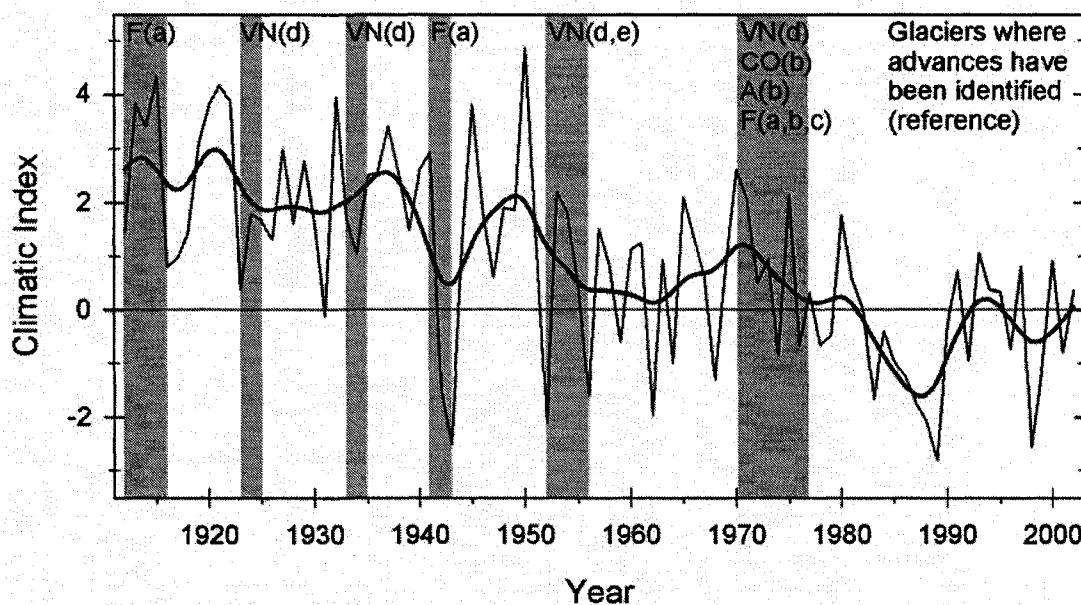


Fig. 3.4. Comparison between the regional climatic index and glacier advances identified in the Tronador Area ($41^{\circ}10'S$) during the 20th-century. A 10-yr, 50% cutoff spline (thick line) is shown to emphasize the low frequency patterns in the climatic series. The shaded bars are approximate dates for observations of glacier advances. Glacier abbreviations are (F) Frías Glacier; (VN) Ventisquero Negro Glacier; (CO) Castaño Overo Glacier; (A) Alerce Glacier. The bracketed lower case letters refer to sources listed in Table 3.4.

Table 3.4. Glacier advances identified in the Tronador Area (41°10'S) during the 20th century.

Glacier	Date of advance	Supporting evidence	Reference
Frías	1912-1916	Age of trees growing on frontal and lateral moraines. 8-13-yr ecesis estimated (a)	(a) Villalba et al. 1990
	1941-1943		
	1970-1977	- Tree-ring patterns in ice-scarred living tree (a) - In situ measurements of glacier front position (b, c)	(b) Rabassa et al. 1978
Alerce	1975-1977	In situ measurements of glacier front position (b)	(b) Rabassa et al. 1978
Castaño Overo	ca. 1902	Age estimations for trees growing on right lateral moraine (d)	(c) Rabassa et al. 1979
	1970-1974 1976-1977	In situ measurements, frontal position of regenerated ice cone (b)	
	Ventisquero Negro	1896-1902 1923-1924 ca. 1933 1952-1956 ca. 1975	Age of trees growing on right lateral moraines. 14-yr ecesis estimated (d) - Age of trees growing outside right lateral moraine. 14-yr ecesis, estimated (d) - Tree-ring patterns in ice-scarred living tree (e) Field observations and air photographs (d)

3.4.4. Regional streamflow variations and relationships with climate records

The PCA performed on the annual discharge of seven Argentinean rivers in the north Patagonian Andes (Table 3.2) confirmed the existence of a strong regional hydroclimatic signal in this area. The only significant Principal Component explains 76.8% of the variance in the annual series over the 1957-2003 common interval. In addition, this regionally-averaged streamflow record shows a strong positive correlation ($r = 0.77$, $p < 0.01$) with the regional climatic index series and remarkable similarities at interannual and interdecadal scales (Fig. 3.5). Regional annual streamflow variations show a highly significant negative trend (-3.9% decade⁻¹, $p < 0.01$) over the 1912-2002 period (Table 3.3). Correlations between the averaged streamflow series and the annual and seasonal temperature and precipitation records revealed the opposite influence of these variables on river discharges in the region. Statistically significant positive (negative) correlations with the regional precipitation (temperature) series were found for all three seasons analyzed (Table 3.5). However, the strongest correlations (up to +0.82) occurred with precipitation records, especially with annual and cold season totals. The highest negative correlations ($r = -0.375$) were found with the annual temperature series (Table 3.5).

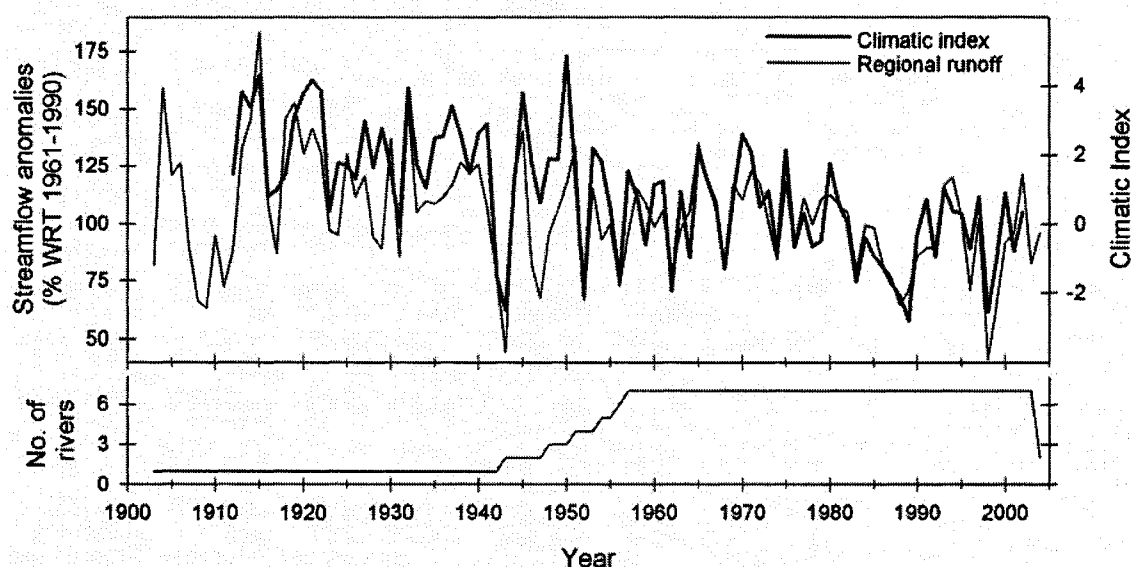


Fig. 3.5. Comparison between the regional climatic index (thick line) and the average of seven annual (April-March) river records from the eastern side of the north Patagonian Andes (thin line), expressed as percentages from their 1961-1990 mean flows. The lower diagram shows the number of gauge stations used in the computation of the regional streamflow series on any given year.

Table 3.5. Paired correlations between the annual (April-March) streamflow record and annual and seasonal (April-September, October-March) precipitation and temperature series for the northwestern Patagonian region between 1912 and 2002. The statistical significance (t test) of the correlations was estimated after accounting for the serial correlation in the intervening time series (Dawdy and Matalas 1964). Notes: (**) Significant at the 95% (99%) confidence level.

		Precipitation			Temperature		
		Apr-Mar	Apr-Sep	Oct-Mar	Apr-Mar	Apr-Sep	Oct-Mar
Runoff Apr-Mar		0.820**	0.798**	0.480**	-0.375**	-0.262*	-0.332**
Precip.	Apr-Mar		0.937**	0.620**	-0.247*	-0.141	-0.252*
	Apr-Sep			0.315**	-0.187	-0.116	-0.181
	Oct-Mar				-0.280*	-0.133	-0.313**
Temp.	Apr-Mar					0.800**	0.781**
	Apr-Sep						0.250*

3.5. Discussion and Conclusions

The preliminary analyses presented here indicate major changes in the climate of northwestern Patagonia over the last century with noticeable impacts on glaciers and river discharge in the region. Conservative statistical analyses revealed a strong, highly significant tendency towards drier and warmer conditions over the 1912-2002 period. For example, averaged warm season (October-March) temperatures have increased by 0.056°C per decade, whereas cold season (April-September) precipitation records (on average ca. 73.5% of annual totals) have declined at a rate of 4.89% per decade (Fig. 3.3AB and Table 3.3). The marked cooling trend between the early 1940s and the late 1970s (Fig. 3.3A) was previously identified as the most noticeable feature in northwestern Patagonian records west of the Andes (e.g. Rosenblüth et al. 1997; Villalba et al. 2003). However, our results indicate that over the 1912-2002 period, this cooling trend is insufficient to counteract the overall warming tendency observed in the region. The comparison with independently measured climate and streamflow records suggests that these regional temperature and precipitation series can be regarded as reliable indicators of climatic conditions for northwestern Patagonia between ca. 38° and 45°S .

The small size of glaciers in the north Patagonian Andes and their relatively short response time to climate fluctuations makes them particularly suitable to complement studies of recent climate changes in this part of the world. The comparison of past and present glacier front positions from repeat ground photographs (Fig. 3.2) provides precise, powerful baseline information about the long term behavior of local ice masses. The good quality paired photographs from six glaciers between 39°S and 43°S document the strong glacier recession over the past century in this region and corroborate the highly significant trends towards warmer and drier conditions over the 20th century based on regionalized temperature and precipitation records. A simple climatic index derived from these records provides a crude proxy for glacier mass balance that is consistent with the observed glacier recession in the region (Fig. 3.3C). Within the marked negative trend depicted by the climatic index, multi-year periods of positive values (i.e. wet winters followed by cool summers) roughly coincide with known dates of glacier readvances during the 20th century (Fig. 3.4 and Table 3.4). For example, the well-documented

interval of glacier advances culminating in 1976-1977 probably took place in response to consecutive years of relatively wet and cool conditions during the early 1970s and thus implies a relatively short (less than a decade) glacier response time to climate. However, these tentative conclusions are drawn on the limited, presently available database. Recent and ongoing glaciological studies (e.g. Bown 2004; Rivera et al. 2005) may ultimately provide more comprehensive data to evaluate the relationships between glaciers and synoptic changes in climate in this area.

The climatic index developed in this paper is strongly correlated with regional streamflow records derived from the seven longest and most complete records from the Argentinean side of the North Patagonian Andes, confirming the validity of this index and highlighting the regional nature of the changes observed in these variables. Correlation with precipitation and temperature series provides further insight into the climate-runoff relationships in the region, indicating a strong regional pattern of discharge primarily controlled by precipitation variability over the last century. These preliminary findings have interesting implications for the evaluation of the relative importance of possible future changes in precipitation and temperatures in this region.

Results from several coupled atmosphere-ocean general circulation models (Cubasch et al. 2001; Bradley et al. 2004) suggest that the temperature and precipitation trends observed in northwestern Patagonia will probably continue well into the 21st century. Although further work is needed to evaluate the potential hydrological and socio-economic impacts of such predictions, basic knowledge about recent (i.e. 20th-century) climate variability in this area is one of the most important factors to consider in future water resource management programs and regional development initiatives. However, present instrumental records remain inadequate to capture the full range of decade- to century-scale hydroclimatic variability in this region. Future developments of multi-proxy climate and streamflow reconstructions (e.g. Lara et al. 2005; Masiokas et al. 2005) may provide the necessary long term climate perspective to improve our understanding of past, present and future changes in this area.

3.6. References

- Aceituno, A., Fuenzalida, H. and Rosenblüth, B. 1993. Climate along the extratropical west coast of South America. In: Mooney, H.A., Fuentes, E.R., Kronberg, B.I., (eds.), *Earth system responses to global change – Contrasts between North and South America*. Academic Press, 61-69.
- Alexandersson, H. 1986. A homogeneity test applied to precipitation data. *Journal of Climatology* 6, 661-675.
- Aniya, M. 1988. Glacier inventory for the Northern Patagonia Icefield, Chile, and variations 1944/45 to 1985/86. *Arctic and Alpine Research* 20(2), 179-187.
- Aniya, M., Sato, H., Naruse, R., Skvarca, P. and Casassa, G. 1996. The use of satellite and airborne imagery to inventory outlet glaciers of the Southern Patagonia Icefield, South America. *Photogrammetric Engineering and Remote Sensing* 62, 1361-1369.
- Bown, F. 2004. Cambios climáticos en la Región de Los Lagos y respuestas recientes del Glaciar Casa Pangué (41°08'S). M.Sc. Thesis, Universidad de Chile, Santiago, 131 pp.
- Bradley, R.S., Keimig, F.T. and Diaz, H.F. 2004. Projected temperature changes along the American cordillera and the planned GCOS network. *Geophysical Research Letters* 31, L16210, doi:10.1029/2004GL020229.
- Coudrain, A., Francou, B. and Kundzewicz, Z.W. 2005. Glacier shrinkage in the Andes and consequences for water resources – Editorial. *Hydrological Sciences Journal* 50(6), 925-932.
- Cubasch, U., Meehl, G.A., Boer, G.J., Stouffer, R.J., Dix, M., Noda, A., Senior, C.A., Raper, S. and Yap, K.S. 2001. Projections of future climate change. In: Houghton, J. T., et al., (eds.), *Climate Change 2001: The Scientific Basis. Contribution of Working Group I to the Third Assessment Report of the Intergovernmental Panel on Climate Change*, Cambridge University Press, 525–582.
- Dawdy, D.R. and Matalas, N.C. 1964. Statistical and probability analysis of hydrologic data, part III: analysis of variance, covariance and time series. In: Chow, V.T., (ed.), *Handbook of Applied Hydrology, A Compendium of Water-Resources Technology*, McGraw-Hill Book Company, New York, 8.68–8.90.
- De Agostini, A.M. 1945. *Viajes de exploración a la Cordillera Patagónica Austral*. 2nd ed. Guillermo Kraft, Buenos Aires, 445 pp.
- Dyurgerov, M.B. and Meier, M.F. 2000. Twentieth century climate change: Evidence from small glaciers. *Proceedings of the National Academy of Sciences* 97, 1406-1411.

- Fonck, F. and Hess, F. 1857. Informe de los señores Francisco Fonck i Fernando Hess sobre la espedicion a Nahuelhuapi. *Anales de la Universidad de Santiago de Chile* XIV, 1-11.
- Haeberli, W. 2005. Mountain glaciers in global climate-related observing systems. In: Huber, U.M., Bugmann, H.K.M., Reasoner, M.A., (eds.), *Global change and mountain regions – An overview of current knowledge*. Springer, 169-175.
- Hamilton, T.D. 1965. Comparative glacier photographs from northern Alaska. *Journal of Glaciology* 5(40), 479-487.
- Hauthal, R. 1904. Gletscherbilder aus der argentinischen Cordillera. *Zeitschrift des Deutschen und Oesterreichischen Alpenvereins* 35, 30-56.
- Hodge, S.M., Trabant, D.C., Krimmel, R.M., Heinrichs, T.A., March, R.S. and Josberger, E.G. 1998. Climate variations and changes in mass of three glaciers in western North America. *Journal of Climate* 11, 2161-2179.
- Hoelzle, M., Haeberli, W., Dischl, M. and Peschke, W. 2003. Secular glacier mass balances derived from cumulative glacier length changes. *Global and Planetary Change* 36(4), 295-306.
- Jakob, C. 1936. Alrededor del Tronador. *Revista Geográfica Americana* V(28), 1-21.
- Jakob, C. 1937. La fiscalización de las reservas acuáticas es una obligación nacional para la Argentina. *Revista Geográfica Americana* V(50), 313-326.
- Johannesson, T., Raymond, C.F. and Waddington, E.D. 1989. A simple method for determining the response time of glaciers. In: J. Oerlemans (ed.), *Glacier Fluctuations and Climatic Change*. Kluwer Academic Publishers, Dordrecht, 343-352.
- Jones, P.D. and Hulme, M. 1996. Calculating regional climatic time series for temperature and precipitation: methods and illustrations. *International Journal of Climatology* 16, 361-377.
- Jones, P.D. and Moberg, A. 2003. Hemispheric and large-scale surface air temperature variations: an extensive revision and an update to 2001. *Journal of Climate* 16, 206-223.
- Klok, E.J. and Oerlemans, J. 2004. Climate reconstructions derived from global glacier length records. *Arctic, Antarctic, and Alpine Research* 36(4), 575-583.

- Kölliker, A., Kühn, F., Reichert, A., Tomsen, A. and Witte, L. 1917. Patagonia: Resultados de las expediciones realizadas en 1910 a 1916. Sociedad Científica Alemana, 2 vols, Buenos Aires, 430 pp.
- Koutche, V. and Ladvoat, H.J. 1937. Parque Nacional Los Alerces: Proyecto de reserva para la creación de un Parque Nacional en el Territorio Nacional del Chubut. In: Dirección de Parques Nacionales (eds.), Nuevos Parques Nacionales, Buenos Aires, 35-94.
- Lara, A., Urrutia, R., Villalba, R., Luckman, B.H., Soto, D., Aravena, J.C., McPhee, J., Wolodarsky, A., Pezoa, L. and Leon, J. 2005. The potential use of tree-rings to reconstruct streamflow and estuarine salinity in the Valdivian Rainforest ecoregion, Chile. *Dendrochronologia* 22, 155-161.
- Lawrence, D.B. and Lawrence, E.G. 1959. Recent glacier variations in southern South America. American Geographical Society Southern Chile Expedition Technical Report, Office of Naval Research Contract 641(04), New York, USA, 39 pp.
- Lliboutry, L. 1998. Glaciers of Chile and Argentina. In: Williams, R.S., Ferrigno, J.G., (eds.), Satellite Image Atlas of Glaciers of the World: South America. USGS Professional Paper 1386-I, Online version 1.02.
- Masiokas, M.H., Villalba, R., Luckman, B.H., Delgado, S. and Ripalta, A., 2005. Tree rings and glacier fluctuations as paleoclimatic indicators in southern Argentina. Proc. Open Science Conference: Global Change in Mountain Regions, 2-6 Oct. 2005, Perth, Scotland, UK.
- McCabe, G.J., Fountain, A.G. and Dyurgerov, M.B. 2000. Variability in winter mass balance of Northern Hemisphere glaciers and relations with atmospheric circulation. *Arctic, Antarctic, and Alpine Research* 32(1): 64-72.
- Miller, A. 1976. The Climate of Chile. In: Schwerdtfeger, W. (ed.) World Survey of Climatology 12, Climate of Central and South America. Amsterdam, Elsevier, pp. 113-145.
- Nesje, A. 2005. Briksdalsbreen in western Norway: AD 1900–2004 frontal fluctuations as a combined effect of variations in winter precipitation and summer temperature. *Holocene* 15(8), 1245-1252.
- Neumeyer, J.J. 1949. En el valle del Río Esperanza (Chubut). *Anuario del Club Andino Bariloche* 17, 47-50.
- Oerlemans, J. 1994. Quantifying global warming from the retreat of glaciers. *Science* 264: 243-245.
- Oerlemans, J. 2001. *Glaciers and Climate Change*. Balkema Publishers, 148 pp.

- Oerlemans, J. 2005. Extracting a climate signal from 169 glacier records. *Science* 308, 675-677.
- Oerlemans, J. and Fortuin, J.P.F., 1992. Sensitivity of glaciers and small ice caps to greenhouse warming. *Science* 258, 115-117.
- Pittock, A.B. 1980. Patterns of climatic variation in Argentina and Chile - I. Precipitation, 1931-1960. *Monthly Weather Review* 108, 1347-1361.
- Porter, S.C. 1981. Glaciological evidence of Holocene climatic change. In: Wigley, T.M.L., Ingram, M.J., Farmer, G., (eds.), *Climate and History*. Cambridge University Press, pp. 83-110
- Prohaska, F. 1976. The climate of Argentina, Paraguay and Uruguay. In: Schwerdtfeger, W. (ed.) *World Survey of Climatology 12, Climate of Central and South America*. Amsterdam, Elsevier, pp. 13-112.
- Rabassa, J., Rubulis, S. and Suarez, J. 1978. Los glaciares del Monte Tronador. *Anales de Parques Nacionales XIV*, 259-318.
- Rabassa, J., Rubulis, S. and Suarez, J. 1979. Rate of formation and sedimentology of (1976-1978) push-moraines, Frías Glacier, Mount Tronador (41°10'S; 71°53'W), Argentina. In: Schluochter, C., (ed.), *Moraines and Varves*. A.A. Balkema, pp. 65-79.
- Rabassa, J., Brandani, A., Boninsegna, J.A. and Cobos, D.R. 1984. Cronología de la "Pequeña Edad del Hielo" en los glaciares Río Manso y Castaño Overo, Cerro Tronador, Provincia de Río Negro. *Actas Noveno Congreso Geológico Argentino* 3, 624-639.
- Rasmussen, L.A. and Conway, H. 2004. Climate and glacier variability in western North America. *Journal of Climate* 17, 1804-1815.
- Rivera, A. 2004. Mass balance investigations at Glaciar Chico, Southern Patagonia Icefield, Chile. Ph.D. Thesis, University of Bristol, UK, 303 pp.
- Rivera, A., Casassa, G., Acuña, C. and Lange, H. 2000. Variaciones recientes de glaciares en Chile. *Revista de Investigaciones Geográficas* 34, 25-52.
- Rivera, A., Acuña, C., Casassa, G. and Bown, F. 2002. Use of remote sensing and field data to estimate the contribution of Chilean glaciers to the sea level rise. *Annals of Glaciology* 34, 367-372.

- Rivera, A., Bown, F., Casassa, G., Acuña, C. and Clavero, J. 2005. Glacier shrinkage and negative mass balance in the Chilean Lake District (40°S). *Hydrological Sciences Journal* 50(6), 963–974.
- Rogers, G.F., Malde, H.E. and Turner, R.M. 1984. *Bibliography of repeat photography for evaluating landscape change*. Salt Lake City: University of Utah Press. 179 pp.
- Rosenblüth, B., Casassa, G. and Fuenzalida, H. 1995. Recent climatic changes in western Patagonia. *Bulletin of Glacier Research* 13, 127-132.
- Rosenblüth, B., Fuenzalida, H. and Aceituno, P. 1997. Recent temperature variations in southern South America. *International Journal of Climatology* 17, 67-85.
- Santer, B.D., Wigley, T.M.L., Boyle, J.S., Gaffen, D.J., Hnilo, J.J., Nychka, D., Parker, D.E. and Taylor, K.E. 2000. Statistical significance of trends and trend differences in layer-average atmospheric temperature time series. *Journal of Geophysical Research*, 105(D6): 7337-7356.
- Secretaría de Energía, 2004. Informe del Sector Eléctrico, Año 2003. Ministerio de Planificación Federal, Inversión Pública y Servicios, Secretaría de Energía, Argentina. 154 pp.
- SSRH, 2004. Estadística Hidrológica de la República Argentina, Edición 2004. CD-ROM, 1st Ed. Subsecretaría de Recursos Hídricos, Buenos Aires, Argentina.
- Steffen, H. 1909. Viajes de Exploracion i Estudio en la Patagonia Occidental: 1892-1902, Vol. I. *Anales de la Universidad de Chile*, Imprenta Cervantes, Santiago. 409 pp.
- Veblen, T.T. and Lorenz, D.C. 1988. Recent vegetation changes along the forest/steppe ecotone in northern Patagonia. *Annals of the American Association of Geographers* 78(1), 93-111.
- Villalba, R., Leiva, J.C., Rubulis, S., Suarez, J. and Lenzano, L.E. 1990. Climate, tree-ring, and glacial fluctuations in the Río Frías Valley, Río Negro, Argentina. *Arctic and Alpine Research* 22(3), 215-232.
- Villalba, R., Lara, A., Boninsegna, J.A., Masiokas, M., Delgado, S., Aravena, J.C., Roig, F., Schmelter, A., Wolodarsky, A. and Ripalta, A. 2003. Large-scale temperature changes across the Southern Andes: 20th-century variations in the context of the past 400 years. *Climatic Change* 59, 177-232.
- Villalba, R., Masiokas, M., Kitzberger, T., and Boninsegna, J.A. 2005. Biogeographical consequences of recent climate changes in the southern Andes of Argentina. In: Huber, U.M., Bugmann, H.K.M., and Reasoner, M.A. (eds.) *Global Change and Mountain Regions, An Overview of current knowledge*. Springer, 157-166.

- Vose, R.S., Schmoyer, R.L., Steurer, P.M., Peterson, T.C., Heim, R., Karl, T.R. and Eischeid, J.K. 1992. The Global Historical Climatology Network: Long-term monthly temperature, precipitation, sea level pressure, and station pressure data, Tech. Rep. NDP-041, Carbon Dioxide Information Analysis Center, Oak Ridge National Laboratory, Oak Ridge, Tennessee, U.S.A.
- Warren, C.R. and Sugden, D.E. 1993. The Patagonian Icefields: a glaciological review. *Arctic and Alpine Research* 25, 316–331.
- Zumbühl, H.J. and Holzhauser, H. 1988. Glaciers des Alpes du Petit âge glaciaire. *Les Alpes* 64(3), 129-322.

The previous chapter dealt with 20th-century glacier and climate changes in the north Patagonian Andes. Chapter 4 develops an original chronology of Little Ice Age (LIA) fluctuations for five small glaciers in the south Patagonian Andes using mainly dendrogeomorphic techniques. Preliminary glacier area changes since the LIA are estimated using Landsat TM satellite imagery.

An earlier version of Chapter 4 has been accepted for publication in July 2007 by *Palaeogeography, Palaeoclimatology, Palaeoecology* (Copyright Elsevier 2007). The list of co-authors is as follows:

Masiokas, M.H.^{1,2}; Luckman, B.H.¹; Villalba, R.²; Delgado, S.²; Skvarca, P.³; Ripalta, A.²

¹ Department of Geography, University of Western Ontario, London, Ontario, Canada.

² Instituto Argentino de Nivología, Glaciología y Ciencias Ambientales (IANIGLA-CONICET), Mendoza, Argentina.

³ Instituto Antártico Argentino, Buenos Aires, Argentina.

Chapter 4: Little Ice Age fluctuations of small glaciers in the Monte Fitz Roy and Lago del Desierto areas, south Patagonian Andes, Argentina

4.1. Introduction

Large outlet glaciers from the North and South Patagonian Icefields (NPI and SPI, respectively) have historically been the foci of most glaciological investigations in Patagonia south of 45°S, and little is known about the smaller glaciers elsewhere in the region (e.g. Mercer 1965; Röthlisberger 1986; Wenzens 1999; Delgado et al. 2002). The studies from the NPI and SPI have supplied most of the evidence for the development of the late Holocene glacier history for this region, which has been used with other multi-proxy climate reconstructions to improve our understanding of Patagonian climate variability during this time frame (see e.g. Glasser et al. 2004, and references therein). However, despite these efforts and the enormous potential for glaciological investigations of this region, current knowledge about past glacier fluctuations and glacier-climate relationships in the south Patagonian Andes remains limited (Warren and Sugden 1993; Porter 2000; Luckman and Villalba 2001; Casassa et al. 2002; Rivera 2004). Mercer (1965, 1968, 1970) used evidence from six outlet glaciers of the SPI and limited data from the San Lorenzo area and Glaciar Narváez (located to the east of the icefields) to identify three main periods of late Holocene glacier advances in this region at ca. 4700-4200, 2700-2000 ¹⁴C yrs BP and during the past few centuries. Aniya (1995, 1996), working subsequently on three different outlet glaciers of the SPI, proposed a revised Neoglacial glacier chronology with glacier advances ca. 3600, 2300, and 1600-1400 ¹⁴C yrs BP, and during the past centuries. More recently, Strelin et al. (2002) proposed up to seven Neoglacial advances for the southern tip of South America and the Antarctic Peninsula region.

In this paper we focus on the last Neoglacial event identified in these regional glacier chronologies, namely the widely recognized Little Ice Age (LIA) (Grove 2004). We develop preliminary LIA and post-LIA glacial chronologies for five glaciers located near the northeast margin of the SPI using dendrogeomorphological techniques plus the analysis of historical documents, aerial photographs and satellite images. The study sites

are Glaciar Torre and Glaciar Piedras Blancas in the Monte Fitz Roy area and three small glaciers on the west margin of Lago del Desierto (Fig. 4.1). There is conspicuous morphological evidence of pre-LIA events at some of these sites but it is not reported in detail here. Although some glacier advances have been identified in the south Patagonian Andes dating from the 12th and 14th centuries (e.g. Glasser et al. 2002), the available evidence suggests that most glaciers reached their LIA maxima between the 17th and 19th centuries (Luckman and Villalba 2001; Delgado et al. 2002; Glasser et al. 2004; Koch and Kilian 2005; Aravena 2007). However, as few glaciers have been studied in detail, little is known about the timing, number and magnitude of glacier events that occurred in the south Patagonian Andes during this time (Espizua et al. in preparation). This is unfortunate because the LIA is usually the period with the most abundant, best preserved and most easily dated evidence: it also comprises the period for which other high resolution proxy climate records (e.g. tree rings) are generally available for comparison with the glacier records. The lack of long (>10 years) direct glacier mass balance records in this region hampers the paleoclimatic interpretation of the available late Holocene glacial chronologies. In addition, most previous studies are from a few large calving glaciers that tend to have complex responses to climate variations (Warren and Sugden 1993; Warren and Aniya 1999). Thus, the detailed study of LIA and post-LIA glacier advances from these smaller glaciers is an important step towards improving our understanding of the influence of climate on glacier behavior and, therefore, the climatic significance of the glacier events identified in Patagonia.

Many factors control the response of individual glaciers to climate changes (e.g. Oerlemans 2001). Larger glaciers tend to have longer response times and more complex dynamic responses to climate than small glaciers (Johannesson et al. 1989) and therefore we specifically targeted several small accessible glaciers that we assume would be more sensitive (and respond more immediately) to climate changes. In addition, selecting several glaciers of similar size minimizes differences due to glacier size and allows a better evaluation of the regional response of the glacier system. These data will hopefully facilitate subsequent studies where the climatic significance of the inherently low resolution glacier records will be analyzed together with higher resolution proxy climate

records and instrumental climate data from this region (see e.g. Grosjean and Villalba 2006). The ultimate goal of this and additional ongoing studies at other small glaciers is to develop robust, reliable regional glacial chronologies for the past ~1000 years in order to evaluate the main spatio-temporal variability of glacier and climate fluctuations in the Patagonian Andes.

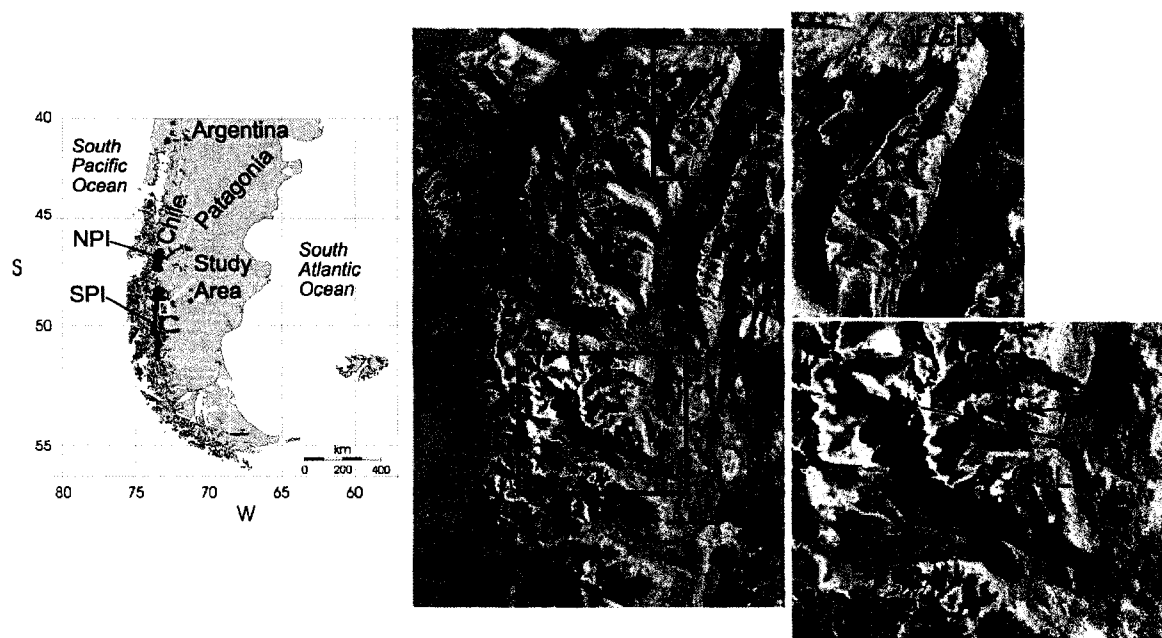


Fig. 4.1. (Left) Location of the study area and the North and South Patagonian Icefields (NPI and SPI). (Center and right) 2005 Landsat TM image showing the location of the glaciers (1-3) studied at the Lago del Desierto (LGD) area, and Glaciar Piedras Blancas (4) and Glaciar Torre (5) in the Monte Fitz Roy (FR) area. Glaciar de los Tres (G3) and Glaciar Río Blanco (GBL) are also indicated. Portions of Glaciar Viedma (GV) and Glaciar Chico (GCH) are shown to illustrate the differences in size between these large SPI outlets and the small glaciers analyzed in this study.

4.2. Study Area

Environmental conditions of southwestern Patagonia are largely determined by the interaction between the dominant westerly winds and the north-south orientation of the Patagonian Andes (Miller 1976; Prohaska 1976). This results in an extremely steep precipitation gradient ranging from ca. 7000-8000 mm of annual precipitation on the SPI

(Escobar et al. 1992) to less than 300 mm within 100 km east of the main divide (Villalba et al. 2003). Temperatures are less variable but exhibit a more maritime (continental) regime on the west (east) side of the Andes, with mean annual temperatures of around 6°C measured at the few low elevation stations that exist around the SPI (Miller 1976). Regional studies using the limited climate records available (rarely >60 years) have found a long-term warming trend (Rosenblüth et al. 1997; Villalba et al. 2003; Rivera 2004; Chapter 2). Long-term changes in precipitation are more variable, and although some studies report a negative trend for some stations in the region (Rosenblüth et al. 1995; Rivera 2004), recent analyses of homogenized precipitation records suggest no trend for this area (Aravena 2007).

The five glaciers studied here are located a few kilometers east and separate from the SPI. They have a predominantly easterly orientation and are between ca. 1-25 km² in size¹ (Fig. 4.1 and Table 4.1). Parts of Glaciar Piedras Blancas and Glaciar Torre are debris-covered and both end in relatively large proglacial lakes confined by recent moraines (Fig. 4.1). Usually the oldest moraines are densely covered by mature forests, and forest colonization in the forefield allows the tree-ring dating of younger glacier deposits. The dominant tree species colonizing these deposits are *Nothofagus pumilio* (lenga) and *N. betuloides* (coihue), but in some humid places *N. antarctica* (ñire) is also common. Unfortunately, some forested portions of the glacier forefields were burned by forest fires associated with the European settlement of this area in the early 20th century.

4.3. Previous studies

The great potential for glaciological research of the study area has been known for decades (e.g. Kölliker et al. 1917; Mercer 1965). Several descriptive studies and glaciological investigations have been carried out (Heim 1951; Lliboutry 1952, 1953a, b, 1993; Bertone 1960, 1972; Mercer 1965, 1968; Röthlisberger 1986; Popovnin et al. 1999; Masiokas et al. 2000, 2001; Rivera 2004), and the well-defined moraine systems located

¹ Glaciar Torre is actually formed by three merging tongues referred to as Glaciar Torre, Adela and Grande in Lliboutry (1953b). Glaciar Piedras Blancas is also known as Glaciar Fitz Roy, whereas the three glaciers studied at Lago del Desierto have adjacent accumulation areas and are referred to as Glaciar Laguna del Desierto 8, 9, and 10 in Bertone (1960). For simplicity, they will be called here Glaciar Lago del Desierto I, II, and III.

in front of the present glacier margins have long been recognized as clear evidence of recent glacier activity in this region. However, as most investigations have usually focused either on a Holocene perspective (e.g. Mercer 1968; Röthlisberger 1986), or on 20th century glacier conditions (e.g. Lliboutry 1953a, b; Aniya et al. 1996, 1997; Rignot et al. 2003), few studies have attempted a precise dating of the conspicuous, relatively recent glacier deposits. Few maps or estimates of LIA moraine ages (e.g. Mercer 1965; Masiokas et al. 2000) and only one very preliminary glacier inventory (Bertone 1960) are available for the glaciers studied in this paper.

Lliboutry (1952, 1953a, b; 1993) analyzed aerial and field photographs, historical documents and local sources to provide detailed descriptions of surficial glacier features and recent glacier front variations in the Fitz Roy area (Fig. 4.1). Although a marked retreat was indicated for Glaciar Río Blanco between 1936 and 1952, relatively little change in frontal position was found at Glaciar Piedras Blancas for the same interval (Lliboutry 1953a). At Glaciar Torre the proglacial lake level dropped by 12-15 m between 1931-1952 and the glacier front remained in approximately the same position. However, the calving (northern) portion of Glaciar Torre had receded 700 ± 50 m between 1952 and 1981 (Lliboutry 1993).

Auer (1956) identified four frontal moraine systems, the youngest of which was still bare and assumed to correspond to the latest glacier readvance of recent centuries. Mercer visited Glaciar Torre in 1963 and described the end moraines in front of the present ice margin (Mercer 1965). He reported an almost bare moraine damming the proglacial lake and another massive moraine almost immediately downvalley with immature forest cover and living trees up to 170 years old on the more sheltered (eastern) slopes. Mercer grouped both ridges as Fitz Roy Moraines IV and identified three older ridges with mature forest cover approximately 100, 700 and 2700 m downvalley as Fitz Roy Moraines III, II, and I. Mercer estimated an ecesis of ca. 100 years for this site based on historical pictures showing virtually no change in glacier front position in 30 years and the lack of vegetation colonizing the moraine damming the lake. Based on these preliminary estimates, Mercer assigned late 19th century and late 17th century ages for the

two Fitzroy Moraine IVs. He estimated Moraine III to be older than 800 ± 85 ^{14}C yrs based on a basal peat date from a site between Moraines II and III where they are only a few meters apart.

Masiokas et al. (2000) and Delgado et al. (2002) presented preliminary tree-ring data from sites on the LIA deposits of Glaciar Piedras Blancas. No ecessis correction values were available for the site, but living 80 yr-old and 250 yr-old trees were used to estimate minimum ages for two massive lateral moraines. Most of the tree-ring samples collected at this glacier were also used to develop a long, well replicated tree-ring width chronology that was utilized to reconstruct regional temperature variability for southern Patagonia during the past four centuries (Villalba et al. 2003). The formation of the moraines identified at Piedras Blancas was tentatively related to two significant cold intervals observed around the mid 17th and 19th centuries in a preliminary version of this reconstruction (Masiokas et al. 2000). The clearly delimited sequence of moraine ridges in front of the small glaciers on the west margin of Lago del Desierto (Fig. 4.1) have not been studied previously. The only available information for these glaciers is the rough areal estimates and basic geographic data in Bertone (1960), and a poor quality photograph published by De Agostini (1945).

Table 4.1. Data sources used in this study. Available historical documents, aerial photographs (AP) and satellite images (SI) for each site are listed. Approximate glacier areas were derived from available satellite imagery (see text for details).

Glacier	Location (elev.)	Area in 2005	Year of available photographs (reference)	AP	SI
Torre	49°19'S 73°01'W (660 m)	24.6 km ²	1931 (DeAgostini 1945); 1946 (Heim 1951); 1950s? (Auer 1956); 1952 (Lliboutry 1953b); 1950s? (Bertone 1960); 1960s? (Wylhelmy and Rohmeder 1963); 1963 (Mercer unpubl.); 1980s? (Clapperton 1993); 2002, 2005 (Villalba, Masiokas unpubl.).	1966 1968 1981	1984 2000 2002 2005
Piedras Blancas	49°16'S 72°58'W (650 m)	5.6 km ²	1931, 1936 (DeAgostini 1945); 1946 (Heim 1951); 1952 (Lliboutry 1953b); 1950s? (Bertone 1960); 2002 (Villalba, Masiokas unpubl.); 2005 (Masiokas, Skvarca unpubl.).		
Lago del Desierto I	49°03'S 72°54'W (1090 m)	0.83 km ²	1930s? (DeAgostini 1945); 2004, 2005 (Villalba, Casteller, Masiokas unpubl.).	1966 1997	
Lago del Desierto II	49°04'S 72°54'W (850 m)	1.92 km ²	2003, 2004, 2005 (Villalba, Casteller, Masiokas unpubl.).		
Lago del Desierto III	49°05'S 72°55'W (1120 m)	0.95 km ²	2004, 2005 (Villalba, Casteller, Masiokas unpubl.).		

4.4. Methods

4.4.1 Dating the glacier deposits

The development of the LIA glacial histories for the five glaciers studied in this paper was primarily based on dendroglaciological techniques (e.g. Luckman 1986, 1988; Schweingruber 1996). The usefulness and inherent limitations of dendroglaciological methods are summarized in Table 4.2. Minimum ages for recent glacial events were usually determined from the age of the oldest trees growing on these deposits. Increment cores were collected from living trees growing on lateral and terminal moraines, prepared using standard dendrochronological procedures (Stokes and Smiley 1996) and counted to determine tree age. Where the pith ring was not present pith offset values were estimated based on ring curvature on the oldest candidate trees. Minimum ages for trees with rotten piths were estimated by adding 20 years to the date of the innermost countable rings. Cores were taken as close to the root collar as possible to minimize potential errors due to sampling height and most samples were taken between 50 and 100 cm from the tree base. Nine young *N. pumilio* trees growing outside the LIA moraines at Glaciar Piedras

Blancas were sampled at the base and at 100 cm height to provide a rough estimate of vertical growth rates. Ring counts indicate that, on average, the trees grew one meter in seven years, suggesting that the error in estimating basal dates from cores sampled up to one meter above the root crown probably does not exceed 10 years. A similar estimate was obtained from seven trees at Glaciar Torre that grew from 25-40 cm to 100 cm height in seven years. Therefore we used a vertical growth rate of 10 cm per year to correct for sampling height.

Table 4.2. Evidence for and limitations of dendroglaciological dating (modified from Luckman, 2000).

Evidence	Precision	Information provided	Limitations
1) Trees growing in the glacier forefield	5-50 years	Age of oldest tree provides minimum age for surface	Eccesis (lag time between moraine stabilization and tree establishment) difficult to estimate. Assumes the oldest tree was sampled
2) Tilted and/or scarred tree	Exact calendar age of damage	Damage date indicates glacier position at a specific time	Moderately rare, dead trees require cross-dating
3) Trees killed by glacier advance	a) Exact calendar date of outer ring by cross-dating with living trees. Dating precision depends on preservation of wood and loss of outer rings b) approx. date by ^{14}C dating ($\pm 50-100$ yrs).	<i>In situ</i> : death date indicates position of glacier at a specific time Reworked wood: only provides a limiting date for death	a) Requires cross-dating, loss of outermost rings b) low temporal resolution, expensive
4) Trees growing outside glacier forefield	Annual resolution	Reference chronologies, paleoclimatic information	Age of oldest tree. Dead material can extend the chronologies but is difficult to find and usually not well preserved in this region

An important limitation in determining moraine ages from trees growing on their surface is to estimate the time interval between the stabilization of the surface and tree seedling establishment (Sigafos and Heindricks 1969; McCarthy and Luckman 1993). This interval (also known as “eccesis”) has been shown to vary widely depending on microclimatic conditions, substrate and the species involved. There have been very few detailed eccesis estimates for glacier deposits in the Patagonian Andes (see e.g. Koch and Killian 2005). Moreover, the presence of proglacial lakes, the sparse vegetation on the

steep bedrock outcrops and the poor temporal coverage of available air photos limited our ability to estimate ecesis correction factors for these glaciers. However, De Agostini (1945) reports on a massive outburst flood that occurred on December 16, 1913 from the proglacial lake of Glaciar Río Blanco (Fig. 4.1) depositing large amounts of sediments throughout the Río Blanco Valley, including numerous boulders especially to the north of Glaciar Piedras Blancas (or “White Boulders Glacier”). Our examination of the site indicates that this outburst probably originated from Glaciar Piedras Blancas and not from Glaciar Río Blanco (see Fig. 4.4 below). In either case, the pith date at the base of the oldest of nine trees sampled on this surface was 1923, suggesting an approximate ecesis of 10 years for this site. Additional evidence suggesting a variable ecesis of about 15-30 years was found at Glaciar Lago del Desierto II. In front of the most conspicuous southern lateral moraine the kill date of a partially buried, *in situ* stump was precisely dated to 1743 by dendrochronological analysis, providing a maximum date for the formation of this deposit. The base of the oldest tree sampled on top of the distal slope of this moraine was dated to 1758, suggesting it took about 15 years for the forest to recolonize this surface. The innermost moraine at this site is formed by coarse material on a steep, unstable bedrock slope and was visible several meters in front of the glacier in 1966 air photographs. However, the only seedling found on this moraine was tree-ring dated to 1994, indicating about 29 years of ecesis at this site. These preliminary data suggest that, where pith is present, the combination of ecesis and the sampling height correction factor introduce a range of 2-4 decades when estimating dates of moraine formation from tree ages. Larger ecesis estimates are expected at sites lacking good soil conditions (e.g. the steep bedrock slopes in front of the glaciers at Lago del Desierto). However, given the small sample size and the heterogeneity of sites and conditions observed at the different glacier forefields, we used a 15-yr ecesis estimate unless otherwise noted.

Precise information about past glacier activity can be obtained from trees that have been directly affected by past glacier advances (Table 4.2). This material can be extremely valuable in providing complementary, limiting calendar dates for past glacial events (e.g. Luckman 2000). Unfortunately very few damaged or killed trees were found at these

study sites. The 400-yr long Piedras Blancas (*Nothofagus pumilio*) reference chronology (Villalba et al. 2003) was used in crossdating trials of tree-ring series from subfossil material. Mature trees located outside the main LIA moraines were also sampled to provide minimum age estimates of surfaces not directly affected by these glacier events. As most tree species in this region rarely exceed 400 years of age, it is difficult to differentiate deposits of older events based solely on the age of the trees colonizing their surface. This limitation, plus forest fire activity and the poor preservation of subfossil wood have usually hampered the dating of glacier fluctuations from the first half of the past millennium in the south Patagonian Andes. In most cases we used complementary evidence such as the health and size of the trees to determine whether the sampling sites were covered by old-growth or first generation forests, but unfortunately some degree of uncertainty will remain until better dating is available.

4.4.2 Estimating glacier area changes since the LIA

Preliminary estimates of glacier area changes since the LIA maximum and between 1984 and 2005 were derived from the analysis of two Landsat Thematic Mapper (TM) scenes with 28.5 m resolution acquired on December 26, 1984 and February 19, 2005. The normal, almost continuous, cloud cover characteristic of the study area and the presence of transient snow on most images hamper the mapping of the true glacier limits and greatly diminish the suitability of most satellite data for analysis. The two images selected were almost entirely cloud free with little transient snow outside the glacier limits and were corrected for geometric and atmospheric distortions (Song et al. 2001; Tucker et al. 2004; SIB 2005) prior to the delimitation of glacier areas. These images were combined with a 30 m resolution digital elevation model (DEM) derived from Terra ASTER imagery to facilitate the identification of individual glacier basins². Ratio images of TM bands 4 and 5 (i.e. TM4/TM5) with an interactive examination of different masking thresholds were used to differentiate glacier ice from other surfaces (Paul 2004). This procedure is considered among the best available for mapping glaciers larger than

² This DEM is processed by The Land Processes Distributed Active Archive Center (LPDAAC), NASA Earth Observing System (EOS). Individual glacier basins were first identified using the HYDRO routine available in ArcInfo and then, based on the visual examination of available satellite imagery, maps and aerial and field photography, corrected manually to exclude minor satellite ice masses and focus only on the main body of selected glaciers.

0.1 km² by remote sensing (e.g. Paul et al. 2002) and was supplemented by the manual delineation of debris covered areas of Glaciar Piedras Blancas and Glaciar Torre. The approximate LIA maximum extent of these glaciers was mapped manually on the 1984 TM scene based on air photo interpretation and field mapping. However, as precise calendar dates often could not be assigned to the LIA maximum, the changes in area should be regarded as approximate and subject to correction as new data become available.

4.5. Results

4.5.1. Glaciar Torre

The main moraine ridges and other relevant features at Glaciar Torre are shown in Fig. 4.2. No precise dating control is available for the two conspicuous, outermost moraines M1 and M2 (Moraines I and II of Mercer 1965, see above). These moraine ridges are clearly discernible, especially on the north side of the valley, and can be followed for several hundred meters upvalley providing strong evidence for at least two major, earlier, glacier events at this site. Mercer (1965) located a peat deposit from a site where M2 and M3 (Moraine III of Mercer) are only a few meters apart (site A in Fig. 4.2). The basal peat date of 800 ± 85 ¹⁴C yrs BP³ provides a minimum age for probably both moraines indicating they pre-date the main LIA advances of the past few centuries. The frontal M3 comprises a broad band of ridges that have been extensively modified by fluvio-glacial activity at this site. Trees growing on two partially destroyed north lateral ridges that are correlated with this moraine indicate they were formed before the early 1600s (M3ab, Fig. 4.2 and Table 4.3). However, the presence of trees of similar or older ages on M4b (see below) implies that M3 predates 1600 and therefore the trees on M3 may not provide closely limiting dates.

³ This ¹⁴C date was calibrated to 1050-1400 A.D. (2-sigma probability distribution) using the CALIB radiocarbon calibration program (<http://calib.qub.ac.uk/calib/>) and the Southern Hemisphere calibration dataset of McCormack et al. (2004).

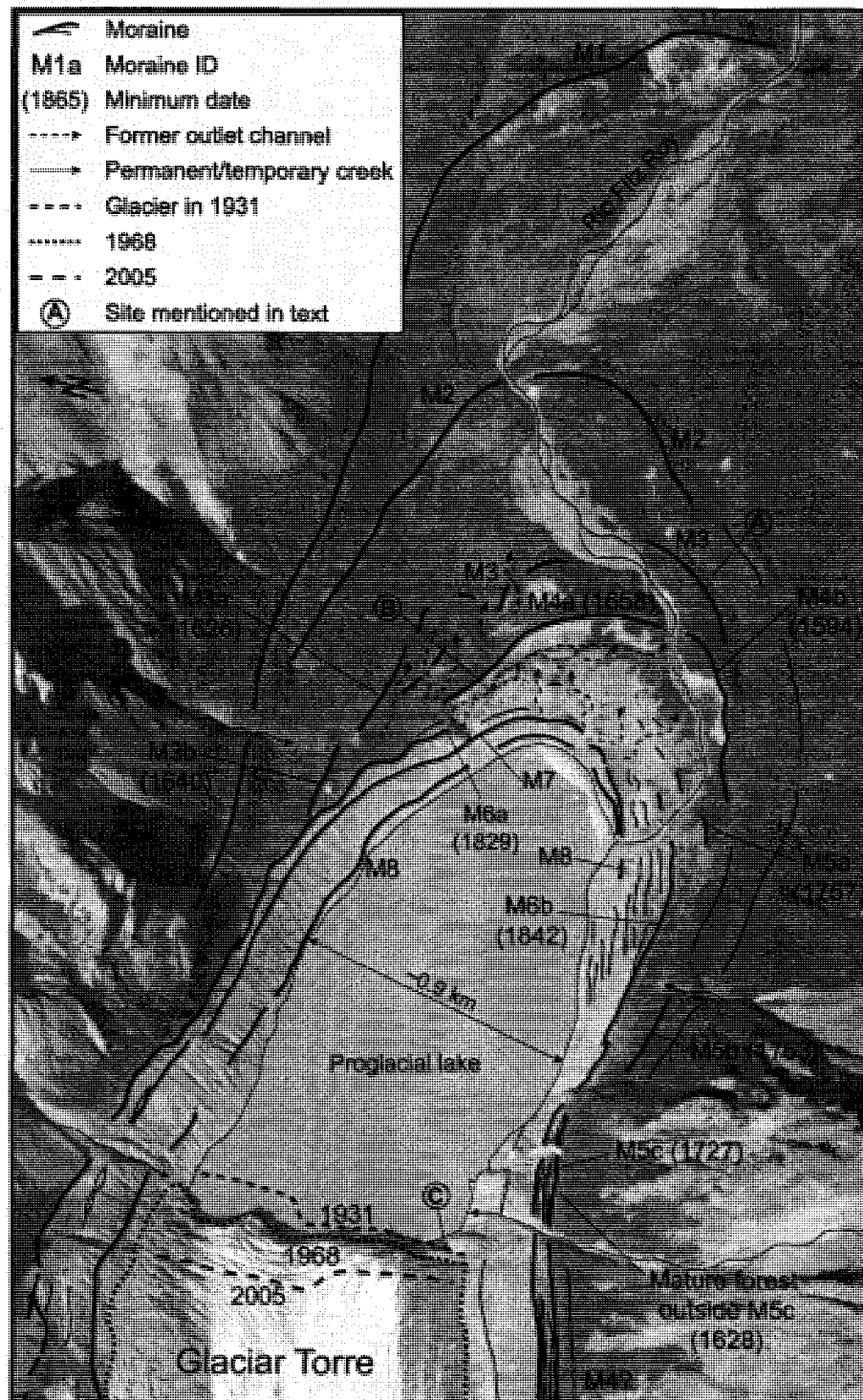


Fig. 4.2. Main features and tree-ring based minimum dates of moraines at Glaciar Torre. The mapping is based on a 1968 air photograph, and the 1931 (2005) glacier frontal position is based on historical documents (field surveys and satellite imagery) (see text for details).

A conspicuous, sharp frontal ridge on both sides of Río Fitz Roy (M4ab, Fig. 4.2) is tentatively interpreted as the LIA maximum at this glacier and represents a clear example of the importance of micro-environmental conditions in the establishment of vegetation that is used for the tree-ring dating of a given surface. The samples from the distal, more sheltered slopes of these moraines indicate that these deposits were formed sometime in the late 16th century (Table 4.3). On the contrary, the proximal unstable slopes of the moraines, constantly exposed to strong westerly winds, remain only barely vegetated. Unfortunately, no evidence has been found yet to provide a maximum, bracketing date for this event.

Table 4.3. Dendrochronological dating of moraines at Glaciar Torre. Number of trees and earliest ring dates from the three oldest trees are indicated with the estimated pith offset and sampling height correction factors. Minimum dates for the deposits after accounting for ecesis are shown in the last column. Notes: (D) distal slope of moraine; (P) proximal slope; (*) date obtained after crossdating with living trees (see text for details).

Sampling site	Number of trees; innermost ring dates (pith offset and sampling height correction factors)		Minimum age for surface (ecesis)
	North margin	South margin	
M3a (D)	16 trees; 1674 (20,13), 1683 (20,9), 1687 (20,8)		1626 (15)
M3b (P)	14 trees; 1685 (20,10), 1696 (10,5), 1730 (20,5)		1640 (15)
M4a and M4b (D)	28 trees; 1690 (10,7), 1705 (10,10), 1708 (20,7)	10 trees; 1635 (20,6), 1669 (15,11), 1676 (5,6)	M4a: 1658 (15) M4b: 1594 (15)
M5a (D)		5 trees; 1797 (15,10), 1815* (15,10), 1824* (20,10)	1757 (15)
M5b (P)		18 trees; 1783 (0,3), 1792 (20,4), 1792 (5,3)	1753 (15)
M5c (P)		27 trees; 1767 (15,10), 1767 (0,4), 1772 (15,13)	1727 (15)
Mature forest outside M5c		11 trees; 1664 (15,6), 1710 (20,10), 1722 (20,10)	1628 (15)
M6a and M6b (D)	20 trees; 1829 (10,5), 1872 (5,5), 1877 (0, 5)	13 trees; 1842 (2,5), 1854 (10,7), 1882 (0,5)	M6a: 1799 (15) M6b: 1820 (15)
M6 (P)		7 trees; 1929 (10,2), 1929 (0,8), 1934 (0,8)	1902 (15)
Former channel outside M7	9 trees; 1885 (0,4), 1894 (0,6), 1913 (3,6)		1866 (15)

Evidence for a subsequent glacier advance (M5) comes from the south margin of the glacier where a series of fragmented but conspicuous ridges occurs along the southern slope of the valley (Fig. 4.2). Although initially assumed to correspond to the M4 frontal moraines, based on morphological continuity, tree-ring dating of numerous trees growing on and immediately outside these ridges indicates that this deposit was formed later, during the early 1700s (M5a-c, Table 4.3 and Fig. 4.2). There is no strong morphological evidence for an equivalent event on the north margin of Río Fitz Roy and only a few large boulders and minor ridges remain as a possible indication of the former frontal glacier position of M5 (Fig. 4.2). The strong fluvio-glacial dissection beyond the former glacier snout has also largely destroyed the frontal moraines associated with the subsequent readvance (M6) of Glaciar Torre. However, the lateral extent of this advance is clearly indicated by two massive lateral moraine ridges at the margins of the proglacial lake (M6ab, Fig. 4.2). Tree-ring dating from trees growing on the more sheltered, distal slopes of M6 suggest a late 18th century minimum age for these deposits (Table 4.3). This determination comes from 20 trees sampled at the eastern end of the north lateral M6 (Fig. 4.2 and Table 4.3). However, recent, extensive sampling of *Rhizocarpon geographicum* lichens along the crest of this lateral moraine and in several other sites at this glacier (Irene Garibotti, pers. comm.) indicate a minimum age of 1740 for this deposit and suggests that in fact M6 may have not completely obliterated the evidence from the lateral M5 on the north side of the lake. Although preliminary, this complementary information may provide further evidence for the lateral extent and date of formation for M5 at this site. Evidence for at least two major subsequent events (M7 and M8) was identified inside M6, but as the moraines have no tree cover it was not possible to obtain direct minimum ages for the events. However, assuming a 15-yr ecesis, the pith date at the base of the oldest tree sampled along a former outlet channel associated with M7 (site B in Fig. 4.2) suggests that this moraine was formed before 1866 (Table 4.3). In addition, the examination of historical documents from 1931 (De Agostini 1945) indicates that the proglacial lake has remained approximately the same size for at least seven decades (Fig. 4.3A). Assuming that the trees at site B established only after the outlet channel was abandoned due to glacier front recession, M8 must have been formed only a few decades after M7, probably by the end of the 1800s or the beginning

of the 20th century. This implies a subsequent, dramatic glacier front recession (and a concurrent proglacial lake expansion) to the 1931 ice front position shown in Fig. 4.3A. The proglacial lake covers any evidence of more recent moraines (if they existed), and no evidence was found for subsequent, 20th-century readvances at Glaciar Torre.

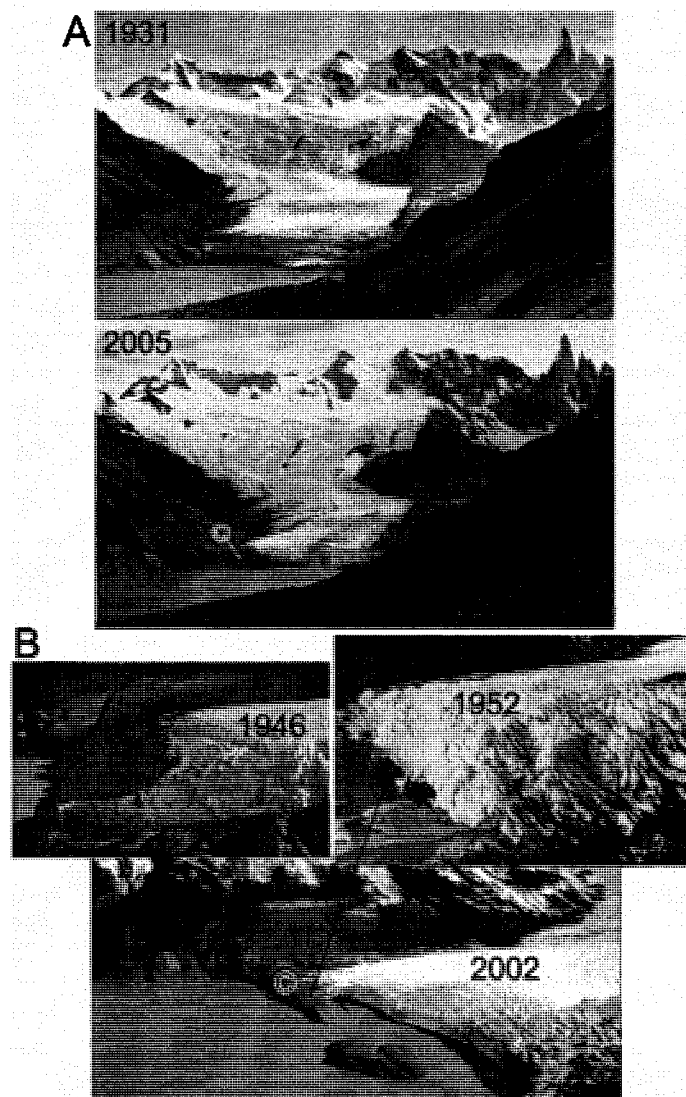


Fig. 4.3. (A) Historical changes of Glaciar Torre between 1931 (De Agostini 1945) and 2005 (photo R. Villalba). The 1931 view is one of the earliest photographs of this glacier. Note the significant thinning of the glacier tongue. (B) Frontal positions of Glaciar Torre in 1946 (Heim 1946), 1952 (Lliboutry 1953b) and 2002 (photo R. Villalba). The frontal bedrock ridge (denoted as C here and in Fig. 2) is about 50 m high.

Although the limited documentation available indicates that the glacier front has retreated a small distance during recent decades, the main loss of glacier ice at this site in the last 75 years has been principally due to a drastic thinning of the glacier tongue (Fig. 4.2 and 4.3). Using the conspicuous bedrock ridge in front of the glacier as a reference (denoted as C in Fig. 4.2 and 4.3), we estimate that the glacier has thinned by at least 50-60 m since 1952. In recent years the glacier snout has almost detached from this ridge and the width of the calving front has increased significantly (Fig. 4.3B). We suggest that this ridge acted as a pinning point that anchored the position of the glacier front for most of the 20th century. However, with recent retreat the snout is no longer protected by this ridge and calving processes will probably accelerate frontal recession in coming years.

4.5.2. Glaciar Piedras Blancas

Several massive frontal and lateral moraine ridges were identified at Glaciar Piedras Blancas (Fig. 4.4). On the eastern side of Río Blanco there are at least four possible moraine ridges (M1-4, Fig. 4.4) built against the steep slopes of Cerro Rosado. Although no dating control is available for these ridges, the small lake with thick organic sediments immediately outside M2 (site A, Fig. 4.4 and 4.5A) could potentially provide limiting dates for these features. Additional information may also be obtained from basal dates of the other peat bogs in this area (see Fig 4.4).

Moraines of at least four glacier advances (M5-M8, Fig. 4.4) have been identified and formed during the last few centuries. As the forest cover on the eastern portion of the moraines has been affected by forest fires, we concentrated sampling on the western sector of the lateral moraines immediately below a massive bedrock ridge (Fig. 4.4). Tree-ring dating from the north and south lateral M5 (Table 4.4) indicates that these ridges were formed during or prior to the early 17th century. Slightly older trees dating to 1573 were cored immediately outside M5 in mature, old-growth forests (Fig. 4.4). An inner moraine ridge (M6) was assigned an early 19th century date of formation based on trees growing on the north lateral ridge. However, the low number of trees colonizing this deposit and the wide disparity in ages for the north and south lateral moraines (1815 and 1886, respectively) suggest that this date may not be closely limiting (Table 4.4). In fact,

the oldest tree sampled on a former outlet channel immediately outside the north lateral M6 was dated to 1759. Assuming this channel was active when M6 was formed, this date suggests the channel was abandoned by the mid 1740s (Table 4.4) and the moraine could date from the mid 18th century.

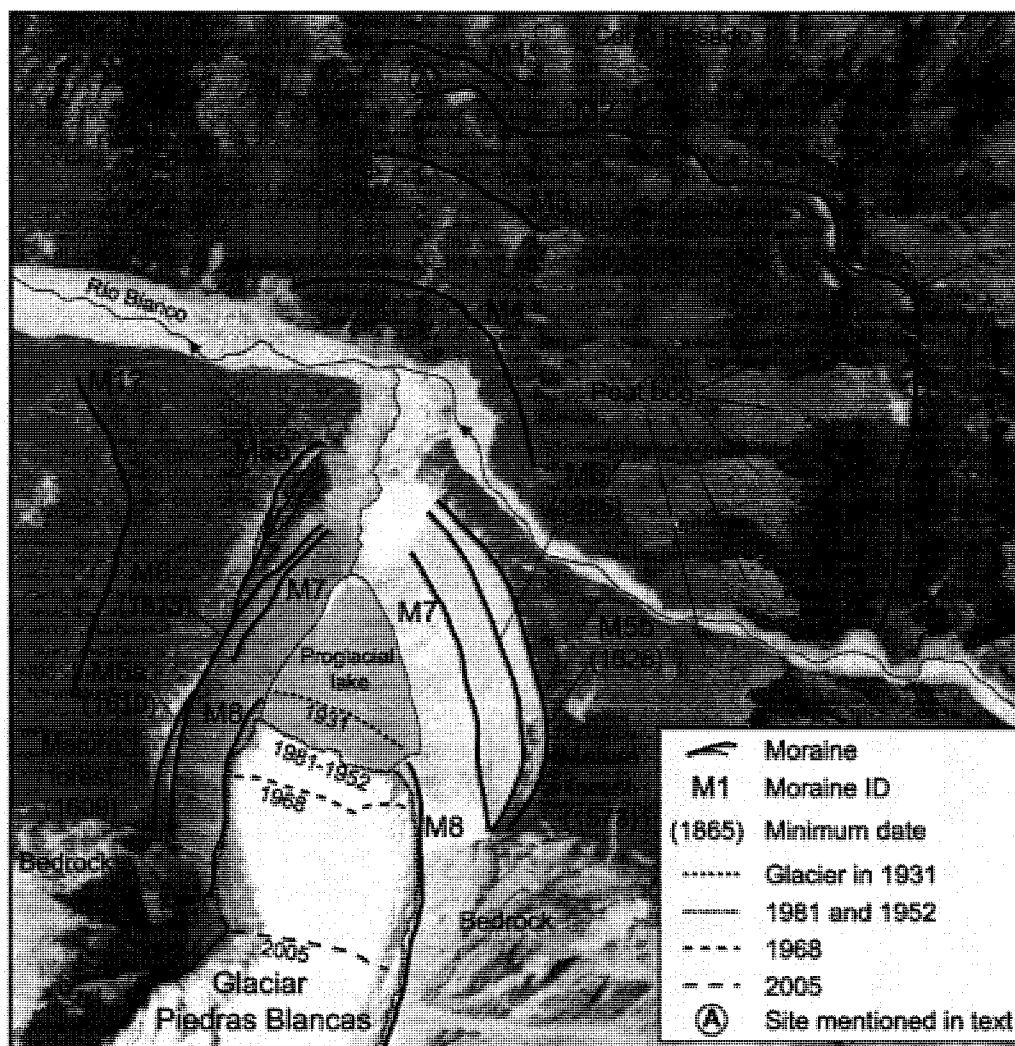


Fig. 4.4. Main features and dendroglaciological dating of moraines at Glaciar Piedras Blancas. The mapping is based on a 1981 air photograph and the widest point in the lake is about 450 m. The 1931 and 1952 glacier frontal positions are derived from photographs in De Agostini (1945) and Lliboutry (1953b), respectively. The 1968 and 2005 positions are based on air photos, field surveys and satellite imagery.

Table 4.4. As Table 4.3, but for Glaciar Piedras Blancas.

Sampling site	Number of trees; innermost ring dates (pith offset and sampling height correction factors)		Minimum age for surface (eaces)
	North margin	South margin	
Mature forest outside M5	17 trees; 1655 (20,11), 1690 (20,5), 1701 (20,10)	18 trees; 1616 (15,13), 1647 (20,10), 1655 (20,12)	North: 1609 (15) South: 1573 (15)
M5a and M5b (D)	7 trees; 1640 (5,10), 1656 (2,9), 1733 (2,13)	14 trees; 1672 (20,9), 1686 (0, 10), 1688 (0,12)	M5a: 1610 (15) M5b: 1628 (15)
M5a and M5b (P)	7 trees; 1670 (0,2), 1774 (15,3), 1806 (10,4)	7 trees; 1750 (20,10), 1777 (20,7), 1803 (20,13)	M5a: 1668 (15) M5b: 1705 (15)
Former channel between M5 and M6	2 trees; 1783 (20,4), 1812 (20,4)		1744 (15)
M6 (D)	4 trees; 1851 (10,11), 1895 (15,10), 1898 (6,4)		1815 (15)
M6 (P)		7 trees; 1931 (20,10), 1945 (4,2), 1946 (9,10)	1886 (15)

The remnants of M7 are poorly preserved on the unstable proximal slopes of M6 on both sides of the proglacial lake and lack tree-ring evidence for dating (Fig. 4.4). The innermost moraines identified at Glaciar Piedras Blancas (M8) mark the lateral limits of a more recent glacier advance during the early 20th century. The glacier front was very close to the M8 position in 1931 (Fig 4.5A, upper) but below it in 1952 (Fig. 4.5B, inset). The analysis of aerial photographs from 1968 and 1981 indicates that the glacier advanced again after 1968 and had reached approximately the 1952 position (i.e. stayed within M8 limits, Fig. 4.5B) by the early 1980s (Fig. 4.4). After this readvance Glaciar Piedras Blancas has retreated and thinned significantly and as a result, the lower, calving portion of the glacier snout is almost disconnected from the upper glacier (see Fig. 4.5A).

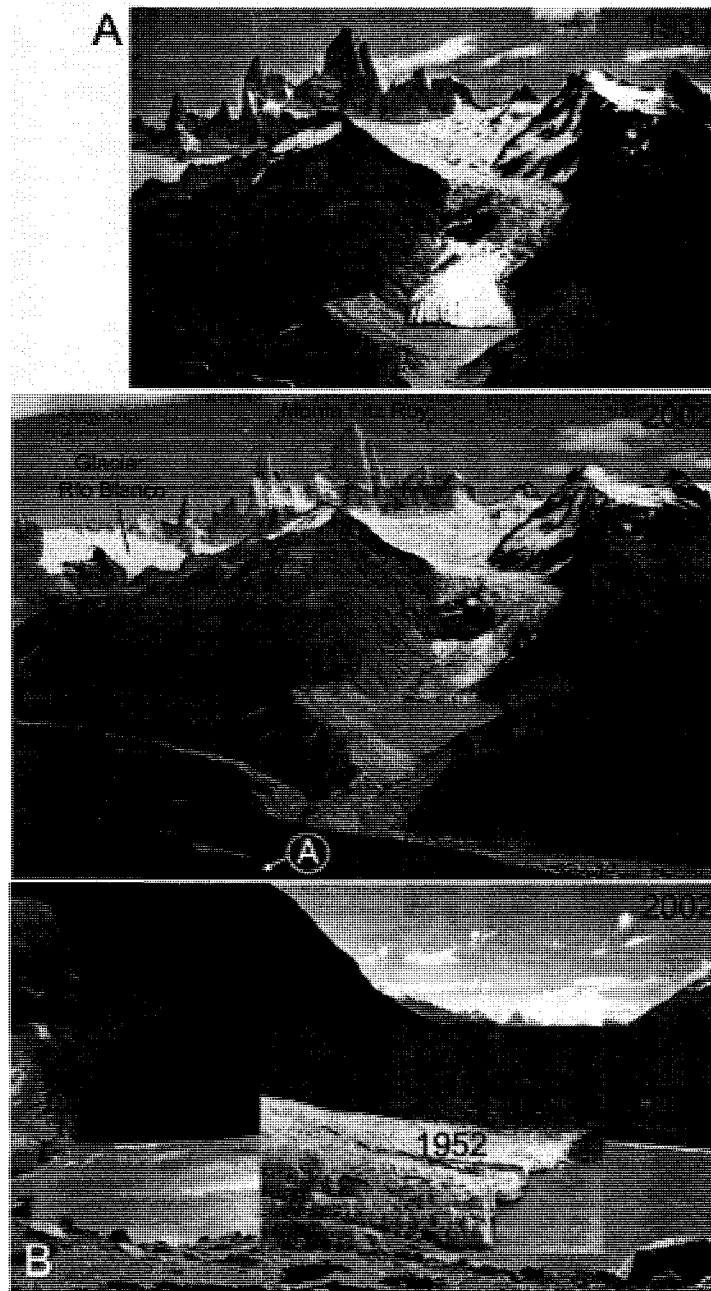


Fig. 4.5. (A) Paired comparison of Glaciar Piedras Blancas between 1931 (De Agostini 1945) and 2002 (photo M. Masiokas). Cerro Fitz Roy and Glaciar Río Blanco are located a few km to the southwest of Glaciar Piedras Blancas. A small moraine-dammed lake with thick organic deposits is denoted as A here and in Fig. 4.4. (B) Glacier front variations between 1952 (Lliboutry 1953b) and 2002 (photo R. Villalba). Note the north lateral M8 outside the glacier in 1952.

4.5.3. Glaciar Lago del Desierto I

The three glaciers investigated at Lago del Desierto all showed a clear sequence of moraines (Fig. 4.6) but in places the forest has been subject to recent fires. The forest on the outer moraines of the northernmost glacier has been burned but we located several trees that escaped these recent fires and a few well preserved *in situ*, burned stumps to provide minimum age estimates for some of these moraines. The oldest of nine mature trees sampled in the forest outside the outermost, northern moraine ridge (M1, Fig. 4.6A) was dated to 1654 (Table 4.5). Nine trees cored on the distal slope of the south lateral M1 showed similar ages with the oldest tree dating back to 1628. Between this outer moraine and the present glacier front position we identified at least seven moraines which were better preserved on the north margin of the glacier (M2-8, Fig. 4.6A). Four trees (including two *in situ* stumps) cored on the distal side of the north lateral M5 (Fig. 4.6A) provided a minimum reference date of 1740 for M5 (Table 4.5). In addition, the oldest tree sampled inside this moraine on the south margin of the central proglacial stream (Fig. 4.6A) was dated to 1830 (Table 4.5). A small, 1-1.5 m high ridge of boulders (M6, Fig. 4.6A) marks the limit of a recent glacier advance at this site, and the innermost ring of the trees inside this moraine was dated to 1901 (Table 4.5). Another small moraine ridge (M7) occurs a few meters inside M6 with trees of similar size and an innermost ring of 1905 (Table 4.5). This similarity in tree age and size between M6 and M7 suggests that M7 may have been formed soon after M6 in the late 1800s or early 20th century, probably during a minor advance or pause in glacier recession. These ridges were also identified on the south margin of the southern branch of the proglacial stream (Fig. 4.6A). A small ridge of boulders (M8), evidence for the most recent advance of this glacier, was found only a few meters in front of the current glacier margin on the steep bedrock slope but no trees had colonized this recently deglaciated surface.

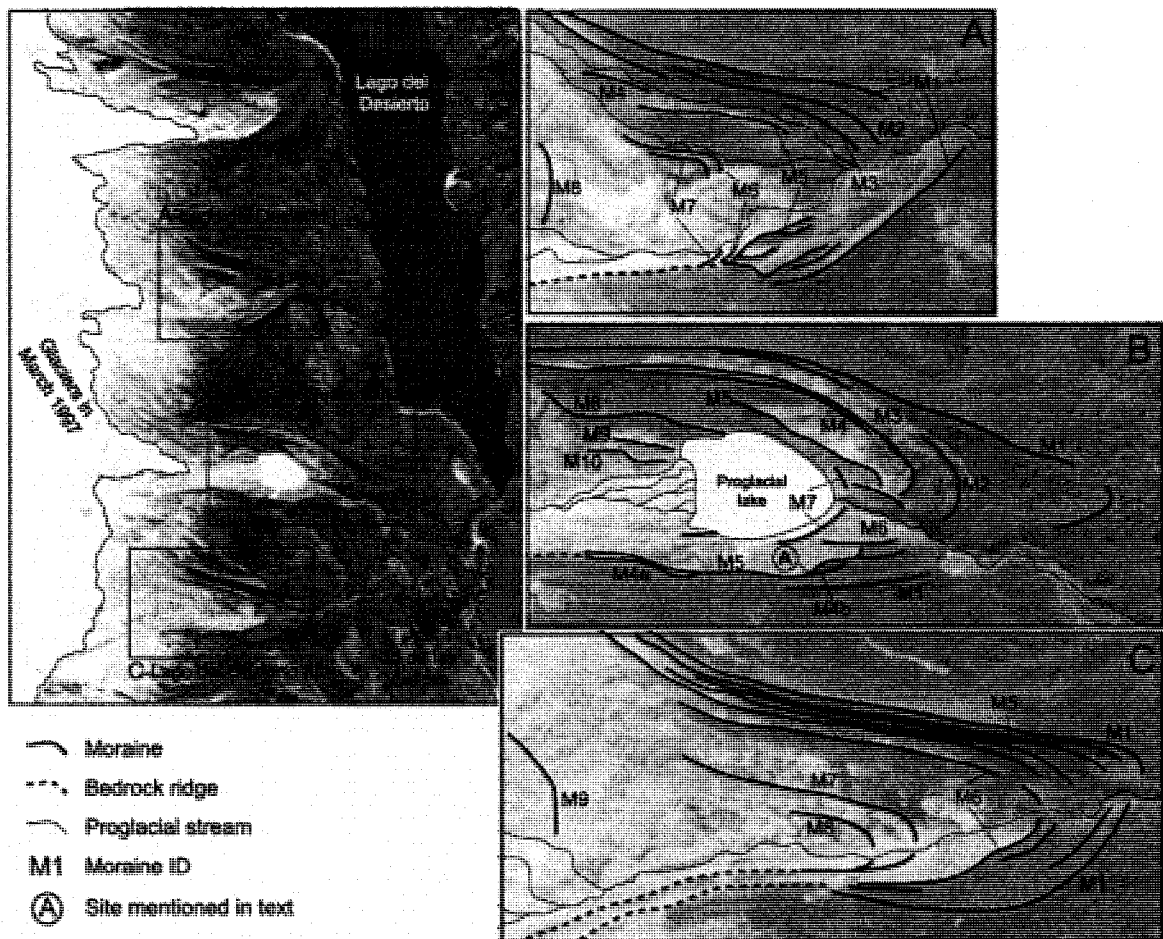


Fig. 4.6. Main features identified at the three glaciers studied in the Lago del Desierto area, identified from north to south as Glaciar Lago del Desierto I, II and III (A, B and C, respectively). The mapping is based on aerial photographs from March 1997 and the lake in front of Glaciar II is about 340 m long. The limit between M5 and older deposits at this same glacier is denoted by A (see text for details).

Table 4.5. As Table 4.3, but for the three glaciers at Lago del Desierto. Note: (#) The outermost ring of a single *in situ* stump on the distal slope of the south lateral M5 was crossdated to 1743 using a living tree-ring width chronology and provides a maximum age for this event. The innermost ring of another partially buried living tree that apparently survived this event was dated to 1725 (see text for details).

Glacier	Sampling site	Number of trees; innermost ring dates (pith offset and sampling height correction factors)		Minimum age for surface (ececis)
		North margin	South margin	
Lago del Desierto I	Mature forest outside M1	9 trees; 1695 (20,6), 1698 (10,8), 1769 (20,10)		1654 (15)
	M1 (D)		9 trees; 1668 (20,5), 1674 (20,8), 1713 (3,13)	1628 (15)
	M5 (D)	4 trees; 1788 (20,13), 1805* (20,5), 1819 (20,3)		1740 (15)
	Inside M5	16 trees; 1849 (0,4), 1862 (3,1), 1864 (10,4)		1830 (15)
	Inside M6	9 trees; 1921 (3,2), 1930 (0,1), 1935 (0,1)		1901 (15)
	Inside M7	17 trees; 1924 (0,4), 1936 (5,2), 1940 (5,4)		1905 (15)
Lago del Desierto II	Mature forest outside M4		3 trees; 1575 (20,12), 1599 (15,10), 1709 (20,15)	1528 (15)
	M4a (P)		6 trees; 1645 (5,10), 1670 (10,8), 1672 (20,6)	1615 (15)
	M4b (D)		3 trees; 1689 (20,13), 1794 (3,7), 1821 (15,12)	1656 (15)
	M5 (D)#		15 trees; 1772 (10,4), 1772 (3,4), 1804 (10,4)	1743 (15)
	M8 (P)	14 trees; 1931 (0,1), 1941 (0,1), 1945 (0,2)		1900 (30)
	M9 (P)	5 trees; 1967 (0,1), 1972 (0,1), 1982 (0,1)		1936 (30)
	M10 (D)	1 tree; 1994 (0,0)		1964 (30)

Table 4.5. Cont'd.

Lago del Desierto III	M1 (D)	9 trees; 1581 (20,13), 1591 (10,13), 1631 (0,5)		1553 (15)
	M1 (P)	2 trees; 1669 (20,15), 1786 (20,13)		1619 (15)
	M5 (P)	4 trees; 1702 (20,12), 1730 (0,10), 1809 (20,10)		1655 (15)
	M6 (D)	25 trees; 1755* (0,6), 1759 (10,10), 1766* (10,5)		1734 (15)
	M6 (C)	1 tree; 1774 (15,10)		1734 (15)
	M6a and M6b (P)	5 trees; 1857 (20,3), 1862 (20,4), 1873 (10,3)	2 trees; 1930 (20,10), 1949 (20,10)	M6a: 1819 (15) M6b: 1885 (15)
	M7 (D)		1 tree; 1951 (0,8)	1928 (15)
	M7a and M7b (C)	2 trees; 1920 (0,2), 1944 (0,2)	2 trees; 1946 (3,2), 1958 (0,2)	M7a: 1903 (15) M7b: 1926 (15)
	M7 (P)	8 trees; 1900 (0,18), 1904 (0,2), 1927 (10,2)		1867 (15)
	M8 (P)	6 trees; 1936 (0,1), 1944 (5,1), 1958 (0,4)		1920 (15)
	Outside M9	3 trees; 1976 (0,1), 1978 (0,1), 1979 (0,1)		1945 (30)
	M9 (C)	1 tree; 1985 (0,0)		1955 (30)

4.5.4. Glaciar Lago del Desierto II

Glaciar Lago del Desierto II (locally known as Glaciar Huemul) is the most easily accessible and is frequently visited by tourists arriving at the southern shores of Lago del Desierto (Fig. 4.6). This glacier is also the only one with a proglacial lake that has developed between the recent moraines and the steep bedrock outcrop where the glacier snout is presently located. At least ten moraines were identified in front of this glacier and on both sides of the lake (Fig. 4.6B). This complex glacial history is difficult to elucidate because some moraines have been partially or completely overridden by subsequent, more extensive events and because recent fires have destroyed potential tree-ring sampling sites, especially on the north side of the lake. As a result, a complete glacial chronology is not available, and we currently do not have precise dating control for the three outermost moraines identified at this site (M1-3, Fig 4.6B). However, on the south margin of the glacier the forest was protected from burning by steep bedrock ridges, and six mature trees cored along the crest and proximal slope of M4 were tree-

ring dated to 1615 providing a minimum age estimate for this event (Table 4.5). Further downglacier, three trees sampled immediately outside M4 were dated to 1528 (Table 4.5). Although preliminary, these tree ages indicate that moraines M1-M3 pre-date 1528 and that M4 was probably formed in the early 1700th century.

M5 is a sharp, arcuate moraine ridge clearly visible on both sides of the proglacial lake (Fig. 4.6B). The south lateral M5 has partially overridden the lateral M4, and at the bottom of the distal slope of M5 we found one *in situ* stump that seemed to have been killed during the formation of the moraine and was partially buried by glacier deposits. A 101 yr-long tree-ring width series was developed from this stump and crossdated with the Glaciar Piedras Blancas chronology. The outer ring was dated to 1743. A living tree with its base also buried by glacier deposits was sampled a few meters from the *in situ* snag and the innermost ring was dated to 1725 by simple tree-ring counting. We interpret these data as indicating that the glacier event forming M5 culminated in the 1740s when relatively fine material was being deposited in front of the moraine, killing the *in situ* stump which therefore provides a precise maximum date for this event. The partially buried living tree at this site was probably a small seedling at the time of moraine formation and may have survived this event. The earliest ring of 15 living trees growing on these deposits at the foot of the distal slope was dated to 1758 (Table 4.5) indicating that deposition from the moraine had ceased by that time. This value also suggests a lag time between moraine stabilization and tree establishment of about 15 years at this site.

Further downvalley along this ridge, the morainic material on the distal slope of M5 becomes much coarser and the trees are much older and larger (site A in Fig. 4.6B). This was interpreted in the field and by re-examination of aerial photographs as the limit between M5 and an older surface (probably M4) that had been partially overridden by M5. The earliest ring of the oldest of three trees sampled on this coarser and apparently older deposit (denoted as M4b in Fig. 4.6B) was dated to 1656. Unfortunately the forest on M6 and M7 (Fig. 4.6B) has been seriously affected by forest fires and no tree-ring based age estimations are available for these events. Three additional, more recent moraines (M8-10, Fig. 4.6B) with no evidence of fire activity are located on the steep

bedrock slope between the proglacial lake and the present glacier margin. The basal pith date of the oldest tree sampled inside M8 (M9) was 1930 (1966), and only one tree (with a basal pith dated to 1994, Table 4.5) was found on the distal slope of the innermost of these moraines (M10). Available air photographs (Table 4.1) indicate that the glacier front was already several meters behind this moraine by 1966, suggesting that it took at least 29 years for this tree to colonize the newly exposed surface. We applied a larger ecesis of 30 years to these more recent moraines (M8-10) and preliminarily dated them to 1900, 1936 and 1964, respectively (Table 4.5).

4.5.5. Glaciar Lago del Desierto III

Glaciar Lago del Desierto III is the southernmost of the glaciers studied in this area (Fig. 4.6). Detailed examination of the glacier forefield and the available documentation revealed the existence of at least nine distinct moraines (M1-9) that are particularly well-preserved as arcuate ridges on the north side of the proglacial stream (Fig. 4.6C). However, as extensive portions of these moraines have been affected by forest fires we focused on those deposits where tree-ring dating was feasible. Several mature trees were sampled on the outermost moraine ridge (M1, Fig. 4.6C) and indicate that this deposit is at least 450 years old (Table 4.5). Inside these deposits on the proximal slope of M5 two trees that apparently survived the fire were about 350 years old. Both living and dead trees (*in situ* stumps killed by recent fires) were sampled along an inner, well-defined moraine ridge with immature forest cover (M6, Fig. 4.6C). The inner and outermost rings of four of the five burned stumps sampled were successfully crossdated using the Piedras Blancas chronology and indicate they established between 1749 and 1784 and were killed between 1949 and 1968. Together with similar minimum ages obtained from living trees (Table 4.5), this suggests that this moraine was probably formed during the early 1700s. The three moraines observed within M6 (M7-9, Fig. 4.6C) showed no evidence of former fires. The age of the oldest tree sampled in association with M7 indicate that this deposit is at least 138 years old. The trees inside M8, on the north margin of the proglacial stream, indicate it was formed before 1920 (Table 4.5). The only seedling found on M9 had a basal date of 1985 and the basal pith of the oldest of three trees immediately outside the moraine was dated to 1975 (Table 4.5). Since these trees are growing in

roughly similar conditions to those at M10 in Glaciar Lago del Desierto II (see above), we assumed a larger, 30-yr ecesis value for this particular site and dated this moraine to about 1945 (Table 4.5).

4.5.6. Changes in glacier area

Preliminary estimates of glacier area changes since the LIA and between 1984 and 2005 were derived from Landsat TM satellite imagery and represent the first attempt to document long term glacier changes in the study area. These data will also be valuable reference measures for future monitoring of these sites (Table 4.6). Glaciar de los Tres and Glaciar Río Blanco, located between Glaciar Torre and Glaciar Piedras Blancas (Fig. 4.1), were included for completeness. The 1995-96 area of Glaciar de los Tres (0.976 km²) is known from field measurements (Popovnin et al. 1999) and agrees reasonably well with our estimates for 1984 and 2005 (Table 4.6), providing an independent validation of our results based on the relatively coarse (~30 m) resolution of Landsat TM sensors. The approximate dates for the LIA maximum at each glacier are based on tree-ring based minimum age estimates from the late 1500s and early 1600s for specific moraines at each site (Table 4.6). As moraine positions are interpolated in some cases, these areas only provide a rough, minimum estimate of LIA surface area for comparison with present conditions. The results in Table 4.6 indicate that these glaciers had lost between 20 and 48% of their LIA area by 2005. The smaller glaciers show the highest proportional reductions: the three small glaciers at Lago del Desierto shrank by an average of 44% whereas Glaciar Torre and Piedras Blancas, though losing a greater absolute area, decreased by only ~21%. In the last two decades these glaciers have lost between 5 and 18% of their 1984 areas. The significant downwasting of glacier surfaces since the LIA maximum suggests that glacier mass losses are proportionally greater than these areal estimates indicate.

Table 4.6. Approximate changes in glacier area (in km²) between the LIA, 1984 and 2005 based on the analysis of Landsat TM satellite imagery (Table 4.1). Maximum extent and dating of LIA advances was based on the location of LIA maximum moraines and tree-ring based estimations (refer to text for details). Area changes between 1984 and 2005 for Glaciar Río Blanco and Glaciar De Los Tres are included for completeness.

Glacier	LIA area (approx. date)	Moraine used	1984 (% change since LIA)	2005 (% change since 1984)
Torre	30.8 (late 1500s)	M4	26.2 (-14.9%)	24.6 (-6.1%)
Río Blanco	N/A	N/A	4.42	4.21 (-4.8%)
De los Tres	N/A	N/A	1.01	0.90 (-10.9%)
Piedras Blancas	7.20 (early 1600s)	M5	6.02 (-16.4%)	5.63 (-6.5%)
Lago del Desierto I	1.60 (early 1600s)	M3/4	0.87 (-45.6%)	0.83 (-4.3%)
Lago del Desierto II	3.03 (early 1600s)	M4	2.21 (-27.1%)	1.92 (-13.1%)
Lago del Desierto III	1.79 (early 1600s)	M5	1.16 (-35.2%)	0.95 (-18.1%)

4.6. Summary and Conclusions

The available evidence from the five small glaciers studied in the Fitz Roy and Lago del Desierto areas (Fig. 4.1) highlights the complex late Holocene glacial history of this region and the existence of numerous glacier advances during the past few centuries (Table 4.7). In most cases there are at least three or four well-defined older moraine ridges downvalley of early 17th century LIA moraines but they could not be accurately dated with the available evidence (Fig. 4.2, 4.4 and 4.6). Provisional minimum age estimations from a single ¹⁴C date inside M2 at Glaciar Torre and tree-ring data from this glacier and Glaciar Lago del Desierto II suggest these moraines probably pre-date 1500 A.D. Recent investigations at Glaciar Seco⁴ revealed several massive bouldery lateral moraines with a mature forest cover similar to those seen at Lago del Desierto.

Radiocarbon dates from subfossil logs preserved beneath the boulders of the outermost of these moraines indicate these boulders were emplaced after 1000 ¹⁴C yrs BP. Given the morphological similarities between the moraine records at these sites, it seems possible that the outermost moraines at Lago del Desierto could be of similar age. Röthlisberger (1986), Luckman and Villalba (2001) and Masiokas et al. (2001) have also reported radiocarbon dates in the 500-1500 ¹⁴C year BP time frame from wood recovered from

⁴ Glaciar Seco is a small, east facing glacier located ca. 95 km to the south of Glaciar Torre that was investigated in 2005.

sub-till localities at several glaciers in the vicinity of the study area (Espizua et al. in preparation). However, correlation of these events will remain problematic until better dating control is available. Future investigations at Glaciar Piedras Blancas could target the small moraine-dammed pond or the peat bogs within the older moraines (see Fig. 4.4 and 4.5) that might provide evidence to date some of these earlier advances.

Table 4.7. Summary of tree-ring based minimum (<) and maximum (>) age estimates for the main moraine systems identified at the five glaciers analyzed in this study. Note: (*) see text for details about the preliminary dating of M6 at Glaciar Piedras Blancas.

Period	Glacier				
	Torre	Piedras Blancas	Lago del Desierto I	Lago del Desierto II	Lago del Desierto III
2000-present					
1975-99		Early 1980s?			
1950-74			M8?	<1964 (M10)	
1925-49		~1931 (M8)		<1936 (M9)	<1945 (M9)
1900-24	M8?		<1905 (M7) <1901 (M6)	<1900 (M8)	<1920 (M8)
1875-99					
1850-74	<1866 (M7)	M7?		M7-M6?	<1867 (M7)
1825-49					
1800-24		<1815 (M6)*			
1775-99	<1799 (M6)				
1750-74					
1725-49	<1727 (M5)	<1744? (M6)*	<1740 (M5)	<1743> (M5)	<1734 (M6)
1700-24					
1675-99					
1650-74					<1655 (M5)
1625-49				<1645 (M4)	
1600-24		<1610 (M5)	M4-M1		M4-M1
1575-99	<1594 (M4)				
Prior to 1574	M3-M1	M4-M1			

The LIA maximum at these glaciers was tentatively identified as a series of massive moraines that tree-ring dating indicates were formed during or before the late 1500s – early 1600s (Tables 4.3, 4.5 and 4.7). Although no closely limiting dating control is currently available for these events, the examination of the tree-ring samples and the conditions at the sampling sites (i.e. health of the forest, size of trees, etc) suggest that, even after accounting for the inherent uncertainties of ecesis and other correction factors,

the potential error associated with these minimum age estimates is ca. ± 20 years. Similar dating of moraines from other glaciers in the south Patagonian Andes (e.g. Glasser et al. 2004; Koch and Kilian 2005; Aravena 2007) seem to corroborate this preliminary dating and suggests the existence of a major glacier event in this area between the late 16th century and the early 17th century.

The best documented glacier advances in the study area were identified immediately inside the massive ridges of the LIA maxima and occurred in the first decades of the 18th century (Table 4.7). The clearest evidence for this event comes from Lago del Desierto with the tree-ring dating of M5 at Glaciar II to ca. 1743 and from moraines M5 at Glaciar I and M6 at Glaciar III dating to ca. 1740 and 1734, respectively (Fig. 4.6 and Table 4.5). Preliminary analyses of available aerial photographs revealed the existence of apparently similar features in other glaciers immediately to the north of Glaciar Lago del Desierto I (Fig. 4.6), suggesting that this was probably a widespread (and likely simultaneous) event throughout this area. An event of similar age (M5, Fig. 4.2 and Table 4.3) was also observed at Glaciar Torre, and although the associated depositional landforms have been largely modified by later readvances, complementary dendrochronological and lichenometric determinations suggest it was formed in the early 1700s. The evidence for a concurrent event at Glaciar Piedras Blancas is not clear as the (apparently) equivalent moraines (M6, Fig. 4.3) inside the LIA maximum were dated to the early 1800s based on the few trees found on their surface. However, tree-ring samples along a former outlet channel immediately outside the north lateral M6 (Table 4.4) suggest that this moraine could in fact have been formed in the first half of the 18th century (see above). In contrast to earlier advances, the moraines of the early 1700s event were dated by bracketing ages from living and sub-fossil trees well within their maximum life span. Since this advance was clearly identifiable at most sites in the study area, it was used here as a relatively well-dated reference event to evaluate the sequence of advances at each site and the relationship with those at other glaciers analyzed in this study (Table 4.7). For example, the moraine sequence at Glaciar Torre (Fig. 4.2) shows that there are no major moraines between the early 1700s and the LIA maximum advance of the late 1500s (M5 and M4, respectively). A similar situation can also be observed at Glaciar Piedras Blancas (Fig.

4.4), and probably applies to other glaciers in the study area, especially those at Lago del Desierto that showed several, poorly dated outer ridges that hampered the identification of the LIA maximum extent (Fig. 4.7).

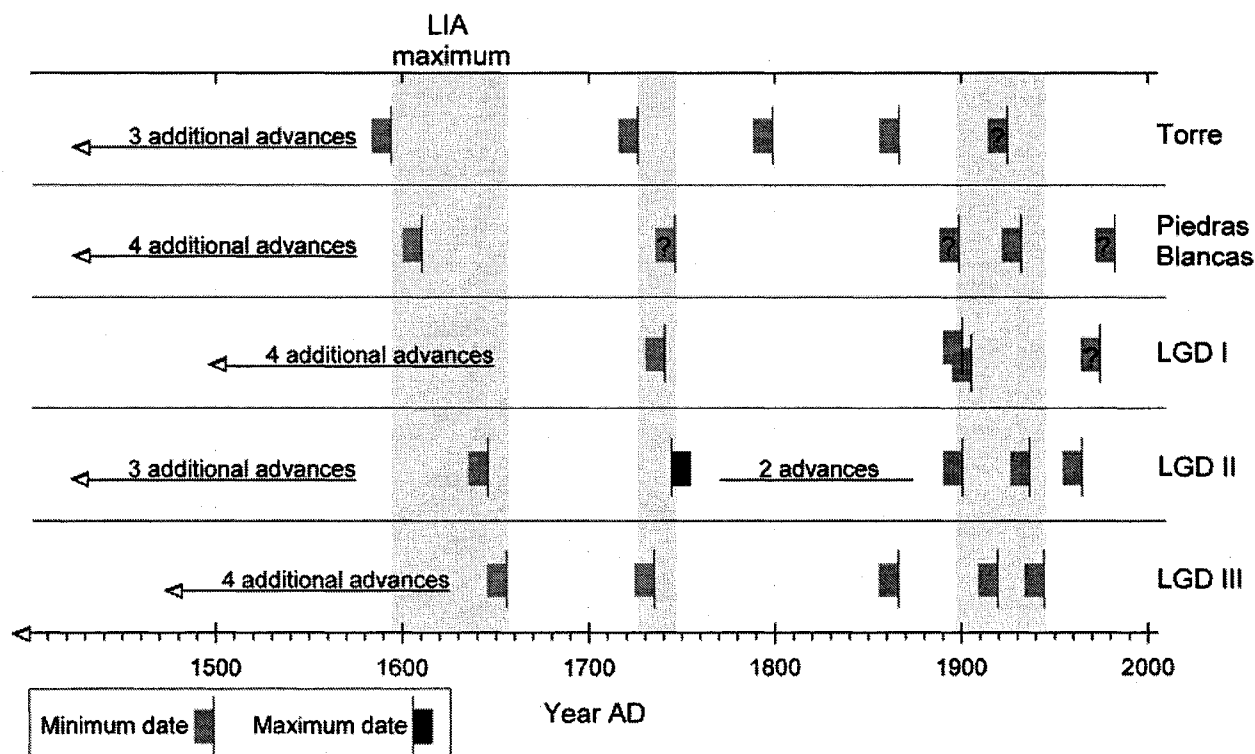


Fig. 4.7. Summary of available age estimates for the main glacier advances identified in the Fitz Roy and Lago del Desierto areas (for details see Table 4.7). Shaded bars indicate probable ages of major glacier events.

We identified three glacial events after the early 1700s at all glaciers studied except for Glaciar Lago del Desierto II, where at least five readvances occurred (M6-10, Fig. 4.6 and Table 4.7). Although the tree-ring based minimum ages for these events span several decades, they indicate a regional glacier reactivation during the late 19th and early 20th centuries when all glaciers experienced readvances within a few decades (Table 4.7 and Fig. 4.7). However, the uncertainties inherent in such dendroglaciological dates prohibit precise evaluation of synchronicity as it is possible that events spaced only a few decades apart could be assigned approximately similar minimum ages (see e.g. M6/M7 at Glaciar Lago del Desierto I, or M8/M9 at Glacier III, Table 4.7). Future research should, if

possible, pay special attention to those sites and situations where evidence could provide more precise, maximum age estimates for these more recent glacier events in the study area.

The analysis of available Landsat TM satellite imagery from the study sites are the first quantitative estimates of the long-term changes in glacier area since the LIA. It also provides important reference material for future studies and complements the evidence from repeat photography of historical documents (Table 4.6 and Fig. 4.3 and 4.5). The results indicate a loss of between 20-48% of the LIA glacier area to 2005 with significant recession (5-18%) in the last two decades. Smaller glaciers have suffered proportionally greater loss of area. These figures underestimate volumetric losses as many glaciers have also thinned considerably in the 20th century. This widespread overall pattern of recession agrees with the results from the majority of glacier studies in the region (e.g. Rignot et al. 2003).

In general, our study highlights the importance of analyzing detailed results from single case studies with caution and the need to build a regional database of well dated records from carefully selected sites before we can fully elucidate the complex late Holocene glacier history of this region. Although these results indicate general patterns of glacier fluctuations, differences between the individual records may reflect real differences in glacier response/behavior or uncertainties inherent in the dating controls presently available. This was particularly evident at the Lago del Desierto area, where three glaciers of similar size, setting and moraine sequences showed a relatively poor agreement in the tree-ring based estimates of the age of the most recent moraines (see Fig. 4.6 and Table 4.7). Although an increased sample of study sites will improve our understanding of the LIA and post-LIA glacier history of this region, they must provide an adequate sample of more precisely dated histories that may not be possible at every site. Bracketed dating, locating glacier damaged trees and improved ecesis estimates may yield better dendrogeomorphic dates but it is also important to evaluate other dating techniques such as lichenometry, glaciolacustrine sedimentary records and basic stratigraphy to complement dendrogeomorphic techniques. The existence of numerous,

additional small valley glaciers surrounded by dense forests neighboring the Patagonian Icefields (see Fig. 4.1) offer many opportunities for such multi-disciplinary, multi-proxy paleoenvironmental initiatives.

4.7. References

- Aniya, M. 1995. Holocene glacial chronology in Patagonia: Tyndall and Upsala glaciers. *Arctic and Alpine Research* 27, 311–322.
- Aniya, M. 1996. Holocene variations of Ameghino Glacier, southern Patagonia. *Holocene* 6, 247–252.
- Aniya, M., Sato, H., Naruse, R., Skvarca, P and Casassa, G. 1996. The use of satellite and airborne imagery to inventory outlet glaciers of the Southern Patagonian Icefield, South America. *Photogrammetric Engineering and Remote Sensing* 62, 1361–69.
- Aniya, M., Sato, H., Naruse, R., Skvarca, P., and Casassa, G. 1997. Recent glacier variations in the Southern Patagonia Icefield, South America. *Arctic and Alpine Research* 29 (1), 1-12.
- Aravena, J.C. 2007. Reconstructing climate variability using tree rings and glacier fluctuations in the southern Chilean Andes. PhD Thesis, Department of Geography, University of Western Ontario, Canada. 236 pp.
- Auer, V. 1956. The Pleistocene of Fuego-Patagonia. Part I: The Ice and Interglacial Ages. *Annales Academia Scientiarum Fennicae, Series AIII*, 226 pp.
- Bertone, M. 1960. Inventario de los glaciares existentes en la vertiente Argentina entre los paralelos 47°30' y 51° S. Instituto Nacional del Hielo Continental Patagónico, Pub. No. 3, Buenos Aires, 104 pp.
- Bertone, M. 1972. Aspectos glaciológicos de la zona del Hielo Continental Patagónico. Instituto Nacional del Hielo Continental Patagónico, Buenos Aires, 130 pp.
- Casassa, G., Rivera, A., Aniya, M., and Naruse R. 2002. Current knowledge of the Southern Patagonia Icefield. In: Casassa, G., Sepúlveda, F., and Sinclair, R. (eds.), *The Patagonian Icefields. A unique natural laboratory for environmental and climate change studies*. Kluwer Academic/Plenum Publishers, New York, pp. 67-83.
- Clapperton C.M. 1993. *Quaternary Geology and Geomorphology of South America*. Elsevier, Amsterdam,
- De Agostini, A.M. 1945. *Andes Patagónicos* (2nd ed.), Guillermo Kraft Ltda., Buenos Aires, 437 pp.

- Delgado, S., Masiokas, M., Villalba, R., Trombotto, D., Ripalta, A., Hernández, J., and Calí, S. 2002. Historical and dendrochronological evidences for glacier fluctuations in Patagonia during the past 1000 years (PATAGON-1000). In: Trombotto, D. and R. Villalba (eds.), IANIGLA, 30 Years of Basic and Applied Research on Environmental Sciences. ZetaEditores, Mendoza, Argentina, pp. 47-51.
- Escobar, F., Vidal, F., and Garin, C. 1992. Water balance in the Patagonia Icefield. *Bulletin of Glacier Research* 4, 109–120.
- Espizua, L., Rivera, A., Masiokas, M.H., Villalba, R., Aravena, J.C., and Delgado, S. In preparation. Glacier fluctuations in extratropical South America during the past 1000 years: A review. To be submitted to *Palaeogeography, Palaeoclimatology, Palaeoecology*.
- Glasser, N.F., Hambrey, M.J., and Aniya, M. 2002. An advance of Soler Glacier, North Patagonian Icefield, at ca. AD 1222–1342. *Holocene* 12, 113–120.
- Glasser, N.F., Harrison, S., Winchester, V. and Aniya, M. 2004. Late Pleistocene and Holocene palaeoclimate and glacier fluctuations in Patagonia. *Global and Planetary Change* 43: 79-101.
- Grosjean, M. and Villalba, R. 2006. Regional climate variations in South America over the late Holocene. *PAGES News, Workshop reports* 14, 26.
- Grove, J.M. 2004. *Little Ice Ages: Ancient and Modern* (2 vols), Routledge, London, 718 pp.
- Heim, A. 1951. Informe sobre un estudio glaciológico en el Parque Nacional Los Glaciares. *Anales de Parques Nacionales*, Buenos Aires, 10 pp.
- Johannesson, T., Raymond, C.F., and Waddington, E.D. 1989. A simple method for determining the response time of glaciers. In: Oerlemans J. (ed.), *Glacier Fluctuations and Climatic Change*, Kluwer, Dordrecht, pp. 343-352.
- Koch, J., and Kilian, R. 2005. "Little Ice Age" glacier fluctuations, Gran Campo Nevado, southernmost Chile. *Holocene* 15, 20-28.
- Kölliker, A., Kühn, F., Reichert, A., Tomsen, A., and Witte, L. 1917. Patagonia: Resultados de las expediciones realizadas en 1910 a 1916. *Sociedad Científica Alemana*, Buenos Aires, (2 vols), 430 pp.
- Lliboutry, L. 1952. Estudio cartográfico, geológico y glaciológico de la zona del Fitz Roy. *Instituto de Geografía, Universidad de Buenos Aires*, 62 pp.

- Lliboutry, L. 1953a. More about advancing and retreating glaciers in Patagonia. *Journal of Glaciology* 2 (13), 168-172.
- Lliboutry, L. 1953b. Snow and ice in the Monte Fitz Roy region (Patagonia). *Journal of Glaciology* 2 (14), 255-261.
- Lliboutry, L. 1993. Thrust of Glaciar Torre over itself. *Journal of Glaciology* 39 (133), 707-708.
- Luckman, B.H. 1986. Reconstruction of Little Ice Age events in the Canadian Rocky Mountains. *Geographic Physique et Quaternaire* 40, 17-28.
- Luckman, B.H. 1988. Dating the moraines and recession of Athabasca and Dome Glaciers, Alberta, Canada. *Arctic and Alpine Research* 20, 40-54.
- Luckman, B.H. 2000. The Little Ice Age in the Canadian Rockies. *Geomorphology* 32, 357-384.
- Luckman, B.H., and Villalba, R. 2001. Assessing the synchronicity of glacier fluctuations in the western cordillera of the Americas during the last millennium. In: Markgraf, V. (ed.), *Interhemispheric Climate Linkages*, Academic Press, London, pp. 119-40.
- Masiokas, M., Casteller, A., Villalba, R., Trombotto, D., Ripalta, A., Hernandez, J., and Lázaro, M. 2000. Latitudinal differences in glacier fluctuations across Patagonia: A dendrogeomorphological approach to characterize climate variability in the southern Andes during the past 1000 years. In: *Abstracts from the International Conference on Dendrochronology for the Third Millennium*, Mendoza, Argentina, pp. 176.
- Masiokas, M., Villalba, R., Delgado, S., Trombotto, D., Luckman, B., Ripalta, A., and Hernandez, J. 2001. Dendrogeomorphological reconstruction of glacier variations in Patagonia during the past 1000 years. In: *Abstracts from the International Conference Tree Rings and People*, Davos, Switzerland, pp. 177.
- McCarthy, D.P., and Luckman, B.H., 1993. Estimating ecesis for tree-ring dating of moraines: a comparative study from the Canadian Cordillera. *Arctic and Alpine Research*. 25, 63-68.
- McCormac, F. G., Hogg, A. G., Blackwell, P. G., Buck, C. E., Higham, T. F. G. and Reimer, P. J. 2004. SHCal04 Southern Hemisphere Calibration, 0-11.0 cal Kyr BP. *Radiocarbon* 46 (3), 1087-1092.
- Mercer, J.H. 1965. Glacier variations in southern Patagonia. *Geographical Review*, 55, 390-413.

- Mercer, J.H. 1968. Variations of some Patagonian glaciers since the Late-Glacial. *American Journal of Science* 266, 91–109.
- Mercer, J.H. 1970. Variations of some Patagonian glaciers since the Late-Glacial: II. *American Journal of Science* 269, 1-25.
- Miller, A. 1976. The Climate of Chile. In: Schwerdtfeger, W. (ed.), *World Survey of Climatology, Volume 12: Climates of Central and South America*. Elsevier, Amsterdam, pp. 113-145.
- Oerlemans, J. 2001. *Glaciers and Climate Change*. Balkema Publishers, Rotterdam, 148 pp.
- Paul, F. 2004. The new Swiss glacier inventory 2000 – Application of remote sensing and GIS. Ph.D. Thesis, Department of Geography, University of Zurich, Switzerland, 198 pp.
- Paul, F., Kääb, A., Maisch, M., Kellenberger, T., and Haeberli, W. 2002. The new remote-sensing-derived Swiss glacier inventory: I. Methods, *Annals of Glaciology* 34: 355–361.
- Popovnin V.V.; Danilova T.A.; Petrakov D.A. 1999. A pioneer mass balance estimate for a Patagonian glacier: Glaciar De los Tres, Argentina. *Global and Planetary Change* 22 (1) 255-267.
- Porter, S.C. 2000. Onset of Neoglaciation in the Southern Hemisphere. *Journal of Quaternary Science* 15 (4), 395–408.
- Prohaska, F., 1976. The Climate of Argentina, Paraguay and Uruguay. In: Schwerdtfeger, W. (ed.), *World Survey of Climatology, Volume 12: Climates of Central and South America*. Elsevier, Amsterdam, pp. 13-73.
- Rignot, E., Rivera, A. and Casassa, G. 2003. Contribution of the Patagonia Icefields of South America to global sea level rise. *Science* 302: 434-437.
- Rivera, A. 2004. Mass balance investigations at Glaciar Chico, Southern Patagonia Icefield, Chile. PhD thesis, University of Bristol, UK, 303 pp.
- Rosenblüth, B., Casassa, G., Fuenzalida, H., 1995. Recent climatic changes in western Patagonia. *Bulletin of Glacier Research* 13, 127–132.
- Rosenblüth, B., Fuenzalida, H.A., and Aceituno, P. 1997. Recent temperature variations in southern South America. *International Journal of Climatology* 17, 76-85.
- Röthlisberger F. 1986. *10,000 Jahre Gletschergeschichte der Erde*. Verlag Sauerländer: Aarau.

- Schweingruber, F.H. 1996. *Tree Rings and Environment – Dendroecology*. Swiss Federal Institute for Forest, Snow and Landscape, WSL/FNP, Haupt Verlag, Bern, 609 pp.
- S.I.B. 2005. *Protocolo para el preprocesamiento de imágenes satelitales Landsat para aplicaciones de la Administración de Parques Nacionales. Sistema de Información de Biodiversidad*, Administración de Parques Nacionales, Buenos Aires, 22 pp.
- Sigafoos, R.S., and Heindricks, E.L. 1969. The time interval between stabilization of alpine glacial deposits and establishment of tree seedlings. US Geological Survey, Professional Paper 650-B, B89-B93.
- Song, C., Woodcock, C.E., Seto, K.C., Lenney, M.P., and Macomber, S.A. 2001. Classifications and change detection using Landsat TM: When and how to correct atmospheric effects? *Remote Sensing of Environment* 75 (2), 230-244.
- Stokes, M.A., and Smiley, T. 1996. *An introduction to tree-ring dating*. University of Arizona Press, Tucson, Arizona, 73 pp.
- Strelin, J.A., Malagnino, E., Sone, T., Casassa, G., Iturraspe, R., Mori, J., and Torielli, C. 2002. Cronología Neoglacial del extremo sur de Sudamérica, Arco de Scotia y Península Antártica. In: *Actas XV Congreso Geológico Argentino*, El Calafate, Argentina, 506-511.
- Tucker, C.J., Grant, D.M., and Dykstra, J.D. 2004. NASA's Global Orthorectified Landsat Data Set. *Photogrammetric Engineering & Remote Sensing* 70 (3), 313–322.
- Villalba, R., Lara, A., Boninsegna, J.A., Masiokas, M., Delgado, S., Aravena, J.C., Roig, F.A., Schmelter, A., Wolodarsky, A., and Ripalta, A. 2003. Large-scale temperature changes across the southern Andes: 20th-century variations in the context of the past 400 years. *Climatic Change* 59, 177-232.
- Warren, C.R., and Sugden, D.E. 1993. The Patagonian Icefields: a glaciological review. *Arctic and Alpine Research* 25, 316–31.
- Warren, C.R., and Aniya, M. 1999. The calving glaciers of southern South America. *Global and Planetary Change* 22, 59–77.
- Wenzens, G., 1999. Fluctuations of outlet and valley glaciers in the Southern Andes (Argentina) during the past 13,000 years. *Quaternary Research* 51, 238–247.
- Wilhelmy, H., and Rohmeder, W. 1963. *Die La Plata Länder, Argentinien-Paraguay-Uruguay*. Braunschweig, Westermann, 584 pp.

Chapter 4 discussed the available dendrogeomorphic evidence for Little Ice Age fluctuations for five small glaciers in the south Patagonian Andes. The following chapter uses a similar approach to develop a late Neoglacial record of fluctuations for two small neighboring glaciers in the north Patagonian Andes. The evidence to aid the dating of glacier deposits at these sites is remarkably rich, and the resulting LIA glacier chronologies are the most detailed available for this region.

This chapter will be submitted for publication in the near future with the following list of co-authors:

Masiokas, M.H.^{1,2}; Luckman, B.H.¹; Villalba, R.²; Rabassa, J.³; Ripalta, A.²

¹ Department of Geography, University of Western Ontario, London, Ontario, Canada.

² Instituto Argentino de Nivología, Glaciología y Ciencias Ambientales (IANIGLA-CONICET), Mendoza, Argentina.

³ Centro Austral de Investigaciones Científicas, CADIC-CONICET, Ushuaia, Tierra del Fuego, Argentina.

Chapter 5: Late Neoglacial fluctuations of Glaciar Río Manso and Glaciar Frías in the north Patagonian Andes of Argentina

5.1. Introduction

The glaciers of the Patagonian Andes in southern South America have an enormous potential as indicators of past and present climatic changes. The close proximity of a dense forest cover and former glacier termini over a latitudinal range of ca. 1500 km make this area particularly suitable for studies using several independent techniques to date glacial deposits and develop multi-proxy paleoclimate reconstructions. However, despite this potential, past glacier fluctuations and glacier-climate relationships in the Patagonian Andes are still not well known. Most glacier investigations in this region have concentrated south of 45°S and have usually focused either on 20th-century glacier changes (e.g. Aniya et al. 1997; Rignot et al. 2003), or on glacial variations during the late Quaternary and the Holocene periods (e.g. Mercer 1982; Rabassa and Clapperton 1990; Clapperton 1993; Glasser et al. 2004; Sugden et al. 2005). In the north Patagonian Andes¹, much more information is available about regional glacier fluctuations that occurred during the last glacial maximum (see e.g. Denton et al. 1999 and references therein) than for glacier fluctuations during the last few centuries. Very few studies have focused on glacial fluctuations of the last ~1000 years (e.g. Villalba et al. 1990, hereafter V90) for which the available glacial evidence is usually relatively abundant, well preserved and most easily dated. This interval also encompasses the period for which high resolution proxy climate information (primarily derived from tree rings) is readily available for comparison with the glacier records. Although the number, magnitude and dating precision of glacial events for this time frame differ from site to site, in general the available information indicates that the most extensive glacier advances in the Patagonian Andes occurred between the 17th and 19th centuries [globally identified as the Little Ice Age (LIA), Grove 2004]. There is additional, scattered evidence of glacier events that occurred between the 12th and 14th centuries (e.g. Glasser et al. 2002), and a few minor glacial advances during the 20th century (e.g. Masiokas et al. 2007, hereafter Chapter 3). However, the small number of glaciers studied and the poor dating control for most of

¹ The north Patagonian Andes are considered here as the portion of the Andes between ~37° and 45°S.

these glacial events suggest that the existing regional glacial chronologies can only be considered provisional until more detailed studies at suitable glaciers are developed. According to Luckman and Villalba (2001:136), “there remains a significant need for detailed, well-dated records of glacier fluctuations, coupled with a better understanding of the factors that control glacier mass balance” during this time frame.

In this paper we present a revised late Neoglacial² chronology of fluctuations for Glaciar Río Manso (locally known as Ventisquero Negro) and Glaciar Frías in the Monte Tronador area (41°10'S, 71°52'W), north Patagonian Andes, Argentina (Fig. 5.1). Although we focus on LIA and post-LIA glacier fluctuations at these sites, available evidence for pre-LIA glacier activity is also discussed as it provides important additional information for placing the more recent glacier events into a longer term, late Holocene perspective. The two study sites are within a few km from each other and represent excellent examples of the usefulness and limitations of dendroglaciological investigations. Our analysis of the Glaciar Río Manso fluctuations integrates the scattered information from previous glaciological studies (Lawrence and Lawrence 1959; Rabassa et al. 1978, 1984; Röthlisberger 1986) with the results from extensive sampling of living and subfossil tree-ring material recently collected at the site. As past variations of Glaciar Frías have already been studied in great detail in V90, we report only recently discovered key pieces of evidence that strengthen the available glacial chronology and improve our understanding of glacier behavior in this region. In conjunction with ongoing investigations at other small glaciers, the ultimate goal of this project is to develop robust, reliable regional glacial chronologies for the past ~1000 years to evaluate the main spatio-temporal variability of glacier and climate fluctuations in the Patagonian Andes.

² The term Neoglaciation usually refers to a geologic-climatic unit characterized by rebirth and/or growth of glaciers during the last half of the Holocene (Porter and Denton 1967; Porter 2000).

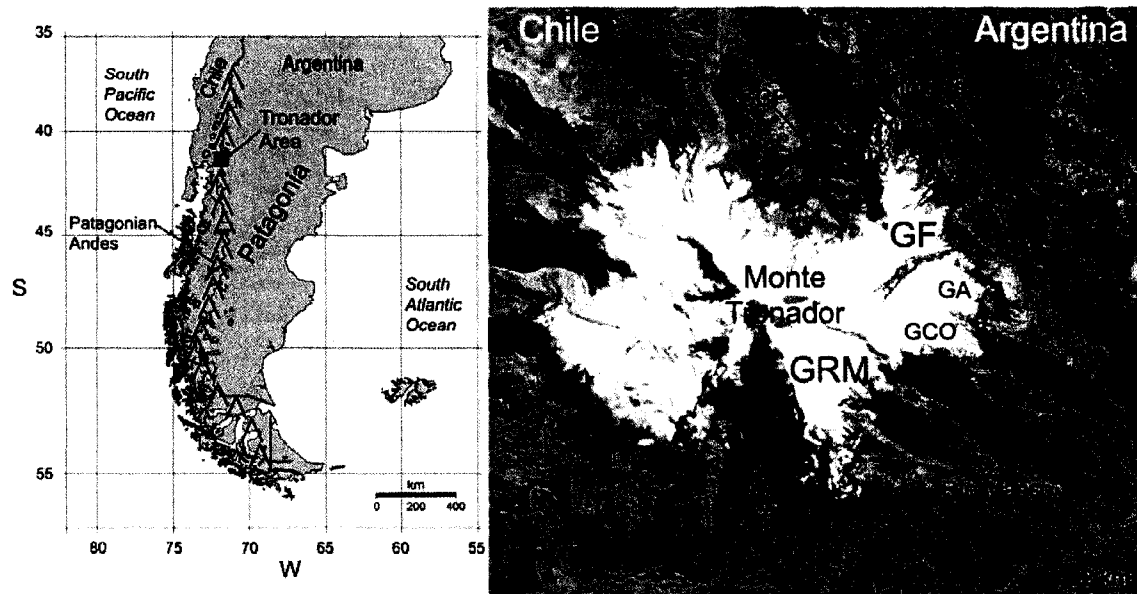


Fig. 5.1. (Left) Location of the Tronador area in the north Patagonian Andes. **(Right)** ASTER image from April 2003 showing the location of Glaciar Frías (GF) and Glaciar Río Manso (GRM) on the eastern side of Monte Tronador. Note the dark, debris covered surface of the regenerated lower portion of GRM and the proglacial lake at the head of Río Manso. Río Frías and the neighboring glaciers Alerce (GA), Castaño Overo (GCO) and Casapangue (GCP) are also shown.

5.2. Study Area

Monte Tronador (3554 m) straddles the international border in the north Patagonian Andes and its upper slopes are completely covered by a thick icecap that feeds several glaciers. Frías, Alerce, Castaño Overo, and Río Manso are the main glaciers on the eastern side (Fig. 5.1). This site is particularly suitable for dendroglaciological investigations because it is a relatively compact area that contains several small valley glaciers with different degrees of forest recolonization of the glacial forefields that allow dendrochronological and/or radiocarbon dating of past glacier fluctuations. The most common tree species colonizing the glacier forefields are *Nothofagus dombeyi* (locally known as coihue) and *N. pumilio* (lenga), but in some humid and protected sites the long-living *Fitzroya cupressoides* (alerce) is also frequent.

Despite having the same source, the glaciers on the Argentinean side of Monte Tronador are quite varied. For example, Glaciar Frías is largely devoid of debris cover with a steep but continuous profile (Fig. 5.1). On the other hand, the upper and lower portions of Glaciar Río Manso are separated by a steep cliff several hundred meters high and the lower glacier is regenerated from snow, ice and debris avalanching from the steep slopes above. The sound of these frequent avalanches is the source of the name Tronador (“The Thunderer”). The lower portion of Glaciar Río Manso has a relatively gentle slope and is covered by a thick debris layer, hence the local name, Ventisquero Negro (“Black Glacier”). In front of this glacier a massive, (presumably late Holocene) terminal moraine has been partially overridden by subsequent readvances giving an unusual fork-like shape to the terminal moraines of more recent glacier advances (Lawrence and Lawrence 1959; hereafter L&L). Available documentary evidence and aerial photographs (Table 5.1) indicate that despite minor readvances, the glacier margin varied relatively little between 1937 and 1991. However, rapid thinning and recession of the lower tongue in subsequent years has resulted in the formation of a large, rapidly growing proglacial lake between the glacier margin and the main moraine ridges (see Fig. 5.2).

Glaciar Frías (Fig. 5.1) is the northernmost ice body in the Argentinean sector of Monte Tronador and over the last millennium it has expanded over a relatively flat valley during several, clearly defined readvances (V90). The last of these events culminated in 1976/77 and has been described in detail by Rabassa et al. (1978, 1979) and V90. A shallow proglacial lake (“Laguna de los Témpanos”) existed for some decades in the early 20th century (it was still visible at the glacier front in a photograph taken by De Agostini in the early 1930s) but is now completely filled with fine outwash material transported by Río Frías. Although no direct mass balance records exist for this area, the marked ice front recession since the late 1970s suggests an extended period of negative mass balances at this site. The glacier toe presently hangs on the steep bedrock slopes several hundred meters above the valley floor.

Table 5.1. Summary of the available sources of information for the Argentinean glaciers on Monte Tronador. The dates of pictures showing partial or complete views of the glaciers were compiled by the authors and include published and unpublished sources. Dates for available air photos and satellite images apply to all glaciers. Notes: (*) Approximate areas based on the semi-automated analysis of a ~15 m resolution 2003 ASTER satellite image and a ~30 m resolution Digital Elevation Model (Delgado et al. 2006). (#) The area of the mostly debris-covered lower tongue of Glaciar Río Manso was delineated manually on the same image.

Glaciers	Area in 2003 (km ²)	References	Dates of available pictures	Available air photos (AP) or satellite images (SI)
Frías	6.69*	Fonck and Hess 1857 Steffen 1909 DeAgostini 1940 Rabassa et al. 1978 Villalba et al. 1990 Masiokas et al. 2007	1856, 1893, late 1930s, 1977, 1985, 1994, 2005, 2007	AP: 1944, 1953, 1961, 1970, 1981, 1998 SI: 1985 and 1987 (Landsat 5), 2000 (Landsat 7), 2003 (ASTER)
Alerce	2.23*	Rabassa et al. 1978 Lliboutry 1998	1977, 2005	
Castaño Overo	3.25*	Jakob 1936 Rabassa et al. 1978, 1984 Röthlisberger 1986 Masiokas et al. 2007	1936, 1982, 2003, 2005	
Río Manso	Upper: 6.57* Lower: 1.73#	Jakob 1937 Auer 1956 Thomasson 1959 Lawrence and Lawrence 1959 Rabassa et al. 1978, 1984 Röthlisberger 1986 Masiokas et al. 2007	1936, 1937, 1942, 1948, 1954, 1982, 1991, 2000, 2001, 2005, 2007	

5.3. Previous work

The relatively easy access and spectacular scenery of this area has attracted explorers, climbers and scientists for over a century and a relatively rich archive of historical documents is available especially for the Río Manso and Frías glaciers (Table 5.1). Most of these early publications contain historic photographs of the glaciers that are invaluable sources for the documentation of recent glacier changes by comparison with the present ice front positions. However, it was not until the late 1950s that a detailed glaciological study was carried out in this area, when L&L presented the first dating of moraines of Glaciar Río Manso using dendrochronology and tephrochronology. In a short visit of

three days in March 1959 they prepared a detailed description of the main features associated with the recent history of this glacier and highlighted the great scientific potential of the area. A thick tephra layer found on top of the massive frontal moraine was assumed to correspond to the tephra recovered in nearby peat samples and dated to 2240 ± 60 ^{14}C yrs BP by Auer (1958), providing a minimum age for this older glacier event. L&L also reported the existence of a drowned forest apparently killed during a glacier advance that dammed a lateral creek forming a temporary lake on the north margin of the glacier. We call this the Río Blanco Site. The innermost rings of living trees sampled on the drained lake bed and inside the moraine formed by this glacier advance (the most extensive of recent centuries) were dated to 1852 and 1855 respectively, and L&L suggested that the ice was in recession, and the lake probably drained, by the early 1850s. They also found several mature trees partially buried by glacial outwash in front of the moraine formed by this event. Some of these trees, killed by the glacial outwash, have since decayed, and several empty cylindrical holes or “tree wells” were reported at this site. A more recent readvance dated to ca. 1952 was inferred from the tree-ring patterns of a young (<35 years) living tree that was being partially buried by fine outwash just 1.5m in front of the easternmost margin of the ice at the origin of the proglacial Río Manso. The presence of year-old seedlings colonizing this fresh, unstable deposit led L&L to suggest an almost immediate tree establishment in the moist, shaded moraines of this glacier and no ecesis correction³ was used in their analysis.

Rabassa et al. (1978) (hereafter Ra78) provided an excellent description of the four Argentinean glaciers and estimated their surface areas from aerial photography. They also used extensive field work, measurements of ice margin positions and topographic profiles to identify a relatively synchronous glacier readvance between the early 1970s and 1976-77 at the glaciers on the Argentinean side of Monte Tronador. This is probably the best documented recent glacier advance in the Patagonian Andes north of 45°S and has subsequently been linked to a period of cooler and wetter conditions across the region

³ The term “equesis” usually refers to the time interval between moraine stabilization and tree seedling establishment (Sigafos and Heindricks 1969; McCarthy and Luckman 1993).

(V90; Chapter 3). Rabassa et al. (1984) (hereafter Ra84) employed dendrochronology and lichenometry to estimate the dates of formation of the most important events associated with the LIA at Glaciar Río Manso and Glaciar Castaño Overo. They identified up to eight moraine ridges on the south margin of Glaciar Río Manso and, based on preliminary tree-ring counts, lichen sizes and a radiocarbon date of a stump associated with the outermost deposit, they suggested that the largest LIA expansion took place at around 1772. Tree ages estimated from tree diameters were used to infer the age of the major LIA deposits on the south margin of Glaciar Castaño Overo (Fig. 5.1). According to this preliminary evidence, the most extensive LIA event at this glacier was dated to ca. 1818-29. In a visit to this glacier in 1982, Röthlisberger (1986) (hereafter Ro86) found a small *in situ* stump and roots that had been overridden by glacier deposits on the south margin of a (now vanished) regenerated ice cone at the bottom of a ~200 m-high cliff. Three samples were ^{14}C dated to “modern” times and Ro86 suggested that a recent advance had buried this material⁴.

Röthlisberger also visited Glaciar Río Manso in 1982 and discovered several *in situ* stumps on the proximal slope of the main north lateral moraine, west of the drowned forest of L&L (Ro86). Four *in situ* stumps located at about 40 m above the glacier surface and 70 m below the moraine crest were dated to 940 ± 110 , 620 ± 50 , 585 ± 50 , and 300 ± 85 ^{14}C yrs BP. An additional rooted stump was found only 10 m below the moraine crest and dated to modern times. Ro86 interpreted these results as representing several glacier advances with the latest (assumed to have occurred during the 19th century) being the most extensive of the last centuries. Near the shoreline of Lago Frías (some 11 km north of Glaciar Frías at the end of Frías valley) Röthlisberger found a 0.4-1.4 m thick tephra layer with *in situ* plant remains that were dated to 2435 ± 65 ^{14}C yrs BP. Ro86 linked this tephra with that described by L&L at Glaciar Río Manso and used this evidence to support the minimum age proposed for that moraine. Masiokas et al. (2001) presented two preliminary tree-ring floating chronologies from stumps sampled at the Río Blanco

⁴ During recent field surveys at Glaciar Castaño Overo and the neighboring Glaciar Alerce (Fig. 5.1) we found several additional *in situ* and reworked stumps associated with glacier deposits. This material together with the samples from living trees collected at these sites is being analyzed and results will be reported in the near future.

Site of L&L and at the north lateral moraine site of Ro86 together with six radiocarbon dates (ranging between 290 ± 70 and 110 ± 60 ^{14}C yrs BP) derived from this material.

V90 used dendrogeomorphology and documentary sources to develop a chronology of fluctuations for the past ~1000 years for Glaciar Frías and linked these events to temperature variations inferred from a local millennial length *Fitzroya cupressoides* tree-ring chronology. Based on the ages of trees growing on the most extensive LIA moraine deposits and growth suppression in the tree-ring series from a tree just outside this moraine, V90 suggested that the LIA advance reached its maximum position by ca. 1638-39. This event was associated with an extensive cold interval between 1520 and 1660 inferred from tree rings. Another ice-scarred tree associated with a moraine immediately inside the main LIA advance was used to provide a maximum date of ca. 1719-21 for this event. Five subsequent glacier advances were dated, mainly by dendrogeomorphic techniques, between the 1719-21 event and the well dated advance that culminated in 1976-77. The outermost moraine identified at this glacier, located about 70-100 m outside the deposits of the LIA maximum advance, was assigned a preliminary minimum date of 1236 based on the age of the oldest *Fitzroya cupressoides* tree sampled on its surface (V90).

Apart from the measurements of 1976-85 ice front positions at Glaciar Frías, only a few additional records are available for Glaciar Alerce and Glaciar Castaño Overo (Rabassa et al. 1978; Lliboutry 1998) (Fig. 5.1). To our knowledge, only Glaciar Casapangue on the Chilean side of Tronador (Fig. 5.1) has been studied for changes in ice thickness and frontal positions during the 20th century (Bown 2004). In Chapter 3 we used photographic comparisons of selected glaciers (including Frías, Castaño Overo and Río Manso) and hydro-climatic records from northwestern Patagonia to show that the drastic ice mass loss observed over the past century can be at least partially explained by a highly significant regional trend towards reduced accumulation in the winter and increased ablation in the summer. They also related some of the 20th-century readvances in the Tronador area to multi-year periods of overall cooler and wetter conditions across this region.

5.4. Methodology

The studies reported here at Glaciar Río Manso and Glaciar Frías involved similar techniques although the emphasis varied between glacier forefields based on the extent and results of previous work. The analysis of historical documents and aerial photographs was used to determine former ice marginal positions and identify recent glacial deposits. These historical references and additional information available are summarized in Table 1. In general, glacial deposits were dated using standard dendrogeomorphic techniques similar to those in Luckman (1988, 2000; see Table 5.2). Briefly these were as follows.

a) Glaciar Río Manso

Minimum ages of surfaces and related glacial events for Glaciar Río Manso were in most cases determined from the age of the oldest trees sampled on these deposits using increment corers. Where the pith was not present, pith offset values were estimated based on ring curvature on the oldest candidate trees. Minimum ages for trees with rotten piths were estimated by adding 20 years to the date of the innermost countable ring. Cores were taken as close to the root collar as possible to minimize errors in estimating tree ages due to sampling height. However, as it was difficult to core low on the stem except for a few very young trees, most cores were taken 50-100 cm above the tree base. Six young *N. pumilio* trees growing on the drained lake floor at the north margin of this glacier were sampled at the base, 50 and 100 cm height to provide estimates of vertical growth rates. Ring counts indicate the trees took an average of 10.3 years to reach 100 cm height, and we used a vertical growth rate of 10 cm per year to correct for sampling height. Tree-ring evidence from a south lateral moraine formed between 1970 and 1981 [based on field observations (Ra84) and air photo interpretation] was used to estimate ecesis. The innermost basal rings of the two oldest trees on this moraine (nine were sampled) were dated to 1983. As this moraine probably corresponds to the well documented glacier event that culminated in 1976-77 at other glaciers in the Tronador area (see Ra78; V90), we used a 6-yr ecesis throughout this study. This relatively rapid recolonization rate is conservative as L&L proposed almost immediate tree seedling establishment based on direct observations of a new push moraine on the eastern margin of the glacier (see above). Overall, these approximations for the sampling height and

ecesis correction factors suggest that, when pith is present, the absolute tree ages obtained at this glacier provide a relatively minor average error (usually <10-15 years) when estimating dates of moraine formation from tree rings⁵.

Table 2. Evidence for and limitations of dendroglaciological dating (modified from Luckman 2000).

Evidence	Precision	Information provided	Limitations
1) Trees growing in the glacier forefield	5-50 years	Age of oldest tree provides minimum age for surface	Ecesis (lag time between moraine stabilization and tree establishment) difficult to estimate. Assumes the oldest tree was sampled
2) Tilted and/or scarred tree	Exact calendar age of damage	Damage date indicates glacier position at a specific time	Moderately rare, dead trees require cross-dating
3) Trees killed by glacier advance	a) Exact calendar date of outer ring by cross-dating with living trees. Dating precision depends on preservation of wood and loss of outer rings b) approx. date by ¹⁴ C dating ($\pm 50-100$ yrs).	<i>In situ</i> : death date indicates position of glacier at a specific time Reworked wood: only provides a limiting date for death	a) Requires cross-dating, loss of outermost rings b) low temporal resolution, expensive
4) Trees growing outside glacier forefield	Annual resolution	Reference chronologies, paleoclimatic information	Age of oldest tree. Dead material can extend the chronologies but is difficult to find and usually not well preserved in this region

Complementary information about past activity at Glaciar Río Manso was obtained from trees that had been killed or tilted by past glacier advances. Several cross-sections were obtained from subfossil stumps below tills in the lateral moraines and along the margins of the proglacial Río Manso. Numerous stumps were also sampled in the bed of the former ice-dammed lake on the left margin of the glacier (the Río Blanco Site). The cross-sections were processed and analyzed following standard dendrochronological procedures (Stokes and Smiley 1996), and a nearby *Nothofagus pumilio* tree-ring width chronology (La Almohadilla chronology, Villalba et al. 1997) was used as a reference

⁵ The number of living trees cored at each sampling station, together with the absolute dates of the oldest trees, pith offset and sampling height corrections, and estimated minimum ages of surfaces is listed in Appendix 5.

series to crossdate the “floating” (undated) tree-ring series derived from these stumps. Crossdating trials were carried out using program COFECHA (Holmes 1983; Grissino-Mayer 2001) to determine precise calendar dates for ring series from subfossil wood. Several complementary radiocarbon dates were also obtained from selected stumps. In rare cases, we found mature, living trees that had been tilted by the glacier or partially buried by glacial outwash during past readvances. These trees were cored using increment borers and provided important information on the chronology of the main glacier events at this site. Mature trees growing outside the main LIA deposits (but not directly affected by glacier events) were also sampled to compare and differentiate minimum ages from this forest with those obtained from the trees colonizing the glacier deposits.

b) Glaciar Frías

The late Neoglacial fluctuations of Glaciar Frías have been described in V90. As this record is entirely based on living trees, we recently examined the glacier forefield for subfossil remnants of trees that had been killed or directly affected by glacier activity and that could provide limiting dates to help bracket the existing age estimates for the moraines. We found two groups of stumps that had been buried by the LIA maximum advance and the outermost, poorly dated moraine of V90. This material, mainly *in situ* *F. cupressoides* stumps⁶, was exposed where the Río Frías cuts through the northernmost portion of the frontal moraines. Tree cores from well preserved *in situ* stumps associated with the outermost moraine were crossdated against a composite reference series from eight *F. cupressoides* chronologies (1104-2338 years in length) from sites between 41° and 43°S in the north Patagonian Andes of Argentina (Villalba et al. 1996). Three samples were also radiocarbon dated to complement the tree-ring dating of these moraines. In addition, we sampled a few young *N. dombeyi* trees growing inside the precisely dated 1976-77 moraine to improve our estimates of ecesis at this glacier.

⁶ With a potential lifespan of over 3000 yrs and a strong regional common signal in tree-ring variations (Villalba et al. 1996), *F. cupressoides* trees can provide millennia-long reference tree-ring chronologies for crossdating subfossil stumps. As the wood has an extremely low decay rate (see e.g. Roig et al. 2001), alerce stumps will usually be better preserved than snags from other tree species.

5.5. Results

5.5.1. Glaciar Río Manso

Detailed investigations were carried out at nine key areas of the Glaciar Río Manso forefield that are identified alphabetically in a clockwise direction (Fig. 5.2). The results will be presented for three major areas: the north lateral moraine (Areas A-D), the terminal zone (Areas E-G), and the south lateral moraine (Areas H and I).

5.5.1.1. The north lateral moraine (Areas A-D)

At station A the north lateral moraine has a steep proximal slope in which Röthlisberger (1986) found several *in situ* stumps that yielded a wide range of radiocarbon ages (Table 5.3) and were interpreted as evidence of several different glacier events over the past 1000 years. We revisited this site and found several *in situ* stumps within ~5-15 m of the moraine crest on a very unstable slope and with no apparent spatial or elevation pattern. Eleven cross-sections and three radiocarbon dates were obtained from these snags. The tree-ring width patterns from seven stumps were successfully combined into a floating tree-ring chronology of 111 years and crossdated with the 450-yr long La Almohadilla chronology to provide calendar dates for the floating tree-ring series (VNF chronology, Fig. 5.3). The outermost ring dates and position of these *in situ* stumps on the steep proximal slope of the north lateral moraine, suggest that they were killed and buried by glacier deposits during the mid to late 18th century as the glacier advanced and thickened. However, the calibrated radiocarbon determinations obtained from these stumps showed a wide range of possible calendar dates (Table 5.3) and a very poor agreement with the tree-ring based results (see Table 5.4). Unfortunately we were unable to locate additional subfossil material to corroborate Röthlisberger's older dates, obtained in 1982 from a site approximately 40m above the glacier surface and 70m from the moraine crest (Table 5.3). These trees had probably been removed or buried by mass wasting processes when we visited this glacier two decades later. They remain the only potential evidence of older LIA advances from the north lateral moraine

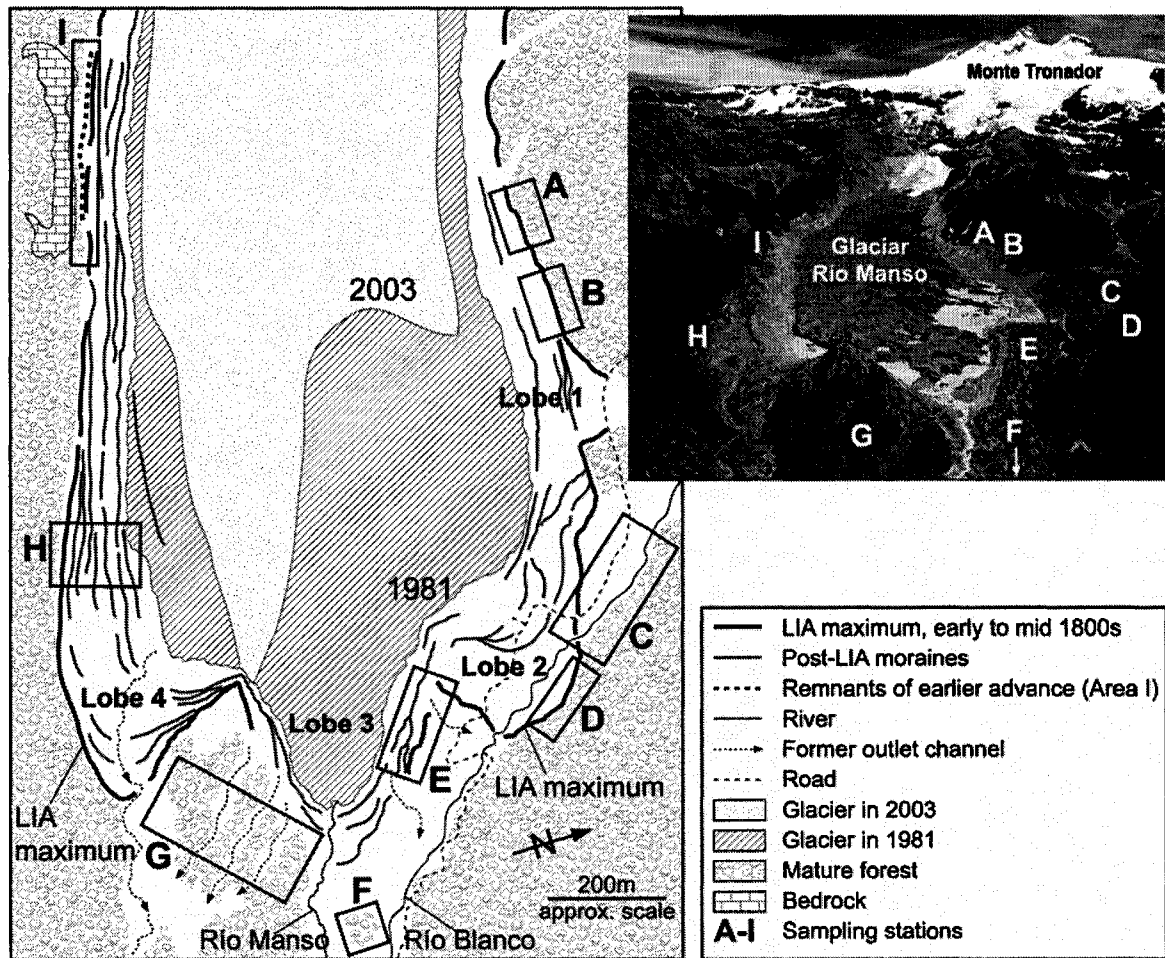


Fig. 5.2. (Left) Map showing the lower portion of Glaciar Río Manso, the location of LIA and post-LIA moraine systems and recent ice margin positions based on field surveys, air photo interpretation, satellite imagery and historical documents (data sources in Table 5.1). **(Upper right)** Oblique view of Monte Tronador and Glaciar Río Manso in the late 1990s showing the location of sampling stations A-I (photo source: <http://www.tronador.com>).

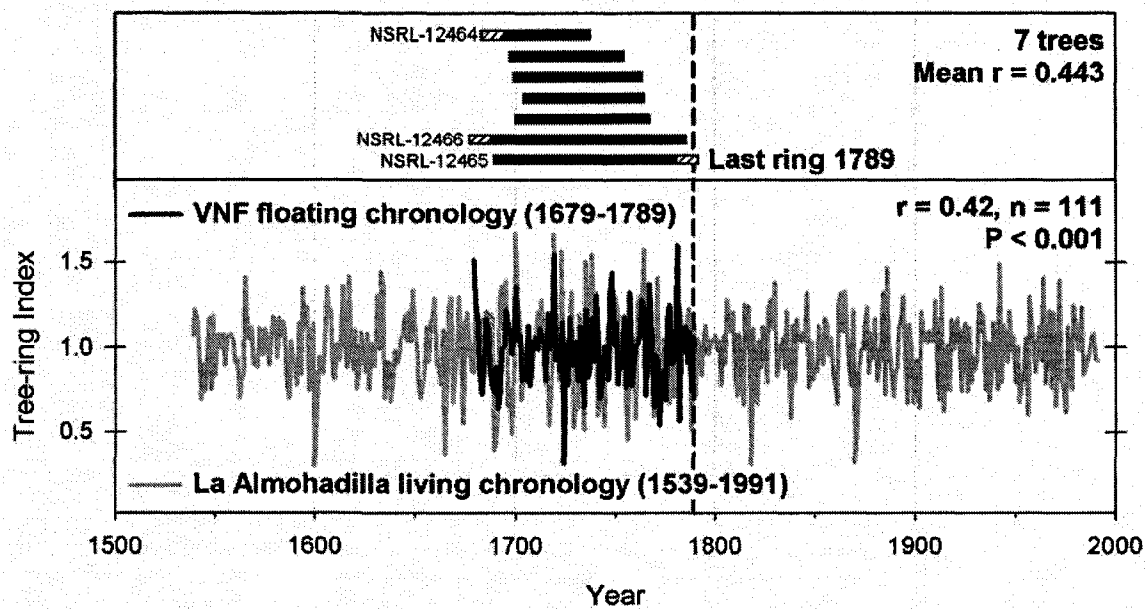


Fig. 5.3. Time span of *in situ* stumps found inside the north lateral moraine of Río Manso Glacier (Area A in Fig. 5.2). Crossdating the floating VNF chronology derived from these stumps with La Almohadilla ring-width chronology indicates that the last of these trees died ca. 1789. White hatched boxes in the upper diagram indicate the location of radiocarbon dated samples within cross-sections (Tables 5.3 and 5.4).

Living trees were sampled on the outer moraine at site B, approximately 150 m downvalley from the stumps in Area A (Table 5.4). Tree diameters on the proximal slope of the moraine ranged between 20 and 50 cm and the earliest ring of the oldest tree was dated to 1892 (Appendix 5). An older, 1.0 m diameter *N. pumilio* tree was found near the bottom of the distal slope of this moraine. This tree had an almost horizontal main trunk tilted towards the mature forest and two (one dead and one alive) vertical branches. The pith of the main trunk was rotten with an innermost ring dating to 1885. The innermost rings at the base of the two vertical branches dated to 1843 (dead) and 1841 (live branch) (Appendix 5). Other trees cored on the distal slope were clearly smaller (20-60 cm in diameter) with an oldest innermost ring dating to 1874. The large old tree at the base of the distal slope seems to have been knocked over during the formation of this moraine and survived, producing two vertical “leaders” that assumed apical dominance. The earliest basal date from these branches suggests the tree was tilted (and moraine emplaced) shortly before 1841-43.

In 2001 we relocated the site of the former ice-dammed lake (Río Blanco Site) on the north margin of Glaciar Río Manso described in L&L (Area C in Fig. 5.2). During the most extensive advance of recent centuries the former marginal lake was blocked by Lobe 2 and received discharge from Lobe 1 and the Río Blanco glaciers some distance upstream (Fig. 5.2). Upstream from Lobe 2, over 20 cross-sections were collected from *in situ* stumps exposed by the incision of Río Blanco into laminated lake sediments. Five radiocarbon dates were obtained from these stumps (Table 5.3). In 2004 a landslide from the steep southern valley-side slope modified the course of Río Blanco exposing many additional *in situ* stumps along the new channel (Fig. 5.4A-C). Radii from 18 cross-sections were used to build a floating tree-ring width series (RBL chronology) that was crossdated against La Almohadilla chronology (Fig. 5.5). Although a few peripheral rings may have been eroded from these samples, the calendar dates obtained for the outer rings of these cross-sections indicate that the last two trees died by ca. 1848 when they were drowned in the former ice-dammed lake. The wide range of kill dates also indicates that this glacier advance may have affected this portion of forest for several decades during which some trees survived longer than others in close proximity to the ice. The earliest date from these *in situ* stumps indicates that Lobe 2 (and by implication Glaciar Río Manso) was less extensive prior to this event and had not dammed Río Blanco between 1569 and the early 1800s. Calibrated ^{14}C ages from the outer portion of selected snags provided a wide range of potential death dates between 1450 and 1950 and, as at Station A, showed only weak agreement with the absolutely dated dendrochronological determinations (Tables 5.3 and 5.4).

Table 5.3. Radiocarbon ages of *in situ* stumps from Glaciar Río Manso (Areas A, C, and H; Fig. 5.2). Calibrated calendar dates A.D. (2-sigma distributions rounded to the nearest 10 yr) and their associated probabilities (most probable calendar date range in bold) were obtained using the CALIB program (Stuiver and Reimer 1993) available online at <http://radiocarbon.pa.qub.ac.uk/calib/> and the Southern Hemisphere calibration dataset of McCormac et al. (2004). Notes: (#) The position of sample within tree was not specified but probably collected from outer rings; (†) Sample taken from outer rings; (‡) Sample from innermost rings; (*) Not included in Río Blanco tree-ring chronology (see text).

Sample code	14C age (BP)	2 σ calibrated calendar date range (probability)	Location	Ref.
HV-11800 #	940 \pm 110	900-920 (0.012) 950-1300 (0.987)	Area A; 40m above glacier, 70m below moraine crest.	Ro86
HV-12865 #	620 \pm 50	1300-1430 (1.000)		
HV-12864 #	585 \pm 50	1310-1360 (0.287) 1380-1450 (0.713)		
HV-11799 #	300 \pm 85	1450-1710 (0.705) 1720-1810 (0.218) 1840-1890 (0.049) 1920-1950 (0.028)		
HV-11798 #	Modern	N/A	Area A; 10m below moraine crest	
NSRL-12465 †	285 \pm 35	1490-1600 (0.592) 1610-1670 (0.374) 1780-1800 (0.034)	Area A; same site as above ~5- 15m below moraine crest	This study
NSRL-12466 ‡	280 \pm 50	1470-1680 (0.917) 1770-1800 (0.061) 1940-1950 (0.015)		
NSRL-12464 ‡	220 \pm 55	1520-1590 (0.102) 1620-1710 (0.300) 1720-1890 (0.466) 1910-1950 (0.133)		
HEL-4547 †	290 \pm 70	1450-1680 (0.864) 1740-1810 (0.107) 1930-1950 (0.029)	Area C; bed of former ice- dammed lake (Río Blanco Site)	
HEL-4549 †	200 \pm 60	1520-1560 (0.034) 1630-1950 (0.967)		
HEL-4548 †	160 \pm 80	1530-1540 (0.011) 1630-1950 (0.989)		
HEL-4546 †	110 \pm 60	1670-1780 (0.389) 1800-1950 (0.611)		
NSRL-12640 †*	90 \pm 35	1680-1740 (0.276) 1800-1940 (0.708)		
LP-82 #	178 \pm 56	1650-1890 (0.831) 1910-1950 (0.169)	Area H; within outermost moraine	Ra84

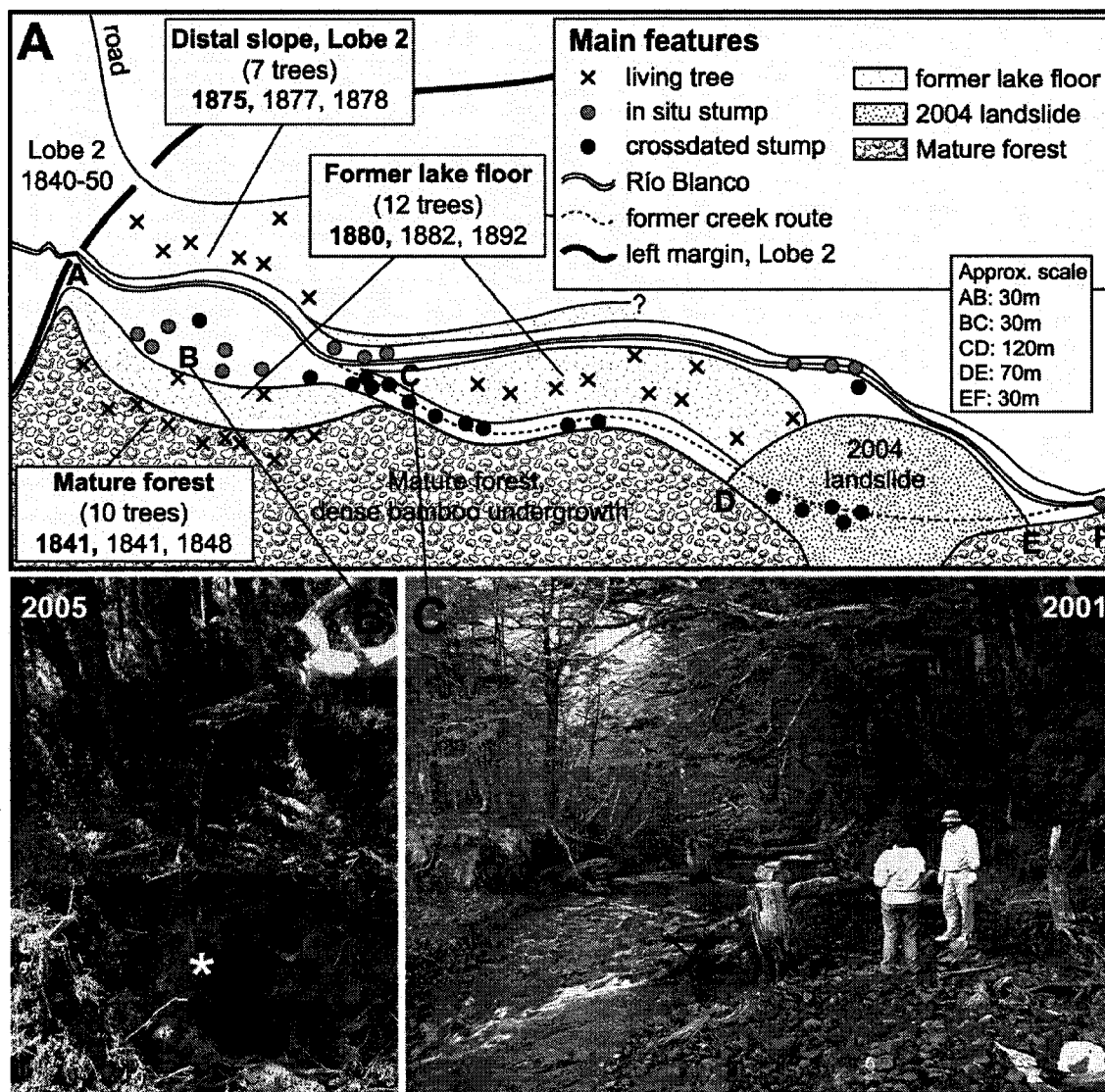


Fig. 5.4 (A) Schematic map showing the location of *in situ* stumps and living trees sampled in Area C (the Río Blanco Site) on the north margin of Glaciar Río Manso. The number of living trees sampled at the different sites is listed together with the age of the three oldest specimens (oldest in bold). (B) Cross-section of the former lake floor sediments at point B in 2005, with the rotten remnants of an *in situ* stump (*) embedded in the deposits. The limit for dense bamboo undergrowth and mature forest starts ~5m behind this pit. (C) 2001 view of Río Blanco channel (abandoned due to a landslide in 2004) showing some of the *in situ* stumps sampled close to point C.

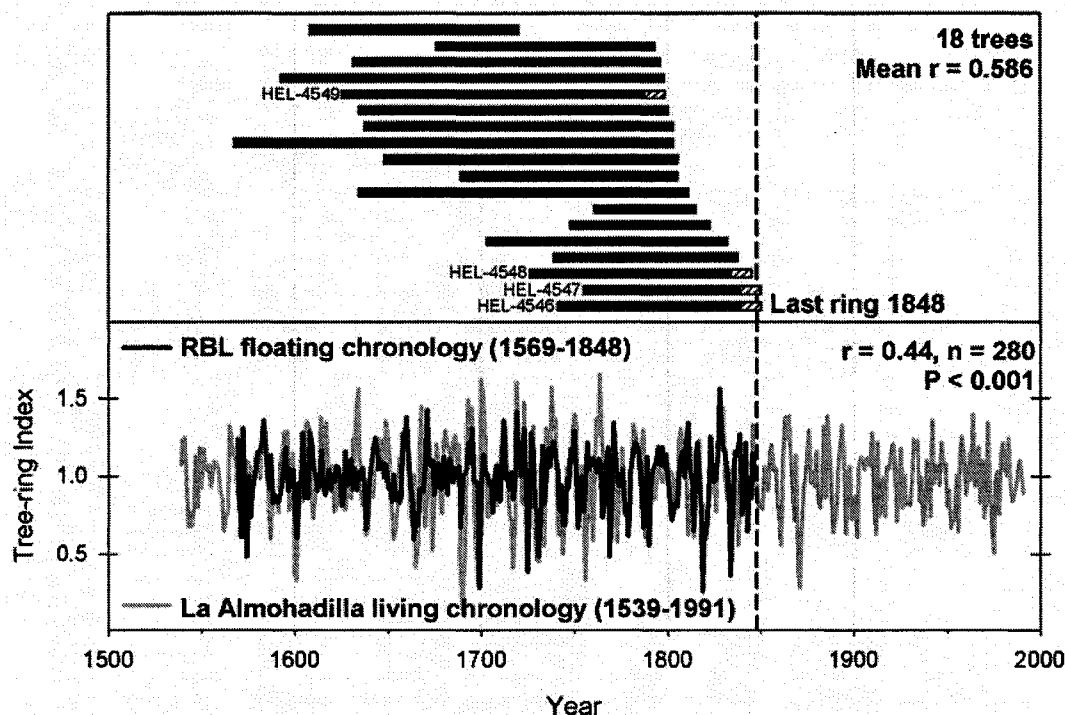


Fig. 5.5. Time span and calendar dating of the floating tree-ring chronology derived from 18 *in situ* stumps found in Area C. The dates obtained for these snags and the setting of the site suggest that the glacier advanced, dammed Río Blanco and created a small lake that killed this portion of forest ca. 1848. The range in kill dates also indicates that this glacier advance may have started affecting these trees by the late 1700s. Complementary radiocarbon dates were obtained from selected portions in the cross-sections (white hatched boxes). For calibrated ^{14}C dates see Tables 5.3 and 5.4.

Several living trees (Fig. 5.4A) were sampled at this site. The estimated germination dates of the oldest living trees cored on the former lake floor and the distal slope of the moraine that formed this marginal lake were 1880 and 1875 respectively⁷ (Appendix 5). This evidence indicates that the lake finally drained some years prior to ca. 1875 and that the outer moraine of Lobe 2 became stabilized and colonized sometime in the late 1860s or early 1870s (Appendix 5). A minimum date of 1841 was obtained from 10 trees in the dense forest north of the creek, just beyond the former lake floor and approximately 3

⁷ Based on field counting of tree rings, L&L reported a minimum date of 1852 from trees sampled on the former lake floor. Our results from Area C suggest that this may be an over estimate.

meters above the current Río Blanco level (Fig. 5.4A and C). The oldest tree found by L&L at this site was dated to 1732, suggesting that this surface was probably not severely affected by the marginal lake that drowned the adjacent portion of forest a few meters to the south⁸ (Fig. 5.4).

Table 5.4. Comparison between ¹⁴C determinations from selected *in situ* stumps at Glaciar Río Manso and their absolute, tree-ring based date range determined by crossdating analyses with a nearby living tree-ring chronology (Fig. 5.3). The samples for radiocarbon dating included 15-25 rings in each cross-section. Notes: (*) Most probable calibrated calendar date range derived from Table 5.3; (#) Calendar dated range of the radiocarbon dated portion of the stump. The maximum/minimum limiting ring dates are shown in bold.

Station	Sample code	¹⁴ C age (BP)	Most probable calibrated cal. range*	Tree-ring based date range#
A	NSRL-12464	220±55	1720-1890	1685-1705
	NSRL-12466	280±50	1470-1680	1679-1699
	NSRL-12465	285±35	1490-1600	1769-1789
C	HEL-4549	200±60	1630-1950	1776-1796
	HEL-4548	160±80	1630-1950	1823-1843
	HEL-4547	290±70	1450-1680	1828-1848
	HEL-4546	110±60	1800-1950	1828-1848

Approximately 200-300 m east of site C, glacier Lobe 2 rode up the opposite (south) valley side and deposited a symmetrical morainic arc (Area D in Fig. 5.2). Although at the highest, central point this moraine is only about one meter high, well-marked differences in tree age and forest characteristics exist on either side of this moraine. Mature trees growing a few meters outside this moraine were up to 387 years old and 1.7 m in diameter, whereas trees growing on the proximal slope were between 30-70 cm diameter and dated to 1862 (Appendix 5). In this sector L&L reported a similar minimum age of 1855 for a tree growing inside the moraine limits. However, the most striking contrast is between the dense, impenetrable undergrowth of bamboo (*Chusquea culeou*,

⁸ In fact, L&L used the multi-year ring-width patterns of this single tree to estimate former water levels of the adjacent lake associated with the frontal variations of glacier Lobe 2 (i.e. narrow rings during high water levels due to more advanced positions of the ice dam, and viceversa).

locally known as caña colihue) in the mature forest beyond the moraine and an almost bamboo-free zone inside the glacial limit. To our knowledge, this “bamboo line” has not previously been described in the scientific literature. Its presence facilitated the identification of the margin of this glacier advance by simply mapping the density of bamboo colonizing the surface. A similar “bamboo line” was seen at other glaciers in the north Patagonian Andes [e.g. Glaciar Torrecillas (42°40’S, 71°54’W) and Glaciar Esperanza Norte (42°09’S, 72°01’W) in Argentina and Glaciar Universo (42°07’S, 72°03’W) in Chile]. Using the limiting dates from the trees and assuming relatively rapid recolonization, these data suggest that the glacier was in recession by the late 1840s or early 1850s when the first trees started colonizing the fresh glacial deposits.

In summary, the tree-ring material and available radiocarbon dates from stumps along the north margin of Glaciar Río Manso provide contrasting evidence for glacier events during the past 1000 years. Röthlisberger (Ro86) identified three different glacier advances dating ca. 950, 600 and 300 ¹⁴C yrs BP based on poorly constrained radiocarbon dates from buried *in situ* stumps at the lower part of the proximal slope of the outermost moraine (Area A in Fig. 5.2). The limited documentation seems to indicate that these samples were collected from the same stratigraphic unit. In addition, the wide error range of these age estimates (Table 5.3), plus discrepancies between other ¹⁴C and tree-ring dates from this site (Table 5.4), suggests these results should be interpreted with caution. The reported position of the stumps, 70 m below the moraine crest, indicates they are from a different population than the trees we sampled higher on the same slope (Fig. 5.3). Although they may represent evidence of an earlier glacier advance(s), the number and timing of these events cannot be resolved based on the available evidence. The most extensive advance of recent centuries occurred between ca. 1790 and the early 1840s and was identified using complementary data from subfossil and living trees directly affected by the glacier and numerous tree-ring samples collected from deglaciated surfaces.

5.5.1.2. The terminal zone (Areas E-G)

In 1983 Rabassa and collaborators collected a set of tree-ring samples from Area E (Fig. 5.2) that were re-analyzed in 2005 to obtain approximate minimum ages for the series of

sub-parallel moraine ridges identified at this site. The oldest tree sampled on the outermost moraine ridge was dated to 1867, and tree-ring counts of trees associated with three inner ridges indicate the ridges were formed in the first half of the 20th century (Appendix 5). However, except for the outermost ridge (which seems to be a continuation of the arcuate moraine described in Area D above), significant fluvio-glacial activity on the distal slopes and recent mass wasting processes on the proximal slopes combined with the complex geomorphological setting of this particular site complicated the interpretation of these moraines in relation to those observed elsewhere along the glacier margin (Fig. 5.2).

Area F is a valley floor site, immediately outside the main morainic complex (Fig. 5.2). L&L described an area of old-growth forest floor that had been partially or completely buried by fine glacial outwash over one meter thick associated with the most extensive glacier advance of recent centuries. Morphological evidence of the terminal moraines of Lobe 3 has been considerably modified by fluvio-glacial activity at this site. Nevertheless, estimates of the date of the glacier advance and its easternmost extent were obtained from several trees sampled in this sector. Five living trees with their lower trunks buried by fluvio-glacial gravels began growth before 1680 and two similarly buried dead trees (crossdated with La Almohadilla chronology) had innermost rings dating to 1730 and 1761 and died in the early 20th century (Appendix 5). Five trees sampled in mature forest growing on a 5-7 m high promontory above this outwash had an oldest innermost date of 1708. Two living trees growing on the fluvio-glacial deposits began growth ca. 1849 and 1863 (Appendix 5). As the trees are highly unlikely to seed successfully in an actively aggrading outwash environment, these dates suggest that the outwash was probably formed sometime after 1761 and the early 1840s. Numerous *in situ* and reworked subfossil snags were found scattered over a ~200 m long stretch of Río Manso adjacent to Area F (Fig. 5.2). Unfortunately, despite numerous attempts, these stumps have not been crossdated. The short, usually distorted, tree-ring patterns in most of these samples suggest that they are *Nothofagus antarctica* (Ñire), a relatively less studied and short-lived tree species generally colonizing lower, flood-prone sites in this region.

On the southern side of Río Manso (Area G in Fig. 5.2), the recent advance appears to have only partially overtopped the older massive moraine. Boulders up to 4 x 4 x 3 meters in size occur on the upper third of this slope and appear to delimit the maximum extent of this advance. The distal, east-facing slope of the massive moraine has been partially dissected by several former stream channels from the maximum limit of the recent advance at the top of the slope. The oldest of 26 trees sampled in the intervening forest patches dates to 1673 (Appendix 5) and scattered bamboo undergrowth also occurs indicating the forest is older than that developed elsewhere on the 1840s moraine.

5.5.1.3. The south lateral moraine (Areas H and I)

Multiple moraine ridges within the LIA maximum position along the south lateral margin of Glaciar Río Manso indicate several readvances during the last two centuries (Fig. 5.2). However, most of the evidence for these events has been destroyed by extensive mass wasting and fluvio-glacial processes at the glacier margin. Area H along the south lateral moraine is the only location where most of this evidence is preserved as a clear sequence of moraine ridges showing an increase in tree age and forest cover between the present proglacial lake and old-growth, mature forest with bamboo outside the LIA limit. Eight vegetated moraine ridges (M1-8) were sampled on both distal and proximal sides to obtain minimum age estimates. These data have been reworked from the original samples collected by Ra84 plus additional samples collected in 2001 and 2006 and a revised chronology is presented here. These samples indicate that M1 was formed some years prior to 1839, whereas trees growing in mature forest with dense bamboo undergrowth on the valley side immediately outside this moraine are over 100 years older (Appendix 5). Trees from Moraines 2-6 indicate minimum ages of 1875, 1890, 1899, 1919 and 1949, respectively (Appendix 5). Moraine 7 forms a conspicuous trimline on the south margin of the glacier and was visible immediately outside the glacier margin in aerial photographs taken in 1961 (Table 5.1). The age of the oldest tree on this moraine (1961) indicates this deposit was probably formed before the mid 1950s (Appendix 5). This event may correspond to the advance dated to the early 1950s by L&L on the eastern margin of the glacier (see above). The two oldest trees cored on M8 were dated to 1983 (Appendix 5). As M8 was likely formed by the mid to late 1970s, these dates suggest that

ecesis is less than 10 years for these moraines. Another minor ridge lacking vegetation was observed between M8 and the southeast margin of the glacier (Fig. 5.2). Available photographic evidence (Table 5.1 and Fig. 5.2) suggests this innermost ridge was probably formed between the late 1990s and 2001.

Several *in situ* stumps that had been buried by the distal slope of M1 (Fig. 5.2) were also sampled but most of the cross-sections were rotten and no tree-ring based maximum age estimates were obtained. Ra84 reported a radiocarbon date of 178 ± 56 yrs BP from an *in situ* stump within glacial deposits on this outer moraine (the most probable calibrated date range for this ^{14}C determination is 1650-1890, Table 5.3). They also reported that the oldest tree on this moraine (13 were dated) was 184 years old and suggested this oldest advance probably occurred ca. 1772. Our recent, extensive tree-ring sampling along this transect did not locate an older moraine of this age and we believe that M1 corresponds to the maximum LIA advance of the early to mid 1800s at this glacier.

Approximately 200-300 m upvalley from Area H (Area I, Fig. 5.2), the outermost moraine is marked by a relatively well preserved ridge with old-growth, bamboo-floored forest over 320 years old (10 trees sampled) on the adjacent slope. Although initially regarded as a continuation of the outermost moraine (M1) at site G, the 23 trees sampled on this upper ridge were significantly older with an innermost ring of 1707 on the distal slope (Appendix 5). A partially dissected moraine ridge was identified inside this outermost moraine at station I, but no tree-ring dates are available for that event and mass wasting of the steep slopes at this site has removed most of the evidence for subsequent glacier advances. The outermost ridge at Area I may represent deposits of an earlier glacier event that was almost completely overridden by the LIA maximum advance elsewhere along the glacier margin. This earlier event could correspond to the advance identified some 300 ^{14}C years ago by Ro86 using *in situ* material from Area A (see Table 5.3). However, more evidence is needed (especially from sites outside sampling stations A-I where remnants and/or subfossil material associated with this earlier event may still be present) before we can clarify this issue.

5.5.2. Glaciar Frías

In their study at Glaciar Frías, V90 dated the moraines based on living trees growing on or immediately outside these deposits. They used indirect, variable ecesis correction factors (ranging between eight and 71 years) that were largely based on the time interval between the dendrogeomorphological dating of the main moraines and the peak in specific periods of cold-wet conditions inferred from *F. cupressoides* tree-ring records. In a recent visit to this glacier we found two young *N. dombeyi* trees growing 10-11 m inside the well dated 1976-77 moraine, and the innermost ring at the base of the oldest tree was dated to 1987. This provided a new 10-yr ecesis estimate for this glacier which was used to adjust the dating for some of the moraine systems in V90. Table 5.5 presents a new moraine chronology for this site.

Table 5.5. Revised chronology of fluctuations for Glaciar Frías over the past ~1600 years. For details see text. Note: (*) except for Moraine A, data taken from Table 1 in Villalba et al. (1990).

	Moraine								
	A	B	C	DEF	G	H	J	K	L
Number of living trees cored*	2	1	18	8	6	3	1	22	9
Oldest tree*	1987	1957	1927	1917	1910	1815	1749	1696	1236
Coring height correction*	0	3	3	3	4	4	6	15	N/A
Date of moraine inferred from ice-damaged trees*							1719-21	1638-39	
Revised, probable date of moraine	1977	<1944	<1914	<1904	<1896	<1801	>1719-21	>1638-39	>450AD

Moraine K, the most extensive LIA event, was dated between 1638-39 and 1671 based on the dating of an ice scar in a tree just outside the moraine and the age of the oldest tree growing on the deposits (see V90 and Table 5.5). Similar evidence was used to estimate the formation of the inner moraine J between ca. 1733 and 1719-21. Minimum dates of ca. 1801, 1896, 1904, 1914 and 1944 were assigned to five younger moraine systems based on the age of the oldest trees sampled on their surface and the new ecesis estimate (Table 5.5). The 1976-77 event remains the most recent advance identified at this site and the best documented 20th-century glacier event in this region (see Rabassa et al. 1978,

1979; and V90). In 2005 the glacier front was hanging over a steep bedrock slope and no evidence was found for readvances after 1977. The approximate frontal position of the main moraines at Glaciar Frías is shown in Fig. 5.6.

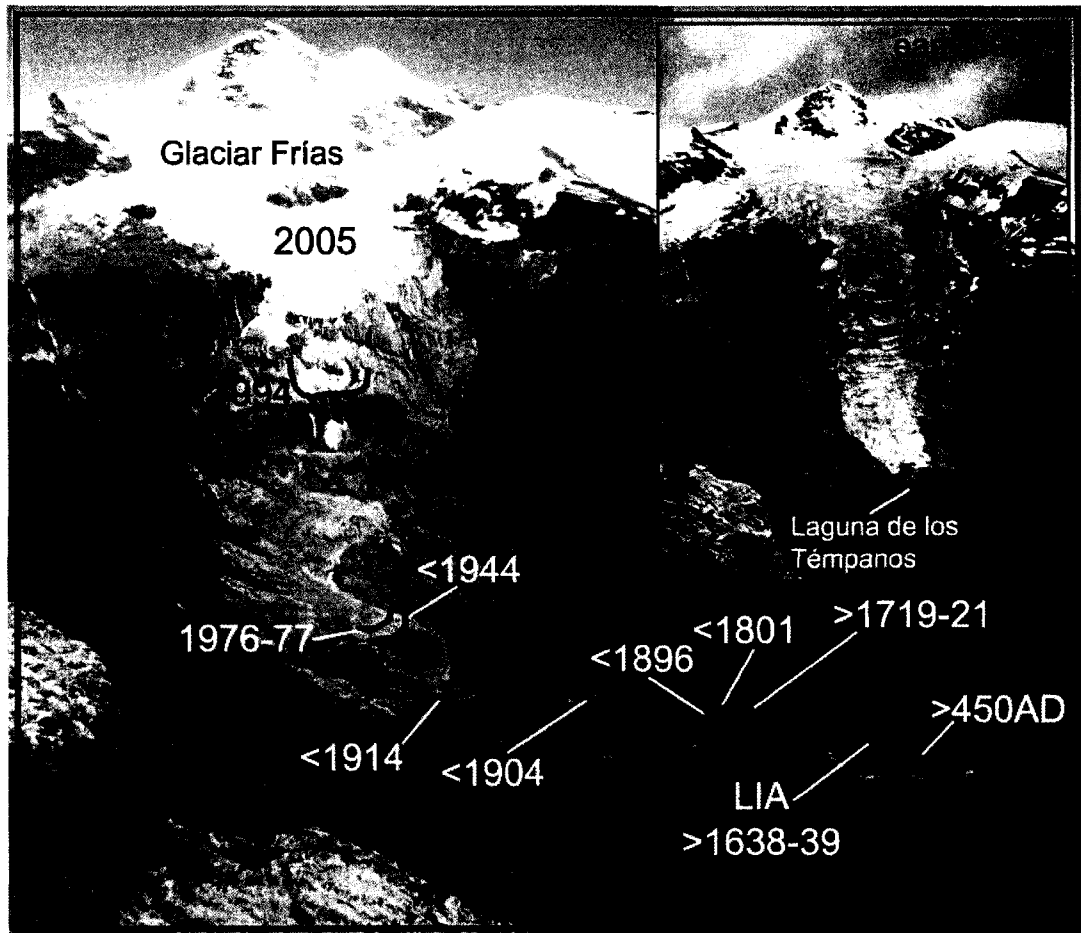


Fig. 5.6. Panoramic view of Glaciar Frías showing the approximate frontal location of the main advances identified during the past ~1600 years. The historical photograph taken in the early 1930s (De Agostini 1949) highlights glacier changes of the past 70 years. The 1994 frontal position is based on a photograph taken by S. Rubulis. The 2005 photo was taken by M. Masiokas.

Recently, two stumps (one *in situ*, the other reworked) were found in an exposure cut by the proglacial stream in Moraine K. However, the wide range of possible calibrated ^{14}C dates from samples in these stumps does not clarify the dating for this event. The most probable calibrated age obtained for the *in situ* stump was 1410-1510 (Table 5.6), but

since the dated sample was not collected from the outer portion of the stump this is not a closely limiting date for this advance. Resampling, future tree-ring analysis and crossdating of subfossil material may resolve this issue.

Table 5.6. As Table 5.3 but for the recently discovered *in situ* and reworked stumps at Glaciar Frías. Notes: (†) Sample taken from 15-30 outer rings; (‡) Sample of ~50 rings, outer portion of stump missing; (§) Sample of 35 rings beneath the outer 15 rings in the stump.

Sample code (tree species)	¹⁴ C age (BP)	2σ calibrated calendar date range (probability)	Location
Gd-19030 (<i>Nothofagus</i> sp.) †	225±60	1520-1540 (0.010) 1630-1950 (0.990)	Reworked. Buried by most extensive LIA advance.
Gd-19032 (<i>F. cupressoides</i>) ‡	470±50	1410-1510 (0.801) 1550-1620 (0.199)	<i>In situ</i> . Buried by most extensive LIA advance.
Beta-231279 (<i>F. cupressoides</i>) §	1720±40	260-460 (0.913) 480-530 (0.087)	<i>In situ</i> . Buried by outermost moraine.

Some 70-100 m outside Moraine K is a poorly dated, partially destroyed frontal moraine system (Moraine L in V90). Based on the tree-ring dating of the innermost ring of a *F. cupressoides* tree growing on this moraine, V90 indicated the deposits are at least 770 years old (Table 5.5). A shift of the main Río Frías channel has cut a new section in this moraine exposing several *in situ* and reworked stumps. We sampled and analyzed the tree-ring patterns of six well-preserved, *in situ* *F. cupressoides* stumps from immediately outside and beneath the moraine and developed a preliminary, floating tree-ring width chronology. Initial crossdating trials using two *F. cupressoides* chronologies spanning the minimum age of this moraine were unsuccessful. We subsequently obtained a date of 1720±40 ¹⁴C yrs BP (Table 6) from one of the stumps sampled in the section within the moraine. Crossdating with a longer composite reference tree-ring chronology (342BC-1995AD) indicated that this tree lived between 196 and 411 AD and that the floating chronology spanned the interval 71-450 AD (Table 5.7). These results suggest the dated tree was overridden by the glacier after 411 AD and other trees at the site died or were killed over the next 40 years. As the tree-ring dating corroborate the ¹⁴C date, these results indicate that the age previously assigned to Moraine L was underestimated and provide the first precise, calendar-dated information for a previously undocumented

glacier event during the first millennium in the north Patagonian Andes. This evidence also suggests that the LIA advance of the early 17th century was probably the most extensive advance during the past 1600 years.

Table 5.7. Tree-ring dating of selected *Fitzroya cupressoides in situ* stumps associated with Moraine L at Glaciar Frías. The reference chronology is based on samples from eight individual sites between 41° and 43°S in the Patagonian Andes of Argentina (Villalba et al. 1996).

	Reference chronology	Radiocarbon dated tree	Subfossil chronology
Period covered	342BC-1995AD (2338 yrs)	196-411AD (216 yrs)	71-450AD (380 yrs)
Number of dated series (trees)	273 (165)	3 (1)	14 (6)
Mean intercorrelation among series	0.513	0.608	0.350
Correlation with reference chronology	1.00	0.477	0.203

5.6. Discussion and Conclusions

The small glaciers and associated forests of the north Patagonian Andes can provide important and complementary information for the study of past and present glacier and climate changes in southern South America. However, to date most glacier studies in Patagonia have concentrated on the larger glaciers south of 45°S and very little is known about late Neoglacial regional glacier behavior in the north Patagonian Andes. Here we present revised chronologies of fluctuations for Glaciar Río Manso and Glaciar Frías on the Argentinean side of Monte Tronador (41°S) during this time frame based on the integration of results from previous studies and extensive new collections of living and subfossil tree-ring material at these sites. This rich array of complementary evidence demonstrates the great potential for dendroglaciological investigations in this area and provides the most detailed chronology of LIA and subsequent glacier fluctuations in the north Patagonian Andes (Fig. 5.7).

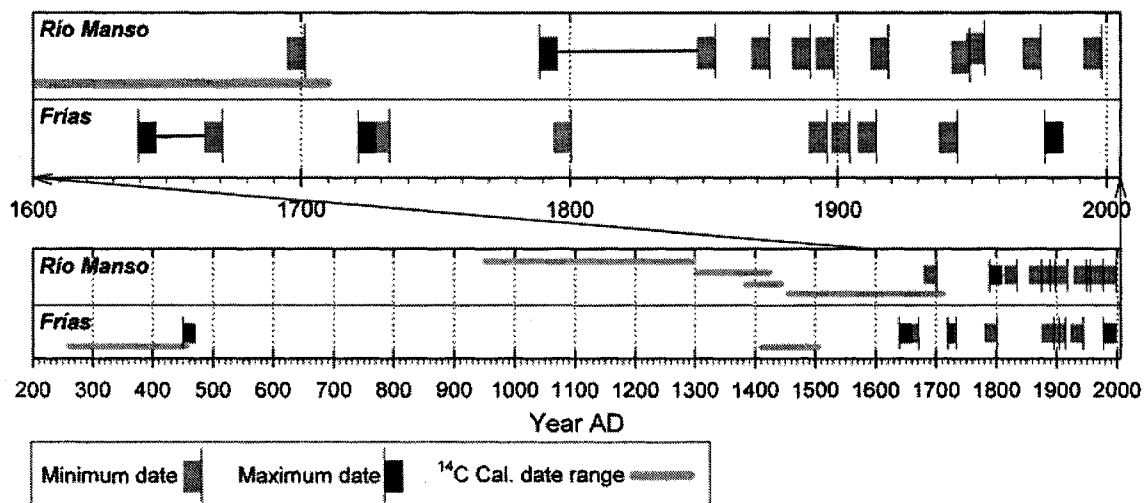


Fig. 5.7. Summary of available late Neoglacial age estimates for the main advances identified at Glaciar Río Manso and Glaciar Frías. Minimum and maximum dates (gray and black boxes, respectively) are based on the tree-ring dating of living trees and *in situ* stumps. The calibrated date ranges (gray bars) for four radiocarbon dated, *in situ* stumps from the north lateral moraine of Glaciar Río Manso (Röthlisberger 1986; Table 5.3) and two *in situ* stumps from the outermost moraines at Glaciar Frías (Table 5.6) are also indicated.

At Glaciar Río Manso a massive, older, frontal moraine apparently predating 2240 ¹⁴C yrs BP was partially overridden by four main glacier lobes during the LIA (Fig. 5.2). Evidence from *in situ* subfossil stumps and living tree-ring samples indicate that the most extensive LIA expansion took place between the late 1700s and the 1830-40s as the lower tongue thickened and advanced into adjacent forests. Overridden *in situ* snags on the inner flank of the north lateral moraine were calendar dated to the late 1700s and provide a maximum age for this event (Fig. 5.3). On the distal side of this moraine a tilted tree and stumps drowned by an ice marginal lake indicate that this glacier advance culminated in the 1840s. Living trees on the proximal side of this north lateral moraine indicate that the glacier was already in recession by the mid 1850s, providing a closely bracketed dating control for this event. Dates from trees downvalley of the moraine corroborate these results and indicate aggradation of proglacial outwash between the 1760s and the early 1840s. On the south margin of the glacier, the peak LIA advance may have

culminated approximately a decade earlier, as the oldest tree growing on the distal slope of the south lateral moraine was dated to 1839. In contrast, the oldest trees in the mature forests immediately outside the LIA maximum moraine date back to the 17th century.

The clearest evidence for subsequent glacier activity at Glaciar Río Manso comes from a sequence of relatively well preserved moraine ridges between the present proglacial lake and old-growth forests on the southern slope of the valley (Area H, Fig. 5.2). This morphological evidence indicates that over the past 150 years the lower glacier tongue has experienced several short periods of readvance or stasis whilst downwasting. Minimum ages obtained from trees growing on these deposits suggest the moraines were formed ca. 1875, 1890, 1899, 1919, 1949, 1955 and during the mid 1970s (Figure 5.7). Historical documents and photographs (Table 5.1) indicate that, despite these minor readvances, the lower tongue remained in approximately the same position between 1937 and 1991 and that the present proglacial lake started to form on the northeastern margin of the glacier by the early 1990s. Although another recent moraine, tentatively dated to around the late 1990s, is present on the southeast margin of the lake, the overall thinning and retreat of the glacier snout and the concurrent, rapid growth of the proglacial lake during the last 10-15 years is clearly evident at this site and was particularly noticeable in January 2007 when we last visited this glacier.

An overall poor agreement was found between the absolute, tree-ring based calendar dates obtained from selected *in situ* stumps and the radiocarbon dates derived from the same samples at this site (Table 5.4). This disparity is related to the non-linearity of the ^{14}C calibration curve during the past few centuries (see Porter 1981) and highlights some of the difficulties associated with radiocarbon dating of glacier events during the last millennium (e.g. Luckman 1986). Similar uncertainties remain in relation to the four ^{14}C dates from *in situ* stumps reported from the north lateral moraine and interpreted as evidence for three glacier events occurring around (or soon after) 950, 600 and 300 ^{14}C yrs BP by Röthlisberger (1986). Unfortunately we could not relocate this site to evaluate this evidence (the stumps were probably buried or eroded by the active mass wasting on this slope). However, given the wide range in calibrated calendar dates (Table 5.3), and

the limited documentation available about the geomorphic and stratigraphic relationships of these stumps, it seems prudent to interpret these results with caution. The only morphological evidence for glacier activity at this site during the last millennium comes from an older lateral moraine section on the south glacier margin (Area I on Fig. 5.2), that is at least 300 years old based on the oldest trees growing on its surface. Thus, the evidence available indicates that, with the exception of a few marginal sites, the main LIA advance of the early-mid 19th century was probably the most extensive event of the past 1000 years. It seems probable that earlier advances were confined within the massive frontal moraine system (tentatively dated to 2240 ¹⁴C yrs BP, see above) and therefore any evidence of such events was overridden by the glacier advance culminating ca. 1840.

A novel finding at Glaciar Río Manso was the strong contrast in the density of the bamboo understorey on either side of the LIA maximum limit. This “bamboo line” is clearly apparent at many places and can be used as a quick, apparently reliable tool for mapping the LIA maximum extent at this glacier (Fig. 5.8). The tree-ring dating of the moraine deposits indicates that, at this site, *Chusquea culeou* needs over 150 years to recolonize the surfaces abandoned after a glacier event. We have observed similar “bamboo lines” at other glaciers in the north Patagonian Andes but the phenomenon has not been reported previously. Although this interesting feature is probably related to the particular reproductive strategy of this species⁹, specific research is needed before we can provide reasonable ecological and physiological explanations for this phenomenon.

⁹ *Chusquea culeou* bamboos are known to flower, seed and die synchronously after a long vegetative period during which they are not aggressive invaders of new areas (Pearson et al. 1994; see also Veblen 1982). Although the regularity and intervals between mast seedings remain uncertain, Pearson et al. (1994) indicate that the flowering cycle may take over five decades in our study area.



Fig. 5.8. A view towards the south showing the location of the “bamboo line” in Area H (Fig. 5.2). Clear differences in forest undergrowth are apparent between the almost bare surface on the outermost LIA moraine in the foreground and the dense bamboo cover of the old-growth forest immediately outside this moraine.

The revised late Holocene chronology of events for Glaciar Frías is based on the detailed study of V90 but incorporates a new, direct ecessis determination for this site and evidence from recently exposed subfossil trees overridden during two glacier advances (Table 5.5). The earliest known advance at this site, previously reported as predating 1236 AD, is shown to have occurred between 411 and 450 AD based on the tree-ring dating of overridden trees. These results are confirmed by a radiocarbon date of 1720 ± 40 ^{14}C yrs BP (calibrated calendar date range 260-460 AD, Tables 5.6 and 5.7) from one of

the crossdated stumps and provide a precise, calendar-dated maximum age estimate for a previously undocumented glacier advance during the 5th century in the north Patagonian Andes. The good agreement between the ¹⁴C and tree-ring dating of this sample contrasts with the generally poor agreement from younger samples at other sites. This illustrates differences in the reliability of ¹⁴C determinations over the last two millennia and suggests that, given the nonlinear relationship between absolute radiocarbon dates and calibrated calendar dates during the past few centuries, most radiocarbon-based moraine age estimates encompassing this interval (i.e. most LIA and post-LIA advances in Patagonia) should be interpreted cautiously unless they are supported by more precise evidence. This result also highlights the great dendroglaciological potential of *Fitzroya cupressoides*. The exceptionally long life span of these trees and their low decay rate make subfossil alerces found in association with glacier deposits one of the best tools for dating glacier advances that occurred within the past few millennia in the north Patagonian Andes.

The most important LIA advance at Frías formed a series of massive moraine ridges located between 70 and 300 m upvalley of the outermost deposits of the 5th century (Fig. 5.6). According to evidence from an ice-scarred tree and several living trees growing on its surface, this main LIA event occurred in the early to mid 17th century (Table 5.5). Radiocarbon dating of two stumps recently found beneath till in this moraine indicate it was formed after ca. 1510 but are not closely limiting (Table 5.6). However, the existence of subfossil alerce stumps associated with this advance suggests that future work at this site may yield additional, tree-ring based information to provide a more precise dating for the main LIA event at this glacier. Glacier readvances occurred in the early 18th and 19th centuries, in the late 19th century and ca. 1904, 1914 and 1944, based on minor revisions of the tree-ring dating of a series of moraine ridges identified in V90 (Table 5.5 and Figs. 5.6 and 5.7). The latest event at this site was precisely identified in 1976-77 by field measurements and tree-ring data (V90, Table 5.5). Despite these 20th-century readvances, Glaciar Frías has experienced marked net frontal recession over the last 100 years that accounts for roughly half of the recession observed since the LIA maximum at this site (see Fig. 5.6).

The recent glacier shrinkage and relatively well documented glacier reactivation during the 1970s suggest that the glaciers at Tronador have been responding to a common regional forcing during the last few decades. In Chapter 3 we suggested that the widespread glacier mass loss in this part of Patagonia was probably the result of the combined effect of decreasing winter accumulation and increased summer ablation across the region. However, despite this evidence of regional synchronicity and the proximity and common accumulation zones for Glaciar Frías and Glaciar Río Manso, there are differences in the number and relative magnitude of glacier events during the last millennium at these two glaciers (Fig. 5.7). The most extensive and conspicuous LIA event at Río Manso occurred between the late 1700s and mid 1800s whereas the most extensive advance at Frías was during the early 17th century (see Figs. 5.2 and 5.6). In addition, Glaciar Río Manso downwasted, remaining relatively close to its LIA maximum position until the 1990s, but Glaciar Frías has receded over one kilometer during this period. These differences may relate to local topographic controls. Río Manso is a reconstituted glacier at the base of a large cliff, is not physically connected with its accumulation area (Fig. 5.2) and the LIA advance terminated against a large topographic obstruction. Frías, on the other hand, is a contiguous glacier tongue that descends a steep slope onto a broad wide, relatively gently sloping valley floor (Fig. 5.6). The lower Río Manso is heavily debris covered, the lower Frías glacier is (and was) not. Such topographic and debris cover controls may result in major differences in the response of these two glaciers to similar climatic forcing. Thus, while the evidence at these two sites allows detailed reconstruction of part of the late Holocene record of glacier fluctuations, these chronologies remain incomplete and give only a partial picture of the regional record. Each glacier record contains unique elements that may reflect local controls on their behavior. This underscores the need for many such detailed studies before a representative regional glacial history can be developed. Ongoing research at other glaciers in the Tronador area and along the north Patagonian Andes will provide complementary evidence to strengthen the available glacier record and allow a better evaluation of past and present glacier and climate variations in this region.

5.7. References

- Aniya, M., Sato, H., Naruse, R., Skvarca, P., and Casassa, G. 1997. Recent glacier variations in the Southern Patagonia Icefield, South America. *Arctic and Alpine Research* 29 (1), 1-12.
- Auer, V. 1956. The Pleistocene of Fuego-Patagonia. Part I: The Ice and Interglacial Ages. *Annales Academia Scientiarum Fennicae, Series AIII*, 226 pp.
- Auer, V. 1958. The Pleistocene of Fuego, Patagonia. Part II: The history of the flora and vegetation. *Annales Academiae Scientiarum Fennicae, Series A-III Geologica-Geographica* 50, 1-239.
- Bown, F., 2004. Cambios climáticos en la Región de Los Lagos y respuestas recientes del Glaciar Casa Pangué (41°08'S). M.Sc. Thesis, Universidad de Chile, 131 pp.
- Clapperton C.M. 1993. Quaternary Geology and Geomorphology of South America. Elsevier, Amsterdam, 779 pp.
- De Agostini, A.M. 1945. Andes Patagónicos (2nd ed.), Guillermo Kraft Ltda., Buenos Aires, 437 pp.
- De Agostini, A.M. 1949. Nahuel Huapi, bellezas naturales de los Andes de la Patagonia Septentrional. *Estudios Fotográficos*, Buenos Aires, 77 pp.
- Denton, G.H., Lowell, T.V., Heusser, C.J., Slüchter, C., Andersen, B.G., Heuser, L.E., Moreno, P.I., Marchant, D.R., 1999. Geomorphology, stratigraphy and radiocarbon chronology of Llanquihue drift in the area of the southern Lake District, Seno Reloncaví, and Isla de Chiloé, Chile. *Geografiska Annaler* 81A, 167-229.
- Fonck, F., Hess, F., 1857. Informe de los señores Francisco Fonck i Fernando Hess sobre la expedición a Nahuelhuapi. *Anales de la Universidad de Santiago de Chile* XIV, 1-11.
- Glasser, N.F., Hambrey, M.J., and Aniya, M. 2002. An advance of Soler Glacier, North Patagonian Icefield, at ca. AD 1222-1342. *Holocene* 12, 113-120.
- Glasser, N.F., Harrison, S., Winchester, V. and Aniya, M. 2004. Late Pleistocene and Holocene palaeoclimate and glacier fluctuations in Patagonia. *Global and Planetary Change* 43: 79-101.
- Grissino-Mayer, H.D. 2001. Evaluating crossdating accuracy: A manual and tutorial for the computer program COFECHA. *Tree-Ring Research* 57(2): 205-221.
- Grove, J.M. 2004. Little Ice Ages: Ancient and Modern (2 vols), Routledge, London, 718 pp.

- Holmes, R.L. 1983. Computer-assisted quality control in tree-ring dating and measurement. *Tree-Ring Bulletin* 43: 69-78.
- Jakob, C., 1936. Alrededor del Tronador. *Revista Geográfica Americana* V(28), 1-21.
- Jakob, C., 1937. La fiscalización de las reservas acuáticas es una obligación nacional para la Argentina. *Revista Geográfica Americana* V(50), 313-326.
- Lawrence, D.B., Lawrence, E.G., 1959. Recent glacier variations in southern South America. American Geographical Society Southern Chile Expedition Technical Report, Office of Naval Research Contract 641(04), New York, USA, 39 pp.
- Lliboutry, L., 1998. Glaciers of Chile and Argentina. In: Williams, R.S., Ferrigno, J.G., (eds.), *Satellite Image Atlas of Glaciers of the World: South America*. USGS Professional Paper 1386-I, Online version 1.02.
- Luckman, B.H. 1986. Reconstruction of Little Ice Age events in the Canadian Rocky Mountains. *Geographic Physique et Quaternaire* 40, 17-28.
- Luckman, B.H. 1988. Dating the moraines and recession of Athabasca and Dome Glaciers, Alberta, Canada. *Arctic and Alpine Research* 20, 40-54.
- Luckman, B.H. 2000. The Little Ice Age in the Canadian Rockies. *Geomorphology* 32, 357-384.
- Luckman, B.H., and Villalba, R. 2001. Assessing the synchronicity of glacier fluctuations in the western cordillera of the Americas during the last millennium. In: Markgraf, V. (ed.), *Interhemispheric Climate Linkages*, Academic Press, London, pp. 119-140.
- Masiokas, M., Villalba, R., Delgado, S., Trombotto, D., Luckman, B., Ripalta, A., and Hernandez, J. 2001. Dendrogeomorphological reconstruction of glacier variations in Patagonia during the past 1000 years. In: Kaennel D.M. and Bräker O.U. (eds). *Abstracts from the International Conference Tree Rings and People*. Davos, Switzerland, p. 177.
- Masiokas, M.H., Villalba, R., Luckman, B.H., Lascano, M.E., Delgado, S. and Stepanek, P. 2007. 20th-century glacier recession and regional hydroclimatic changes in northwestern Patagonia. *Global and Planetary Change*, doi:10.1016/j.gloplacha.2006.07.031.
- McCarthy, D.P., and Luckman, B.H. 1993. Estimating ecesis for tree-ring dating of moraines: a comparative study from the Canadian Cordillera. *Arctic and Alpine Research*. 25, 63-68.

- McCormac, F. G., Hogg, A. G., Blackwell, P. G., Buck, C. E., Higham, T. F. G., and Reimer, P. J. 2004. SHCal04 Southern Hemisphere Calibration, 0-11.0 cal Kyr BP. *Radiocarbon* 46 (3), 1087-1092.
- Mercer, J.H. 1982. Holocene glacier variations in southern South America. *Striae* 18, 35-40.
- Pearson, A.K., Pearson, O.P., and Gomez, I.A. 1994. Biology of the bamboo *Chusquea culeou* (Poaceae: Bambusoideae) in southern Argentina. *Vegetatio* 111: 93-126.
- Porter, S.C. 1981. Glaciological evidence of Holocene climatic change. In: Wigley, T.M.L., Ingram, M.J. and Farmer, G. (eds.), *Climate and History*. Cambridge University Press, pp. 83-110.
- Porter, S.C. 2000. Onset of Neoglaciation in the Southern Hemisphere. *Journal of Quaternary Science* 15 (4) 395-408.
- Porter, S.C. and Denton, G.H. 1967. Chronology of Neoglaciation in the North American cordillera. *American Journal of Science* 265, 177-210.
- Rabassa, J. and C.M. Clapperton. 1990. Quaternary glaciations of the Southern Andes. *Quaternary Science Reviews*, 9: 153-174.
- Rabassa, J., Rubulis, S., Suarez, J. 1978. Los glaciares del Monte Tronador. *Anales de Parques Nacionales XIV*, 259-318.
- Rabassa, J., Rubulis, S., Suárez, J. 1979. Rate of formation and sedimentology of (1976-1978) push-moraines, Frías Glacier, Mount Tronador (41°10'S; 71°53'W), Argentina. In: Schluëchter, C., (ed.), *Moraines and Varves*. A.A. Balkema, pp. 65-79.
- Rabassa, J., Brandani, A., Boninsegna, J.A. and Cobos, D.R. 1984. Cronología de la "Pequeña Edad del Hielo" en los glaciares Río Manso y Castaño Overo, Cerro Tronador, Provincia de Río Negro. *Actas Noveno Congreso Geológico Argentino*, 3: 624-639.
- Rignot, E., Rivera A. and Casassa, G. 2003. Contribution of the Patagonia icefields of South America to global sea level rise. *Science* 302, 434-437.
- Roig, F.A., Le-Quesne, C., Boninsegna, J.A., Briffa, K.R., Lara, A., Grudd, H., Jones, P.D. and Villagrán, C. 2001. Climate variability 50,000 years ago in mid-latitude Chile as reconstructed from tree rings. *Nature* 410, 567-570.
- Röthlisberger F. 1986. 10,000 Jahre Gletschergeschichte der Erde. Verlag Sauerländer: Aarau.

- Sigafoos, R.S., and Heindricks, E.L. 1969. The time interval between stabilization of alpine glacial deposits and establishment of tree seedlings. US Geological Survey, Professional Paper 650-B, B89-B93.
- Steffen, H., 1909. Viajes de Exploracion i Estudio en la Patagonia Occidental: 1892-1902, Vol. I. Anales de la Universidad de Chile, Imprenta Cervantes, Santiago. 409 pp.
- Stokes, M.A., and Smiley, T. 1996. An introduction to tree-ring dating. University of Arizona Press, Tucson, Arizona, 73 pp.
- Stuiver, M. and Reimer, P.J. 1993. Extended ^{14}C data base and revised CALIB 3.0 ^{14}C age calibration program. Radiocarbon 35, 215–230.
- Sugden, D.E., Bentley, M.J., Fogwill, C.J., Hulton, N.R.J., McCulloch, R.D., and Purves, R.S. 2005. Late-glacial glacier events in southernmost South America: a blend of 'northern' and 'southern' hemispheric climatic signals? Geografiska Annaler 87 A, 273-288.
- Thomasson, K. 1959. Plankton of some lakes in an Argentine National Park with notes on terrestrial vegetation. Acta Phytogeographica Suecica 42, 83 pp.
- Veblen, T.T. 1982. Growth patterns of *Chusquea* bamboos in the understory of Chilean *Nothofagus* forests and their influences in forest dynamics. Bulletin of the Torrey Botanical Club 109(4): 474-487.
- Villalba, R. 1990. Climatic fluctuations in northern Patagonia during the last 1000 years as inferred from tree-ring records. Quaternary Research 34, 346-360.
- Villalba, R., J.A. Boninsegna, T.T. Veblen, A. Schmelter, and S. Rubulis. 1997. Recent trends in tree-ring records from high elevation sites in the Andes of northern Patagonia. Climatic Change, 36: 425-454.
- Villalba, R., Leiva, J.C., Rubulis, S., Suarez, J., Lenzano, L.E., 1990. Climate, tree-ring, and glacial fluctuations in the Río Frías Valley, Río Negro, Argentina. Arctic and Alpine Research 22(3), 215-232.
- Villalba, R., Boninsegna, J.A., Lara, A., Veblen, T., Roig, F., Aravena, J.C., Ripalta, A. 1996. Interdecadal climatic variations in millennial temperature reconstructions from Southern South America. In: Jones, P.D., Bradley, R.S. and Jouzer, J. (eds) Climatic variations and forcing mechanisms of the last 2000 years. NATO ASI Series 141. Springer-Verlag, pp. 161-189.

The great variety of evidence for dating glacier deposits discussed in Chapter 5 allowed a relatively detailed chronology of glacier fluctuations to be developed for the past few centuries. Chapter 6 presents a potential improvement to this record by using an extensive, updated network of tree-ring width chronologies from the NW Patagonian region to develop a “glacier mass balance” proxy reconstruction over the past 520 years. The basis for this reconstruction is similar to the climate-based glacier mass balance proxy developed in Chapter 3. However, in this case the homogenized temperature data from Chapter 2 are used together with regional precipitation records to develop the proxy series. The tree-ring based reconstruction is compared with the LIA and post-LIA moraine records developed in Chapter 5 and the usefulness and limitations of both approaches are discussed.

This chapter will be submitted for publication in the near future with the following list of co-authors:

Masiokas, M.H.^{1,2}; Luckman, B.H.¹; Villalba, R.²; Lara, A.³; Urrutia, R.³.

¹ Department of Geography, University of Western Ontario, London, Ontario, Canada.

² Instituto Argentino de Nivología, Glaciología y Ciencias Ambientales (IANIGLA-CONICET), Mendoza, Argentina.

³ Instituto de Silvicultura, Universidad Austral de Chile, Valdivia, Chile.

Chapter 6: Tree-ring based reconstruction of a glacier mass balance proxy record for the past five centuries in the north Patagonian Andes

6.1. Introduction

The scarcity and shortness of direct glacier mass balance records in the Patagonian Andes is one of the main limitations for the proper evaluation of the impacts of inter-annual and inter-decadal climate variations on glacier behavior in this region (see e.g. Hodge et al. 1998; McCabe et al. 2000; Rasmussen and Conway 2004; Nesje 2005). The lack of long, reliable high-elevation climate records from sites near glaciers aggravates this problem and makes it difficult to estimate the relative influence of the main climate variables on recent glacier changes in this extensive and heavily glaciated mountain range¹. Several studies have linked the generalized state of recession observed in Patagonian glaciers during recent decades to large-scale changes towards warmer and drier conditions but few (e.g. Rivera 2004) have undertaken direct mass balance-climate analyses to corroborate this hypothesis. In a recent study, Masiokas et al. (2008) (hereafter Chapter 3) used regionally-averaged temperature and precipitation records from the NW Patagonian region to estimate the relative magnitude of two hypothetical “accumulation” and “ablation” seasons and developed a simple climatic index or “mass balance proxy” for 1912-2002. This exercise allowed an exploratory analysis of possible causes for the noticeable glacier shrinkage observed throughout the north Patagonian Andes² during the 20th century. A significant tendency towards drier winters and warmer summers was suggested as the most likely reason for this regional shrinkage. Short lived intervals of cool-wet conditions were found to correspond approximately with the timing of the most recent glacier readvances identified in this region, suggesting that the climate-based series could be used as a preliminary indicator of the most important changes that have occurred in the mass balance components of north Patagonian glaciers during the last century.

¹ The southern portion of the Patagonian Andes contains the largest glacierized area in the Southern Hemisphere outside Antarctica.

² The north Patagonian Andes are considered here as the portion of the Andes between ca. 37° and 45°S.

In this study we build on the results from Chapter 3 and develop a tree-ring based reconstruction of a regional, climate-based, glacier mass balance proxy estimate for the north Patagonian Andes that extends over the past 520 years. This proxy series is derived from an extensive collection of tree-ring chronologies from species sensitive to those climatic variables (i.e. total winter/annual precipitation and mean summer/annual temperatures) likely affecting glacier mass balances in this region. The reconstructed “mass balance proxy” can be compared with the history of glacier advances that occurred in NW Patagonia during the last 500 years and allows previous related studies (e.g. Bown 2004; Rivera et al. 2005; Bown and Rivera 2007; Chapter 3) to be put into a long term context. The simplicity of the climate-based indices used and the absence of long, measured glacier mass balance records for comparison/validation mean this reconstruction must be considered preliminary. However, the results suggest that it can provide useful baseline information about inter-annual and inter-decadal changes in these records. This information is significantly more detailed than the few low resolution Little Ice Age (LIA) and post-LIA glacier histories currently available for this region (Chapter 5).

6.2. Study area

The north Patagonian Andes and surrounding areas (Fig. 6.1) are characterized by relatively mild environmental conditions and steep precipitation gradients produced by the interaction between the mountain range and the westerly air masses that dominate circulation in this region. At ca. 40°-41°S, precipitation totals at the Pacific coast are almost 2000 mm per year and increase to over 4000 mm per year over the main cordillera. Precipitation levels decrease drastically east of the Andes: on the xeric Patagonian steppe (less than 100 km from the mountains) annual rainfall totals can be less than 200 mm per year (Prohaska 1976; Veblen and Lorenz 1988; Villalba et al. 2003). Most of this precipitation falls during the austral winter months, with 65-80% of the annual totals between April and September (Chapter 3). Mean annual temperatures vary from around 11°C at the Chilean coast to ca. 8°C in the forest-steppe limit in Argentina (Miller 1976; Prohaska 1976). Although absolute minimum temperatures in this region can fall below -15°C, mean temperatures for July vary between 4°- 8°C in

Chile to 2°- 4°C in Argentina. Mean temperatures for January range from 14° to 18°C (Prohaska 1976). These moderate climate conditions and the low elevations of the north Patagonian Andes result in limited glacierization with relatively small glaciers on the highest peaks and volcanoes (Lliboutry 1998). This probably explains why the glaciers in this area have been studied relatively less frequently than those associated with the extensive North and South Patagonian Icefields further south (e.g. Rignot et al. 2003). Twentieth-century glacier changes in NW Patagonia have been analyzed using aerial photographs, satellite imagery, historical documents, tree-ring records, and field measurements (e.g. Rabassa et al. 1978; Villalba et al. 1990; Bown 2004; Rivera et al. 2000, 2002, 2005; Bown and Rivera 2007; Chapters 3 and 5). However, these analyses are focused on limited areas and few preliminary glacier inventories are available. Lliboutry (1998) indicates that glaciers cover ca. 300 km² in the Andes between 35°S and 45°S, mainly west of the continental divide. The most noticeable feature in the glacier history of the past century is the significant recession throughout the region (e.g. Rivera et al. 2005; Chapters 3 and 5).

The late Neoglacial chronology of glacier fluctuations in the study area is poorly documented. The most detailed information available is based on Glaciar Frías and Glaciar Río Manso in the Monte Tronador area at around 41°10'S (Fig. 6.1). This information indicates two main pulses of the LIA culminating in the early-mid 1600s (Frías) and early-mid 1800s (Río Manso) followed by several readvances (Villalba et al. 1990; Chapters 3 and 5). The best documented readvance culminated in the mid to late 1970s and has been precisely identified using field observations, aerial photography and tree-ring samples from trees directly affected by the advance (e.g. Rabassa et al. 1978; Villalba et al. 1990).

Although no long (>10 yr), direct glacier mass balance records exist for this area (Rivera et al. 2005), the network of meteorological stations in the NW Patagonian region is denser and of better quality than the sparse network in southern Patagonia (see Rosenblüth et al. 1995, 1997; Rivera 2004; Villalba et al. 2003, Aravena 2007; Chapter 2). This improves our ability to examine the relationship between different climatic

variables and the recent glacier changes in this region. The NW Patagonian region also contains a good database of river discharge that can be used as an independent record to verify some of the climatic information available for this area (see e.g. Chapter 3).

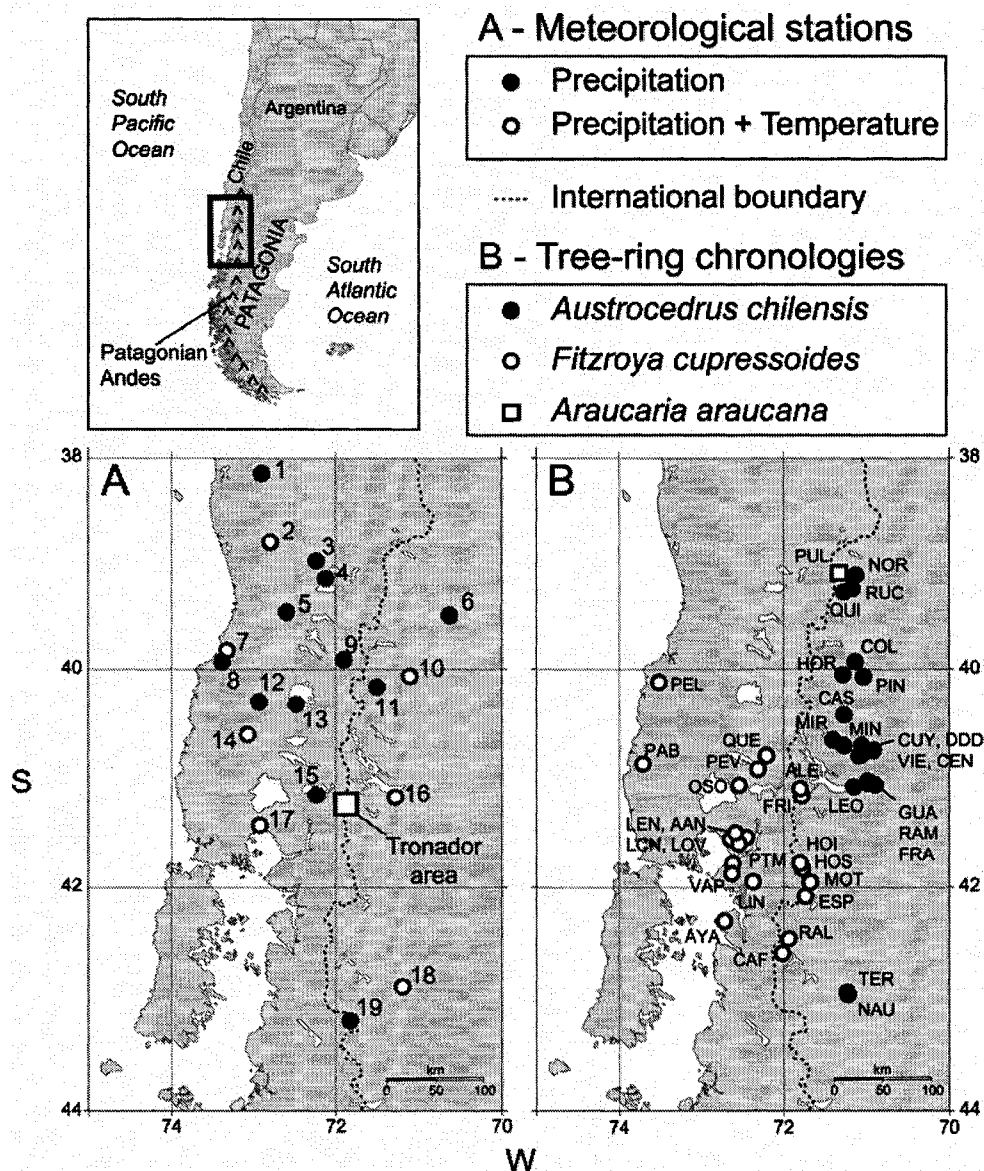


Fig. 6.1. Map of northwestern Patagonia showing (A) the location of the meteorological stations and (B) tree-ring sites used in this study (for identifications see Table 6.1 and Appendix 6). Additional climate data and glacier records from the Tronador area (white box in A) are discussed in the text.

Table 6.1. Stations used to develop regionally-averaged series of annual and seasonal temperature (T) and precipitation (P) variations for northwestern Patagonia between 38° and 44°S. Data sources: A: Dirección General de Aguas (DGA), Chile; B: Global Historical Climatology Network; C: World Weather Records; D: Dirección Meteorológica de Chile (DMC); E: Autoridad Interjurisdiccional de Cuencas de los Ríos Neuquén, Limay y Negro (AIC), Argentina; F: Universidad Austral de Chile; G: Empresa Nacional de Electricidad (ENDESA), Chile; H: Servicio Meteorológico Nacional (SMN), Argentina.

Station (code in Fig. 1A)	Lat. (S)	Long. (W)	Elev. (m)	Var.	Period (% missing)	Data source
Lumaco (1)	38.15	72.90	60	P	1948-2001 (1.2)	A
Temuco (2)	38.80	72.80	114	P	1912-2003 (1.5)	B
				T	1930-2005 (2.6)	B,C,D
Los Laureles (3)	38.98	72.23	190	P	1947-2001 (1.2)	A
Flor del Lago (4)	39.15	72.12	300	P	1961-2001 (0.2)	D
Purulón (5)	39.47	72.60	95	P	1936-2000 (0.5)	D
Ea. Campo Grande (6)	39.50	70.63	960	P	1947-1998 (3.7)	E
Valdivia (7)	39.80	73.10	13	P	1912-2003 (1.5)	B
				T	1912-2003 (7.3)	B,C,D
Isla Teja (8)	39.85	73.20	9	T	1960-2001 (0.2)	F
Puerto Fuy (9)	39.87	71.90	596	P	1961-1996 (0.7)	G
Ea. Collun Co (10)	40.07	71.17	875	P	1912-1998 (1.5)	E
				T	1912-1989 (0.6)	E
Ea. Quechuquina (11)	40.15	71.58	640	P	1957-1998 (6.3)	E
Río Bueno (12)	40.30	72.93	70	P	1940-2000 (2.0)	D
Lago Ranco (13)	40.32	72.48	79	P	1931-2000 (1.1)	D
Osorno (14)	40.60	73.07	65	P	1961-2001 (0.2)	D
				T	1961-2003 (5.3)	B,C,D
Punta Huano (15)	41.13	72.28	200	P	1961-2000 (0.4)	D
Bariloche (16)	41.20	71.20	840	P	1931-2003 (5.4)	B
				T	1914-2005 (0.0)	B,C,H
Puerto Montt (17)	41.40	73.10	85	P	1907-2003 (1.9)	B
				T	1911-2005 (4.5)	B,C,D
Esquel (18)	42.90	71.20	785	P	1916-2003 (4.8)	B
				T	1901-2005 (0.4)	B,C,H
Futaleufú (19)	43.20	71.82	317	P	1961-2001 (0.6)	D

The sharp precipitation gradients and complex topography of the north Patagonian Andes result in a wide variety of forest environments with great potential for dendrochronological studies. Schulman (1956) published the first tree-ring studies in South America from this region and highlighted the potential for obtaining long, clearly-

defined and climate-sensitive tree-ring records from a few key species. Since the early 1970s many studies have confirmed Schulman's conclusions using tree-ring chronologies collected from many sites in Chile and Argentina (e.g. Holmes et al. 1979; LaMarche et al. 1979; Villalba and Veblen 1997; Villalba et al. 1996, 1997; Lara et al. 2000, 2001, 2007). The majority of the chronologies are derived from *Austrocedrus chilensis* (ciprés de la cordillera), *Fitzroya cupressoides* (alerce), *Nothofagus pumilio* (lenga), or *Araucaria araucana* (Araucaria) trees. They are usually 300-500 years long for *A. chilensis* and *N. pumilio*, but can exceed 700 years for *A. araucana*. The chronologies from *F. cupressoides* are significantly longer³: most composite series exceed 1400 years in length (Villalba et al. 1996; Lara et al. 2000) and in a few cases they can extend for millennia (Lara and Villalba 1993; Wolodarsky-Franke 2002). Chronologies from these species have been used successfully in several tree-ring based reconstructions of annual and seasonal temperatures (Lara and Villalba 1993; Villalba et al. 1997, 2003), precipitation (Villalba et al. 1998), river discharges (Holmes et al. 1979; Lara et al. 2007), and large-scale circulation indices (Villalba 1990, 1994). Recent sampling has updated many key chronologies and has added new, promising sites to the extensive database of tree-ring records from this region.

6.3. Data and Methods

6.3.1. Developing glacier mass balance proxy series from climate records

We employed a similar method to that used in Chapter 3 to develop two simple, regional “glacier mass balance” proxy records from selected surface temperature and precipitation data for the NW Patagonian region. The two proxies cover the same 1912-2002 interval but differ in the length of the “seasons” used to estimate the relative magnitude of the hypothetical accumulation and ablation components of regional glacier mass balances in any given year. The first series (MBPsea) uses equally-weighted “long winter” (April-September) precipitation totals and “long summer” (October-March) mean temperatures as surrogates for winter accumulation and summer ablation in the north Patagonian Andes (see Chapter 3). The second series (MBPann) is based on “annual” (April-March) precipitation and temperature data.

³ Alerces are considered the second longest living tree species (Brown 1996).

Monthly total precipitation records for sites between 38°S and 44°S were obtained from Version 2 of the Global Historical Climatology Network (Vose et al. 1992) and various institutions in Chile and Argentina (Table 6.1). Since many of these records are short or incomplete, we selected 18 stations that provided the most complete (< 7% missing) and longest (>30 years long) records covering the 1961-1990 interval (Fig. 6.1 and Table 6.1). These are the same precipitation records as those used in Chapter 3. Missing months were estimated by linear regression using reference series created from up to 10 neighboring stations significantly correlated ($p < 0.05$) with the candidate series. These reference series were also used to evaluate potential inhomogeneities in the data for each station. The standard normal homogeneity test for single shifts (Alexandersson 1986) was used to obtain adjustment coefficients, identify the location and evaluate the statistical significance of potential inhomogeneities in the “long winter” and “annual” precipitation totals for each candidate site. Each series was adjusted only when Alexandersson’s test reached the 95% critical level.

The temperature series used in this study differ from those used in Chapter 3. Instead of using gridded temperature data from the CRUTem2v dataset (Jones and Moberg 2003), the ablation component of the glacier mass balance proxy records developed here is based on a more regionally representative temperature dataset from selected stations in NW Patagonia between 38° and 44°S (Fig. 6.1 and Table 6.1). These series were obtained from a recent, extensive compilation of mean monthly surface temperature station records for southern South America (Chapter 2). In some cases where the temperature records for individual stations were gathered from several sources (Table 6.1), they were averaged using the approach of Hansen et al. (1999) to obtain the longest and most complete possible series for each site. Reference series were created using first-differenced mean monthly series from 3-10 highly-correlated neighboring stations (Chapter 2). We selected the eight stations from both sides of the north Patagonian Andes with the longest and most complete records (Fig. 6.1 and Table 6.1). The homogeneity testing employed here is similar to that used for precipitation series but uses “long summer” and “annual” temperature averages as candidate series for each station.

The regional “long winter” and “annual” precipitation anomaly series were developed by averaging standardized anomalies (Z scores) of the April-September and April-March homogenized precipitation totals from the 18 stations in Table 6.1. We used the 1961-88 period common to all precipitation and temperature stations as a reference. Changes in the variance of the regional record due to changes in sample size were adjusted using the method of Osborn et al. (1997). The “long summer” and “annual” homogenized temperature records from the eight selected stations were also converted to Z scores and averaged into a variance adjusted regional record. The glacier mass balance proxies or climatic indices were developed by subtracting the temperature anomalies from the precipitation anomalies such that relatively wet winters/years and cool summers/years result in positive indices (overall “positive” mass balance conditions in the region), and viceversa. For example, in years when heavy winter precipitation was followed by warm summers the mass balance index is close to zero. Each year or season is identified by the year of the earliest month (e.g. the 2002 year runs from April 2002 to March 2003). The regional representativeness of these mass balance proxy series was evaluated using independent climatic data from the Mascardi station located near the Argentina-Chile border in the Tronador area (Fig. 6.1) and from seven rivers on the eastern side of the mountains (see Chapter 3). The low frequency patterns in these proxy series were also compared to the revised moraine record from glaciers in the Tronador area (Chapter 5).

As discussed in Chapter 3, the choice of specific months and length of season in the development of the proxy series based on long winter – long summer data is somewhat arbitrary and only intended to provide a simple yet reasonable surrogate for the relative importance of accumulation vs. ablation in any given year. It is not known whether precipitation or temperature variability is the more significant driver of mass balance variations in this region. Obviously, more realistic selection and weighting for this proxy series can be developed as north Patagonian glacier mass balance data become available in the future (e.g. Rivera et al. 2005). Preliminary, extensive comparisons between different seasonal combinations of mass balance proxy series and individual and regionally averaged tree-ring chronologies (not shown) indicated that the series based on

annualized April-March records invariably showed stronger correlations with the tree-ring series and significantly improved the statistical significance of the reconstruction models. Thus, as both winter-summer and annual mass balance proxy series are extremely similar at inter-annual and inter-decadal timescales (see below), the annual mass balance proxy (MBPann) was used as the predictand variable in the tree-ring based reconstruction trials described below.

6.3.2. Tree-ring data

We focused on tree-ring width chronologies from *A. chilensis*, *F. cupressoides* and *A. araucana* which have shown (or were inferred to have) some sensitivity to the precipitation and temperature records that were used to develop the glacier mass balance proxy series. All of the *A. chilensis* chronologies were collected from relatively open stands in xeric environments along the eastern side of the north Patagonian Andes (Fig. 6.1). At most of these sites summer/annual precipitation and spring/summer temperatures are the main climatic variables affecting tree growth (Villalba and Veblen 1997; Villalba et al. 1998). Most *A. araucana* chronologies come from similar sites. Holmes et al. (1979) used five *A. araucana* and two *A. chilensis* chronologies to reconstruct streamflow variations on the eastern side of the north Patagonian Andes. As river discharges in this region are strongly correlated with winter precipitation and summer temperatures (Chapter 3), we hypothesized that the *A. araucana* records available would show a somewhat similar climatic response to *A. chilensis* (i.e. wide rings during cool/wet years and narrow rings during warm/dry years). *F. cupressoides* trees grow in more humid/cooler environments, and, although they have been used to reconstruct regional summer temperature variations (e.g. Lara and Villalba 1993), other studies (e.g. Villalba et al. 1990) show that cool and wet conditions result in wider rings in this species.

Initially 71 tree-ring width chronologies (28 from *A. chilensis*, 20 from *A. araucana* and 23 from *F. cupressoides*) were selected for evaluation. The ring-width measurements for these chronologies were obtained from the International Tree-Ring Data Bank and from the Tree-Ring Laboratories in Valdivia, Chile and Mendoza, Argentina. Most of these chronologies have been described and analyzed elsewhere (LaMarche et al. 1979;

Villalba and Veblen 1997; Villalba et al. 1996; Lara and Villalba 1993; Lara et al. 2000, 2007). After removing series shorter than 100 years, the quality of the raw tree-ring measurements in each chronology was assessed using program COFECHA (Holmes 1983; Grissino-Mayer 2001). Series with an average correlation <0.4 (0.3 for *F. cupressoides*) with the site “master” chronology built from all remaining series were discarded to ensure a strong common signal, and only chronologies ≥ 300 years and ending in 1989 or later were used in further analyses. Only one *A. araucana* chronology met these criteria (Appendix 6).

The program ARSTAN (Cook and Holmes 1984; Cook and Krusic 2005) was used to remove the non-climatic age-related trend in the individual tree-ring width records and obtain dimensionless, stationary tree-ring index series (Fritts 1976, Cook et al. 1990). We used a fixed 150-yr spline with a 50% cutoff (Cook and Peters 1981) to standardize each series and preserve approximately the same amount of low frequency variability in all records⁴. A biweight robust averaging technique and the ARSTAN chronologies (Cook 1985) were used to minimize the influence of endogenous, non-synchronous disturbances and maximize the common signal at each site. The variance of the chronologies was stabilized using the method of Osborn et al. (1997). Subsequently, the main regional patterns of common variability in the *A. chilensis* and *F. cupressoides* chronologies were identified using principal component analysis (PCA). Based on the PCA results, the raw measurements for the chronologies that loaded most strongly on each PC were grouped and processed in a similar manner as described above to obtain regionally-averaged ARSTAN chronologies (Table 2). The strength of the common signal within these composite chronologies was evaluated using the Expressed Population Signal (EPS) statistic (Wigley et al. 1984) via a moving window analysis. We selected an EPS threshold of 0.8 to denote reasonable signal strength. Averaging individual chronologies based on PCA results significantly reduced the number of variables employed in the multiple regression reconstruction trials (eight final series in total including the individual *A. araucana* chronology, Table 6.2) and resulted in an important improvement in the

⁴ This particular standardization method preserves 50% of the variance at wavelengths of 150 years and 99% of the variance at wavelengths of 47 years or shorter.

useful length of these records. The common period for the final chronologies with reasonable signal strength is 1650-1989.

Table 6.2. The eight tree-ring chronologies used to develop the mass balance proxy reconstructions. In each case, the earliest year with reasonable signal strength ($EPS \geq 0.8$) is indicated. Correlations with the MBPann series for different lags and over the 1942-89 common interval are shown and denoted by an asterisk if $p < 0.10$ (see text for discussion). Notes: (SIC) sample intercorrelation; (AC1) first-order autocorrelation; (AR order) autoregressive order of the chronology determined using the minimum Akaike Information Criterion (Akaike 1974).

Chron.	Cores	SIC	Full period	EPS \geq 0.8	AC1	AR order	Corr. with MBPann (1942-89)			
							t-1	t	t+1	t+2
AUS1	416	0.562	1461-2003AD	1480	0.402	AR (2)	-0.445*	0.398*	0.339*	-0.166
AUS2	224	0.567	1508-2003AD	1650	0.458	AR (3)	-0.368*	0.460*	0.374*	-0.247*
AUS3	121	0.649	1540-2002AD	1580	0.505	AR (1)	-0.228	0.407*	0.314*	0.004
FIT1	319	0.466	1992BC-2003AD	1340BC	0.543	AR (3)	0.157	-0.322*	0.004	0.237
FIT2	321	0.485	342BC-1995AD	60	0.521	AR (3)	0.002	-0.105	0.285*	-0.055
FIT3	100	0.458	354BC-1994AD	600	0.702	AR (3)	0.182	-0.101	0.051	0.312*
FIT4	90	0.397	500-1996AD	1250	0.635	AR (2)	0.006	0.138	0.237	0.155
ARA1	28	0.609	1589-1989AD	1640	0.424	AR (1)	-0.164	0.239	0.141	-0.259*

6.3.3. Reconstruction Method

The regional glacier mass balance proxy reconstruction for the north Patagonian Andes is based on the application of point-by-point regression (PPR, Cook et al. 1996, 1999). This methodology is based on principal components regression analysis and allows an objective control over which tree-ring chronologies and their principal component scores enter the regression equation for reconstructing the mass balance proxy series. The multiple predictor – single predictand case relevant for this study uses four stages of model development (which result in four “pools” of tree-ring variables that successively concentrate the common climatic signal of interest) that are applied in sequence prior to

the development of the final reconstruction model (see description in Cook et al. 1999). We applied this technique to develop five PPR regression models using different combinations of predictor series (i.e. the eight well replicated chronologies developed above) with variable periods of overlap. These combinations were intended to find the best, longest and most updated reconstruction(s) of the glacier mass balance proxy series. For example, Model 1 included the maximum number of potential predictors but resulted in the shortest reconstruction, namely 1650-1989 (Table 6.3). Each reconstruction model was calibrated using post-1941 data and verified using data for the 1912-41 period. This allowed the objective evaluation of the performance of each model over the same independent dataset (see below).

First, all chronologies with data for the selected overlapping interval were lagged at $t-1$, $t=0$, $t+1$ and $t+2$ and grouped in Pool 1 as potential predictors for the April-March based glacier mass balance proxy (Table 6.3). The lagging approach was used to capture the tree-growth preconditioning and lagged response to climate often seen in tree-ring series (Fritts 1976). In order to simplify the tests of association between the tree-ring series and the mass balance proxy, both predictand and predictor series were prewhitened using low-order autoregressive (AR) models in which the order is objectively determined using the minimum Akaike Information Criterion (AIC, Akaike 1974) with a correction for small sample bias (Hurvich and Tsai 1989; Cook et al. 1999).

The prewhitened tree-ring series from Pool 1 were correlated against the prewhitened mass balance proxy record over their corresponding calibration interval and only those series correlated at $p < 0.10$ (two-tailed test) with the predictand data were selected for further analysis. This reduced the number of variables in Pool 1 to only those (Pool 2, Table 6.3) with a reasonable regional climate signal(s). PCA was subsequently used to reduce the number of variables in Pool 2 and concentrate their common climatic information further: Pool 3 contains the corresponding principal components with an eigenvalue ≥ 1 (Guttman 1954; Kaiser 1960). These orthogonal tree-ring variables were then correlated with the predictand series over the calibration period and based on their correlation coefficients they were entered into the regression model in order of decreasing

magnitude until the minimum AIC was achieved. Pool 4 is formed by the series included in this regression equation, which was used to reconstruct the predictand series over the full length of the series (Table 6.3). The final step was to add back to the reconstruction the autocorrelation that had been modeled and removed from the mass balance proxy series at the initial stages of analysis (see Cook et al. 1999 for further details).

Table 6.3. Calibration/verification statistics and details of the five trial models developed for the reconstruction of the MBPann proxy series. The models were calibrated using post-1941 data. For verification we used MBPann data between 1912-41 and an equivalent series for 1853-79 created from climate records from Valdivia, Chile. For each model the number of input variables is progressively reduced from Pool 1 to Pool 4 via point-by-point regression (see text for details). The final reconstruction is based on Models 3 and 4 (results in bold). **Calibration statistics:** (adj r²) coefficient of determination adjusted to account for the number of predictors in each model and used to estimate the proportion of variance explained by regression; (s_e) standard error of the estimate; (DWd) the Durbin-Watson d statistic used to test for first-order autocorrelation (AC1) of the regression residuals (Ostrom 1990). The DWd values indicate that the null hypothesis (AC1=0) cannot be conclusively rejected at the 95% significance level. **Verification statistics:** (r_v²) squared Pearson correlation coefficient; (RMSE) root-mean-squared error of validation; (RE) reduction of error; (CE) coefficient of efficiency; (rVal) correlation with 1853-79 “mass balance proxy” series from Valdivia. All correlations are highly significant (p<0.01).

Model (calib. period)	Pool				Calibration				Verification (1912-41)				Valdivia	Reconstr. length
	1	2	3	4	Adj r ²	s _e	DWd	AC1	r _v ²	RMSE	RE	CE	rVal	
1 (1942-1987)	32	13	5	2	0.474	1.137	1.759	0.054	0.366	1.559	0.315	0.037	0.702	1651-1987
2 (1942-1992)	28	8	4	3	0.503	1.079	1.773	0.050	0.379	1.500	0.437	0.108	0.636	1581-1992
3 (1942-2000)	12	6	3	3	0.504	1.131	1.627	0.105	0.426	1.403	0.507	0.220	0.608	1581-2000
4 (1942-1992)	20	5	3	2	0.347	1.225	1.907	0.002	0.322	1.571	0.382	0.023	0.635	1481-1992
5 (1942-2000)	8	4	2	2	0.264	1.344	1.805	0.050	0.163	1.609	0.351	-0.026	0.573	1481-2000

The goodness of fit of the five reconstruction models over their calibration interval was evaluated based on the proportion of variance explained by regression and the first-order autocorrelation of the regression residuals (see Table 6.3). The predictive skill of the models outside the calibration period was evaluated using the 1912-41 portion of the glacier mass balance proxy series not used in the calibration of these models. We

employed three verification statistics commonly used in dendroclimatological analyses (Fritts 1976; Cook and Kairiukstis 1990; Cook et al. 1994), namely the square of the Pearson correlation coefficient (r^2_v), the Reduction of Error (RE) statistic, and the Coefficient of Efficiency (CE) statistic (Table 6.3). As measures of shared variance between the actual and estimated series, r^2_v is the least rigorous of the three tests because it is not sensitive to differences in mean levels between the series. A positive value for either RE or CE indicates that the regression model has some skill; CE is however the most rigorous test because the benchmark for determining skill is the verification period mean (Cook et al. 1994, 1999). The root-mean-square error statistic (RMSE, Weisberg 1985) was also calculated to estimate the expected error of the reconstructions. Additional independent verification of the models was undertaken by correlating the reconstructed MBPann values to those developed from historical monthly temperature and precipitation data from Valdivia (39°48'S, 73°06'W, Fig. 6.1 and Table 6.3) available for 1853-79 (J.C. Aravena, personal communication). Finally, the LIA and post-LIA moraine record from the Tronador area was compared to the low frequency patterns in the annual and cumulative values of the reconstructed series.

6.4. Results

6.4.1. Instrumental climate records and mass balance proxy series, 1912-2002

The regionally-averaged “long winter” (Apr-Sep) precipitation and “long summer” (Oct-Mar) temperature records in NW Patagonia show distinct intra- to multi-decadal patterns between 1912 and 2002 (Fig. 6.2A). Winter precipitation records show a marked long term negative trend, with several short-lived periods of increased precipitation during the early 1920s, 1940s, 1950s and 1980s and the late 1990s (Fig. 6.2A). The most noticeable feature in this smoothed series is a step-like decrease in precipitation totals in 1955-56 with generally higher values before 1955 and lower values and a steeper negative trend thereafter (Fig. 6.2A, dark green line). The long summer temperature series (Fig. 6.2A, light green line) shows a moderate negative trend that contrasts with the positive trend reported in Chapter 3 for the same season using a slightly different area and set of

stations⁵. Sustained cool summer conditions occurred during the mid-late 1930s and the early-mid 1970s. Temperatures increased markedly following the 1970s but have remained relatively stable and slightly above the long term average since the early 1980s (Fig. 6.2A).

The glacier mass balance proxy series derived from the seasonal Apr-Sep precipitation and Oct-Mar temperature records (MBP_{sea}) shows high inter-annual variability superimposed on a marked long term negative trend (Fig 6.2B). Although the negative trend is less steep, this series is remarkably similar to that developed in Chapter 3. This suggests that the cooling trend in the summer temperatures reported here has been insufficient to counter the overall 20th-century trend towards increasingly negative glacier mass balance conditions inferred from the climate record.

The mass balance proxy record derived from annually-averaged climate data (MBP_{ann}, Fig. 6.2B) is very similar to the MBP_{sea} series at inter-annual and inter-decadal scales. This probably reflects the dominant influence of winter precipitation in annual totals in this region (see Chapter 3) and the similarity between the relative magnitude of summer and annual temperatures in any given year (i.e. warm summers will probably result in overall warm years, and viceversa). Both mass balance proxy series show a few synchronous short-lived periods of overall “positive” conditions within their negative long term trends (Fig. 6.2B). Although these periods generally occur when regional precipitation levels are relatively high and temperature levels are relatively low (shaded dark grey in Fig. 6.2A), the analysis of the temporal variations in these series allows a more detailed interpretation regarding their causes and a preliminary assessment of the relative influence of regional precipitation and temperature changes on these features. For example, the “positive” mass balance peak observed in the early-mid 1990s (Fig. 6.2B) occurred during a period with relatively stable temperatures and is therefore directly and

⁵ In Chapter 3 we used temperature data from the CRUTem2v gridded dataset (Jones and Moberg 2003) for the grid cell between 40°-45°S and 70°-75°W and reported a statistically significant warming trend for long summer temperatures between 1912 and 2002. The record is based on up to five stations within this grid cell. In the present chapter we incorporated additional station records for NW Patagonia between 38° and 44°S derived from Chapter 2 and used well-replicated reference series for adjusting (where necessary) non-climatic inhomogeneities in the long summer records.

almost entirely related to the sharp increase in precipitation levels during those years (Fig. 6.2A).

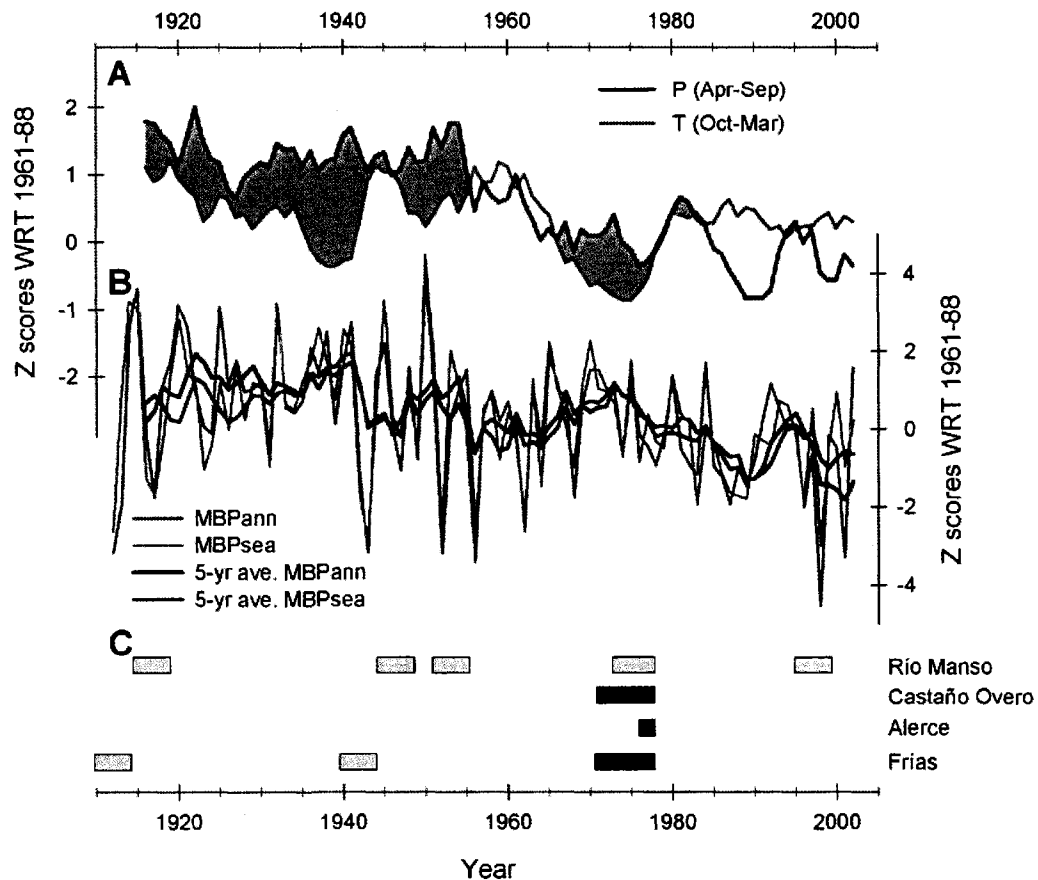


Fig. 6.2. Temperature, precipitation, proxy mass balance and moraine records for NW Patagonia, 1912-2002. **(A)** Five-year running averages of regionally-averaged cold season (April-September) precipitation (P) and warm season (October-March) temperatures (T) expressed as standardized anomalies (Z scores) with respect to the 1961-88 period. Shaded areas denote intervals when precipitation levels (dark green line) are collectively high and/or temperature levels (light green line) are low, implying overall “positive” mass balance conditions in this region. **(B)** Regional “glacier mass balance” proxy series calculated as (i) the difference between the Z scores of cold season precipitation totals and warm season mean temperatures (MBPsea, thin red line), and (ii) annual (April-March) precipitation and temperature data (MBPann, thin blue line). In general, positive values are interpreted as the result of wet winters/years and cool summers/years, and viceversa. The thick lines are five-year running averages for each series. **(C)** 20th-century moraine record for four glaciers in the Tronador area. Dates of moraine formation are inferred from dendrochronology (gray boxes) or field measurements (black boxes) (for details see Rabassa et al. 1978; Villalba et al. 1990; Chapter 5).

The reliability of this climate-based series as a surrogate for glacier mass balance conditions was partially validated using the available glacier record from the Tronador area (Fig. 6.1 and 6.2C). The comparison of the records shows that peaks in the mass balance indices generally precede the formation of moraines identified in this area (Fig. 6.2B and C). The clearest example is the good correspondence between the more positive MBPs between the mid 1960s and the mid 1970s and the well documented glacier readvances during or immediately after that period (see Fig. 6.2B). Independent information from the Mascardi climate station (located a few km east of the Tronador glaciers, Fig. 6.1) and also from a regionally-averaged streamflow record from seven gauge stations on the eastern side of the north Patagonian Andes (Fig. 6.3) further validate the regional representativeness of the mass balance proxy series. Equivalent mass balance proxy series derived from the Mascardi records show correlations of 0.915 and 0.908 with the corresponding regional mass balance proxy series over the 1969-94 overlapping period, whereas the correlations of the MBP_{sea} and MBP_{ann} series with the regional streamflow record are 0.769 and 0.750, respectively, for the 1912-2002 overlapping interval (see Fig. 6.3).

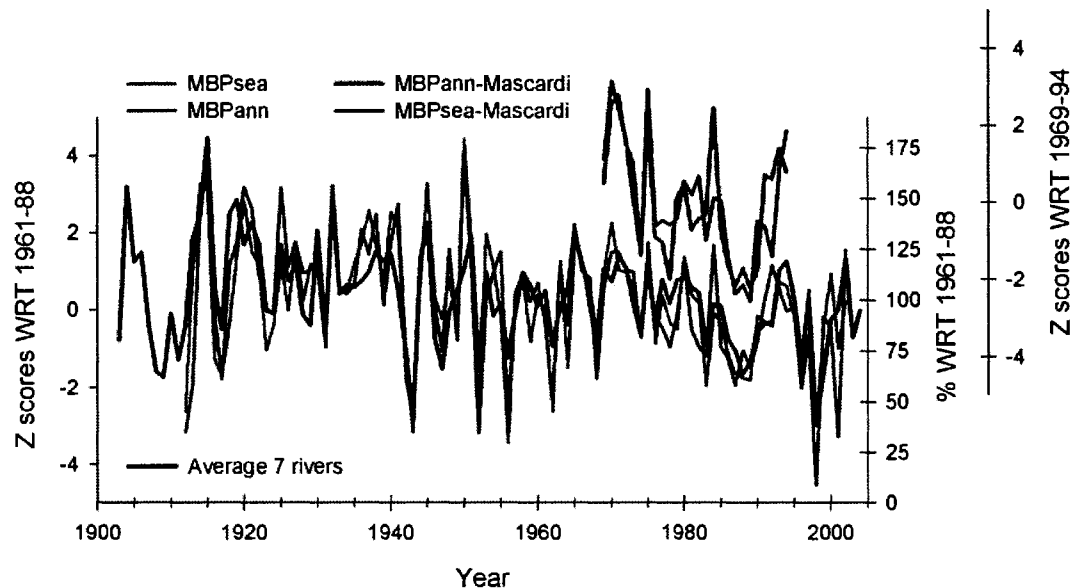


Fig. 6.3. Comparison between the regional “glacier mass balance” proxy series and independent data sets. The proxy series developed in Fig. 6.2 (MBPsea: red line, MBPann: blue line) are compared with the average annual (April-March) discharge of seven rivers from the eastern side of the north Patagonian Andes (thick black line, expressed as percentages from the 1961-1988 mean flows), and two equivalent seasonal and annual glacier mass balance proxy series calculated using data from the Mascardi station in the Tronador area (brown and green lines, expressed as standardized anomalies from the 1969-94 period). Note the strong similarities between all series.

6.4.2. Tree-ring records

The analysis of the original *A. chilensis* chronologies using PCA identified three groups (AUS1-3, Appendix 6 and Table 6.2) that roughly reflect the geographical location of the sampling sites. AUS1 groups 13 chronologies in the central portion of the distribution, AUS2 is formed by four of the northernmost sites, and AUS3 is formed by the two southernmost sites (Fig. 6.1 and Appendix 6). The three resulting composite tree-ring width chronologies show a remarkably strong common signal and corroborate the findings of previous studies (e.g. Schulmann 1956; Villalba and Veblen 1997) which have highlighted the great dendrochronological potential of this species. Despite the variety of sites and the large number of samples, the mean series intercorrelation for the

composite records ranges between 0.56 and 0.65 (Table 6.2). The chronologies are updated to 2002-03 and have reasonable signal strength ($EPS \geq 0.80$) starting between 1650 (AUS2) and 1480 (AUS1). PCA identified four groups of *F. cupressoides* chronologies (Appendix 6). FIT1 contains eight Chilean sites in the SE portion of their distribution, FIT3 groups three Chilean sites located towards the NE, and FIT4 contains the two westernmost chronologies in the study area (Fig. 6.1 and Appendix 6). All the eight Argentinean chronologies are grouped in FIT2. The four composite *F. cupressoides* records are significantly longer than the *A. chilensis* series and have a reasonable signal strength that begins in 1250 or earlier in all cases (Table 6.2). These series are also relatively well replicated but only FIT1 is updated to 2003; the rest end between 1994 and 1996. The Estancia Pulmari *A. araucana* chronology is located near the northern *A. chilensis* sites (Fig. 6.1), shows a strong mean series intercorrelation of 0.609, and has adequate signal strength between 1640 and 1989 (Table 6.2).

6.4.3. Mass balance proxy reconstruction, 1481-2000

Preliminary tests of association between the tree-ring chronologies and the MBP_{sea} and MBP_{ann} series (not shown) generally showed stronger correlations with the latter. These results were consistent for different overlapping intervals and may reflect a better sensitivity of these tree-ring series to annually-averaged precipitation and temperature variations in this region. We therefore focused on reconstructing MBP_{ann} as it resulted in stronger regression models and improved predictive skill. The strong similarities between the two climate-based mass balance proxy series (Fig. 6.2B) suggest however that a good quality reconstruction of the MBP_{ann} series should also provide useful information regarding the past inter-annual and inter-decadal fluctuations based on seasonal (MBP_{sea}) data.

In general, the composite *A. chilensis* chronologies showed the strongest correlations with the mass balance proxy series. This is illustrated in Table 6.2 for the 1942-89 calibration period which includes all series. Positive, statistically significant correlations (at $p \leq 0.1$) were found for all three *A. chilensis* chronologies for lags $t=0$ and $t+1$, whereas the other lags generally showed negative (and in some cases statistically significant)

correlations. The strong positive correlations with this species at lags $t=0$ and $t+1$ would be anticipated given the relatively xeric conditions of the original sites in which cool-wet years would promote tree-growth and viceversa. A similar, weaker, response was found for the *A. araucana* chronology (Table 6.2). The *F. cupressoides* composite chronologies showed contrasting results that were unexpected, based on previous analyses which have shown a positive response to cool and wet conditions for this species (e.g. Villalba et al. 1990). The negative correlations between series FIT1-3 at lag $t=0$ and the MBPann proxy record (Table 6.2) imply a reduced tree-growth during cool-wet years and viceversa. The other lags usually showed weak but positive correlations for these three composite *F. cupressoides* series. The correlations with FIT4 were invariably weaker but usually positive for all lags.

Five reconstruction models derived from different combinations of the eight available predictors were developed for the MBPann series using PPR. These models explain between 26% and 50% of the observed variance over their calibration periods (Table 6.3) and all contain at least one *A. chilensis* series, highlighting the importance of this species as predictor of this variable. Other regression equations including only the longer *F. cupressoides* chronologies (that could potentially provide the longest reconstructions) were not statistically significant. Therefore, the length of the final reconstructions was limited to the length of the *A. chilensis* chronologies with reasonable signal strength (350-520 years, Table 6.3). It is worth noting that the combined use of composite chronologies and PPR effectively reduced the number of independent variables in each regression model to a maximum of three (see Pool 4 in Table 6.3). This represents a significant simplification of the regression equations considering the very extensive number of potentially useful individual chronologies available from the study area (Fig. 6.1).

The analysis of the first-order autocorrelation coefficients in the regression residuals of Models 1-5 indicates these series have very little persistence (Table 6.3). Thus, the selection of the best model(s) to develop the final mass balance proxy reconstruction was based on the percentage of variance accounted for by each model and the analysis of verification statistics obtained using data outside the calibration periods. This analysis

revealed the superior predictive skill of Model 3, which showed the highest percentage of explained variance over both the calibration and verification periods (50.4% and 42.6%, respectively), the lowest expected errors in the reconstruction (RMSE), and the highest RE and CE values (Table 6.3). The correlation with the Valdivia “mass balance” proxy series between 1853-79 was not the highest but still highly statistically significant. Based on this information, Model 3 was used to estimate the MBPann series between 1581 and 2000. Model 4 was the only one with reasonable predictive skill outside the calibration period that could extend the reconstruction of the MBPann series (back to 1481 in this case, Table 6.3). The observed vs. predicted records for these models during the calibration/verification intervals are shown in Fig. 6.4. The final reconstructed series was created by splicing together the relevant portions from Models 3 and 4, each rescaled to have zero mean and unit standard deviation over the 1912-92 period in common with the instrumental record (Fig. 6.5A). This approach was taken to standardize the variance of the reconstructed series and facilitate the interpretation of the results in terms of 20th-century conditions.

The reconstructed series (Fig. 6.5A) shows a strong year-to-year variability embedded within several well defined periods of overall positive or negative conditions ranging from a few years to several decades in length. The most noticeable positive proxy balances in this series occurred during the late 1500s, ca. 1660, between ca. 1720-40 and 1860-80, and between the mid 1960s and 70s (Fig. 6.5A). Periods with strong negative “mass balance” conditions occurred around 1620-50, 1670-1700, 1820-40, 1880-1920 and during last decades of the 20th century. The lowest value on record for both instrumental and reconstructed series is 1998 (Fig. 6.5A). This agrees with previous studies (e.g. Suarez et al. 2004; Kitzberger and Suarez 2007) that highlighted the severity of the extreme dry-warm conditions during 1998-99 and linked this phenomenon to a massive dieback and subsequent shift in forest composition of mature mixed *Nothofagus-Austrocedrus* forests along the eastern margin of the north Patagonian Andes.

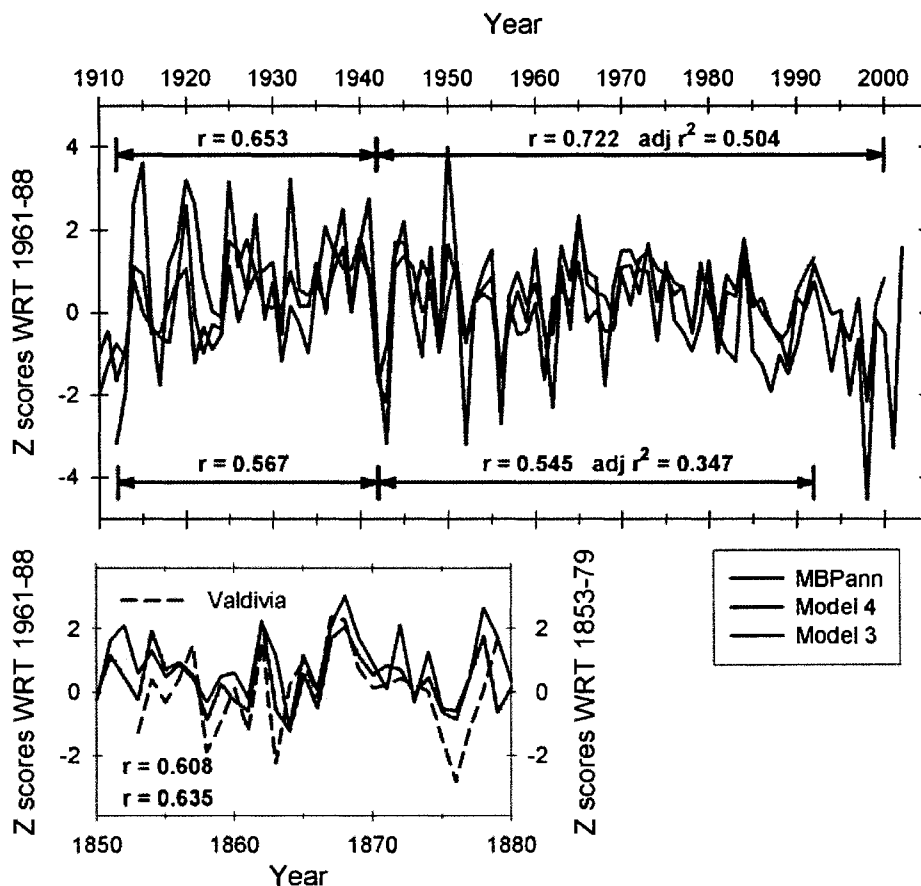


Fig 6.4. (A) Comparison of the calculated glacier mass balance proxy series (MBPann, blue line) with values predicted from Models 3 and 4 (dark red and dark green lines, respectively). The regression equations were calibrated over the 1942-2000 (Model 3) and 1942-92 (Model 4) intervals. The proportion of variance explained by regression adjusted for loss of degrees of freedom ($\text{adj } r^2$) is shown together with the square of the Pearson correlation coefficient (r^2_v) over the 1912-41 verification period (see Table 6.3). **(B)** As above using an equivalent MBPann series (dashed blue line) developed from climate data for 1853-79 from Valdivia, Chile (Fig. 6.1 and Table 6.1). In this case the Pearson correlation is shown.

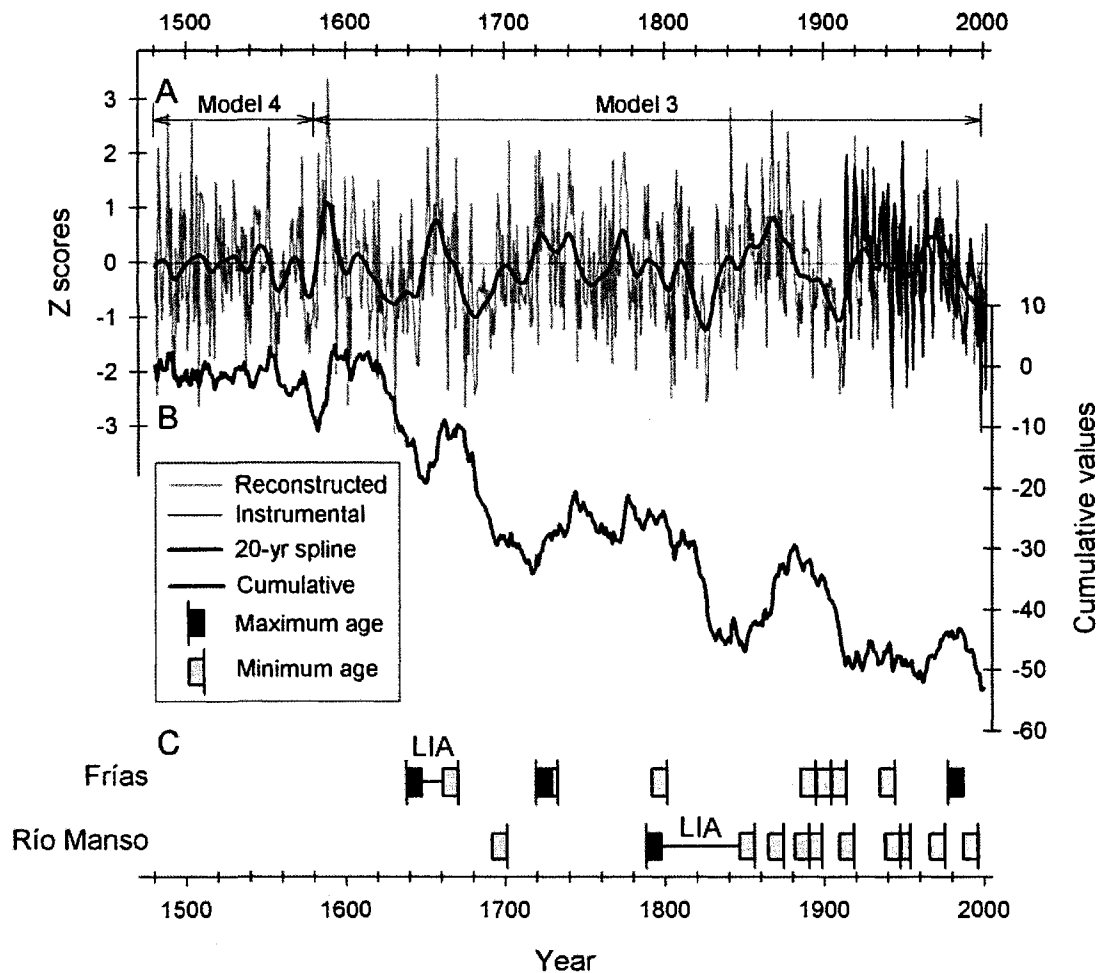


Fig. 6.5. (A) Reconstruction of the MBPann series for the NW Patagonian region based on tree-ring data. The 1481-1580 (derived from Model 4) and the 1581-2000 portions of the reconstruction (Model 3) were spliced together after rescaling the original reconstructions to the 1912-92 period in common with the instrumental series (shown here as a blue line and rescaled to the same reference period). (B) Cumulative record of the reconstructed MBPann series. (C) Tree-ring dated moraine records for Glaciar Frías and Glaciar Río Manso in the Tronador area. Maximum ages for the deposits (black squares) are largely based on the dendrochronological dating of trees directly affected by the glacier advance, whereas minimum dates (gray squares) are derived from the age of the oldest trees sampled growing on the moraines (Chapter 5).

Fig. 6.5B displays the cumulative values of the reconstructed mass balance proxy series. The most striking features of this record are the strong negative trend since the early 1600s and the five relatively well defined, extended periods of “positive” (or “less negative”) conditions within the overall decreasing trend (Fig. 6.5B). These peaks can be interpreted as periods when conditions were relatively more favorable for glaciers and should therefore provide useful information for the cross-validation of the independent glacier record from this region. This hypothesis is partially validated using the moraine record from Glaciar Frías and Glaciar Río Manso in the Tronador area (Chapter 5) (Fig. 6.5C). The most extensive LIA advances at Frías (early-mid 17th century) and Río Manso (late 18th-early 19th century) occurred soon after two major intervals of positive, cumulative mass balance conditions during the late 16th-early 17th century and between the mid-late 18th and early 19th century. In addition, several readvances identified at both glaciers during the late 1800s-early 1900s seem to be associated with another major peak in cumulative mass balances that culminated in the early 20th century (Fig. 6.5B and C). However, the correspondence between the cumulative mass balance proxy series and other glacier advances is not as clear. This may well be related to the inherent uncertainties associated with the tree-ring dating of the moraines and/or the tree-ring based reconstruction models developed here. The complex dynamic response of individual glaciers to climate and site specific factors such as topographic profile and debris cover may have also influenced the lag time and relative magnitude of any given advance to a change in mass balance conditions. Data from studies at an increased number of glaciers to develop a larger, more regionally representative moraine record, together with improved mass balance reconstructions from more realistic regression models, are needed to elucidate these issues.

6.5. Discussion and Conclusions

The study of glacier fluctuations in the north Patagonian Andes is of particular interest for the better understanding of glacier-climate relationships and changes in southern South America. The relatively small size of these ice masses makes them particularly sensitive to synoptic changes in climate (Oerlemans and Fortuin 1992), and thereby valuable sources of information for studies of hydro-climatic variations in this region.

The existence of several tree species with great dendrochronological potential along the north Patagonian Andes offers the opportunity to evaluate such variations in a multi-century to multi-millennia perspective using high-resolution tree-ring based reconstructions of a variety of environmental parameters. In addition, the network of hydro-climatic stations with long, complete records is relatively much denser and of better quality than those available further south where most Patagonian glaciers are located. However, despite this great potential, the limited information available for north Patagonian glaciers and the lack of long (>10 yr), direct glacier mass balance records make it difficult to estimate the relative influence of the main climate variables on glacier behavior and relate the glacier growth/recession to a specific change in climate conditions.

This paper presents an exploratory approach to the estimation and reconstruction of regional “glacier mass balance” conditions in the north Patagonian Andes over the past five centuries using climate records and tree-ring width chronologies. Mass balance conditions between 1912-2002 are estimated using regionally-averaged long winter (April-September) precipitation totals and long summer (October-March) mean temperatures as indirect measures of the “accumulation” and “ablation” components of a hypothetical annual mass balance proxy series for 1912-2002 (MBP_{sea}, see Fig. 6.2). This is the same approach and almost the same dataset as used in Chapter 3, except that here we use individual temperature station data instead of gridded values for the estimation of the long summer regional temperature averages⁶. The variation results in an important shift in regional temperature trends from a strong positive to a slightly negative tendency that likely reflects differences in the number of stations and homogeneity adjustments used in each case. The temperature series developed here is probably a more reliable depiction of regional variations in the study area because of the larger number of stations used to create this series and to develop reference series for testing the homogeneity of the individual records (see Chapter 2). However, this discrepancy has not had a significant influence on the resulting mass balance proxy series: the overall, strong negative trend and roughly the same inter-annual and inter-decadal features can still be

⁶ The individual station records were not available when Chapter 3 was written.

observed using this improved dataset (Fig. 6.2B). Similar features are also observed in an equivalent record developed using data from the Mascardi station (one of the very few stations located within the mountain range) and a regional streamflow record derived from seven rivers east of the mountains (see Fig. 6.3 and Chapter 3). The glacier record also seems to validate the usefulness of this series as an indicator of the most important changes in glacier mass balance conditions observed throughout the north Patagonian Andes during the 20th century. As discussed in Chapter 3, the widespread glacier recession observed in this region could be explained by the marked tendency towards more negative glacier mass balance conditions inferred from the proxy series. Although data are available for a very small number of sites, most glacier advances identified during the last century also show a relatively good agreement with the proxy record and the few short-lived periods of overall “positive” mass balance conditions evidenced in the MBPsea series generally precede the formation of moraines (Fig. 6.2).

The results from previous dendroclimatic studies in the NW Patagonian region indicate that some key tree species usually have a reasonable sensitivity to a combination of precipitation and temperature records (e.g. Villalba and Veblen 1997; Villalba et al. 1990, 1998) or to the strongly related river discharge records (e.g. Holmes et al. 1979; Lara et al. 2007). This suggests that many of the tree-ring chronologies available for this region could be used for developing a tree-ring based reconstruction of the climate-based mass balance proxy records discussed above. Preliminary comparisons between the mass balance proxy series and tree-ring records derived from selected *A. chilensis*, *F. cupressoides* and *A. araucana* chronologies (Appendix 6 and Table 6.2) generally confirmed this hypothesis. This is especially true for *A. chilensis* chronologies, which consistently showed the strongest correlations with the mass balance proxy record. These preliminary correlation analyses also showed that the strongest correlations were usually associated with an equivalent and very similar instrumental series created from annually averaged (April-March) temperature and precipitation data (the MBPann series, Fig. 6.2). This improvement in the correlations seem to indicate that, despite the minimal differences between the MBPsea and MBPann series at inter-annual and inter-decadal scales, the annual records are probably reflecting a more appropriate “window” to capture

the climatic signal in the tree-ring records. Thus, the MBPann series is the basis of the tree-ring based reconstructions presented here. The similarities between the proxy series suggest however that the interpretation of the results should also roughly apply to the season-based MBPsea record.

Five multiple regression equations were developed using point-by-point regression (PPR, Cook et al. 1999) and different combinations of the tree-ring chronologies as potential predictors of the mass balance proxy series. The PPR approach and the use of regionally-averaged tree-ring chronologies effectively concentrated the climatic signal in the tree-ring records reducing the number of final predictors in these models to a maximum of three (Table 6.3). The critical importance of the *A. chilensis* records as predictors of the mass balance proxy series was corroborated further at this stage as only models containing at least one chronology from this species reached statistical significance. The climatic signal contained in the much longer *F. cupressoides* records seems to provide useful additional information to the regression models but is not strong enough to successfully explain the variations in the mass balance series without the information provided by the *A. chilensis* chronologies.

Tests of the predictive skill of the regression equations using instrumental data specifically withheld from the calibration process greatly facilitated the selection of the best, longest and most updated reconstruction(s) of the glacier mass balance proxy series. The model that emerged from this process (Model 3, Table 6.2) explains over 50% of the variance in the instrumental record and is the basis for the mass balance proxy reconstruction between 1581 and 2000. A lower quality regression model (Model 4) that explains 35% of the variance extends the final reconstruction back to 1481. This combined record (Fig. 6.5A) is the first tree-ring based glacier mass balance proxy reconstruction for the Patagonian Andes. The proportion of variance explained by Model 3 is among the highest reported to date in dendroclimatic studies from this region. The relatively good agreement with an equivalent “mass balance proxy” series developed from early (1853-79) climate records from Valdivia, Chile provide truly independent evidence for the validity of the reconstructed series. Additional supporting evidence

comes from exceptional recent climatic events, such as the well documented extreme warm-dry conditions in the NW Patagonian region in 1998-99 observed by other researchers using completely different approaches (e.g. Suarez et al. 2004; Kitzberger and Suarez 2007) and effectively identified in both the instrumental and the reconstructed series developed in this study (see Fig. 6.5A).

A strong year-to-year variability and several well defined low frequency modes of variability characterize the mass balance proxy reconstruction (Fig. 6.5A and B). A cumulative series of this record provides an interesting, alternative way of assessing the relative magnitude and extent of these variations over a long term perspective and allows a better evaluation of this series in terms of the regional glacier record. In this sense, extended periods of “positive” or “less negative” values can be interpreted as periods during which climatic conditions were relatively more favorable for glaciers (probably resulting in glacier growth) and viceversa. A marked negative trend is the most noticeable feature of the cumulative series especially since about the late 1500s (Fig 6.5B) and coincides with the overall pattern of glacier recession during the past few centuries in the north Patagonian Andes. Interestingly, the reconstructed mass balance proxy series also shows several “peaks” of progressively lesser magnitude that roughly coincide with the general pattern of progressively smaller glacier advances observed in the region during the past few centuries (see e.g. Villalba et al. 1990; Chapter 5). In two cases the reconstructed positive mass balance conditions precede the main LIA advances identified at two local glaciers (Fig. 6.5C). The other “positive” periods also precede or overlap identified glacier advances but the correspondence is not consistent for both glaciers. This reflects some of the limitations associated with this comparative approach. Among other factors, the rather coarse nature of the glacier record, the inherent uncertainties associated with dating glacier deposits with tree-rings, and especially the extremely small number of glaciers studied to date should be considered in the interpretation of the results. The comparison is also hampered by the inherent uncertainties of the mass balance proxy series (and the resulting tree-ring based reconstruction models) which mainly result from the current lack of appropriate data for testing the glacier-climate relationships in this region.

Our results confirm the existence of a strong common hydro-climatic signal across NW Patagonia and seem to validate, using an improved climate dataset, the previously reported strong tendency towards increasingly negative mass balance conditions between 1912 and 2002 (Chapter 3). Strong linkages were also observed during the 20th century with regional tree-ring chronologies and to a lesser extent with localized glacier records from sites at the heart of the study area. These linkages provide an excellent opportunity for improving our understanding of past and present regional climate variability and change at different timescales using different environmental indicators that can be effectively cross-validated. The reconstruction presented here is a first attempt to evaluate the main past and present changes in the climate conditions likely affecting glaciers in this region during the past few centuries. Despite the rather simplistic approach used in the development of both the mass balance proxy record and the resulting multiple regression equations, our findings provide promising perspectives for improved reconstructions once more detailed glacier-climate linkages are established and a larger and more up to date network of glacier mass balance and tree-ring records become available.

6.6. References

- Akaike, H. 1974. A new look at the statistical model identification. *IEEE Transactions on Automatic Control*, AC-19, 716-723.
- Alexandersson, H. 1986. A homogeneity test applied to precipitation data. *Journal of Climatology* 6, 661-675.
- Aravena, J.C. 2007. Reconstructing climate variability using tree rings and glacier fluctuations in the southern Chilean Andes. Ph.D. Thesis, University of Western Ontario, 236 pp.
- Bown, F., 2004. Cambios climáticos en la Región de Los Lagos y respuestas recientes del Glaciar Casa Pangué (41°08'S). M.Sc. Thesis, Universidad de Chile, Santiago, 131 pp.
- Bown, F. and Rivera, A. 2007. Climate changes and recent glacier behaviour in the Chilean Lake District. *Global and Planetary Change* 59, 79-86.

- Brown, P.M. 1996. OLDLIST: A Database of Maximum Tree Ages. In: J.S. Dean, D.M. Meko, and T.W. Swetnam (eds). *Proceedings of the International Conference on Tree Rings, Environment, and Humanity: Relationships and Processes*, May 1994, Tucson, Arizona, 727-731.
- Cook E.R. 1985. A time series analysis approach to tree-ring standardization. Ph.D. Thesis, University of Arizona, Tucson, USA, 183 pp.
- Cook E.R. and Peters, K. 1981. The smoothing spline: a new approach to standardizing forest interior ring-width series for dendroclimatic studies. *Tree-Ring Bulletin* 41, 45-53.
- Cook E.R. and Holmes R.L. 1984. Program ARSTAN user manual. Laboratory of Tree-Ring Research, University of Arizona, Tucson Arizona USA.
- Cook, E.R. and Krusic, P.J. 2005. Program ARSTAN: A tree-ring standardization program based on detrending and autoregressive time series modeling, with interactive graphics. Tree-Ring Laboratory, Lamont-Doherty Earth Observatory, Columbia University, NY.
- Cook, E.R., Briffa, K.R., Shiyatov, S. and Mazepa, V. 1990. Tree Ring Standardization and Growth-Trend Estimation. In: Cook, E.R. and L.A. Kairiukstis (eds.) *Methods of Dendrochronology: Applications in the Environmental Sciences*, Kluwer Academic Publishers, Dordrecht, 104-123.
- Cook E.R., Briffa K.R. and Jones P.D. 1994. Spatial regression methods in dendroclimatology: A review and comparison of two techniques. *International Journal of Climatology* 14: 379-402.
- Cook, E.R., D. M. Meko, D. W. Stahle, and M. K. Cleaveland, 1996. Tree-ring reconstructions of past drought across the coterminous United States: Tests of a regression method and calibration/verification results. In: J.S. Dean, D.M. Meko, and T.W. Swetnam (eds). *Proceedings of the International Conference on Tree Rings, Environment, and Humanity: Relationships and Processes*, May 1994, Tucson, Arizona, 155-169.
- Cook, E.R., Meko, D.M., Stahle, D.W. and Cleaveland, M.K. 1999. Drought reconstructions for the continental United States. *Journal of Climate* 12, 1145-1162.
- Fritts H.C. 1976. *Tree rings and climate*. Academic Press, London, 567 pp.
- Grissino-Mayer, H.D. 2001. Evaluating crossdating accuracy: A manual and tutorial for the computer program COFECHA. *Tree-Ring Research* 57(2): 205-221.

- Guttman, L. 1954. Some necessary conditions for common-factor analysis. *Psychometrika*, 19, 149–161.
- Hansen, J., Ruedy, R., Glascoe, J. and Sato, M. 1999. GISS analysis of surface temperature change. *Journal of Geophysical Research* 104, 30997-31022.
- Hodge, S.M., Trabant, D.C., Krimmel, R.M., Heinrichs, T.A., March, R.S., Josberger, E.G, 1998. Climate variations and changes in mass of three glaciers in western North America. *Journal of Climate* 11, 2161-2179.
- Holmes R.L. 1983. Computer-assisted quality control in tree-ring dating and measurement. *Tree-Ring Bulletin* 44, 69-75.
- Holmes, R.L., Stockton, C.W., and LaMarche, V.C. 1979. Extension of river flow records in Argentina from long tree-ring chronologies. *Water Resources Bulletin* 15, 1081–1085.
- Hurvich, C.M. and Tsai, C. 1989. Regression and time series model selection in small samples. *Biometrika* 76, 297–307.
- Jones, P.D. and Moberg, A. 2003. Hemispheric and large-scale surface air temperature variations: an extensive revision and an update to 2001. *Journal of Climate* 16, 206-223.
- Kaiser, H.F. 1960. The application of electronic computers to factor analysis. *Educational and Psychological Measurement* 20, 141-151.
- Kitzberger, T. and Suarez, M.L. 2007. Rapid forest dieback and warm drought in Northern Patagonia, South America. Proceedings of the Joint Annual Meeting of the Ecological Society of America/ The Society of Ecological Restoration, August 2007, San José, California, OOS 42-7.
- LaMarche, Jr., V.C., Holmes, R.L., Dunwiddie, P.W., and Drew, L.G. 1979. Tree-ring chronologies of the Southern Hemisphere. *Chronology Series V. Vol. 1: Argentina*. Laboratory of Tree-Ring Research, University of Arizona, Tucson.
- Lara, A. and Villalba R. 1993. A 3620-year temperature record from *Fitzroya cupressoides* tree rings in Southern South America. *Science* 260: 1104-1106.
- Lara, A., R. Villalba, JC Aravena, A. Wolodarsky-Franke and E. Neira. 2000. Desarrollo de una red de cronologías de *Fitzroya cupressoides* (alerce) para Chile y Argentina. In: Roig (ed.) *Dendrocronología en América Latina*. EDIUNC, Mendoza, Argentina, 217-244.
- Lara, A., Aravena J.C., Villalba R., Wolodarsky-Franke A., Luckman B.H. and Wilson R. 2001. Dendroclimatology of high-elevation *Nothofagus pumilio* forests at their

- northern distribution limit in the Central Andes of Chile. *Canadian Journal of Forest Research* 31, 925-936.
- Lara, A., Villalba R. and Urrutia R. 2007. A 400-year tree-ring record of the Puelo River summer-fall streamflow in the Valdivian Rainforest eco-region, Chile. *Climatic Change*, doi:10.1007/s10584-007-9287-7.
- Lliboutry, L. 1998. Glaciers of Chile and Argentina. In: Williams, R.S., Ferrigno, J.G., (eds.), *Satellite Image Atlas of Glaciers of the World: South America*. USGS Professional Paper 1386-I, Online version 1.02.
- Masiokas, M.H., Villalba, R., Luckman, B.H., Lascano, M.E., Delgado, S. and Stepanek, P. 2008. 20th-century glacier recession and regional hydroclimatic changes in northwestern Patagonia. *Global and Planetary Change* 60, 85-100.
- McCabe, G.J., Fountain, A.G. and Dyurgerov, M.B. 2000. Variability in winter mass balance of Northern Hemisphere glaciers and relations with atmospheric circulation. *Arctic, Antarctic, and Alpine Research* 32(1): 64-72.
- Miller, A. 1976. The Climate of Chile. In: Schwerdtfeger, W. (ed.) *World Survey of Climatology 12, Climate of Central and South America*. Amsterdam, Elsevier, pp. 113-145.
- Nesje, A. 2005. Briksdalsbreen in western Norway: AD 1900–2004 frontal fluctuations as a combined effect of variations in winter precipitation and summer temperature. *Holocene* 15(8), 1245-1252.
- Oerlemans, J. and Fortuin, J.P.F. 1992. Sensitivity of glaciers and small ice caps to greenhouse warming. *Science* 258, 115-117.
- Osborn, T.J., Briffa, K.R. and Jones, P.D. 1997. Adjusting variance for sample-size in tree-ring chronologies and other regional-mean time-series. *Dendrochronologia* 15, 89-99.
- Ostrom, C.W., Jr. 1990. *Time Series Analysis: Regression Techniques (2nd Ed.)*. Quantitative Applications in the Social Sciences, Newbury Park, Sage Publications, 96 pp.
- Prohaska, F. 1976. The climate of Argentina, Paraguay and Uruguay. In: Schwerdtfeger, W. (ed.) *World Survey of Climatology 12, Climate of Central and South America*. Amsterdam, Elsevier, pp. 13-112.
- Rabassa, J., Rubulis, S. and Suarez, J. 1978. Los glaciares del Monte Tronador. *Anales de Parques Nacionales XIV*, 259-318.

- Rasmussen, L.A. and Conway, H. 2004. Climate and glacier variability in western North America. *Journal of Climate* 17, 1804-1815.
- Rignot, E., Rivera A. and Casassa, G. 2003. Contribution of the Patagonia icefields of South America to global sea level rise. *Science* 302, 434-437.
- Rivera, A. 2004. Mass balance investigations at Glaciar Chico, Southern Patagonia Icefield, Chile. Ph.D. thesis, University of Bristol, UK, 303 pp.
- Rivera, A., Casassa, G., Acuña, C. and Lange, H. 2000. Variaciones recientes de glaciares en Chile. *Revista de Investigaciones Geográficas* 34, 25-52.
- Rivera, A., Acuña, C., Casassa, G. and Bown, F. 2002. Use of remote sensing and field data to estimate the contribution of Chilean glaciers to the sea level rise. *Annals of Glaciology* 34, 367-372.
- Rivera, A., Bown, F., Casassa, G., Acuña, C. and Clavero, J. 2005. Glacier shrinkage and negative mass balance in the Chilean Lake District (40°S). *Hydrological Sciences Journal* 50(6), 963-974.
- Rosenblüth, B., Casassa, G. and Fuenzalida, H. 1995. Recent climatic changes in western Patagonia. *Bulletin of Glacier Research* 13, 127-132.
- Rosenblüth, B., Fuenzalida, H. and Aceituno, P. 1997. Recent temperature variations in southern South America. *International Journal of Climatology* 17, 67-85.
- Schulman E. 1956. *Dendroclimatic change in semiarid America*. University of Arizona Press, Tucson Arizona, USA.
- Suarez, M.L., Ghermandi, L., and Kitzberger, T. 2004. Factors predisposing episodic drought-induced tree mortality in *Nothofagus* – site, climatic sensitivity and growth trends. *Journal of Ecology* 92 (6), 954-966.
- Veblen, T.T., Lorenz, D.C., 1988. Recent vegetation changes along the forest/steppe ecotone in northern Patagonia. *Annals of the American Association of Geographers* 78(1), 93-111.
- Villalba, R. 1990. Latitude of the surface high-pressure belt over western South America during the last 500 years as inferred from tree-ring analysis. *Quaternary of South America and Antarctic Peninsula* 7, 273-303.
- Villalba R. 1994. Tree-ring and glacial evidence for the Medieval Warm Epoch and the Little Ice Age in southern South America. *Climatic Change* 26: 183-197.

- Villalba, R. and Veblen, T.T. 1997: Spatial and temporal variation in tree growth along the forest-steppe ecotone in northern Patagonia. *Canadian Journal of Forest Research* 27, 580–97.
- Villalba, R., Leiva, J.C., Rubulis, S., Suarez, J. and Lenzano, L.E. 1990. Climate, tree-ring, and glacial fluctuations in the Río Frías Valley, Río Negro, Argentina. *Arctic and Alpine Research* 22(3), 215-232.
- Villalba, R., Boninsegna, J.A., Lara, A., Veblen, T., Roig, F., Aravena, J.C. and Ripalta, A. 1996. Interdecadal climatic variations in millennial temperature reconstructions from Southern South America. In: Jones, P.D., Bradley, R.S. and Jouzer, J. (eds) *Climatic variations and forcing mechanisms of the last 2000 years*. NATO ASI Series 141. Springer-Verlag, pp. 161-189.
- Villalba, R., J.A. Boninsegna, T.T. Veblen, A. Schmelter, and S. Rubulis. 1997. Recent trends in tree-ring records from high elevation sites in the Andes of northern Patagonia. *Climatic Change*, 36: 425-454.
- Villalba R., Cook E.R., Jacoby G.C., D'Arrigo R.D., Veblen T.T. and Jones P.D. 1998. Tree-ring based reconstructions of northern Patagonia precipitation since AD 1600. *The Holocene* 8 (6): 659-674.
- Villalba, R., Lara, A., Boninsegna, J.A., Masiokas, M., Delgado, S., Aravena, J.C., Roig, F.A., Schmelter, A., Wolodarsky, A., and Ripalta, A. 2003. Large-scale temperature changes across the southern Andes: 20th-century variations in the context of the past 400 years. *Climatic Change* 59, 177-232.
- Vose, R.S., Schmoyer, R.L., Steurer, P.M., Peterson, T.C., Heim, R., Karl, T.R., Eischeid, J.K., 1992. *The Global Historical Climatology Network: Long-term monthly temperature, precipitation, sea level pressure, and station pressure data*, Tech. Rep. NDP-041, Carbon Dioxide Information Analysis Center, Oak Ridge National Laboratory, Oak Ridge, Tennessee, U.S.A.
- Weisberg, S. 1985. *Applied Linear Regression*, 2nd ed., John Wiley, New York, 324 pp.
- Wigley T.L., Briffa K.R. and Jones P.D. 1984. On the average value of correlated time series, with applications in Dendroclimatology and Hydrometeorology. *Journal of Climate and Applied Meteorology* 23: 201-213.
- Wolodarsky-Franke, A. 2002. Fluctuaciones ambientales de los últimos 1000 años a partir de anillos de crecimiento de *Fitzroya cupressoides* (Molina Johnston) en el área del Volcán Apagado, Décima Región, Chile. M.Sc. Thesis, Universidad Austral de Chile.

This final chapter summarizes the main results obtained in this thesis and discusses their relevance in terms of the original objectives described in Chapter 1. The most important original contributions of this thesis are outlined, and final conclusions and recommendations for future related research are presented.

Chapter 7: Summary and conclusions

7.1. Introduction

The primary objective of this research was to improve understanding of the main spatial and temporal patterns of climate and glacier variability across the Patagonian Andes over the past few centuries using instrumental climate data, tree rings and glacier records. This goal was achieved in a series of analyses presented as individual manuscripts in this thesis. Chapter 2 presented the first comprehensive analysis of homogenized, updated mean monthly temperature records across southern South America (SSA) and the neighboring Antarctic Peninsula region (AP). This combined data set represents the largest compilation for these regions, including data from numerous discontinued stations that have usually been neglected in previous studies. This denser network of station records was crucial to the development of relatively homogeneous temperature series, and provides a more regionally-representative perspective for the study of recent temperature variations at the selected glacier sites (see below) and a robust basis for differentiating their main modes of variability during the observational period. Chapter 3 and Appendix 1 presented detailed analyses of rainfall and snowfall records across NW Patagonia and the central Andes of Chile and Argentina. These analyses provide important complementary information to improve understanding of climate and streamflow variability in SSA.

Chapters 4 and 5 presented reconstructions of the history of recent glacier fluctuations in two areas of the north and south Patagonian Andes using dendrogeomorphic techniques. Each area contained several small glaciers of relatively easy access with different degrees of forest recolonization of the glacier deposits and a rich collection of supporting historical documentary materials. Such small glaciers were considered more responsive to climate variations than the large or calving glaciers usually studied heretofore elsewhere in Patagonia. In both areas several glacier advances were identified, some of which were previously undocumented. The resulting Little Ice Age (LIA) and post-LIA chronologies of glacier events are among the most detailed available for the Patagonian Andes. Although the major advances and the generalized pattern of late 20th century

glacier recession observed in these two areas generally agree with the regional pattern of fluctuations described in the literature, some important differences were observed that relate to large-scale climatic forcings and/or the specific characteristics of the glaciers studied. These differences indicate that the regional glacier history in the Patagonian Andes is probably more complex than commonly assumed and underscore the need for additional detailed studies at many more sites before a truly representative picture can be extracted from the limited glacier records currently available.

A central question in the analysis of past glacier records in this region is the relative importance of temperature and precipitation variability on glacier fluctuations in this region. In an attempt to address this issue, hydro-climatic data, historical documents and the moraine record of glaciers were used in Chapter 3 to develop an exploratory assessment of the impacts of recent climate changes on 20th-century glacier behavior in the north Patagonian Andes. This combined use of multiple sources of evidence is an original attempt to overcome the limitations associated with the lack of appropriate glacier mass balance data and high-elevation climate records needed for the proper evaluation of climate-glacier relationships. The resulting “glacier mass balance proxy” series showed a marked negative trend and provided strong evidence of the generalized glacier mass loss of the past century in this region. Independent streamflow records and climate data from the mountains validated the regional representativeness of this proxy series at inter-annual and inter-decadal timescales. A relatively good agreement between the low frequency variations in this series and 20th century glacier advances in the north Patagonian Andes corroborated these findings. These preliminary results suggested that such data could be used as a reasonably reliable regional estimate of the relative magnitude of the accumulation and ablation components of the mass balance of local glaciers between 1912 and 2002.

The simple glacier mass balance proxy series developed in Chapter 3 was subsequently revised in Chapter 6 to incorporate a better representation of temperature variations, and an extensive multi-species network of tree-ring width chronologies from NW Patagonia was used to reconstruct this series over the past 520 years. Although there have been

other attempts to develop glacier mass balance reconstructions from tree-rings records in the Northern Hemisphere (e.g. Watson and Luckman 2004), this was the first attempt for a Southern Hemisphere site and employed quite different techniques. The results have shown the great potential for dendroclimatological investigations of this region to provide baseline information that places the 20th century glacier and hydro-climatic variations in a longer term perspective. The annually resolved reconstructed record shows important variations at inter-annual and inter-decadal scales and is significantly more detailed than the few, presently available low resolution LIA glacier histories for this region.

Preliminary comparisons with the LIA moraine record revealed broad similarities but the linkages remain provisional until more detailed glacier records and improved mass balance proxy estimates become available.

In most cases the results reported in this thesis are original contributions to current knowledge about climate-glacier-tree growth inter-relationships and variability in southern South America. However, in carrying out this work we encountered some limitations related to the basic data and/or the methodologies used that were not anticipated during the planning stages of this thesis. Identification and discussion of these limitations in the appropriate chapters constitutes an important contribution of this thesis. Recognizing these limitations will lead to the better understanding and interpretation of the results of this and other related studies in the region and will hopefully facilitate and improve future research of glacier and climate variability in the Patagonian Andes.

The following sections summarize the main findings of this thesis in more detail.

7.2. 20th-century climate variations in southern South America

A key objective of this thesis was to develop and evaluate improved climate records that could be used to document recent climate variability in SSA and provide calibration data for subsequent proxy climate reconstructions. In this context, several new databases were developed and analyzed, including surface temperature data for SSA and the AP (Chapter 2), precipitation and streamflow records for NW Patagonia (Chapter 3), and snowpack and streamflow records for the central Andes (Appendix 1).

A series of relatively homogeneous records of mean annual temperatures that cover most of the 20th century were developed using an updated, greatly expanded surface station dataset for SSA and the AP between 36° and 70°S (Chapter 2). In SSA these records showed four distinct regional patterns centered in the NW, NE, central-northern and southernmost sectors. When averaged into regional series, the NE and southernmost sectors showed statistically significant positive linear trends of 0.059°C and 0.037°C per decade, respectively, over the 1912-2005 period. In contrast, mean annual temperatures from Northern Patagonia west of the Andes showed a significant cooling trend of -0.053°C per decade. Central-northern Patagonia showed a positive, non-significant linear trend of 0.016°C decade⁻¹. Several statistically significant shifts in mean conditions were identified in these records using a robust regime shift detection technique, with the significant increase in temperatures in 1977-78 in the NE, NW and southern sectors of SSA emerging as the most salient feature. The regional series were also analyzed using an innovative nonparametric approach that identifies the location, magnitude and statistical significance of the major intra- to multi-decadal (IMD) patterns in these records. This analysis showed that the three SSA subregions with positive linear trends have experienced, especially after 1977, extended warm periods that have reached highly significant levels with respect to an essentially stationary reference time series. In contrast, in NW Patagonia the warmest and coldest IMD conditions occurred during 1912-32 and 1964-76, respectively.

The results in Chapter 2 indicated that most of the instrumental temperature variability observed in SSA can be explained by few, well defined and relatively time-stable regional dominant modes with distinct low frequency patterns. In general, these regional patterns agreed with previously reported analyses from this region (e.g. Villalba et al. 2003), but the use of a denser network and updated, homogenized records allowed a more detailed spatial characterization and a improved assessment of the magnitude of change over the last few decades in the context of the 20th century.

The combined analysis of SSA and AP data indicated that the temperature variability observed in the southern sector of South America is not strongly related to that observed over the AP. It is, therefore, proposed that the significant 20th-century warming trends observed in these two regions are probably related to different forcing mechanisms. The comparison of these regional series against large-scale atmospheric variables and indices (see e.g. Appendix 1) can provide important insights into this issue. Future analyses will be carried out that should improve our understanding of the inter-relationships between these series and evaluate their potential influence on the temperature variations observed in SSA and the AP.

The more complete network of hydro-climatic stations in the NW Patagonian region allowed a comprehensive analysis of 20th-century climate variability and change in this region. Linear trends in regionally-averaged annual and cool season precipitation records indicate a significant decrease in precipitation totals over the 1912-2002 interval (Chapter 3). Although this strong tendency towards drier conditions has been reported in previous studies (e.g. Aravena 2007; Bown and Rivera 2007), in most cases the data used only covered the second half of the 20th century. Thus, the regionally-averaged record developed in this thesis provides a more appropriate framework to evaluate these changes over the observational period. Interestingly, the analysis of temperature data for this region showed contrasting results depending on the dataset used. In Chapter 3, mean annual and warm season temperatures calculated from gridded data (Jones and Moberg 2003) showed positive and highly significant trends over the 20th century, whereas subsequent analyses (Chapter 6) based on improved data developed in Chapter 2 showed a cooling tendency for this area that is more in agreement with the results from previous studies (Rosenblüth et al. 1997; Villalba et al. 2003).

Snowfall is a critical factor in glacier mass balance and streamflow variability in this region. Appendix 1 developed the first regional trans-Andean snowpack and streamflow records for SSA between ca. 32° and 37°S and identified a remarkably strong common signal in these variables. These records showed a slightly positive linear trend over the second half of the 20th century but an overall negative trend over the last 100 years.

Analyses of inter-relationships with large-scale atmospheric features showed a strong association with conditions in the tropical Pacific but also striking linkages with atmospheric conditions in the Amundsen-Bellinghaussen Seas to the west of the AP. These results provide important new information for water management programs at a local scale but also an interesting, larger scale perspective for the analysis of the hydro-climate changes observed further south in the Patagonian region.

7.3. Glacier fluctuations in the Patagonian Andes during the past five centuries

7.3.1. Southern study area: Monte Fitz Roy and Lago del Desierto

Dendrogeomorphic techniques were used to reconstruct the Little Ice Age (LIA) and post-LIA activity for five small glaciers near the northeast margin of the South Patagonian Icefield. The study sites include Glaciar Torre and Piedras Blancas in the Monte Fitz Roy area, and three adjacent glaciers near Lago del Desierto. At these sites the LIA maximum position was identified by massive moraines with mature trees dating to the late 1500s-early 1600s growing on their surfaces. Several older moraines occur beyond these limits but could not be precisely dated. Relatively synchronous advances occurred at most glaciers in the early 1700s and were dated using living trees and *in situ*, subfossil material. All glaciers showed three to five subsequent advances mostly during the mid 19th and early 20th centuries. Despite some site-specific discrepancies, this preliminary pattern of fluctuations (advances in the early 17th and 18th centuries, 19th century and early 20th century) agrees reasonably well with the LIA glacier history derived from other sites across the Patagonian Andes (see e.g. Masiokas et al. 2006 and Aravena 2007 for updated compilations of the moraine record available). These results provide important new information on the glacier history of this area but additional, more precisely-dated records are needed from many more sites before we can fully elucidate the complex late Holocene glacial history of this region.

Estimates based on Landsat TM imagery indicated that the glaciers studied in the Fitz Roy-Lago del Desierto areas lost between 15 and 46% of their LIA areas by 1984 and a further 5-18% by 2005. The smallest glaciers showed the greatest proportional loss. Paired comparisons of the earliest known and contemporary photographs for the glaciers

in the Fitz Roy area confirmed this mass loss. Despite the lack of long, good quality climate records in the vicinity of these study sites, the large-scale pattern of warming identified between 1912 and 2005 for the south Patagonian region (Chapter 2) provides support for a primary role of temperature in this regional phenomenon.

7.3.2. Northern study area: Monte Tronador

A revised late Neoglacial chronology of fluctuations for Glaciar Río Manso and Glaciar Frías in the Monte Tronador area (41°10'S, 71°52'W), north Patagonian Andes, Argentina was developed based on extensive sampling of living and subfossil tree-ring material recently collected at these sites and the information available from previous studies. Although focused on LIA and post-LIA glacier fluctuations at these sites, available evidence for pre-LIA glacier activity provided important additional information, placing the more recent glacier events into a longer term, late Holocene perspective. These results constitute the most detailed chronology of LIA glacier fluctuations for the north Patagonian Andes.

At Glaciar Río Manso, a massive, frontal moraine apparently predating 2240 ¹⁴C yrs BP was partially overridden during the LIA. Evidence from *in situ* subfossil stumps and a tilted tree indicate that the most extensive LIA expansion took place between the late 1700s and the 1830-40s. This confirms the results from an early, preliminary study at this site (Lawrence and Lawrence 1959) and constitutes the first case in the north Patagonian Andes where the tree-ring patterns of *in situ* snags were successfully crossdated with those from living trees to provide a maximum age for a glacier advance. Minimum dates from several living trees growing on the deposits from this advance provide closely bracketed dating control for this event. The almost complete lack of evidence of glacial landforms outside this limit indicates that, with the exception of a few marginal sites, the main LIA advance was the most extensive event of the past millennium. Earlier advances were probably confined by and within the older massive frontal moraine system (tentatively dated to 2240 ¹⁴C yrs BP), and evidence of intervening events was overridden by the glacier advance that culminated ca. 1840. Subsequent glacier activity at Glaciar Río Manso was inferred from moraine ridges on the southern slope of the valley.

Minimum ages from trees growing on these deposits suggest the moraines were formed ca. 1875, 1890, 1899, 1919, 1949, 1955 and during the mid 1970s. Despite these minor readvances, historical documents and photographs indicate that the lower tongue of the glacier has thinned but remained in approximately the same position between 1937 and 1991. After 1991 there has been drastic thinning and recession with the formation of a rapidly growing proglacial lake. A minor readvance was tentatively dated to the late 1990s from available aerial and ground photographs.

A hitherto undescribed phenomenon at Glaciar Río Manso is the strong contrast in the density of the bamboo (*Chusquea culeou*) understory across the LIA maximum limit. This “bamboo line” has subsequently been observed at other glaciers in the north Patagonian Andes and is probably related to the particular reproductive strategy of this species. It can therefore be used as a quick, apparently reliable, tool for mapping the maximum extent of this 150-yr old advance. When used in combination with the tree-ring dating of recently glaciated vs. non-glaciated surfaces, this feature could facilitate the identification and mapping of glacier advances at other glaciers in the region.

The revised late Holocene chronology of events for Glaciar Frías was based on a detailed previous study (Villalba et al. 1990) plus new evidence from living trees and recently exposed subfossil trees that were overridden during two separate glacier advances. The earliest known advance at this site occurred between 411 and 450 AD based on the tree-ring dating of overridden trees. These results were confirmed by a radiocarbon date of 1720 ± 40 ^{14}C yrs BP (calibrated calendar date range 260-460 AD) from one of the crossdated stumps and provide a precise, calendar-dated maximum age estimate for a previously undocumented glacier advance during the 5th century in the north Patagonian Andes. The most important LIA advance at Frías occurred in the early to mid 17th century based on evidence from an ice-scarred tree and several living trees growing on the moraine surface. A new, direct estimate of ecesis for this site was used to revise the tree-ring dating of most of the moraine ridges identified within the LIA limits. Glacier readvances occurred in the early 18th and 19th centuries, in the late 19th century and ca. 1904, 1914 and 1944. The latest event at this site occurred in 1976-77 and was

documented by field observation and tree-ring data (Rabassa et al. 1978; Villalba et al. 1990). Despite these 20th-century readvances, Glaciar Frías has experienced a dramatic net frontal recession over the last 100 years.

The successful tree-ring dating of several subfossil stumps that had also been dated through radiocarbon determinations allowed a direct comparison between these two dating techniques. For those samples associated with LIA advances at both sites, there was generally poor agreement between the absolute, tree-ring based calendar dates and their corresponding radiocarbon dates. This disparity is most likely related to the non-linearity of the ¹⁴C calibration curve during this time frame (Porter 1981) and highlights some of the difficulties associated with radiocarbon dating of glacier events during the past few centuries. In contrast, a much better agreement was found between the ¹⁴C and tree-ring dating of the older *Fitzroya cupressoides* sample (1720±40 ¹⁴C yrs BP) obtained at Glaciar Frías. This finding not only illustrates an interesting cross-validation of results but also highlights an additional, undocumented application of *F. cupressoides* (alerce) in the study of past glacier fluctuations in the north Patagonian Andes. The extremely low decay rate of buried stumps of this species and the possibility of crossdating their tree-ring patterns with existing millennia-long tree-ring chronologies make subfossil alerces found in association with glacier deposits one of the best tools for dating glacier advances that occurred within the past few millennia in this region.

The drastic, widespread glacier recession observed at the study sites and by repeat photography of early glacier views indicated that, over the past several decades, the overall conditions in this region have clearly favored glacier ice ablation over accumulation at high elevation sites across the mountains. The regional nature of this phenomenon suggests the existence of a large-scale common climatic forcing mechanism operating relatively synchronously across this region. However, the pre- 20th century chronologies from Glaciar Frías and Glaciar Río Manso differ: Río Manso reaches its maximum in the 1830-40s whereas Glaciar Frías has several older moraines outside the mid 19th century position. The proximity of these glaciers and their relatively similar sizes and common accumulation zones would suggest a similar mass balance history but

differences in their topographic profiles, debris cover and presence of local topographic barriers downvalley seems to have resulted in differences in the sequence of moraines that are preserved. At Río Manso the massive, older ridge in front of the glacier probably confined most pre- or early LIA advances and any evidence of earlier advances was overtopped by the mid-19th century event. In contrast, at Glaciar Frías the unconfined older advances extended much further down the flat valley floor and were not subsequently overridden. Minor differences in the dates assigned to the glacier deposits may also relate to the inherent uncertainties of dendroglaciological determination of moraine ages. Overall, these results highlight the need for a significantly larger and more robust sample of glacier records to be developed that allow a truly regional chronology of glacier events to be defined by replication at many sites, minimizing the importance of localized differences in glacier response to climate.

7.4. North Patagonian glacier mass balance proxy estimates

In Chapter 3 a regional climatic index or “glacier mass balance proxy” series for the 1912-2002 period was developed based on winter precipitation and summer temperature records from the NW Patagonian region. This series was intended to mimic glacier mass balance relationships and showed a marked negative trend which agrees with the drastic glacier recession across this region shown by repeat photography of some of the earliest photographs of glaciers in southern South America. Short periods of positive climate indices broadly corresponded with known evidence of glacier advances in the region. Regionally-averaged mean annual streamflow records east of the mountains provided an independent verification check of the climatic series and showed a similarly strong negative trend and a remarkable agreement at inter-annual and inter-decadal timescales. This highlighted the existence of a strong, regionally coherent hydroclimatic signal in northwestern Patagonia between ca. 38° and 44°S.

Chapter 6 improved the instrumental mass balance proxy record developed in Chapter 3 and presented an original tree-ring based reconstruction of a climate-based proxy series over the past 520 years. This reconstruction, which is derived from an extensive collection of climate-sensitive tree-ring width chronologies, was compared with the

history of glacier advances identified in Chapter 5 and partially cross validates these independent records. Taking into consideration the inherent limitations of the glacier record discussed above, the results indicated the potential utility of this mass balance proxy reconstruction as an indicator of the most important changes in glacier mass balance conditions observed throughout the north Patagonian Andes. When viewed as a cumulative series, this reconstruction showed a marked negative trend since the late 1500s that coincides with the overall pattern of glacier recession in this region. Embedded in this long term trend there are several intervals of overall “positive” or “less negative” conditions (implying overall “positive” glacier mass balances across the region) that become progressively less marked towards the present in a similar pattern to the progressively smaller glacier advances observed in the north Patagonian Andes during the past few centuries (see e.g. Villalba et al. 1990; Chapter 5). The main LIA advances identified at Glaciar Frías in the early 1600s and at Glaciar Río Manso in the early 1800s occur shortly after two of these extended “peaks”. Some discrepancies were found between the other “positive” periods and subsequent glacier advances, which may reflect uncertainties associated with the dating control for these events. These include the rather coarse nature of the glacier record, the inherent uncertainties associated with dating glacier deposits with tree-rings, and especially the extremely small number of glaciers studies available. The comparison is also hampered by the lack of adequate mass balance data for glaciers in this region against which to calibrate the mass balance proxy series (and the resulting tree-ring based reconstruction models). Nevertheless, the results indicate that the regional signal observable in instrumental hydro-climatic data can also be identified in well-replicated tree-ring chronologies that in most cases extend for several centuries. This presents an excellent opportunity for using this diverse group of environmental indicators in the study of past and present glacier and climate variability and change in this region.

7.5. Recommendations for future related research and final conclusions

This thesis has discussed several inter-related approaches for studying past and present climate and glacier variations in southern South America using a wide variety of instrumental and proxy climate data. Several limitations in these data and methodology

have been identified and partially addressed but they also provide possibly significant avenues for future research in this region.

The exhaustive approach adopted in the development of relatively homogeneous individual temperature series (see Chapter 2) sought to maximize the information available while minimizing the manipulation of the original records. However, as additional station records and metadata become available, further testing will be required to validate these results and adjust, where necessary, any remaining inhomogeneities in these series. Further work with these new homogenized series could therefore incorporate other climate data and attempt more sophisticated analyses e.g. by looking at seasonal and monthly data, analyzing site-specific homogeneity issues, or examining inter-relationships of specific areas/stations with large-scale atmospheric variables and indices. These data will also be invaluable for calibrating tree-ring series against climate records to develop dendroclimatic reconstructions or for more detailed analysis of climate-glacier links across the Patagonian Andes.

As discussed in Chapters 3 and 6, the assessment of impacts of the relative significance of temperature and precipitation changes on glaciers in the Patagonian Andes will remain provisional until appropriate measurements of glacier mass balances and high elevation climate data become available. This information could be complemented with systematic measurements of recent changes in glacier length and area from additional sites such as those used in this thesis. In this sense, a regional survey and inventory of glaciers accompanied by a regular monitoring of changes (see e.g. Rivera et al. 2002) will ultimately provide the best framework for a consistent analysis of regional glacier variations and their relationship with observed changes in climate conditions.

The glaciers selected for study are excellent examples of the importance of site-specific factors on the resulting glacial chronologies, highlighting the need for a much larger group of carefully selected study sites as a prerequisite for the development of a regionally representative glacier chronology for the past few centuries. Ongoing investigations at other small glaciers across the Patagonian Andes (see Masiokas et al.

2006) will hopefully provide the necessary evidence to develop robust, reliable regional glacial chronologies for this region and will probably facilitate the identification and isolation of variations related to site-specific factors in these records. In this sense, the most frequent uncertainty found in association with dendroglaciological determinations at the southern study site was the assessment of the age of older surfaces whose age is close to or exceeds the maximum ages of the trees growing on their surface. In such situations future researchers need to attempt to locate additional evidence from subsurface material e.g. subfossil stumps, soils or peat deposits that could ultimately provide bracketing information to complement the minimum age determinations obtained from the oldest trees sampled on the moraines. The results also indicate that the accuracy of the minimum ages for the moraine formation could also be improved using more detailed and site-specific sampling height and ecessis correction factors.

Although the network of meteorological and dendrochronological records is relatively less dense in southern Patagonia, the recent development of a quality controlled database of precipitation records and several new tree-ring chronologies with a discernible sensitivity to precipitation variability for this area (Aravena 2007) represent an excellent complement to the results from this thesis and provide an unprecedented opportunity for improved analyses of glacier-climate-tree growth inter-relationships in this region.

Southern South America has the greatest potential for the development of high resolution records of past climate variability in the Southern Hemisphere for the last millennium. Evaluation of these records is critical to the examination and modeling of hemispheric patterns affecting the global climate system. Therefore, the particular location of the Patagonian Andes extending through mid to high latitudes in the Southern Hemisphere makes the study of past and present climate fluctuations in this region of crucial importance at local, regional and global scales. This thesis presented some novel approaches and demonstrated the potential of the forests and glaciers along this mountain range to provide records from complementary environmental indicators at high and low temporal resolution. The results presented herein are a significant contribution to ongoing

large-scale multi-proxy research projects in this fascinating region (see Grosjean and Villalba 2006) and can provide a springboard for future research endeavors.

7.6. References

- Aravena, J.C. 2007. Reconstructing climate variability using tree rings and glacier fluctuations in the southern Chilean Andes. Ph.D. Thesis, Department of Geography, University of Western Ontario, 236 pp.
- Bown, F. and Rivera, A. 2007. Climate changes and recent glacier behaviour in the Chilean Lake District. *Global and Planetary Change* 59, 79-86.
- Grosjean, M. and Villalba, R. 2006. Regional climate variations in South America over the late Holocene. *PAGES News, Workshop reports* 14, 26.
- Jones, P.D. and Moberg, A. 2003. Hemispheric and large-scale surface air temperature variations: an extensive revision and an update to 2001. *Journal of Climate* 16, 206-223.
- Lawrence, D.B. and Lawrence, E.G. 1959. Recent glacier variations in southern South America. American Geographical Society Southern Chile Expedition Technical Report, Office of Naval Research Contract 641(04), New York, USA, 39 pp.
- Masiokas, M.H., Villalba, R., Luckman, B.H., Delgado, S. and Ripalta, A. 2006. Recent dendroglaciological investigations in the Patagonian Andes of Argentina. Abstracts, International Symposium: Reconstructing Past Regional Climate Variations in South America over the late Holocene: A new PAGES Initiative. Malargue, Mendoza, Argentina, 4-7 October 2006, p. 30.
- Porter, S.C. 1981. Glaciological evidence of Holocene climatic change. In: Wigley, T.M.L., Ingram, M.J., Farmer, G., (eds.), *Climate and History*. Cambridge University Press, pp. 83-110
- Rabassa, J., Rubulis, S. and Suarez, J. 1978. Los glaciares del Monte Tronador. *Anales de Parques Nacionales XIV*, 259-318.
- Rivera, A., Acuña, C., Casassa, G. and Bown, F. 2002. Use of remote sensing and field data to estimate the contribution of Chilean glaciers to the sea level rise. *Annals of Glaciology* 34, 367-372.
- Rosenblüth, B., Fuenzalida, H. and Aceituno, P. 1997. Recent temperature variations in southern South America. *International Journal of Climatology* 17, 67-85.

- Villalba, R., Leiva, J.C., Rubulis, S., Suarez, J. and Lenzano, L.E. 1990. Climate, tree-ring, and glacial fluctuations in the Río Frías Valley, Río Negro, Argentina. *Arctic and Alpine Research* 22(3), 215-232.
- Villalba, R., Lara, A., Boninsegna, J.A., Masiokas, M., Delgado, S., Aravena, J.C., Roig, F., Schmelter, A., Wolodarsky, A. and Ripalta, A. 2003. Large-scale temperature changes across the Southern Andes: 20th-century variations in the context of the past 400 years. *Climatic Change* 59, 177-232.
- Watson, E. and Luckman, B.H. 2004. Tree-ring estimates of mass balance at Peyto Glacier for the last three centuries. *Quaternary Research* 62, 9-18.

The following pages include the Appendices discussed in this thesis. Appendix 1 was published in December 2006 in the Journal of Climate (Volume 19, pages 6334-6352) with the following list of co-authors:

Mariano H. Masiokas^{1,2}, Ricardo Villalba¹, Brian H. Luckman², Carlos Le Quesne³, and Juan Carlos Aravena^{2,4}

¹ Instituto Argentino de Nivología, Glaciología y Ciencias Ambientales (IANIGLA-CRICYT-CONICET), Mendoza, Argentina.

² Department of Geography, University of Western Ontario, London, Ontario, Canada.

³ Instituto de Silvicultura, Universidad Austral de Chile, Valdivia, Chile.

⁴ Centro de Estudios Cuaternarios (CEQUA), Punta Arenas, Chile.

Appendix 1: Snowpack variations in the central Andes of Argentina and Chile, 1951-2005: Large-scale atmospheric influences and implications for water resources in the region

A1.1. Introduction

The snowpack accumulated in the central Andes¹ is the main water source of the major rivers in central Chile and central western Argentina and therefore represents a critical resource for local domestic consumption, irrigation, industries and hydroelectric generation. Since the main road connecting Santiago de Chile with Mendoza and Buenos Aires in Argentina crosses the Cordillera at these latitudes, snow accumulation also has significant economic impacts on surface transportation, trade and winter tourism along this portion of the Andes. Thus, the analysis of recent snowpack variations and their relationships with large-scale atmospheric features is of fundamental socio-economic importance in developing water management strategies and seasonal snowpack and snowmelt forecasts for the region.

Careful investigation of recent snowpack variability in the central Andes is also of particular interest in view of the potential climate changes predicted for this area. In an analysis of seven coupled atmosphere-ocean general circulation models especially targeted to investigate high elevation sites, Bradley et al. (2004) showed that for the next 80 years the central Andes will probably experience significant temperature increases of $\geq 2^{\circ}\text{C}$. Independent general circulation model simulations also predict a significant decrease in precipitation over the region for the next five decades (Cubasch et al. 2001), with likely impacts on the hydrological cycle and long-term water resource availability. Basic knowledge about the causes and amount of recent snowpack variability and change in this mountainous area is probably one of the most important factors to consider in planning mitigation of possible future effects of climate change on the socio-economic activities in this region.

¹ Considered here as the portion of the Andes between 30° and 37°S

Prior studies of observed snowpack records in the central Andes have mainly been restricted to the government agencies dealing with water resources in Chile and Argentina, and few results have been published in the scientific literature. Snowmelt-runoff simulation models for isolated basins on both sides of the Andes have been developed from some of these data by Peña and Nazarala (1987) and Maza et al. (1995). Escobar and Aceituno (1998) utilized data from 17 snow courses in central Chile to evaluate the influence of May-August sea surface temperatures (SST) from the tropical Pacific (Niño 3 Region) on winter snow accumulation. They found a higher probability for increased (decreased) winter snowpack between 30° and 35°S during positive (negative) Niño 3 SST anomalies. Prieto et al. (2000, 2001) used a hundred year record (1885-1996) from a local newspaper reporting the annual number of snow days and maximum snow depth for the high elevation highway between Santiago and Mendoza to analyze the frequency domain and the influence of El Niño-Southern Oscillation (ENSO) on these records. They found significant periodicities centered around 28 and five years, together with a positive trend over the 20th century in the number of snow days per year. Prieto and coworkers also report a strong association between above-average winter snow accumulation and El Niño events. To our knowledge, no combined temporal and spatial assessment of snow course data integrated across the central Andes has been undertaken.

The main purposes of the present paper are: a) to develop a regional snowpack record for the central Andes utilizing updated snow water equivalent (SWE) data from both Chile and Argentina, b) to assess the spatial and temporal influence of large-scale atmospheric variables on snow accumulation in this region, c) to investigate the possibility of predicting snowpack in the central Andes using climatic indices, and d) to quantify the relationship between recent snowpack variations and water availability in the adjacent lowlands.

A1.2. Study area

The central Andes separate the two key agricultural and industrial regions of central Chile and central western Argentina (Fig. A1.1). The Metropolitan Region of Santiago and Regions V and VI contain about 55% of the Chilean population (ca. 8.4 million

people, INE 2003) with a rapidly growing demand for water for urban, agricultural and industrial uses (Brown and Saldivia 2000; Rosegrant et al. 2000; Ribbe and Gaese 2002; Cai et al. 2003). The average annual (1961-1990) rainfall for Santiago is ca. 290 mm and most water needs are met from river runoff from melting mountain snowpack. In the mid 1990s about 48% of the annual discharge of the Maipo River (the main water source for Santiago) was withdrawn to meet these needs (Cai et al. 2003). Central Chile also accounts for about 45% of the total irrigated area of the country (Brown and Saldivia 2000). On the drier Argentinean side of the central Andes the rivers originating in the mountains serve a population of ca. 2.2 million people in the provinces of San Juan and Mendoza (INDEC 2001). With less than 200 mm of precipitation per year the vast majority of the agriculture must rely on irrigation (Díaz Araujo and Bertranou 2004). Snowmelt runoff is also the main source of water for hydroelectric power generation in the region. Between 1986 and 2003, hydropower plants fed by rivers coming from the Cordillera generated, on average 62% and 86% of the total domestic energy generation in the provinces of Mendoza and San Juan, respectively (Secretaría de Energía 2004 and earlier reports available through <http://energia.mecon.gov.ar>).

The mean elevation of the central Andes is around 3500 m, with several peaks reaching over 6000 m. The weakening and northward displacement of the subtropical Pacific anticyclone during the austral winter enhances the westerly flow across central Chile, producing a marked cold season peak of precipitation in central Chile and over the mountains (Miller 1976; Aceituno 1988, Lliboutry 1998). The high elevation and north-south orientation of the Cordillera are an effective topographic barrier for Pacific air masses and little Pacific moisture reaches the easternmost slopes of the Cordillera. In fact, cold season (March-September) precipitation on the easternmost slopes and adjacent lowlands in Argentina are not correlated with precipitation in Santiago during the same period (Compagnucci and Vargas 1998). The region east of the central Andes experiences a continental regime with a marked warm season precipitation peak associated with moist air masses from the northeast as well as non-frontal convective processes (Prohaska 1976). Unfortunately, the lack of high elevation climate stations in

the mountains prevents a more detailed analysis of the spatial and temporal patterns of climate over the central Andes (Lliboutry 1998).

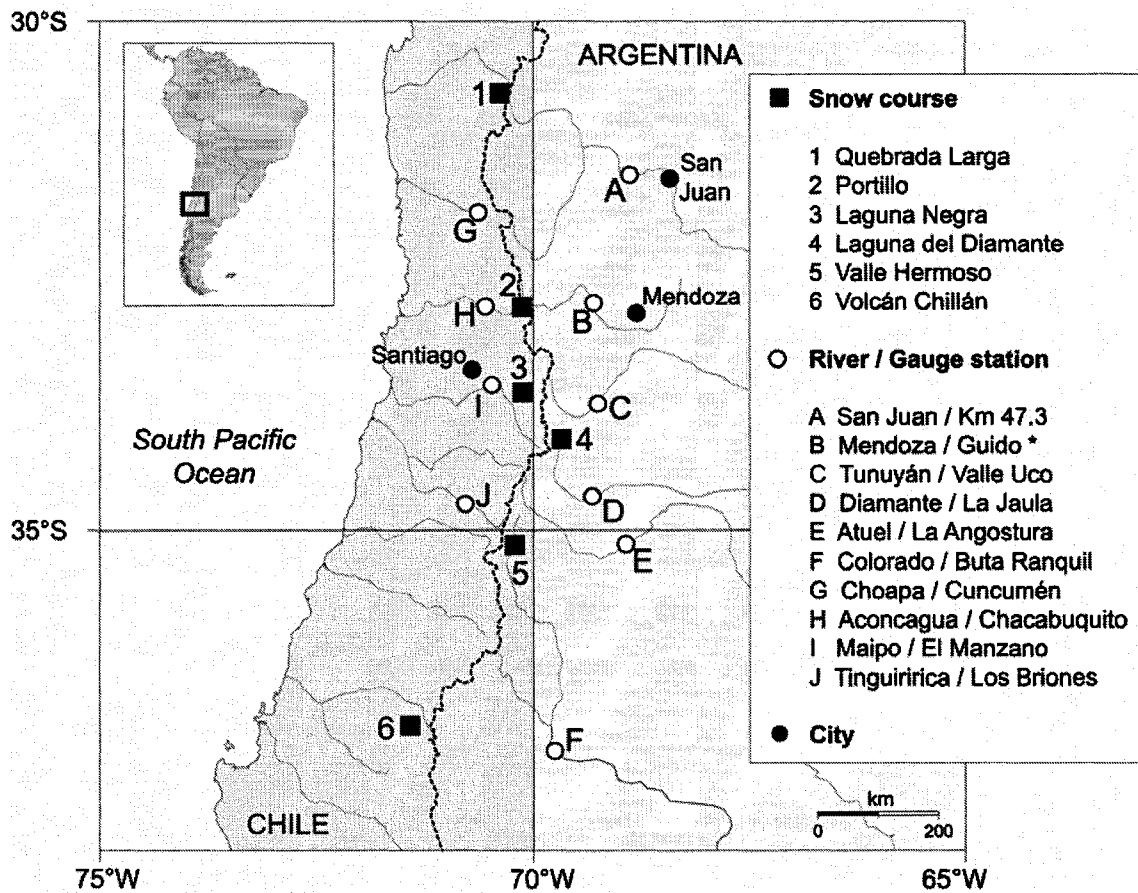


Fig. A1.1. Map of central Chile and central western Argentina, showing the location of snow courses and gauge stations used in this study. The international boundary between Chile and Argentina runs along the drainage divide in the Cordillera. Note: (*) The Guido gauging station also provided precipitation records for this study (see text for details).

Numerous studies have analyzed rainfall variations in the lowlands of central Chile and the significant influence of tropical Pacific atmospheric features associated with ENSO has been known for decades (Pittock 1980; Quinn and Neal 1983; Aceituno 1988; Rutland and Fuenzalida 1991; Montecinos et al. 2000; Montecinos and Aceituno 2003; Quintana 2004). Above-average winter rainfall anomalies generally coincide with El Niño events and below-average winter rainfall anomalies are more likely to occur during

La Niña years. Rutlland and Fuenzalida (1991) and Montecinos and Aceituno (2003) further describe a strong relationship between above-average winter rainfall conditions in central Chile and enhanced blocking activity over the Amundsen-Bellinghshausen Seas (Am-Be) in the southeast (SE) Pacific, a known ENSO-related atmospheric teleconnection occurring during El Niño events (Karoly 1989, Renwick 1998; Kiladis and Mo 1998).

During the 20th century, annual and winter rainfall variations in central Chile between 30° and 33°S show strong interdecadal variability with an overall negative trend (Quintana 2004). However, within this period of general negative trend, increased rainfall anomalies occurred between ca. 1900-1940 and 1970-2000, whereas negative anomalies were more frequent between 1940 and 1970. In general, studies of streamflow variations also show that ENSO-related features in the tropical Pacific play a predominant role in regulating the hydrological variability in the region, with increased (decreased) summer and annual river discharges following El Niño (La Niña) events (Waylen and Caviedes 1990; Caviedes 1998; Compagnucci and Vargas 1998; Norte et al. 1998; Waylen et al. 2000). Temperature variations in the lowlands of central Chile and central western Argentina show different trends over the 1960-1992 interval (Rosenblüth et al. 1997). Mean annual, summer and winter temperatures show significant positive trends ($>0.3^{\circ}\text{C decade}^{-1}$) west of the Cordillera centered at around 33°S. However, lowland stations east of the Andes show cooling (though non-significant) trends for the mean annual and seasonal temperatures (Rosenblüth et al. 1997).

Studies of recent glacier fluctuations in central Chile (Casassa 1995; Rivera et al. 2000, 2002) indicate a general reduction in glacier mass. Detailed analysis of seven glaciers between 32° and 35°S indicate they lost ca. 16% of their area in the second half of the 20th century and ice thicknesses measured at four glaciers indicated an average thinning of -0.775 m a^{-1} (Rivera et al. 2002). Generalized recession has also been reported from the small number of Argentinean glaciers that have been studied (Leiva 1999). These changes have been mainly linked to the observed rise in elevation of the 0°C isotherm and the equilibrium line altitude of glaciers in central Chile during the last quarter of the

20th century (Casassa et al. 2003; Carrasco et al. 2005). Localized studies (Peña and Nazarala 1987; Milana 1998) indicate that glacier meltwater has been particularly critical to maintain minimum water flows during extreme dry years. However, the potential hydrological impacts of the observed ice mass loss in this region have not been studied in detail.

A1.3. Data and Methods

Since streamflow variability in this region is dominated by snowmelt runoff, snow data have been monitored to forecast spring and summer water supply for over five decades by Dirección General de Aguas (DGA) in Chile, and Subsecretaría de Recursos Hídricos (SSRH), in Argentina. Between 28°S and 37°S, there are fewer than 30 available snow course records in Chile and Argentina and they cover a large altitudinal range from 1380 to 3600 m. Generally, these data consist of measurements of snow depth, density, and snow water equivalent (SWE) averaged over several samples per snow course. The longest snowpack records are from Portillo, Chile (1951-2004) and Valle Hermoso, Mendoza (1952-2005). However, the snow data available vary in quality and length, and the majority of snow courses have missing data for one or several years. During the cold season (early April to late November) most key stations have been monitored on a monthly to bimonthly basis (and since 2000, daily snow pillow measurements are also available for a few Argentinean stations), but numerous circumstances (budget limitations, difficulty of access to the sites, etc) have produced considerable variability in the frequency and timing of the snow measurements across the network. The analysis of records with four or more measurements per winter indicates that the timing of peak SWE values is variable, with 31.0% occurring in August, 43.4% in September, and 14.2% in October. Thus the use of a standard measuring date² to estimate the true SWE peak during the cold season could result in substantial error.

To overcome these limitations, the maximum value of SWE (MSWE) for each year was used as a surrogate of total snow accumulation at each site. This was deemed to be the

² equivalent to the April 1 date extensively used in the western United States as a surrogate for winter snow accumulation; e.g. Cayan 1996; Bohr and Aguado 2001; McCabe and Dettinger 2002; Mote et al. 2005.

best option available, but we acknowledge the likely existence of minor differences (probably not larger than 10%) between the true SWE winter peak and the MSWE values used in this study. The MSWE values for the six longest (>30 yr) and most complete (<10% missing years) snow course records were retained to develop a regional snowpack time series for the central Andes (Table A1.1). Following Jones and Hulme (1996), annual MSWE values for each snow course were converted to percentages of their 1966-2004 mean and subsequently averaged to create a regional MSWE record from 1951-2005.

Table A1.1. Snow courses used to develop a regional averaged series of annual maximum snow water equivalent (MSWE) record for the central Andes, 1951-2005. Data sources: (DGA) Dirección General de Aguas, Chile; (SSRH) Subsecretaría de Recursos Hídricos, Argentina. Note: (#) 2000-2005 MSWE values derived from daily snow pillow records available through <http://www.irrigacion.gov.ar>.

Snow course	Lat.	Long.	Elev.	Period	Missing years (%)	MSWE mean	Data source
Quebrada Larga	30°43'S	70°22'W	3500 m	1956-2004	1970, 1971, 2002 (6.5%)	201 mm	DGA
Portillo	32°50'S	70°07'W	3000 m	1951-2004	1980, 1981 (3.8%)	616 mm	DGA
Laguna Negra	33°40'S	70°08'W	2768 m	1965-2004	None	573 mm	DGA
Laguna del Diamante	34°15'S	69°42'W	3310 m	1956-2005#	None	463 mm	SSRH
Valle Hermoso	35°09'S	70°12'W	2275 m	1952-2005#	None	805 mm	SSRH
Volcán Chillán	36°50'S	71°25'W	2400 m	1966-2004	None	771 mm	DGA

The lack of a representative network of long, complete high-elevation climate records has hampered the assessment of long-term climatic variations in the central Andes and their impacts on mountain snow accumulation and the regional hydrological cycle. These issues were investigated by correlating the regional MSWE series with 4-month moving sums (January-April, ..., September-December) and January-December annual precipitation totals (1961-1990) from three stations located at ca. 110 km west (Santiago-Pudahuel, 33° 23'S, 70° 47'W, 475m), and ca. 110 km (Guido, 32° 51'S, 69° 16'W,

1550m) and 200 km (Mendoza-Observatorio, 32° 54'S, 68° 54'W, 828m) east of the continental divide (Fig. A1.1). Monthly total precipitation records for Santiago and Mendoza were downloaded from the Global Historical Climatology Network website (<http://www.ncdc.noaa.gov/oa/climate/research/ghcn/ghcn.html>) and data from Guido were provided by Subsecretaría de Recursos Hídricos, Argentina. MSWE data were also correlated with 5° x 5° gridded mean seasonal and annual temperature records for central Chile (30°-35°S, 70°-75°W) and central western Argentina (30°-35°S, 65°-70°W) from the HadCRUT2v dataset (Jones and Moberg 2003; Rayner et al. 2003) to examine relationships between regional temperature variations and winter snow accumulation in the mountains. The annual and seasonal time series (and in particular the temperature averages) are strongly autocorrelated. If unaccounted for, this would make the statistical tests of significance of correlations too liberal (i.e. too often rejection of the null hypothesis, $r = 0$). To ensure that all records are serially random prior to correlation, each series was prewhitened using an autoregressive (AR) model where the AR(p) order was estimated following the minimum Akaike Information Criterion (AIC, Akaike 1974). By prewhitening all series under analysis, the significance tests of the moving correlations do not require any degrees-of-freedom adjustment for the serial persistence seen in the original data (e.g. Dawdy and Matalas 1964).

Previous studies have reported a strong ENSO-related tropical and subtropical Pacific influence on snow accumulation in the central Andes (e.g. Escobar and Aceituno 1998) and rainfall variations in central Chile (e.g. Pittock 1980; Aceituno 1988; Montecinos and Aceituno 2003). In general, the warm (cold) phases of ENSO, usually associated with El Niño (La Niña) events in the tropical Pacific, have been related to wet (dry) years in central Chile. Enhanced blocking over the Am-Be area in the SE Pacific during El Niño events has also been linked to increased winter rainfall in central Chile (Rutland and Fuenzalida 1991; Montecinos and Aceituno 2003). However, the identification and timing of El Niño or La Niña events (i.e. the months covered by such events) varies depending on the parameters used to define those events (Trenberth 1997). In this analysis we define El Niño (La Niña) events as periods when the five-month running means of SST anomalies in the Niño 3.4 region (5°N-5°S, 120°-170°W) were above

0.4°C (below -0.4°C) for six months or more (Trenberth 1997). These objectively-defined events were used to examine the warm-wet/cold-dry hypothesis in the central Andes by comparing their occurrence with the 10 highest and lowest snowpack values in the 1951-2005 MSWE regional record. Subsequently, we used the 2.5° x 2.5° gridded monthly mean 500-hPa geopotential height dataset from the National Centers for Environmental Prediction-National Center for Atmospheric Research (NCEP-NCAR) Reanalysis (Kalnay et al. 1996) to investigate the influence of tropospheric circulation anomalies during these extreme years. For each event year and grid point, mean peak winter (June-September) height anomalies from the 1968-1996 reference period were calculated from monthly data and subsequently averaged to create separate composite 500-hPa height anomaly maps for the 10 snowiest and driest years on record.

We also compared the regional MSWE record with seasonally averaged 2.5° x 2.5° gridded SST and sea level pressure (SLP) time series derived from the Reanalysis global database (Kalnay et al. 1996). Mean monthly gridded SST and SLP data were composited into October-January (spring-early summer), February-May (summer-early winter) and June-September (mid-winter) averages and correlated against the regional MSWE series using the linear correlation and mapping routines available at the Climate Diagnostics Center, National Oceanic and Atmospheric Administration (CDC-NOAA) website (<http://www.cdc.noaa.gov/Correlation/>).

Given the socio-economic importance of mountain snow accumulation in central Chile and central western Argentina, better management of water resources could be achieved with the development of reliable models for the prediction of winter snowpack from atmospheric variables or climatic indices (e.g. McCabe and Dettinger 2002). We performed exploratory multiple regression analyses using several climate indices as potential predictors of snow accumulation in the study area. These climate indices (see Table A1.2) have been widely used to characterize atmospheric conditions in the Pacific, Atlantic and Antarctic regions, and were thus possibly linked to interannual snowpack variations in the central Andes. As some of these candidate predictors are not statistically independent (the N34, SOI, and PDO, in particular, exhibit strong intercorrelation), a

stepwise regression approach (F-to-enter 0.05, F-to-remove 0.10) was used to avoid multicollinearity among the predictors and develop a more reliable regression model. The analyses were performed separately for four three-month seasons starting in November of the previous year and ending in October of the current year. Since most of the seasonal climatic index series exhibit strong serial correlations we utilized the prewhitened versions of the seasonal climatic indices as predictors of the prewhitened MSWE snowpack record (see discussion above). While minimizing the impacts of serial persistence on the estimation of the regression models, this approach allowed us to isolate the partial seasonal influences of each candidate predictor on interannual snowpack variations during the 1953-2002 interval common to all series.

Table A1.2. Climatic indices used in this study. The data sources are (CPC) Climate Prediction Center; (NOAA) National Oceanic and Atmospheric Administration; (NCEP) National Centers for Environmental Prediction; (CRU) Climatic Research Unit, University of East Anglia, UK; (JISAO) Joint Institute for the Study of the Atmosphere and Ocean, University of Washington; (CDC) Climate Diagnostics Center; (CIRES) Cooperative Institute for Research in Environmental Sciences.

Climate index description	Period	Data source	Reference
Niño 3.4 Index (N34): Mean monthly SST anomalies for the Niño 3.4 Region, east central Tropical Pacific (5°N-5°S, 170°-120°W).	1950-2004	CPC, NOAA-NCEP http://www.cpc.ncep.noaa.gov/data/indices/	Trenberth 1997
Southern Oscillation Index (SOI): Normalized pressure difference between Tahiti and Darwin.	1866-2004	CRU http://www.cru.uea.ac.uk/cru/data/	Ropelewski and Jones 1987
Pacific Decadal Oscillation (PDO): Leading Principal Component of monthly SST anomalies in the north Pacific Ocean, poleward of 20°N.	1900-2004	JISAO http://jisao.washington.edu/pdo/	Mantua et al. 1997
Atlantic Oscillation (AMO): Mean monthly Atlantic SST anomalies north of the equator, computed with respect to the 1951-2000 base period.	1948-2004	CDC, NOAA-CIRES http://www.cdc.noaa.gov/ClimateIndices/	Enfield et al. 2001
Tropical Southern Atlantic Index (TSA): Mean monthly SST anomalies from the Equator to 20°S, and 10°E to 30°W.	1948-2004	CDC, NOAA-CIRES http://www.cdc.noaa.gov/ClimateIndices/	Enfield et al. 1999
Antarctic Oscillation (AAO): Leading PC of 850 hPa geopotential height anomalies south of 20°S.	1948-2002	JISAO http://www.jisao.washington.edu/data/aa/	Thompson and Wallace 2000

Mean monthly streamflow data for the main rivers in central western Argentina and central Chile were used to examine the influence of the regional MSWE records on runoff (Fig. A1.1 and Table A1.3). Gauge station records were selected for maximum overlap with the MSWE regional series and to avoid major anthropogenic influences on river discharge. Earlier and overlapping monthly records from discontinued stream gauges in the same basin were used to extend (through simple linear regression) the records from active gauge stations on the Mendoza and Diamante Rivers and provide a set of complete and updated (up to June 2004) monthly streamflow series for the most important rivers in central western Argentina. Missing monthly values in the Chilean records were estimated using a reference series created from the remaining streamflow records in the region. Mean annual values were calculated using the July-June water year, and each year is identified by the year of the earliest month (i.e. the 2003 water year extends from July 2003 to June 2004). Mean monthly and annual streamflow series were prewhitened prior to correlation with the regional snowpack record.

Finally, linear trends in the MSWE regional record and the mean annual and seasonal temperatures from the HadCRUT2v grid cells on both sides of the Cordillera were analyzed to explore relationships with river discharges and glaciers over the 20th century. Annual (July-June) and warm season (November-February) river discharges for the region were calculated as the average of the individual streamflow series expressed as percentages from their 1966-2004 mean. Linear trends were computed for the 1951-2004 interval common to all series, and for the 1906-2004 interval common to the gridded temperature and regional runoff records. The statistical significance of trends was assessed following a conservative approach which accounts for the temporal autocorrelation in the regression residuals of each time series (the AdjSE + AdjDF approach, Santer et al. 2000).

Table A1.3. Argentinean and Chilean streamflow records used in this study. Annual data refer to a July-June water year. The statistical significance of least-squares linear trends during the common period was estimated after accounting for the lag-1 autocorrelation in the regression residuals of each series (Santer et al. 2000). Notes: (†) July 1909 – June 1956 estimated from Cacheuta (33° 01'S, 69° 07'W, 1238m); (‡) July 1938 – June 1977 estimated from Los Reyunos (34° 35'S, 68° 39'W, 850m); (ns) Linear trend is not significant ($P>0.05$); * (**) significant at the 0.05 (0.01) level. Data sources: Subsecretaría de Recursos Hídricos (SSRH 2004), Argentina; Dirección General de Aguas (DGA), Chile.

River (basin area)	Gauge station	Lat., Lon.	Elev. (m)	Period of record (% miss.)	Mean annual discharge ($\text{m}^3 \text{s}^{-1}$)	1954-2003 linear trend ($\text{m}^3 \text{s}^{-1} \text{yr}^{-1}$)	Nov-Feb contrib. to annual runoff (%)
San Juan (25670 km ²)	Km. 47.3	31°32'S 68°53'W	945	July 1909- June 2004	65.2	+0.54 ns	53.5 %
Mendoza (9040 km ²)	Guido †	32°51'S 69°16'W	1550	July 1909- June 2004	48.9	+0.37 ns	58.7 %
Tunuyán (2380 km ²)	Valle de Uco	33°47'S 69°15'W	1200	July 1954- June 2004	28.6	+0.12 ns	59.7 %
Diamante (2753 km ²)	La Jaula ‡	34°40'S 69°19'W	1500	July 1938- June 2004	30.9	+0.23 ns	57.0 %
Atuel (3800 km ²)	La Angostura	35°06'S 68°52'W	1200	July 1906- June 2004	35.2	+0.24 ns	51.3 %
Colorado (15300 km ²)	Buta Ranquil	37°05'S 69°44'W	850	April 1940- June 2004	148.3	+0.77 ns	55.8 %
Choapa (1172 km ²)	Cuncumén	31°58'S 70°35'W	955	Jan. 1941- June 2005 (3.0%)	9.6	+0.08 ns	56.5 %
Aconcagua (2059 km ²)	Chacabucuito	32°51'S 70°31'W	1030	Oct. 1913- June 2005 (0.8%)	33.0	+0.18 ns	61.0 %
Maipo (4769 km ²)	El Manzano	33°36'S 70°23'W	890	Nov. 1946- June 2005 (1.6%)	107.8	+0.93 *	55.8 %
Tinguiririca (1424 km ²)	Bajo Los Briones	34°43'S 70°49'W	518	Jan. 1942- June 2005 (9.3%)	50.7	+0.38 **	55.3 %

A1.4. Results

A1.4.1. Regional snowpack record, 1951-2005

In this paper we have developed the first regional snowpack series (expressed as annual Maximum Snow Water Equivalent, MSWE) using snow course data from both sides of

the central Andes in Chile and Argentina. This series covers the 1951-2005 period and is derived from the six longest and most complete snow course records in the region (Table A1.1). Despite the large latitudinal range (ca. 30°-37°S) of these six snow courses and other data limitations discussed above, the individual MSWE records show similar year-to-year variability and share a high percentage of common variance (Fig. A1.2a-f). The mean correlation coefficient from all possible paired combinations is 0.697 and only one significant Principal Component explains 77% of the total variance in these records over the 1966-2004 period. The regional MSWE record (Fig. A1.2g) is approximately normally distributed and shows a non-significant positive linear trend (+3.95% decade⁻¹, $P = 0.543$) over the 1951-2005 interval. The negative first-order autocorrelation coefficient for this series is not statistically significant (-0.258, $p > 0.05$), but reflects the strong year-to-year variability present in both the individual snow course records and the regional MSWE series. Regional MSWE annual values can vary widely from 6% (1968) to 257% (1982) of the 1966-2004 mean (Fig. A1.2g).

A1.4.2. Relationship with local climate conditions

Lagged correlation analysis of the regional MSWE series with seasonal and annual precipitation and temperature records from both sides of the Cordillera revealed the much stronger influence of western (Pacific) conditions on winter snow accumulation at high elevation sites (Fig. A1.3). Using the prewhitened versions of each series, the MSWE series showed highly significant positive correlations with Santiago precipitation for several four-month periods during winter (e.g. $r = 0.878$ with June-September totals, Figure A1.3a) and also with the annual total ($r = 0.893$). Correlations with winter precipitation east of the mountains at Guido were lower but still significant (at the 0.05 level) for the May-August and June-September periods. However, only June-September precipitation totals in Mendoza (further east of the continental divide) were significantly correlated with the regional snowpack record (Fig. A1.3a).

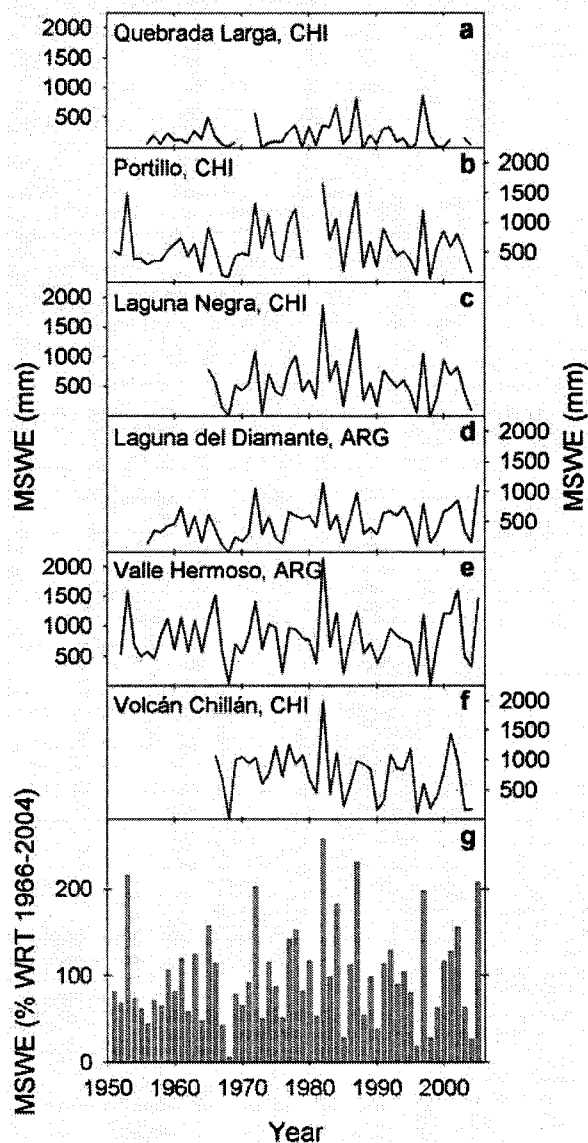


Fig. A1.2. (a-f) Plot of the annual Maximum Snow Water Equivalent (MSWE) records for the six snow courses used in this study. CHI: Chile, ARG: Argentina. **(g)** Regional snowpack series (1951-2005) developed by averaging the above 6 series expressed as percentages of their 1966-2004 common period mean.

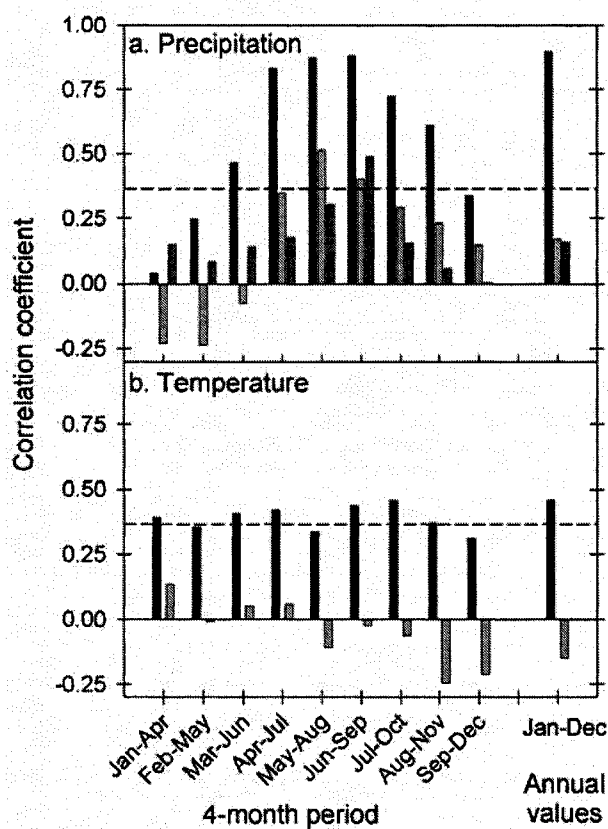


Fig. A1.3. (a) Correlations over the 1961-1990 period between the prewhitened MSWE regional series and four-month seasonal and annual precipitation totals. The stations are Santiago (black bars) west of the Andes, and Guido (light gray bars) and Mendoza (dark gray bars) east of the water divide. **(b)** Correlations between the prewhitened MSWE regional series and $5^{\circ} \times 5^{\circ}$ gridded mean seasonal and annual temperature data for central Chile (30° - 35° S, 70° - 75° W, black bars) and central western Argentina (30° - 35° S, 65° - 70° W, gray bars). The 95% confidence level is depicted by horizontal dashed lines.

The gridded temperature record for central Chile was significantly positively correlated at the 95% level with the regional snowpack record for most of the four-month periods analyzed and the mean annual values (Fig. A1.3b). However, none of the gridded temperature data from east of the mountains were significantly correlated with snowpack, further demonstrating that, at these latitudes, conditions in the Andes are much more strongly related to climate variations west of the continental divide. The significant

positive correlations with temperature variations in central Chile are surprising, as we would expect mountain snowpack records to be positively correlated with nearby precipitation data (e.g. Selkowitz et al. 2002) but mostly negatively correlated with temperature records (e.g. Mote et al. 2005). However, this could partially be explained if the variables involved are not fully independent, where for example increases in precipitation may result from warmer air masses with potentially higher water vapor contents (Barry 1990). The 1961-1990 annual total precipitation values in Santiago and the mean annual gridded temperature series in central Chile are significantly positively correlated ($r = 0.463$, $p < 0.01$).

A1.4.3. Influence of ENSO events and relationship with 500-hPa geopotential height anomalies

Fig. A1.4 shows that above-average snow accumulation in the central Andes is generally associated with the warm phases of ENSO (El Niño events), as was earlier reported by Escobar and Aceituno (1998), and Prieto et al. (2000, 2001). However, comparison of the 10 highest and 10 lowest MSWE years with El Niño and La Niña events (Table A1.4) revealed that this relationship is complex: two of the 10 snowiest years on record did not correspond to El Niño events (as defined by positive SST anomalies in the Niño 3.4 region). In fact, 1984 and 1978 (7th and 10th snowiest years, respectively) actually occurred during extended negative SST anomalies in the Niño 3.4 region (Table A1.4). Extremely low snowfall years in the central Andes show a weaker association with the cold phase of ENSO, and 5 of the 10 driest years (1968, 1996, 2004, 1990 and 1967) did not correspond with concurrent La Niña events in the tropical Pacific (Table A1.4).

Numerous studies have analyzed the 1976-1977 climatic shift throughout the Pacific basin and the changes in ENSO activity toward more warm phases after 1976 (e.g. Mantua et al. 1997; Zhang et al. 1997; Trenberth et al. 2002). This large-scale atmospheric shift and the associated higher frequency and intensity of El Niño events seem to have impacted the snowpack records in the central Andes. During the 1951-1976 interval, only eight years are above the long-term mean, compared with 15 years during the 1977-2005 period. The average snowfall is higher during this latter part of the record

although the means are not significantly different due to the high interannual variability (Fig. A1.4). This agrees with the positive trend in central Chile rainfall records between 1970 and 2000 (Quintana 2004), and is likely responsible for the positive trend observed in the regional MSWE series.

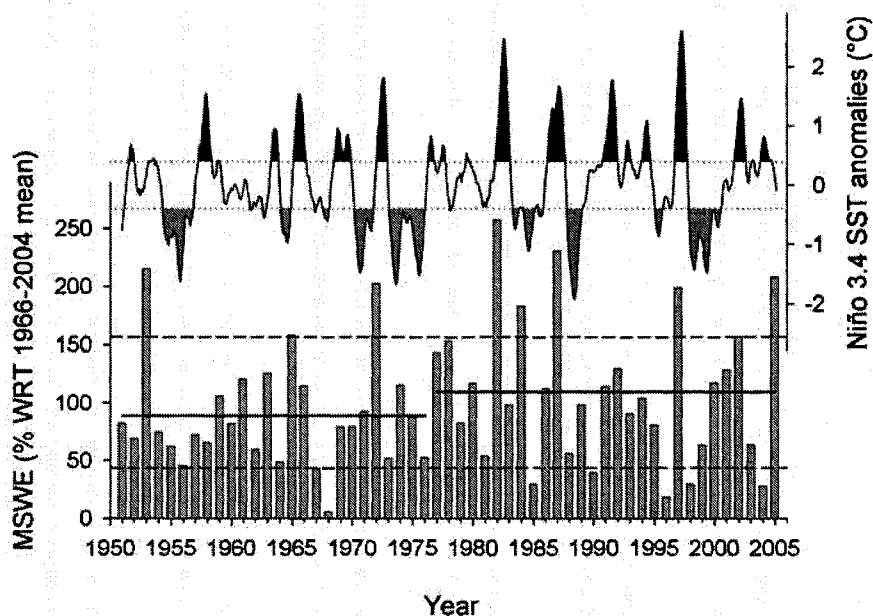


Fig. A1.4. Comparison between (top) five-month moving averages of monthly SST anomalies for the Niño 3.4 region and (bottom) the regional snowpack series from the central Andes. MSWE (SST) records are expressed as percentages (anomalies) from the 1966-2004 (1971-2000) base period. El Niño (La Niña) events are identified following Trenberth (1997) and are shaded black (gray) in the upper diagram. The dashed lines indicate ± 1 standard deviations in the 1951-2005 regional snowpack record. MSWE means for the 1951-1976 and 1977-2005 periods are shown as thick horizontal lines.

Table A1.4. The 10 highest and lowest snow accumulation years in the central Andes (1951-2005), expressed as percentages from the 1966-2004 base period. El Niño and La Niña events (as defined by Trenberth 1997) that overlap at least two of the snow season months (April-October) are also listed. Note that not all the highest (lowest) ranked annual MSWE values coincide with El Niño (La Niña) events.

Rank	10 snowiest years			10 driest years		
	Year	Averaged MSWE	El Niño?	Year	Averaged MSWE	La Niña?
1	1982	257.2%	Yes	1968	5.6%	No ³
2	1987	230.7%	Yes	1996	18.5%	No ⁴
3	1953	215.1%	Yes	2004	27.6%	No ⁵
4	2005	208.2%	Yes	1985	29.1%	Yes
5	1972	202.6%	Yes	1998	29.2%	Yes
6	1997	198.9%	Yes	1990	39.1%	No ⁶
7	1984	183.4%	No ¹	1967	42.8%	No ⁷
8	1965	158.2%	Yes	1956	45.3%	Yes
9	2002	156.9%	Yes	1964	48.6%	Yes
10	1978	152.8%	No ²	1973	51.6%	Yes

Notes:

¹ Niño 3.4 SST anomalies remained negative from August 1983 through May 1986. A La Niña event occurred between August 1984 and August 1985.

² Negative Niño 3.4 SST anomalies occurred between April and December 1978.

³ La Niña event from October 1967 to April 1968 (early winter). Niño 3.4 region SST anomalies remained negative until June 1968, turned positive in July 1968 and El Niño event started in September 1968 (late winter).

⁴ Strictly, an 8-month La Niña event ended in April 1996. Nevertheless, SST anomalies remained negative throughout the winter of that year.

⁵ Positive Niño 3.4 SST anomalies were observed during 2004, with values above +0.4°C between June 2004 and May 2005.

⁶ Positive SST anomalies (between 0 and 0.4°C) were observed during 1990.

⁷ Strictly, a La Niña event only started in October 1967, but SST anomalies had remained negative throughout that year.

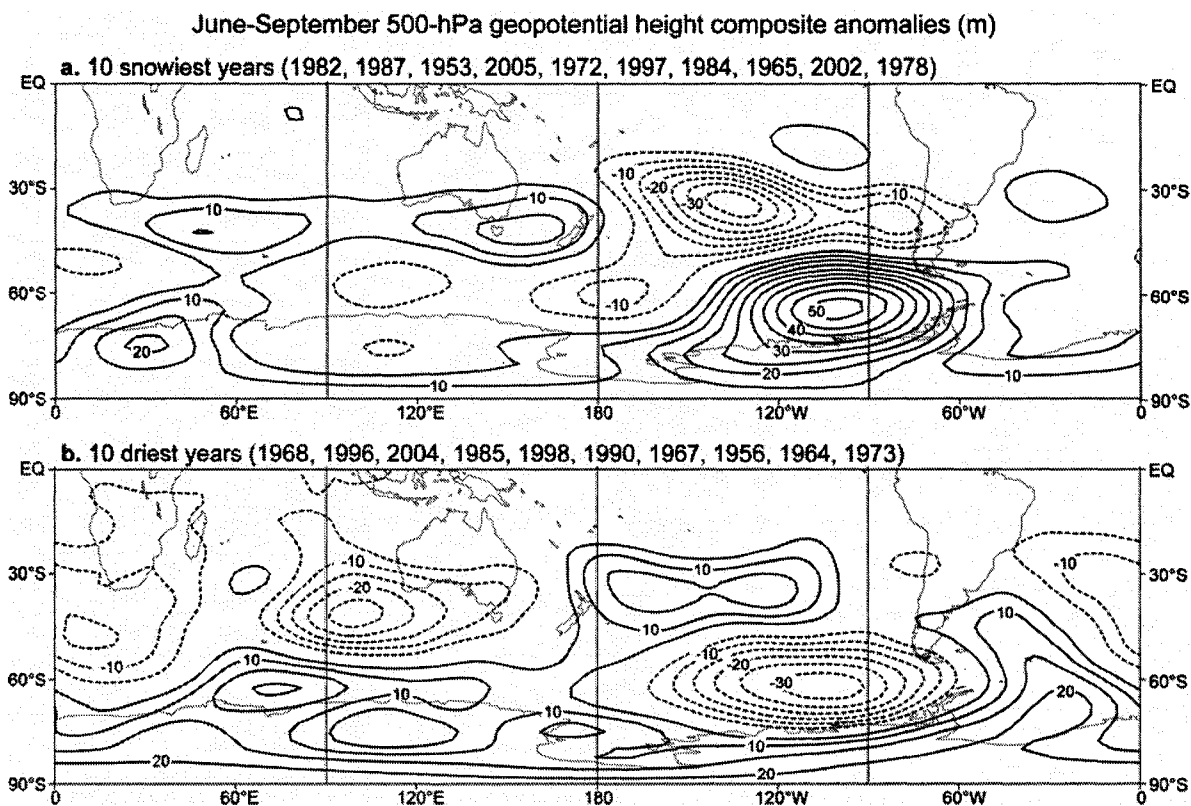


Fig. A1.5. (a) June-September mean 500-hPa geopotential height anomalies for the 10 snowiest years in the central Andes. Mean monthly gridded data were obtained from the NCEP/NCAR Reanalysis global dataset (Kalnay et al. 1996). Contours are in meters with a 5-m contour interval, and zero lines are omitted. Positive (negative) contour anomalies are shown as solid (dashed) lines. **(b)** Same as (a), but for the 10 driest years in the central Andes.

The 500-hPa geopotential height anomaly maps (Fig. A1.5) suggest a clear association between peak winter, large-scale tropospheric circulation anomalies in the mid- to high-latitudes of the Southern Hemisphere and extreme snowfall years in the central Andes. The most noticeable features associated with the ten snowiest years on record are the extensive and well-defined regions of averaged positive and negative height anomalies concentrated between 60°-70°S and 90°-120°W (Am-Be area), and 30°-40°S and 130°-150°W in the subtropical south Pacific (Fig. A1.5a). These patterns confirm the results from previous studies (e.g. Rutlland and Fuenzalida 1991; Montecinos and Aceituno

2003) and indicate that enhanced blocking activity around the Am-Be area and the concurrent weakening of the subtropical Pacific anticyclone are key features influencing above-average snow accumulation in the study area. Interestingly, the 10 driest years on record corresponded with almost an exact opposite anomaly pattern, with negative winter 500-hPa geopotential height anomalies over the Am-Be region and positive anomalies in the subtropical south Pacific between 25° and 40°S (Fig. A1.5b). High snow years also corresponded with generalized positive height anomalies between New Zealand and the southern tip of South Africa, whereas negative anomalies occurred over the Southern Ocean between the date line and 90°E and the eastern Antarctic sector around 70°-80°S and 105°-120°E (Fig. A1.5a). A similar, opposite, anomaly pattern in these remote regions is apparent for the 10 driest years (Fig. A1.5b), providing evidence of the large-scale, relatively time-stable nature of these atmospheric relationships.

A1.4.4. Relationships with gridded SST, SLP and climate indices

In addition to the results described above, correlations of the regional MSWE series with mean seasonal gridded global SST and SLP data (Fig. A1.6) revealed interesting spatial patterns that may help to understand the relative temporal and spatial significance of these variables on snow accumulation in the central Andes. In general, the seasonally-averaged spring-early summer (October-January) gridded SST values showed non-significant correlations with the regional MSWE series (Fig. A1.6a). The February-May (late summer-early winter) SST gridded records show some negative correlation fields centered south and east of Australia and in the southeast Pacific, whereas positive correlations were found over most of the tropical and subtropical eastern Pacific and the southwest Atlantic (Fig. A1.6b). The highest correlations occurred during the June-September (peak winter) period showing the strong and well known ENSO-like wedge pattern over the tropical and subtropical Pacific (e.g. Trenberth and Caron 2000; Trenberth et al. 2002) (Fig. A1.6c). Strong positive correlations were found during this four-month period especially over the Niño 3 and 4 regions in the Tropical Pacific. Conversely, negative correlations occurred mostly over the subtropical western Pacific. Negative correlations were also found on the eastern Pacific off the coast of central Chile. This correlation pattern resembles that obtained by Montecinos and Aceituno (2003) for

June-August central Chile rainfall variations and SST gridded fields over the tropical and subtropical Pacific.

Regional MSWE series vs. Sea Surface Temperatures (SST) and Sea Level Pressures (SLP)

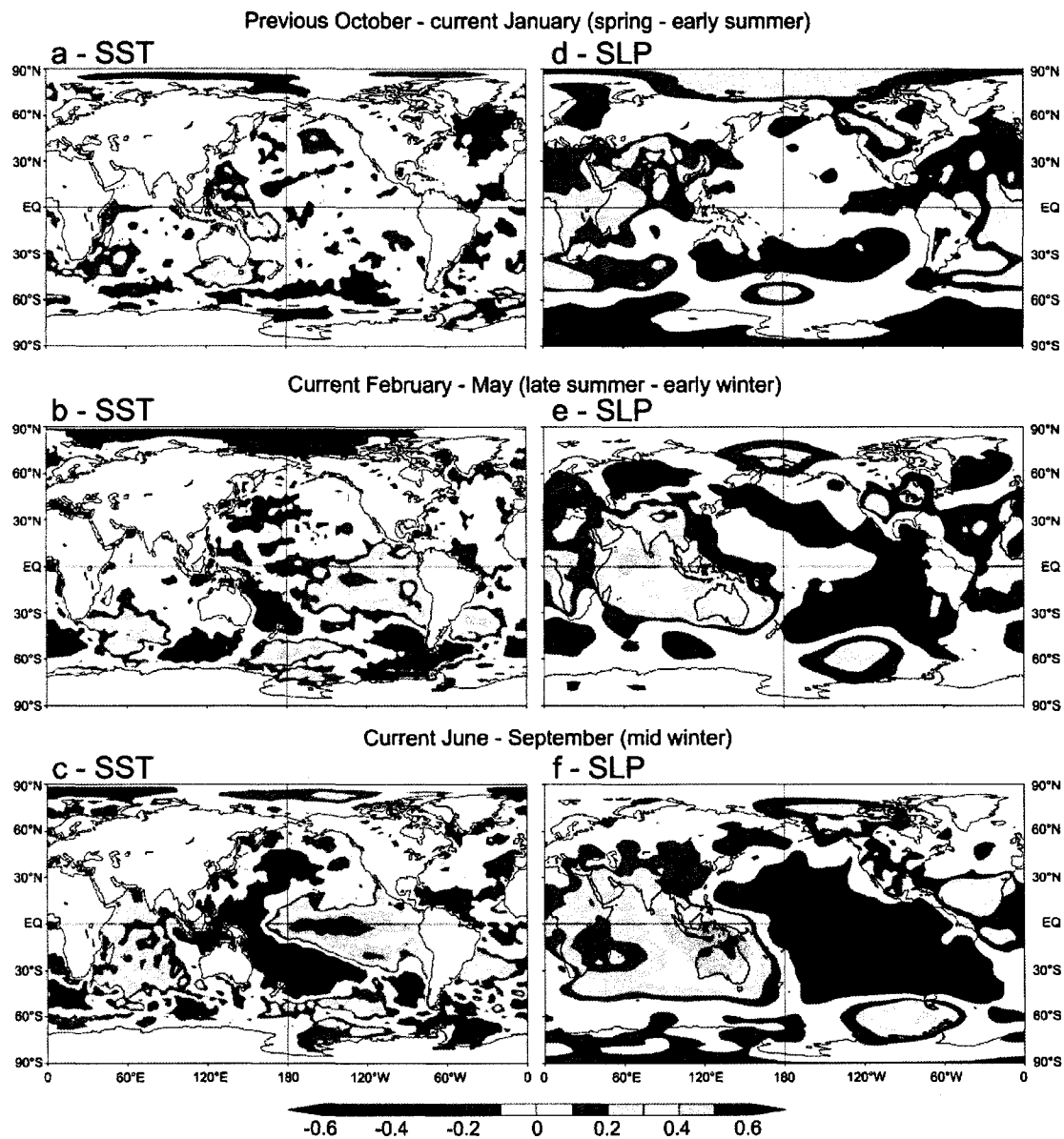


Fig. A1.6. Correlation maps showing the changing seasonal strength in the relationships between the regional MSWE series and seasonally averaged NCEP-NCAR reanalysis $2.5^\circ \times 2.5^\circ$ SST (**a-c**) and SLP (**d-f**) gridded data over the 1952-2003 interval.

Field correlations between the MSWE series and SLP gridded seasonal averages (Fig. A1.6d-f) also showed a temporal pattern with a noticeable ENSO-related structure (Trenberth and Caron 2000). In general, low or non-significant field correlations were found with gridded SLP October-January seasonal averages. Negative correlations, concentrated over the subtropical south Pacific, were found with February-May SLP averages, while the grid cells over the northern Indian Ocean and around Australia were positively correlated with the snowpack series. The strongest gridded SLP-MSWE correlations also occurred in the June-September period during the current winter season (Fig. A1.6f) with negative correlations over the subtropical Pacific and southeast Atlantic oceans. Figure A1.6f also shows positive correlations concentrated around northern Australia and over the Am-Be area in the SE Pacific, closely resembling the Pacific SLP-central Chile winter rainfall correlation pattern obtained by Montecinos and Aceituno (2003). As expected, the pattern in Fig. A1.6f is also roughly similar to the 500-hPa geopotential height anomaly map shown in Fig. A1.5a.

The analysis of the anomaly maps and correlation fields depicted in Figs. A1.5 and A1.6 suggests that, in addition to the strong ENSO-related influence in the Pacific basin, snowpack variations in the central Andes might also be related to large-scale atmospheric features that extend beyond the tropical and subtropical Pacific. If physically and statistically meaningful, these relationships could be used to develop winter snowpack forecasts for the study region. Our multivariate regression trials revealed that none of the climatic indices for the November-April period is significantly correlated with the snowpack record and therefore they are not useful predictors of winter snow accumulation in the central Andes (Table A1.5). However, significant correlations were found between the MSWE record and May-July (early-mid winter) averages of the N34, SOI, and AAO, but due to intercorrelation among these variables only the SOI was included in a regression model which explains about 44% of the variance in the snowpack record (Table A1.5). The predictive skill of these candidate variables decreases later in the winter season. Although the August-October (late winter) averages for the N34, SOI, and PDO showed statistically significant correlations with the regional

snowpack record, only the N34 series was selected in the stepwise regression procedure to explain about 31% of the variance in the MSWE regional series (Table A1.5).

Table A1.5. Multivariate regression trials between 1953-2002 prewhitened versions of the regional snowpack record and seasonally-averaged estimates for the six climatic indices described in Table A1.2. Four three-month seasons starting in November of the previous year were used, and candidate predictors were selected following a stepwise regression approach (F-to-enter 0.05, F-to-remove 0.10). Notes: (r) Correlation coefficient between the snowpack series and seasonal averages for each climatic index; (Beta) Standardized regression coefficients used to compare the relative strength of the various predictors within each model; (Adj r2) Coefficient of determination adjusted for the number of predictors in the model; * (**) Coefficient is significant at the 95% (99%) level; (#) None of the predictors passed the threshold value for F-to-enter.

Clim. Index	NDJ			FMA			MJJ			ASO		
	r	Beta	Adj r2	r	Beta	Adj r2	r	Beta	Adj r2	r	Beta	Adj r2
N34	0.091	-0.147	#	0.273	0.368	#	0.526**	0.038	0.437	0.567**	0.567**	0.307
SOI	-0.154	-0.163		-0.240	0.153		-0.670**	-0.670**		-0.509**	-0.079	
PDO	0.235	0.253		0.170	0.083		0.105	-0.108		0.299*	-0.101	
AMO	-0.017	0.080		0.074	-0.076		-0.073	-0.138		-0.065	-0.096	
TSA	-0.189	-0.198		-0.141	-0.130		-0.087	0.075		0.105	0.071	
AAO	-0.109	-0.055		-0.195	-0.152		-0.247*	-0.045		0.050	0.085	

A1.4.5. Relationships between regional streamflow records and winter snowpack

All of the rivers studied display typical unimodal annual hydrographs with a November to February (late spring-early summer) snowmelt peak that represents about 57% of the annual discharge (Table A1.3). Over the 1954-2003 common period, only one significant Principal Component (PC1) explains 85.5% of the total variance in mean annual discharge of these rivers indicating a strong similarity in flow regimes on both sides of the Cordillera. A similar coherent pattern is shown by PCA of the mean summer (November-February) flows with PC1 explaining 86.1% of the total variance. All 10 rivers showed positive linear trends in annual runoff over the 1954-2003 period (Table

A1.3). However, after accounting for the serial correlation in the regression residuals of each series (Santer et al. 2000), only the Maipo and Tinguiririca Rivers in Chile showed positive linear trends that are statistically significant at the 95% level. Positive linear trends were also observed in the November-February mean seasonal values, but none of these trends reached statistical significance at the 95% level.

The strong, positive association between winter snowpack and spring-summer river discharges is a well-known hydro-meteorological relationship in the study area. However, to our knowledge no published studies have actually quantified this relationship. In Fig. A1.7 we show that highly significant correlations (particularly for the warm-season peak flows) exist between the regional MSWE series and mean monthly streamflow records from both sides of the Cordillera, even after accounting for serial persistence in the individual series. Extremely high correlation values (ranging between 0.778 and 0.908) were also found with the annualized July-June river discharges. Over the 1951-2004 period, the correlation between the MSWE record and the regionally averaged November-February (July-June) river discharges were as high as 0.945 (0.926) (Fig. A1.8), reflecting the crucial influence of mountain snowpack on fresh water availability in the adjacent lowland areas in Chile and Argentina. However, month-by-month correlation analysis (Fig. A1.7) revealed some interesting differences in the relationship between the western and eastern sides of the Cordillera. Although the hydrographs of these rivers have a simple unimodal warm season peak centered around December-January, correlations with the Chilean (western) rivers (light bars, Fig. A1.7) were statistically significant approximately two months prior (even including June, in the middle of the snow season) to the Argentinean (eastern) rivers (dark bars, Fig. A1.7). Significant correlations with the Chilean rivers also ended earlier in the following year than the Argentinean rivers (Fig. A1.7).

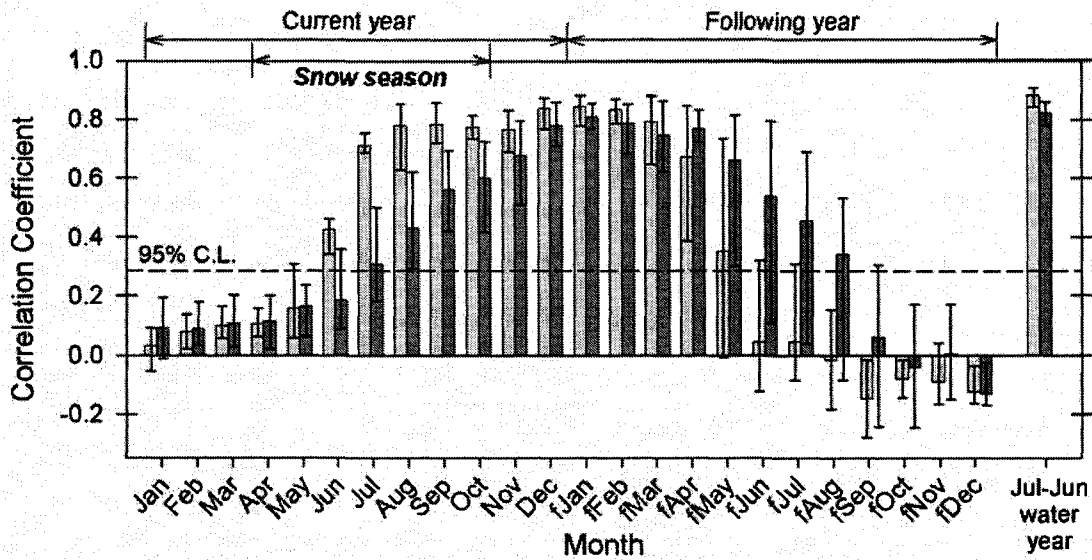


Fig. A1.7. Correlations between the prewhitened regional snowfall MSWE record and streamflow over the 1955-2002 period. The mean and range of the correlations coefficients for the four Chilean (light bars) and six Argentinean (dark bars) rivers are shown for each month and the July-June water year. The 95% confidence level is depicted by the dashed line.

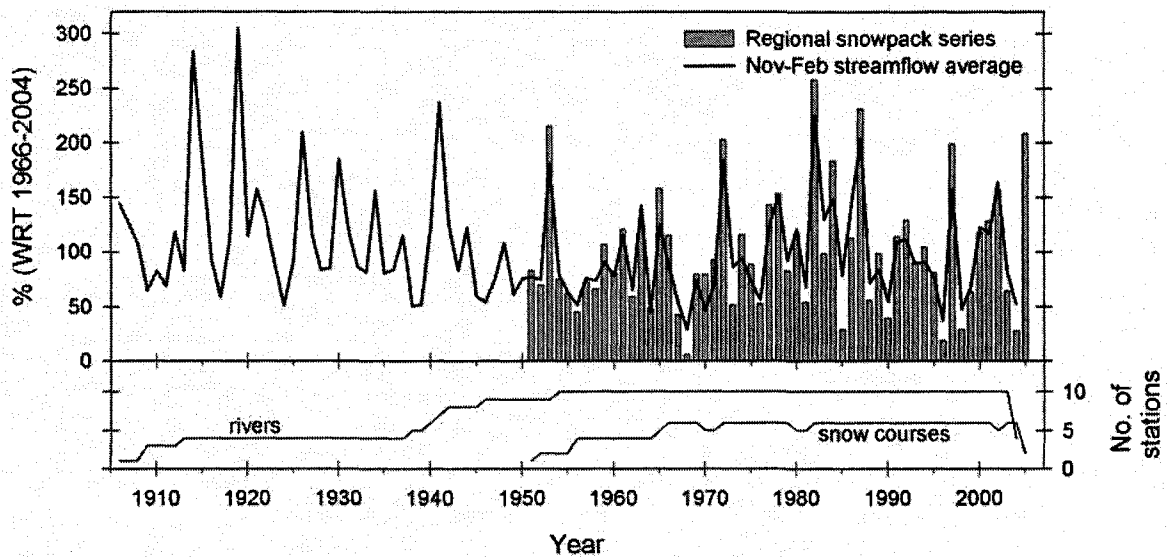


Fig. A1.8. Relationship between the 1951-2005 MSWE series (bars) and the 1906-2004 regionally-averaged November-February discharge from central Chile and central western Argentina (solid line). Both series are expressed as percentages with respect to the 1966-2004 base period. The correlation between these raw series is extremely high ($r = 0.945$, $p < 0.001$). Correlations with the prewhitened data showed similar results.

All winter snowpack and annual and seasonal streamflow and temperature series showed positive trends over the 1951-2004 period, but only the trends for mean annual and warm-season temperatures from central western Argentina were significant at the 0.05 level when the conservative approach of Santer et al. (2000) was used (Table A1.6). Temperature trends on both sides of the Andes remained positive for all seasons when the extended 1906-2004 period was considered, but in this case only the central Chile records reached statistical significance at the 95% level or higher. In contrast, mean annual regional and warm season runoff series showed negative (though non-significant) linear trends over this interval (Table A1.6).

Table A1.6. Linear trends over the 1951-2004 and 1906-2004 periods for several hydroclimatic parameters. Moisture related variables are the regional MSWE series and averaged annual (July-June) and warm season (November-February) regional streamflow records, expressed as percentages from the 1966-2004 common period. Temperature data ($^{\circ}\text{C}$ anomalies from the 1961-1990 period) are from the Climatic Research Unit $5^{\circ} \times 5^{\circ}$ HadCRUT2v gridded dataset (Jones and Moberg 2003; Rayner et al. 2003) averaged over the year (January-December), and six-month warm (October-March), and cold (April-September) seasons. The grid cells used are CRU A = 30° - 35°S , 70° - 75°W (central Chile); CRU B = 30° - 35°S , 65° - 70°W (central western Argentina). The statistical significance (t test) of the least-squares linear trends was estimated after accounting for the lag-1 autocorrelation in the regression residuals of each series (Santer et al. 2000).

Variable	Slope (values per decade)	
	1951-2004	1906-2004
MSWE	+ 1.9%	N/A
Streamflow Jul-Jun	+ 4.4%	- 2.3%
Streamflow Nov-Feb	+ 3.7%	- 2.8%
CRU A Jan-Dec	+ .068 $^{\circ}\text{C}$	+ .081 $^{\circ}\text{C}$ **
CRU A Apr-Sep	+ .065 $^{\circ}\text{C}$	+ .057 $^{\circ}\text{C}$ *
CRU A Oct-Mar	+ .066 $^{\circ}\text{C}$	+ .104 $^{\circ}\text{C}$ **
CRU B Jan-Dec	+ .122 $^{\circ}\text{C}$ *	+ .023 $^{\circ}\text{C}$
CRU B Apr-Sep	+ .101 $^{\circ}\text{C}$	+ .033 $^{\circ}\text{C}$
CRU B Oct-Mar	+ .139 $^{\circ}\text{C}$ *	+ .017 $^{\circ}\text{C}$

A1.5. Discussion and Conclusions

Either directly or indirectly, over 10 million people in central Chile and central western Argentina depend on the fresh water originating from the winter snowpack in the central Andes to meet water demands for drinking, domestic consumption, irrigation, industry and hydroelectric generation. Winter snow accumulation has been systematically monitored for over 50 years for spring-summer snowmelt discharges on both sides of the mountain range, but few published studies are available and little is known about winter snowpack variability in the region. In this paper we present the first attempt to integrate snowpack data from the Andes in Chile and Argentina (Fig. A1.1). Our results generally agree with previous climatic and hydrometeorological studies showing a marked Pacific, ENSO-related influence on precipitation in this area (e.g. Rutlland and Fuenzalida 1991; Compagnucci and Vargas 1998, Escobar and Aceituno 1998, Montecinos and Aceituno 2003). However, using updated snow course data our analyses provide further insight into a) the main temporal and spatial patterns in the snowpack records; b) their relationships with local climate, ENSO events, large-scale atmospheric variables (500-hPa geopotential height, SST and SLP) and climatic indices indicative of conditions in the Pacific, Atlantic and Antarctic regions; c) the temporal importance of the winter snow records on river discharges in the region; and d) possible causes for the observed streamflow and glacier trends over the second half of the 20th century.

Unlike western North America or the European Alps, the snow course data available in the southern South American Andes are very limited in temporal and spatial extent. Between ca. 30° and 37°S only two snow course records exceed 50 years, and only six stations with >30 yrs of records and <10% of missing data were deemed appropriate for this study (Table A1.1). However, these records demonstrate a strong regional signal indicating they are reliable indicators of interannual and interdecadal snowpack variations in the central Andes over the 1951-2005 period. In contrast to the decreasing trends observed in snowpack records across western North America (Mote et al. 2005), the averaged regional MSWE series displays a positive (though non significant) trend with marked interannual variability ranging from 6 to 257% of the 1966-2004 mean.

The most noticeable feature evidenced by the correlation analyses between the regional snowpack series and climate records from both sides of the Cordillera is the highly significant positive correlations with winter and annual rainfall totals in central Chile, which reflect the importance of moist westerly air masses in regulating snowfall over the mountains. Lower (though marginally significant) positive correlations were also found with central Chile gridded temperature records. Precipitation and gridded temperature data east of the continental divide showed a much weaker association with the MSWE series. While highlighting the predominant influence of western conditions on snowpack accumulation in the central Andes, these results revealed an intriguing positive association between temperature and snowpack variations that agrees with a theoretical model of possible effects of warming trends in mountain regions (see Barry 1990). According to this model, warmer air masses with a potentially higher specific humidity may lead to a temporary increase in snowfall at high elevation sites. The positive trends observed in our snowpack series and in surface and tropospheric temperature records in central Chile during winter (Aceituno et al. 1993; Rosenblüth et al. 1997) are in line with this hypothesis. However, the limited empirical information available and the complex nature of the atmospheric processes and feedbacks involved (Allen and Ingram 2002) hamper our ability to assess the possible implications of this positive snowpack-temperature association in the near future. Nonetheless, the analysis of several climate and hydrologic models (Jacobs et al. 2001) suggests that substantial increases in temperature will ultimately result in a reduction of the mountain snowpack, with potential impacts on the hydrological cycle and water supply for the region.

We found a clear correspondence between the warm phases of ENSO (El Niño events) and above-average snow accumulation in the central Andes, but two of the snowiest years on record did not correspond with concurrent positive SST anomalies in the Niño 3.4 region. Moreover, only 50% of the driest years in the central Andes coincided with La Niña events in the tropical Pacific, suggesting the existence of additional factors outside the tropical Pacific that contribute to explain snowfall variability in the central Andes. The analysis of 500-hPa geopotential height anomaly maps associated with the extreme years in the study region revealed that tropospheric conditions in the mid- to high-

latitudes in the Pacific are key factors modulating extreme snowpack variations in the study region. Enhanced blocking activity (associated with positive height anomalies) in the Am-Be area and a weakening of the subtropical Pacific anticyclone during winter result in a northward migration of the westerly storm tracks and above-average snow accumulation in the study area. A remarkably similar height anomaly pattern of opposite sign for the driest years suggests that a stronger Pacific anticyclone and depleted height anomalies in the SE Pacific during winter determine a southward displacement of westerly air masses with a marked reduction in snowfall in the central Andes. These results coincide with previous related studies in the region (e.g. Rutland and Fuenzalida 1991).

Lagged correlations between the regional MSWE series and global gridded SST and SLP data averaged over previous and current seasons showed the well-known association between central Chile precipitation and ENSO-conditions in the tropical and subtropical Pacific (see e.g. Montecinos and Aceituno 2003). Interestingly, the higher correlations with the SST and SLP records were mostly observed during the austral winter season (June-September), suggesting that conditions preceding the cold season have little or no influence on winter snow accumulation in this region (see Fig. A1.6). This was further corroborated by multivariate regression trials between the MSWE series and 3-month moving averages of large-scale climatic indices (Tables A1.2 and A1.5), which revealed serious limitations in predicting snow accumulation before the onset of the winter season using these candidate predictor variables alone. These results also confirmed that the predominant Pacific, ENSO-related influence on snowpack in the central Andes is mainly concentrated during the cold season months, but even during this period the variance explained by the stepwise regression models was relatively modest (44-31%). Given the socio-economic importance of the central Andes snowpack, improved predictive skills are desirable and more research is needed to identify better predictors of snowpack records from the period prior to the austral winter. Since the most serious challenges in managing the mountain water supply will likely occur during below-average snowfall years, special attention should be paid to those large-scale atmospheric linkages associated with (or leading to) extreme dry years in the central Andes. One possibility is

the development of a north-south index utilizing SLP or geopotential height data from the subtropical Pacific off the coast of central Chile combined with those from the Am-Be area in the SE Pacific (see Figs. A1.5 and A1.6f). Although blocking activity in this area is strongly associated with ENSO variability (see e.g. Renwick 1998), a better understanding of additional atmospheric teleconnections affecting conditions in the SE Pacific (e.g. Jacobs and Comiso 1997; Marques and Rao 1999) may in turn lead to improved predictive skills for snowpack in this region.

River discharges on both sides of the central Andes are strongly correlated with the snowpack record and show remarkably similar interannual variability and trends, highlighting the existence of a marked regional hydrologic signal between 31° and 37°S. The correlation between the MSWE record and regionally-averaged river discharges suggests that over the past 55 years >85% of the streamflow variance could be explained by the snowpack record alone (Fig. A1.8). As expected from a snowmelt-dominated streamflow regime, the late spring-early summer months (November-February) account for almost 60% of the annual total flows and show the highest correlations with the snowpack record (Table A1.3 and Fig. A1.7). However, the Chilean rivers also showed highly significant correlations during July-September in the middle of the snow season. Although additional work is needed to elucidate these previously undocumented differences in the snowpack-streamflow relationships between Chilean and Argentinean rivers, we hypothesize that as winter rainfall in central Chile and snow accumulation in the central Andes are strongly correlated (see Fig. A1.3a), the higher correlations of the Chilean rivers during the snow season probably reflect the influence of winter rainfall over the gauge stations located west of the Cordillera.

Linear trend analyses of snowpack, streamflow and local climate records during the 1951-2004 period showed a consistent pattern of positive trends for all these variables. However, conservative estimates revealed that most of these trends are not statistically significant and therefore should be interpreted with caution. During the extended 1906-2004 period, trends in annual and warm season streamflow records changed in sign but remained within the 95% confidence levels, whereas temperatures on both sides of the

central Andes showed a sustained warming tendency, especially in the annual and warm season series from central Chile. This consistent pattern of positive trends found in the temperature records, together with the generalized recession of glaciers observed in the central Andes (Casassa 1995; Rivera et al. 2000) suggest that significant changes in climate have already impacted glacier mass balances in the region. The higher average in snow accumulation during recent decades (which has likely been influenced by the higher frequency and intensity of the warm phases of ENSO after 1976, Trenberth et al. 2002) does not seem to have counteracted the negative impacts of increased glacier ablation associated with higher temperatures across the region. Although largely speculative, these analyses also suggest that the positive trends observed in river discharges during this most recent period (Tables A1.3 and A1.6) may be related to both the higher snow inputs and increasing snow and ice ablation due to higher temperatures during the snowmelt season. Even when increased glacier recession may result in higher runoff in the short-term, the observed and predicted climate tendencies for this region indicate that ultimately the glacier melt contribution to streamflow will diminish, with substantial and widespread socio-economic impacts especially during extreme dry years.

Higher temperatures are also expected to influence the amount of precipitation that falls as rain rather than snow and produce earlier snowmelt peaks which will change the seasonal availability of water supply (Jacobs et al. 2001; Stewart et al. 2005). If such projections are correct, local water management authorities will likely face increasing challenges to allocate the scarce mountain water among the rapidly growing urban, industrial, and agricultural sectors. Further work is needed to quantify the relative influences of rainfall, snowmelt and glacier ablation on the rivers west and east of the continental divide and properly evaluate the potential hydrological and socio-economic impacts of the predicted climate changes in this region. This will also require detailed information about the inherent long-term variability and change in snow accumulation over the central Andes. The remarkably strong association between winter snowpack and summer runoff suggests that streamflow records could be used as surrogates of snowpack variations for most of the past century (see Fig. A1.8). However, this interval may still be inadequate to capture the full range of decade- to century-long fluctuations in the

snowpack record. Examination of the long and well replicated moisture-sensitive tree-ring width chronologies available from the Chilean side of the central Andes (Boninsegna 1988; Le Quesne et al. 2006) indicates that these proxy records could provide a much longer (and thus more appropriate) perspective to assess the low-frequency snowpack variability and improve our understanding of past changes and possible future scenarios for winter snow accumulation in this mountainous region.

A1.6. References

- Aceituno, P., 1988: On the functioning of the Southern Oscillation in the South American sector. Part I: surface climate. *Mon. Wea. Rev.*, 116, 505-524.
- Akaike, H., 1974: A new look at the statistical model identification. *IEEE Trans. Autom. Control*, AC19(6), 716-723.
- Allen, M.R., and W.J. Ingram, 2002: Constraints on future changes in climate and the hydrologic cycle. *Nature*, 419, 224-232.
- Barry, R.G., 1990: Changes in mountain climate and glacio-hydrological responses. *Mountain Res. Development*, 10(2), 161-170.
- Bohr, G.S., and E. Aguado, 2001: Use of April 1 SWE measurements as estimates of peak seasonal snowpack and total cold-season precipitation. *Water Resour. Res.*, 37(1), 51-60.
- Boninsegna, J.A., 1988: Santiago de Chile winter rainfall since 1220 as being reconstructed by tree rings. *Quat. South Am. Antarct. Pen.*, 6, 67-87.
- Bradley, R.S., F.T. Keimig, and H.F. Diaz, 2004: Projected temperature changes along the American cordillera and the planned GCOS network. *Geophys. Res. Lett.*, 31, L16210, doi:10.1029/2004GL020229.
- Brown, E., and J.E. Valdivia, 2000: Water management in Chile (in Spanish), Comité Asesor Técnico de América del Sur (SAMTAC), Asociación Mundial del Agua (GWP). <http://www.eclac.cl/DRNI/proyectos/samtac/InCh01100.pdf>
- Cai, X., M.W. Rosegrant, and C. Ringler, 2003: Physical and economic efficiency of water use in the river basin: Implications for efficient water management. *Water Resour. Res.*, 39 (1), 1013, doi:10.1029/2001WR000748
- Carrasco, J.F., G. Casassa, and J. Quintana, 2005: Changes of the 0°C isotherm and the equilibrium line altitude in central Chile during the last quarter of the 20th century. *Hydrol. Sci. J.*, 50(6), 933-948.

- Casassa, G., 1995: Glacier inventory in Chile: current status and recent glacier variations. *Ann. Glaciol.*, 21, 317-322.
- Casassa, G., A. Rivera, F. Escobar, C. Acuña, J. Carrasco, and J. Quintana, 2003: Snow line rise in central Chile in recent decades and its correlation with climate. *Geophys. Res. Abs.*, 5, 14395.
- Caviedes, C.N., 1998: ENSO influences on the interannual variations of South American rivers (in Spanish). *Bull. Inst. fr. études andines*, 27(3), 627-641.
- Cayan, D., 1996: Interannual climate variability and snowpack in the western United States. *J. Climate*, 9, 928-948.
- Compagnucci, R.H., and W.M. Vargas, 1998: Inter-annual variability of the Cuyo rivers' streamflow in the Argentinean Andes Mountains and ENSO events. *Int. J. Climatol.*, 18, 1593-1609.
- Cubasch, U., and Coauthors, 2001: Projections of future climate change. *Climate Change 2001: The Scientific Basis. Contribution of Working Group I to the Third Assessment Report of the Intergovernmental Panel on Climate Change*, J. T. Houghton et al., Eds., Cambridge University Press, 525-582.
- Dawdy D.R., and N.C. Matalas, 1964: Statistical and probability analysis of hydrologic data, Part III. Analysis of variance, covariance, and time series. *Handbook of Applied Hydrology. A Compendium of Water-Resources Technology*, Chow V.T., ed., McGraw-Hill, 8.68-8.90.
- Díaz Araujo, E., and A. Bertranou, 2004: Systemic Study of Water Management Regimes, Mendoza, Argentina. Comité Asesor Técnico de América del Sur (SAMTAC), Asociación Mundial del Agua (GWP). <http://www.eclac.cl/DRNI/proyectos/samtac/InAr00404.pdf>
- Enfield, D.B., A.M. Mestas-Núñez, D.A. Mayer, and L. Cid-Serrano, 1999: How ubiquitous is the dipole relationship in tropical Atlantic sea surface temperatures? *J. Geophys. Res.*, 104, 7841-7848.
- Enfield, D.B., A. M. Mestas-Núñez, and P.J. Trimble, 2001: The Atlantic multidecadal oscillation and its relation to rainfall and river flows in the continental U.S. *Geophys. Res. Lett.*, 28, 2077-2080.
- Escobar, F., and P. Aceituno, 1998: ENSO influence on Andean winter snowfall in central Chile (in Spanish). *Bull. Inst. fr. études andines*, 27(3), 753-759.
- INDEC, 2001: National Census, 2001 (in Spanish). Instituto Nacional de Estadística y Censos, Argentina. <http://www.indec.mecon.gov.ar>.

- INE, 2003: National Census, 2002 (in Spanish). Instituto Nacional de Estadísticas, Chile.
<http://www.ine.cl>.
- Jacobs, K., D.B. Adams, and P. Gleick, 2001: Potential consequences of climate variability and change for the water resources of the United States. *Climate Change Impacts on the United States: The Potential Consequences of Climate Variability and Change*. National Assessment Synthesis Team, US Global Change Research Program, Cambridge University Press, 405-435.
- Jacobs, S.S., J.C. Comiso, 1997: Climate variability in the Amundsen and Bellingshausen Seas. *J. Climate*, 10, 697-709.
- Jones, P.D., and M. Hulme, 1996: Calculating regional climatic time series for temperature and precipitation: methods and illustrations. *Int. J. Climatol.*, 16, 361-377.
- Jones, P.D., and A. Moberg, 2003: Hemispheric and large-scale surface air temperature variations: an extensive revision and an update to 2001. *J. Climate*, 16, 206-223.
- Kalnay, E., and Coauthors, 1996: The NCEP/NCAR Reanalysis 40-year Project. *Bull. Amer. Meteor. Soc.*, 77, 437-471.
- Karoly, D.J., 1989: Southern Hemisphere circulation features associated with El Niño-Southern Oscillation events. *J. Climate*, 2, 1239-1252.
- Kiladis, G.N., and K.C. Mo, 1998: Interannual and intraseasonal variability in the Southern Hemisphere. *Meteor. Monogr.*, 27(49), 307-336.
- Le Quesne, C., D.W. Stahle, M.K. Cleaveland, M.D. Therrell, J.C. Aravena, and J. Barichivich, 2006: Ancient ciprés tree-ring chronologies used to reconstruct central Chile precipitation variability from A.D. 1200-2000. *J. Climate*, 19, 5731-5744.
- Leiva, J.C., 1999: Recent fluctuations of the Argentinian glaciers. *Global Planet. Change*, 22, 169-177.
- Lliboutry, L., 1998: *Glaciers of the Dry Andes*. *Satellite Image Atlas of Glaciers of the World: South America*. Williams, R.S., and J.G. Ferrigno, Eds., USGS Professional Paper 1386-I. Online version:
<http://pubs.usgs.gov/prof/p1386i/index.html>.
- Mantua, N.J., S.R. Hare, Y. Zhang, J.M. Wallace, and R.C. Francis, 1997: A Pacific Interdecadal Climate Oscillation with impacts on salmon production. *Bull. Amer. Meteor. Soc.*, 78, 1069-1079.

- Marques, R.F.C., and V.B. Rao, 1999: A diagnosis for a long-lasting blocking event over the southeast Pacific Ocean. *Mon. Wea. Rev.*, 127, 1761-1776.
- Maza, J., L. Fornero, and H. Yañez, 1995: Simulating and forecasting snowmelt (in Spanish). *Bull. Inst. fr. études andines*, 24(3), 651-659.
- McCabe, G.J., and M.D. Dettinger, 2002: Primary modes and predictability of year-to-year snowpack variations in the western United States from teleconnections with Pacific Ocean climate. *J. Hydrometeorol.*, 3, 13-25.
- Milana, J.P., 1998: Forecasting river discharges in glacierized basins using energy balance models in the Andes Centrales, Argentina (in Spanish). *Rev. Asoc. Arg. Sedimentol.*, 5(2), 53-69.
- Miller, A., 1976: The climate of Chile. *World Survey of Climatology*, Vol. 12. W. Schwerdtfeger, Ed., Elsevier, 113-218.
- Montecinos, A., and P. Aceituno, 2003: Seasonality of the ENSO-related rainfall variability in Central Chile and associated circulation anomalies. *J. Climate*, 16, 281-296.
- Montecinos, A., A. Diaz, and P. Aceituno, 2000: Seasonal diagnostic and predictability of rainfall in subtropical South America based on tropical Pacific SST. *J. Climate*, 13, 746-758.
- Mote, P.W., A.F. Hamlet, M.P. Clark, and D.P. Lettenmaier, 2005: Declining mountain snowpack in western North America. *Bull. Amer. Meteor. Soc.*, 86(1), 39-49.
- Norte, F., S. Simonelli, and N. Heredia, 1998: Impacts of ENSO on the hydrometeorological regime in Mendoza, Argentina (in Spanish). *Bull. Inst. fr. études andines*, 27(3), 761-770.
- Peña, H., and B. Nazarala, 1987: Snowmelt-runoff simulation model of a central Chile Andean basin with relevant orographic effects. *Large Scale Effects of Seasonal Snow Cover*, Goodison, B.E., Barry, R.G., Dozier, J., Eds., IAHS Publ. 166, 161-172.
- Pittock, A.B., 1980: Patterns of climatic variation in Argentina and Chile - I. Precipitation, 1931-1960. *Mon. Wea. Rev.*, 108, 1347-1361.
- Prieto, M.R., H.G. Herrera, T. Castrillejo, and P.I. Dussel, 2000: Recent climatic variations and water availability in the central Andes of Argentina and Chile (1885-1996). The use of historical records to reconstruct climate (In Spanish). *Meteorologica*, 25(1-2), 27-43.

- Prieto, M.R., H.G. Herrera, P. Doussel, L. Gimeno, and P. Ribera, 2001: Interannual oscillations and trend of snow occurrence in the Andes region since 1885. *Australian Meteor. Mag.*, 50(2), 164-168.
- Prohaska, F., 1976: The climate of Argentina, Paraguay and Uruguay. *World Survey of Climatology*, Vol. 12. W. Schwerdtfeger, Ed., Elsevier, 13-112.
- Quinn, W.H., and V.T. Neal, 1983: Long-term variations in the Southern Oscillation, El Niño, and the Chilean subtropical rainfall. *Fish. Bull.*, 81, 363-374.
- Quintana, J.M., 2004: Factors affecting Central Chile rainfall variations at interdecadal scales (in Spanish). M.Sc. Thesis, Universidad de Chile, 88 pp.
- Rayner, N.A., and Coauthors, 2003: Globally complete analyses of sea surface temperature, sea ice and night marine air temperature, 1871-2000. *J. Geophys. Res.* 108, 4407, doi 10.1029/2002JD002670
- Renwick, J.A., 1998: ENSO-related variability in the frequency of South Pacific blocking. *Mon. Wea. Rev.*, 126, 3117-3123.
- Ribbe L., and H. Gaese, 2002: Water management issues of the Aconcagua watershed, Chile. *Technology Resource Management & Development: Water Management*, Vol. 2. Institute of Technology in the Tropics, Eds., Univ. of Applied Sciences, Cologne, 86-108.
- Rivera, A., G. Casassa, C. Acuña, and H. Lange, 2000: Recent glacier variations in Chile (in Spanish), *Invest. Geogr.*, 34, 29-60.
- Rivera, A., C. Acuña, G. Casassa, and F. Bown, 2002: Use of remotely sensed and field data to estimate the contribution of Chilean glaciers to eustatic sea-level rise. *Ann. Glaciol.*, 34, 367-372.
- Ropelewski, C.F., and P.D. Jones, 1987: An extension of the Tahiti-Darwin Southern Oscillation Index. *Mon. Wea. Rev.*, 115, 2161-2165.
- Rosegrant, M.W., C. Ringler, D.C. McKinney, X. Cai, A. Keller, and G. Donoso, 2000: Integrated economic-hydrologic water modeling at the basin scale: the Maipo river basin. *Agric. Economics*, 24, 33-46.
- Rosenblüth, B., H. Fuenzalida, and P. Aceituno, 1997: Recent temperature variations in southern South America. *Int. J. Climatol.*, 17, 67-85.
- Rutland, J., and H. Fuenzalida, 1991: Synoptic aspects of the central Chile rainfall variability associated with the Southern Oscillation. *Int. J. Climatol.*, 11, 63-76.

- Santer, B.D., and Coauthors, 2000: Statistical significance of trends and trend differences in layer-average atmospheric temperature time series. *J. Geophys. Res.*, 105(D6), 7337-7356.
- Secretaría de Energía, 2004: Electric Sector Annual Report, 2003 (in Spanish). Ministerio de Planificación Federal, Inversión Pública y Servicios, Secretaría de Energía, Argentina. <http://energia.mecon.gov.ar/Publicaciones/Informe%202003.pdf>
- Selkowitz, D.J., D.B. Fagre, and B.A. Reardon, 2002: Interannual variations in snowpack in the Crown of the Continent Ecosystem. *Hydrol. Process.*, 16, 3651-3665.
- SSRH, 2004: Hydrological Statistics of Argentina (in Spanish), CD-ROM, 1st Ed. Subsecretaría de Recursos Hídricos, Buenos Aires, Argentina.
- Stewart, I.T., D.R. Cayan, and M.D. Dettinger, 2005: Changes toward earlier streamflow timing across western North America. *J. Climate*, 18, 1136-1155.
- Thompson, D.W.J., and J.M. Wallace, 2000: Annular modes in the extratropical circulation. Part I: Month-to-month variability. *J. Climate*, 13, 1000-1016.
- Trenberth, K.E., 1997: The definition of El Niño. *Bull. Amer. Meteor. Soc.*, 78(12), 2771-2777.
- Trenberth, K.E., and J.M. Caron, 2000: The Southern Oscillation revisited: Sea level pressures, surface temperatures, and precipitation. *J. Climate*, 13, 4358-4365.
- Trenberth, K. E., J.M. Caron, D.P. Stepaniak, and S. Worley, 2002: Evolution of El Niño–Southern Oscillation and global atmospheric surface temperatures, *J. Geophys. Res.*, 107(D8), 4065, doi:10.1029/2000JD000298.
- Waylen, P.R., and C.N. Caviedes, 1990: Annual and seasonal fluctuations of precipitation and streamflow in the Aconcagua River basin. *J. Hydrol.*, 120, 79-102.
- Waylen, P.R., R. Compagnucci, and R.M. Caffera, 2000: Interannual and interdecadal variability in streamflow from the Argentine Andes. *Phys. Geog.*, 21, 452-465.
- Zhang, Y., J.M. Wallace, and D.S. Battisti, 1997: ENSO-like interdecadal variability: 1900-93. *J. Climate*, 10, 1004-1020.

Appendix 2: Techniques used to identify the main modes of temporal variability in regionally averaged temperature records

A2.1. Statistical significance of linear trends

The statistical significance of the linear trend in each regional time series of size n was assessed using an “effective” sample size n_{eff} (based on the lag-1 autocorrelation coefficient of the linear regression residuals) in the calculation of the standard error of the regression estimate of the trend and the threshold values used in the Student’s t -test (i.e. the AdjSE + AdjDF approach, Santer et al. 2000).

$$n_{eff} = n \frac{1 - r_1}{1 + r_1}$$

If the regression residuals $e(t)$ are statistically independent, then the lag-1 autocorrelation coefficient $r_1 = 0$ and the effective sample size $n_{eff} = n$. However, it is common to find some degree of temporal persistence in the records, and studies where the statistical significance of linear trends is (erroneously) calculated without taking into account this persistence tend to give inflated (too liberal) results. By substituting n_{eff} for n in the calculation of the standard error of the regression estimate of the trend, one obtains an adjusted estimate of its standard error (s'_b). This adjusted estimate is then used to compute an adjusted ratio (t'_b) between the estimated trend and its adjusted standard error:

$$t'_b = b / s'_b$$

To test the significance of the trend, we can then use a t -test where the adjusted t ratio (t'_b) is compared with a critical value (t_{crit}) for a specified significance level α and $n_{eff} - 2$ degrees of freedom (see Santer et al 2000).

A2.2. Identification of regime shifts

The existence of significant shifts in mean conditions in the annually averaged subregional series was examined using the sequential regime shift detection technique developed by Rodionov (2004, 2006). Using the mean of the first l observations in a given time series of size n as a “current”, starting point (\bar{X}_{R1}), this technique first identifies the difference *diff* necessary for the mean (\bar{X}_{R2}) of a hypothetical regime of length l to become statistically significantly different than \bar{X}_{R1} according to a two-tailed Student’s t -test:

$$diff = |\bar{X}_{R2} - \bar{X}_{R1}| = t\sqrt{2\sigma_l^2/l}$$

Here l is assumed to be contained several times in n , t is the value of the t -distribution with $2l - 2$ degrees of freedom at a given probability level p , and the variances of both regimes are assumed the same and equal to the average variance σ_l^2 for running l -intervals in the time series under analysis (Rodionov 2004). Starting with year $i = l + 1$, each new data is added in sequence and a test is performed to determine whether the new value is outside $\bar{X}_{R1} \pm diff$. If the new value is within this expected range it is assumed that the current regime has not changed and observation x_i is included in the calculation of a new mean value \bar{X}_{R1} . Otherwise, x_i is flagged as a possible starting point j of a new regime $R2$ and subsequent data are used to accept or reject this hypothesis. The identification of a regime shift is based on calculating a Regime Shift Index (RSI) for each year $i = j + 1$ to $i = j + l - 1$. RSI represents a cumulative sum of normalized deviations from the hypothetical mean level (\bar{X}_{R2}) of the new regime, and if RSI remains positive during a time period equal to the cut-off length l , a shift is declared at year j . The search for the next shift $R3$ starts at year $i = j + 1$ to ensure that the timing of the next regime is identified correctly even if the actual duration of $R2$ was less than l years (see Rodionov 2004).

In its simplest form, three parameters control the magnitude and scale of the regimes to be detected by the testing algorithm. The significance level p is the level at which the null hypothesis will be rejected. Therefore if a regime shift is detected, the difference in mean values before and after the shift will be statistically significant at least at this given level. Regimes longer than the cut-off length l will all be detected, and although shorter regimes can also pass the test as long as their magnitude is sufficiently large, the ability to detect them depends on the selected cut-off segment length and the target significance level (see Rodionov 2004). The third parameter is the Huber weight parameter h that controls the weights assigned to outliers. Absolute standardized anomalies larger than this parameter (i.e. values larger than h standard deviations) will be weighted inversely proportional to their distance from the expected mean value of their corresponding regime. After experimenting with several combinations of parameter values, we selected a cut-off length $l = 15$ years, a target probability level $p = 0.05$, and a weighting factor $h = 2$ to focus on the most significant decadal and multi-decadal step-like changes that may have occurred in the regionalized mean annual records from SSA and the AP. To ensure that the identified shifts are not simply the manifestation of a red noise process, the series were prewhitened prior to testing using a first order autoregressive parameter estimated by Inverse Proportionality with four corrections (IP4) for subsamples $m = 9$ (Rodionov 2006).

A2.3. Identification of intra- to multi-decadal (IMD) patterns

The Mann-Whitney U test (Wilcoxon 1945; Mann and Whitney 1947) is the nonparametric analogue of the t-test of difference of two independent sample means, and instead of using the raw data, this test assumes that they have been ranked and divided into two classes. For example, if we are interested in testing the significance of the last decade in a 1901-2000 mean annual temperature series, the records are divided into two classes of n_I and n_{II} elements: the 90 years between 1901 and 1990 (class I), and the 10 years between 1991 and 2000 (class II). The U statistic for class II is equivalent to the total number of elements in class I that precede each member of class II when all data values are arranged by rank. That is

$$U_{II} = \sum \sum \varphi(\text{Rank } I_i, \text{Rank } II_j)$$

Here Rank I_i is the rank of the i th member of class I, and Rank II_j is the rank of the j th member of class II. $\varphi(\text{Rank } I_i, \text{Rank } II_j) = 1$ if Rank $I_i < \text{Rank } II_j$, 0 otherwise. From the previous equation it can be seen that the maximum U_{II} statistic would result when that class accounts for the 10 highest rankings ($U_{II} = 90 \times 10$), while the smallest statistic would occur when class II accounts for the 10 lowest rankings ($U_{II} = 0 \times 10$). The $100!/90!10!$ possible arrangements that the rankings in class II might assume produce a series of normally distributed U statistics with a given mean (μ_U) and standard deviation (σ_U). These parameters can be used to Z-transform the U statistics, with significantly high (low) Z values indicating a significant incidence of high (low) rankings in a sample relative to a null hypothesis that assumes random sampling (Mauget 2003).

However, we might be interested in comparing U statistics against a more climate-specific null hypothesis that assumes climate variations have a certain level of persistence but are essentially stationary over the long term. This approach is the basis of the technique used in our study, and briefly the main steps are:

- 1- As the climate variations tested here are (to follow the example above) of 10 years or longer duration, remove that variation from the data by using a high-pass filter. In this case we use a 10-year high-pass Lanczos filter (Duchon 1979), but the window lengths essentially depend on the length of the segment under study.
- 2- Calculate the autoregressive AR(1), AR(2), and AR(3) regression coefficients of the high-passed data obtained above and select the most appropriate AR model by using the minimum Akaike information criterion (Akaike 1974).
- 3- From the results of the previous step, form autoregressive red noise processes which will therefore have essentially the same persistence of the actual high-pass series. Then, adjust the mean and variance of the red noise processes to agree with those of the data.
- 4- Select red noise series of appropriate length (in this case 100 years) and rank those values.

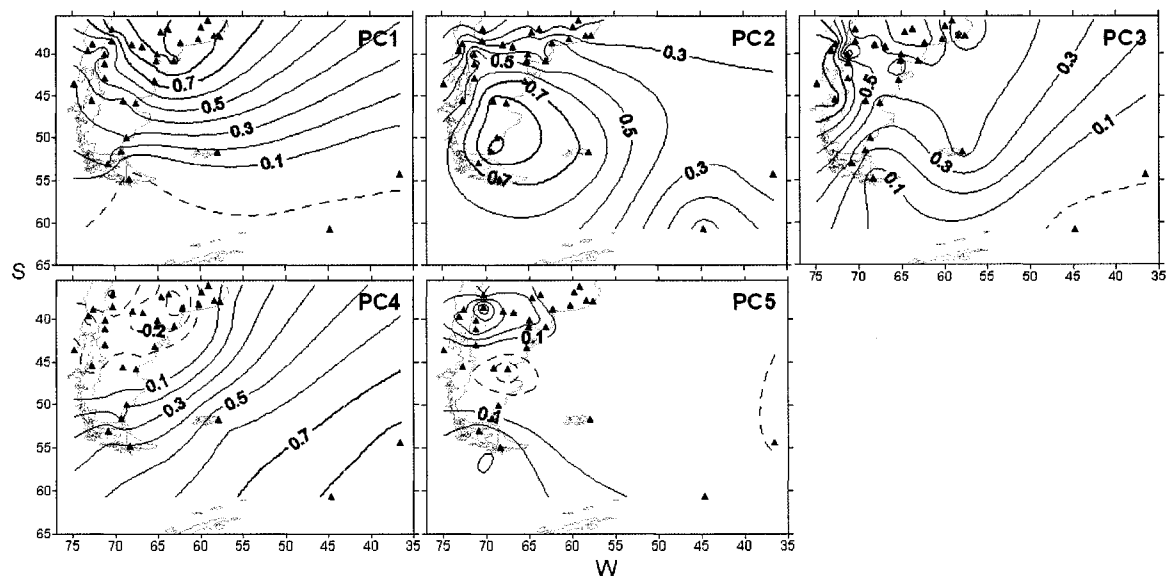
- 5- From the ranked red noise processes resulting from step d, calculate appropriate null statistics, which in the current example would be the U_{II} statistics derived from all possible non-overlapping 10-yr segments of each red noise series.
- 6- Repeat (1-5) until 10 000 independent null realizations are calculated, and determine the distribution parameters of the resulting U_{II} null statistics.

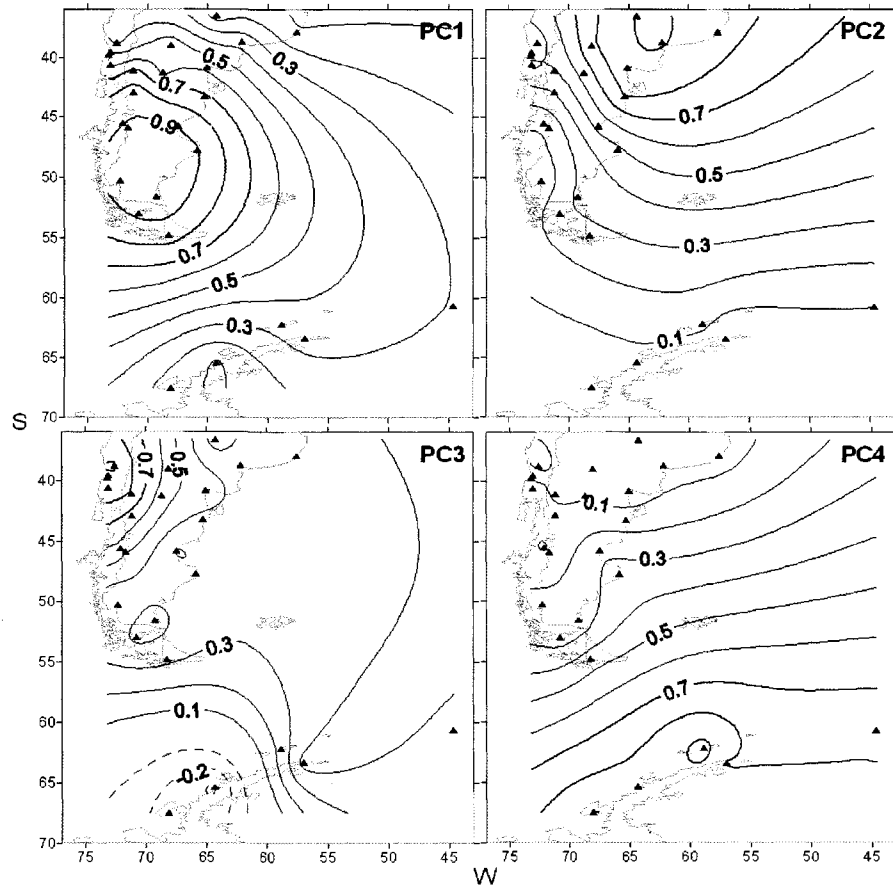
The mean (μ_{MC}) and standard deviation (σ_{MC}) derived from these Monte Carlo simulations can then be used to Z-transform the U statistics obtained from the undetrended series of annual data. The Mann-Whitney Z (MWZ) statistics are then

$$MWZ = (U - \mu_{MC}) / \sigma_{MC}$$

Since MWZ statistics are assumed to be normally distributed with zero mean and unit standard deviation, the positive and negative 90%, 95% and 99% confidence intervals are defined by the ± 1.645 , ± 1.960 and ± 2.576 MWZ values, respectively. Similarly, the ± 3.290 MWZ threshold can be used to denote the 99.9% confidence level.

Instead of testing the significance of a limited, arbitrary single window length (e.g. 10-yr running time window), we generalize the procedure described above and evaluate the significance of climate variations over a wider range of timescales by simply repeating the MWZ tests using sampling windows of varying length (e.g. 6-30 years). Given the dependence of the MWZ mean (μ_{MC}) and standard deviation (σ_{MC}) on sample size, we must repeat the Monte Carlo trials for each window length (see e.g. Mauget 2004). Apart from being an innovative application to climate change studies for this region, this analysis introduces an element of objectivity in the identification of the onset, duration and statistical significance of the main IMD regimes in the homogenized regional series derived from each area.

Appendix 3: As Fig. 2.3, but based on the 32 stations for the 1931-60 interval.

Appendix 4: As Fig. 2.3, but for the 26 stations over the 1961-2001 interval.

Appendix 5: Summary of available dendrochronological evidence from selected living and dead trees cored at sampling stations B-I, Glaciar Río Manso (Fig. 5.2). Number of trees and earliest ring dates from the three oldest trees are indicated. Pith offset and sampling height correction factors are shown in brackets. Estimated minimum ages for surfaces are based on a 6-yr ecesis. Notes: (D) distal slope of moraine; (P) proximal slope; (B) dense bamboo undergrowth; (*) an older tilted tree on the same surface suggests the moraine was emplaced ca. 1841-43 (see text for details); (#) dead trees, minimum ages obtained after crossdating with La Almohadilla living chronology.

Station	Sampling site	Number of trees; innermost ring dates (pith offset and sampling height correction factors)	Minimum age for surface
B	Outer moraine (P)	7 trees; 1905 (10,3), 1924 (0,2), 1926 (0,2)	1886
	Outer moraine (D)	3 trees*; 1883 (5,4), 1904 (10,2), 1923 (2,4)	1868
	Mature forest (B)	8 trees; 1840 (5,8), 1852 (10,15), 1853 (0,10)	1821
C	Outer moraine (D)	7 trees; 1895 (10,8), 1899 (20, 4), 1902 (20,4)	1869
	Former lake floor	12 trees; 1883 (0,3), 1896 (0,4), 1897 (10,5)	1874
	Mature forest (B)	10 trees; 1847 (0,6), 1856 (5,10), 1857 (0,9)	1835
D	Outer moraine (P)	8 trees; 1866 (0,4), 1866 (0,3), 1876 (3,4)	1856
	Mature forest (B)	7 trees; 1650 (20,12), 1715 (10,12), 1755 (20,12)	1612
E	Outer moraine (D)	18 trees; 1896 (3,5), 1899 (5,5), 1903 (5,5)	1882
	Outer moraine (P)	13 trees; 1894 (10,5), 1894 (5,5), 1902 (10,5)	1873
	Inner moraine 1	25 trees; 1930 (10,4), 1931 (0,4), 1932 (0,4)	1910
	Inner moraine 2	4 trees; 1944 (0,4), 1949 (0,4), 1956 (0,4)	1936
	Inner moraine 3	2 trees; 1957 (0,4), 1960 (0,4)	1947
F	Trees with base buried by outwash	6 trees; 1712 (20,12), 1760# (20,10), 1791# (20,10)	1674
	Mature trees not affected by outwash	5 trees; 1724 (5,11), 1853 (0,12), 1857 (3,9)	1702
	Trees growing on top of outwash	2 trees; 1859 (0,10), 1870 (3,4)	1843
G	Mature forest (B)	26 trees; 1706 (20,13), 1731 (15,12), 1731 (15,10)	1667
H	Mature forest (B)	21 trees; 1764 (20,12), 1785 (20,12), 1806 (20,11)	1726
	M1	32 trees; 1854 (5,10), 1854 (3,10), 1870 (15,10)	1833
	M2	24 trees; 1891 (0,10), 1898 (0,5), 1902 (3,8)	1875
	M3	17 trees; 1897 (0,1), 1912 (3,3), 1912 (0,3)	1890
	M4	21 trees; 1911 (5,1), 1920 (0,4), 1931 (3,4)	1899
	M5	19 trees; 1943 (15,3), 1956 (20,3), 1958 (20,4)	1919
	M6	9 trees; 1958 (0,3), 1960 (0,3), 1961 (0,3)	1949
	M7	18 trees; 1963 (0,2), 1972 (5,1), 1973 (0,3)	1955
	M8	9 trees; 1984 (0,1), 1985 (0,2), 1988 (1,1)	1977
I	Mature forest (B)	10 trees; 1700 (20,8), 1763 (0,4), 1790 (20,12)	1666
	Channel between outer moraine and mature forest	3 trees; 1748 (0,12), 1793 (20,10), 1798 (20,10)	1730
	Outer moraine (D)	23 trees; 1737 (20,10), 1785 (20,9), 1817 (0,10)	1701
	Outer moraine (P)	14 trees; 1864 (20,10), 1881 (20,8), 1884 (3,8)	1828

Appendix 6: Selected tree-ring chronologies used in Chapter 6. Notes: (A) *A. chilensis*; (F) *F. cupressoides*; (ARA) *A. araucana*; (SIC) Mean series intercorrelation; (MS) Mean sensitivity: relative measure of year-to-year variability in ring widths (Fritts 1976); (MSL) Mean series length; (PC) Composite record based on separate PCA of *A. chilensis* and *F. cupressoides* chronologies (see text). Note that ARA1 is formed by one site. Sources: (A) Laboratorio de Dendrocronología, Universidad Austral de Chile, Valdivia; (B) Villalba and Veblen (1997); (C) LaMarche et al. (1979); (D) Villalba et al. (1996), Lara et al. (2000); (E) Laboratorio de Dendrocronología, Instituto Argentino de Nivología, Glaciología y Ciencias Ambientales (IANIGLA), Mendoza, Argentina; (*) Available at the International Tree-Ring Data Bank (ITRDB, <http://www.ncdc.noaa.gov/paleo/treering.html>). Multiple sources indicate subsequent updates.

Site (species-site code in Fig. 1)	Lat (S)	Long (W)	Elev.	Period	Yrs	Cores	SIC	MS	MSL	PC	Source
Co. Castillo (A-CAS)	40.50	71.15	1100	1576-2003	428	32	0.667	0.275	248	AUS1	A
El Centinela (A-CEN)	40.73	71.10	1050	1489-2002	514	43	0.682	0.284	230	AUS1	B*,A
Collunco Alto (A-COL)	39.93	71.13	870	1596-1989	394	18	0.505	0.216	249	AUS1	B*
Cuyin Manzano (A-CUY)	40.72	71.13	900	1543-2003	461	39	0.638	0.319	201	AUS1	C*,A
Dedo de Dios (A-DDD)	40.73	71.10	900	1461-1989	529	37	0.701	0.375	287	AUS1	B*
La Fragua (A-FRA)	41.07	71.98	1000	1690-2002	313	23	0.543	0.208	169	AUS1	A
Co. El Guanaco (A-GUA)	41.03	70.98	1150	1497-2002	506	36	0.566	0.260	260	AUS1	B*,A
Co. Los Leones (A-LEO)	41.08	71.15	1020	1539-2003	465	73	0.626	0.228	266	AUS1	C*,B*,A
Arroyo Minero (A-MIN)	40.70	71.27	1050	1589-1991	403	16	0.670	0.274	254	AUS1	B*
El Mirador (A-MIR)	40.65	71.40	1050	1484-2003	520	52	0.589	0.236	226	AUS1	B*,A
Co. Los Pinos (A-PIN)	40.07	71.03	1100	1508-2003	496	67	0.542	0.215	220	AUS1	B*,A
San Ramón (A-RAM)	41.05	70.98	1100	1650-1991	342	17	0.567	0.244	224	AUS1	B*
Paso del Viento (A-VIE)	40.70	71.13	910	1679-1991	313	14	0.586	0.215	229	AUS1	B*
Co. La Hormiga (A-HOR)	40.05	71.28	920	1508-2003	496	61	0.677	0.263	212	AUS2	B*,A
Norquinco (A-NOR)	39.12	71.12	1150	1562-2003	442	102	0.590	0.291	169	AUS2	B*,A
Quillén (A-QUI)	39.28	71.27	1100	1676-1989	314	19	0.601	0.285	194	AUS2	B*
Rucachoroi (A-RUC)	39.25	71.17	1300	1572-2003	432	50	0.606	0.262	185	AUS2	C*,A
Nahuel Pan (A-NAU)	42.97	71.22	850	1567-2002	436	84	0.677	0.283	234	AUS3	B*,A
Ea. Teresa (A-TER)	42.95	71.23	820	1540-2002	463	39	0.636	0.301	203	AUS3	C*,A
Alerce Andino (F-AAN)	41.50	72.50	800	205-2000	1796	27	0.414	0.268	946	FIT1	A
Ayacara (F-AYA)	42.27	72.77	800	354BC-1993AD	2348	30	0.492	0.313	726	FIT1	D

Appendix 6: (cont'd).

Cerro Nevado (F-LCN)	41.40	72.30	850	526-2002	1477	54	0.470	0.256	533	FIT1	A
Lenca (F-LEN)	41.55	72.60	875	1932BC-2001AD	3934	97	0.485	0.258	907	FIT1	D,A
Lago Inexplorado (F-LIN)	41.95	72.28	1000	501-1993	1493	46	0.513	0.250	506	FIT1	D
Oro Verde (F-LOV)	41.60	72.55	800	576-2003	1428	18	0.441	0.269	685	FIT1	A
Patamay (F-PTM)	41.87	72.53	875	832-1994	1163	16	0.423	0.324	621	FIT1	D
Volcán Apagado (F-VAP)	41.58	72.50	975	448-1994	1547	41	0.445	0.271	718	FIT1	D
Río Alerce (F-ALE)	41.17	71.78	1100	864-1991	1128	71	0.533	0.252	471	FIT2	D*
Puerto Café (F-CAF)	42.73	71.97	535	311-1992	1682	58	0.515	0.273	556	FIT2	D*
La Esperanza (F-ESP)	41.25	71.90	750	342BC-1995AD	2338	58	0.571	0.267	463	FIT2	D*
Río Frías (F-FRI)	41.10	71.80	950	888-1991	1104	17	0.498	0.259	571	FIT2	D*
Horqueta Inferior (F-HOI)	41.83	71.77	950	539-1993	1455	31	0.494	0.292	596	FIT2	D*
Horqueta Superior (F-HOS)	41.83	71.78	1230	574-1993	1420	24	0.440	0.278	653	FIT2	D*
Río Motoco (F-MOT)	42.08	71.83	1200	320-1993	1674	36	0.477	0.252	629	FIT2	D*
Río Alejandro (F-RAL)	42.58	71.95	570	568-1993	1426	37	0.440	0.271	556	FIT2	D*
Volcán Osorno (F-OSO)	41.17	72.50	990	788-1994	1207	51	0.472	0.265	557	FIT3	D
Puntiagudo (F-PEV)	40.92	72.35	970	354BC-1994AD	2349	36	0.531	0.211	659	FIT3	D
Los Quetros (F-QUE)	40.83	72.33	900	992-1993	1002	23	0.447	0.266	435	FIT3	D
Pabilos (F-PAB)	40.90	73.75	800	350-1996	1647	42	0.408	0.221	402	FIT4	D
Pelada (F-PEL)	41.00	73.72	850	448BC-1992AD	2441	57	0.412	0.222	498	FIT4	D
Ea. Pulmari (ARA1)	39.08	71.30	1890	1589-1989	401	28	0.609	0.232	252	ARA1	E*

Appendix 7: Permission to reprint Chapter 3

Subject RE: permission to reprint article "in press" in doctoral thesis
From "Truter, Clare (ELS-OXF)"
Date Tuesday, November 6, 2007 6:43 am
To Mariano H Masiokas

October 31, 2007

Dear Mr Masiokas

We hereby grant you permission to reprint the material detailed below at no charge in **your thesis** subject to the following conditions:

1. If any part of the material to be used (for example, figures) has appeared in our publication with credit or acknowledgement to another source, permission must also be sought from that source. If such permission is not obtained then that material may not be included in your publication/copies.
2. Suitable acknowledgment to the source must be made, either as a footnote or in a reference list at the end of your publication, as follows:

“This article was published in Publication title, Vol number, Author(s), Title of article, Page Nos, Copyright Elsevier (or appropriate Society name) (Year).”

3. Your thesis may be submitted to your institution in either print or electronic form.
4. Reproduction of this material is confined to the purpose for which permission is hereby given.
5. This permission is granted for non-exclusive world **English** rights only. For other languages please reapply separately for each one required. Permission excludes use in an electronic form other than submission. Should you have a specific electronic project in mind please reapply for permission.
6. This includes permission for the Library and Archives of Canada to supply single copies, on demand, of the complete thesis. Should your thesis be published commercially, please reapply for permission.

Yours sincerely

Clare Truter

Rights Manager

From: Mariano H Masiokas
Sent: 31 October 2007 16:55
To: Rights and Permissions (ELS)
Cc:
Subject: permission to reprint article "in press" in doctoral thesis

Clare Truter
Rights Manager
Global Rights Department
Elsevier Ltd
PO Box 800
Oxford OX5 1DX, UK

Tel: (+44) 1865 843830 (UK) or (+1) 215 239 3804 (US)
Fax: (+44) 1865 853333
Email: XXXXXXXXX

Dear Clare,

I would like to request permission to reprint the following article in my doctoral thesis:

Masiokas, M.H., Villalba, R., Luckman, B.H., Lascano, M.E., Delgado, S. and Stepanek, P. 20th-century glacier recession and regional hydroclimatic changes in northwestern Patagonia. *Global and Planetary Change* (2007), doi:10.1016/j.gloplacha.2006.07.031.

This article is still "in press", and I could not find the "Request Permission" link to the right of the abstract like with other papers already published in this journal. Could you please indicate me what steps should I follow to obtain such permission?

Thank you very much in advance, and best regards,

Mariano H. Masiokas
Department of Geography
University of Western Ontario
London, Ontario, N6A 5C2
Canada

This email is from Elsevier Limited, a company registered in England and Wales with company number 1982084, whose registered office is The Boulevard, Langford Lane, Kidlington, Oxford, OX5 1GB, United Kingdom.

Appendix 8: Permission to reprint Chapter 4

Subject RE: permission to reprint "accepted" article in doctoral thesis
 From "Truter, Clare (ELS-OXF)"
 Date Wednesday, November 7, 2007 4:29 am
 To Mariano H Masiokas

November 6, 2007

Dear Mr Masiokas

We hereby grant you permission to reprint the material detailed below at no charge **in your thesis** subject to the following conditions:

7. If any part of the material to be used (for example, figures) has appeared in our publication with credit or acknowledgement to another source, permission must also be sought from that source. If such permission is not obtained then that material may not be included in your publication/copies.
8. Suitable acknowledgment to the source must be made, either as a footnote or in a reference list at the end of your publication, as follows:

“This article was published in Publication title, Vol number, Author(s), Title of article, Page Nos, Copyright Elsevier (or appropriate Society name) (Year).”

9. Your thesis may be submitted to your institution in either print or electronic form.
10. Reproduction of this material is confined to the purpose for which permission is hereby given.
11. This permission is granted for non-exclusive world **English** rights only. For other languages please reapply separately for each one required. Permission excludes use in an electronic form other than submission. Should you have a specific electronic project in mind please reapply for permission.
12. This includes permission for the Library and Archives of Canada to supply single copies, on demand, of the complete thesis. Should your thesis be published commercially, please reapply for permission.

Yours sincerely

Clare Truter

Rights Manager

From: Mariano H Masiokas
Sent: 06 November 2007 16:57
To: Truter, Clare (ELS-OXF)
Cc:
Subject: permission to reprint "accepted" article in doctoral thesis

Clare Truter
Rights Manager
Global Rights Department
Elsevier Ltd
PO Box 800
Oxford OX5 1DX, UK

Tel: (+44) 1865 843830 (UK) or (+1) 215 239 3804 (US)
Fax: (+44) 1865 853333
Email: XXXXXXXXX

Dear Clare,

I am sorry for not including this request in my previous message, but another chapter of my thesis has recently been accepted for publication in Palaeogeography, Palaeoclimatology, Palaeoecology and I would also like to request permission to reprint this material in my doctoral thesis. The article is:

Masiokas, M.H.; Luckman, B.H.; Villalba, R.; Delgado, S.; Skvarca, P.; Ripalta, A.. Little Ice Age fluctuations of small glaciers in the Monte Fitz Roy and Lago del Desierto areas, south Patagonian Andes, Argentina. Accepted for publication, Palaeogeography, Palaeoclimatology, Palaeoecology, July 2007.

Thank you very much again, and best regards,

Mariano H. Masiokas
Department of Geography
University of Western Ontario
London, Ontario, N6A 5C2
Canada

This email is from Elsevier Limited, a company registered in England and Wales with company number 1982084, whose registered office is The Boulevard, Langford Lane, Kidlington, Oxford, OX5 1GB, United Kingdom.

Appendix 9: Permission to reprint Appendix 1

Subject Re: [Fwd: permission to reprint article in doctoral thesis]
 From Melissa Weston
 Date Friday, November 2, 2007 5:09 pm
 To Mariano H Masiokas

Hi Mariano,
 This will be fine as long as you acknowledge the source of the material.
 Best regards,
 Melissa

October 31, 2007

Gwendolyn Whittaker
 Publications Coordinator
 American Meteorological Society

Dear Gwendolyn,

I would like to request permission to reprint the following article in my doctoral thesis:

Masiokas, M.H., Villalba, R., Luckman, B.H., Le Quesne, C. and Aravena, J.C. 2006. Snowpack variations in the central Andes of Argentina and Chile, 1951-2005: Large-scale atmospheric influences and implications for water resources in the region. *Journal of Climate* 19, 6334-6352. Could you please direct me to the appropriate person to obtain such permission?

Thank you very much in advance, and best regards,

Mariano H. Masiokas
 Department of Geography
 University of Western Ontario
 London, Ontario, N6A 5C2
 Canada

Melissa S. Weston, Executive Officer
 American Meteorological Society
 45 Beacon Street
 Boston, Massachusetts 02108-3693 USA
 E-MAIL: XXXXXXXXXXXX
 TEL: (617) 227-2426, ext. 250
 FAX: (617) 742-8718
 AMS Web Site: <http://www.ametsoc.org>

=====
 "If there is no wind, row."—Latin proverb

Curriculum Vitae

Name: Mariano H. Masiokas

Place of birth: Mendoza, Argentina

Date of birth:

Post-Secondary Education and Degrees: Universidad Nacional de Cuyo
Mendoza, Argentina
1995-2000 Agronomic Engineer

The University of Western Ontario
London, Ontario, Canada
2002-2003 M.Sc. student, upgraded to Ph.D. Program

The University of Western Ontario
London, Ontario, Canada
2003-2008 Ph.D.

Honors and Awards: Universidad Nacional de Cuyo Young Scientists Scholarship
1999-2000

Inter-American Institute for Global Change Research
Fellowship
2000-2002

Environmental Science Graduate Scholarship, UWO
2003-2006

Special University Scholarship, UWO
2002-2005

International Graduate Student Scholarship, UWO
2002-2005

Western Graduate Research Scholarship, UWO
2005-2007

Province of Ontario Graduate Scholarship
2006-2007

- Related Work Experience:** Teaching Assistant
Universidad Nacional de Cuyo, Mendoza, Argentina
1999-2002
- Research Assistant
Instituto Argentino de Nivología, Glaciología y Ciencias Ambientales (IANIGLA-CONICET), Mendoza, Argentina
2000-2002
- Teaching Assistant
The University of Western Ontario
2002-2007
- Research Assistant
The University of Western Ontario
2002-2008

Publications:

- Delgado, S., Masiokas, M., Villalba, R., Trombotto, D., Ripalta, A., Hernández, J. and Calí, S. 2002. Historical and dendrochronological evidences for glacier fluctuations in Patagonia during the past 1000 years (PATAGON-1000). In: Trombotto, D. and Villalba, R. (eds.) IANIGLA, 30 Years of Basic and Applied Research on Environmental Sciences. ZetaEditores, Mendoza, Argentina, p. 47-51.
- Villalba, R., Lara, A., Boninsegna, J.A., Masiokas, M., Delgado, S., Aravena, J.C., Roig, F.A., Schmelter, A., Wolodarsky, A. and Ripalta, A. 2003. Large-scale temperature changes across the southern Andes: 20th-century variations in the context of the past 400 years. *Climatic Change* 59 (1-2), 177-232.
- Masiokas, M., and Villalba, R. 2004. Climatic significance of intra-annual bands in the wood of *Nothofagus pumilio* in southern Patagonia. *Trees: Structure and Function* 18 (6), 696-704.
- Rodríguez, R., Mabres, A., Luckman, B.H., Evans, M. and Masiokas, M. 2005. "El Niño" events recorded in dry-forest species of the lowlands of northwest Peru. *Dendrocronologia* 22(3), 181-186.
- Villalba, R., Masiokas, M., Kitzberger, T., and Boninsegna, J.A. 2005. Biogeographical consequences of recent climate changes in the southern Andes of Argentina. In: Huber, U., Reasoner, M., and Bugmann, H. (eds.) *Global Change and Mountain Regions, A State of Knowledge Overview*. Springer, p. 157-168.

Masiokas, M.H., R. Villalba, B.H. Luckman, C. Le Quesne, and J.C. Aravena. 2006. Snowpack variations in the central Andes of Argentina and Chile, 1951-2005: Large-scale atmospheric influences and implications for water resources in the region. *Journal of Climate* 19 (24), 6334-6352.

Masiokas, M.H., Villalba, R, Luckman, B.H., Delgado, S., Lascano, M., and Stepanek, P. 2008. 20th-century glacier recession and regional hydroclimatic changes in northwestern Patagonia. *Global and Planetary Change* 60, 85-100.
doi:10.1016/j.gloplacha.2006.07.031.

Masiokas, M.H., Luckman, B.H., Villalba, R., Delgado, S., Skvarca, P. and Ripalta, A. (Accepted). Little Ice Age fluctuations of small glaciers in the Monte Fitz Roy and Lago del Desierto areas, south Patagonian Andes, Argentina. *Palaeogeography, Palaeoclimatology, Palaeoecology*.